SUMMARY

Fachreza Akbar, Department of Civil Engineering, Faculty of Engineering, Universitas Brawijaya. January 2018, Staple Shape Rebar as Flexural Strength Repair on Preloaded Reinforced Concrete Beam. Academic Supervisor: Wisnumurti and Ari Wibowo.

Staple shape rebar is widely known as repair device in repairing surface structure such wall and floor slab combined with patching. Patching of reinforced concrete beam also has been widely used in repair practice whether by addition of strengthening device or without any addition of strengthening device. The easiness of use and cheap price make this repair system has potential to use in deteriorate reinforced concrete beam.

In this study, the two repair procedures have been applied as one repair system and the behavior of repair system correspond to the repaired substrate system is observed and analyzed. With deteriorate of the reinforced concrete members was built by a development of plastic hinge in the mid-span area with three point bending load, staple repair rebar combined with patching mortars has resulting 22-32% higher load capacity during post-repair reload than normal beam for the specimens with 700mm repair rebar. While shorter repair rebar with 400mm long showing 4-8% higher load.

The results of repaired specimens with staple shape repair rebar were also compared with repair system with straight shape rebar. The result shows that specimens repaired with straight shape rebar always show sudden drop of load curve during collapse process. Specimens repaired with straight shape rebar also have lower load capacity than staple shape rebar with the same length of repair system.

According to crack path observation, behavior of the repaired specimens with staple repair rebar shows that collapse is caused combination of shear-flexural mechanism. Wide diagonal cracks were always occurs before the repaired specimens is start to collapse. In the other hand, specimens with straight shape rebar showing debonding and bond-slip mechanism during collapse process.

Keyword : staple repair rebar, reinforced concrete, preload, patching

RINGKASAN

Fachreza Akbar, *Jurusan Teknik Sipil, Fakultas Teknik Universitas Brawijaya, Januari 2018, Tulangan Perbaikan dengan Bentuk Staple Sebagai Perbaikan Kuat Lentur pada Beton Bertulang yang diberikan Pembebanan Awal,* Dosen Pembimbing: Wisnumurti dan Ari Wibowo.

Tulangan berbentuk staple *sudah dikenal sebagai alat perbaikan pada struktur dinding dan lantai, dimana sering kali dikombinasikan dengan teknik penambalan. Tenik tambal juga telah banyak digunakan baik dengan penambahan perkuatan atau tanpa tambahan perkuatan. Kemudahan penggunaan dan nilai ekonomis membuat sistem perbaikan tersebut memiliki potensi untuk digunakan dalam perbaikan beton bertulang yang mengalami kerusakan.*

Pada studi ini, dua metode perbaikan tersebut dipadukan menjadi satu kesatuan sistem perbaikan. Pengamatan dan analisis juga dilakukan untuk mengetahui perilaku dari sistem perbaikan yang diaplikasikan pada struktur asli. Kerusakan pada struktur dibuat dengan membentuk sendi plasti ditengah bentang dengan pembebanan awal. Perbaikan yang dilakukan dengan metode tersebut menghasilkan peningkatan kapasitas 22-32% lebih tinggi dari balok normal untuk balok yang diperbaiki dengan tulangan staple *panjang 700mm. Sedangkan balok yang diperbaiki dengan panjang tulangan 400mm mengalami peningkatan kapasitas sebesar 4-8%. Hasil tersebut juga dibandingkan dengan balok yang diperbaiki menggunakan tulangan berbentuk lurus. Hasil observasi menunjukkan pada balok yang diperbaiki menggunakan tulangan berbentuk lurus selalu mengalami penurunan grafik secara tiba-tiba, dengan nilai beban yang lebih rendah.*

Berdasarkan pengamatan rambatan retak, perilaku dari balok yang diperbaiki dengan tulangan berbentuk staple menunjukkan perilaku kegagalan akibat kombinasi geser-lentur. Retak lebar dengan arah diagonal selalu muncul sebelum balok mengalami kegagalan struktur. Di sisi lain, balok dengan tulangan perbaikan lurus menunjukkan adanya perilaku kegagalan akibat debonding *dan* bondslip.

Kata kunci : tulangan staple*, perbaikan beton bertulang, pembebanan awal, teknik tambal*

FOREWORDS

Repair generally means an activity by replacing a part or putting together what is torn or broken. The object to be repaired usually something that has been used for particular time then get broke by either during its service uses or by accidental force. Therefore, a new part replacement or may be patch were united to the repaired. Generally, repaired object always has tendency to break again with the same manner or may be in different way according to how good the repair was conducted.

Same condition may also be happen in civil engineering works. Even a well-built structure still has probability to deteriorate by many factors. For example, a reinforced beam may experience a sudden surcharge load by unexpected activity above it, which could make the concrete experience and pass its maximum load capacity and failure. In ideal condition, this part of structure should be replaced by new structure, however this may not always possible. Therefore repair work is conducted to restore the failed member strength. This repair work has to be reliable and properly assessed for its probability and behavior of its failure mechanism, so the repaired structure may not harm the user.

In this study, staple repair rebar which has been widely used in repairing surface structure such wall and floor are applied and observed as flexural beam repair device. The easiness of application and cheap price of the devices are several benefits of proposed repair system. However, better understanding of how the proposed repair system will behave during service load and ultimate load is needed before the repair system may be widely used. As there are few information and conducted research on such repair system, therefore, this study is conducted as a preliminary study aiming to open the problems of such repair system, and also similar system with abrupt section change along the length of member. Discussion of the result and repair process is open so there will be a continuity and deliberate discussion to this research topic.

Malang, January 16th 2018

Fachreza Akbar

TABLE OF CONTENTS

TABLE OF CONTENTS ..... Error! Bookmark not defined.

TABLE OF FIGURES ..... Error! Bookmark not defined.

TABLE OF TABLES ..... Error! Bookmark not defined.

APPENDIX LIST ..... Error! Bookmark not defined.

SYMBOL AND NOTATION ..... Error! Bookmark not defined.

CHAPTER 1 INTRODUCTION ..... Error! Bookmark not defined.

1.1 Study Background ..... **Error! Bookmark not defined.**

1.1.1 Repair Problem ..... **Error! Bookmark not defined.**

1.1.2 Residual Strength of a Deteriorated Structure **Error! Bookmark not defined.**

1.1.3 Practical of Insufficient Repair of Patching and Strengthening ..... **Error! Bookmark not defined.**

1.2 Research Problems ..... **Error! Bookmark not defined.**

1.3 Research Question ..... **Error! Bookmark not defined.**

1.4 Limitations ..... **Error! Bookmark not defined.**

1.5 Objectives ..... **Error! Bookmark not defined.**

1.6 Implications ..... **Error! Bookmark not defined.**

CHAPTER 2 LITERATURE REVIEW ..... Error! Bookmark not defined.

2.1 Concrete Beam Stress-Strain Behavior ..... **Error! Bookmark not defined.**

2.1.1 Confinement Effect of Rectangular Stirrups **Error! Bookmark not defined.**

2.2 Limit State of a Structure ..... **Error! Bookmark not defined.**

2.3 Deterioration of Reinforced Concrete Structure . **Error! Bookmark not defined.**

2.3.1 Cracks on Concrete Beam ..... **Error! Bookmark not defined.**

2.4 Concrete Deterioration ..... **Error! Bookmark not defined.**

2.4.1 Composer Deteroriation ..... **Error! Bookmark not defined.**

2.4.2 Microscopic Deterioration during Loading **Error! Bookmark not defined.**

2.5 Concrete Behavior during Repeated Loading ..... **Error! Bookmark not defined.**

2.5.1 Repeated loading by Otter and Naaman .... **Error! Bookmark not defined.**

2.5.2 Unloading and Reloading Branches by Mander, Priestley and Park.. **Error! Bookmark not defined.**

2.5.3 Mathmatical Model of Stress-Strain for Concrete Under Cyclic Loading by Ashlani and Jowkarmeimandi. ..... **Error! Bookmark not defined.**

2.5.4 Repeated Loading of Steel Reinforcement **Error! Bookmark not defined.**

2.6 Bond Strength and Anchorage Development of Steel Reinforcement ..... **Error! Bookmark not defined.**

2.6.1 Yield Penetration Mechanism ..... **Error! Bookmark not defined.**

2.6.2 Analysis of Hook Development ..... **Error! Bookmark not defined.**
2.7 Reinforced Concrete Failure Mechanism on Shear **Error! Bookmark not defined.**
2.8 Repair Method using Strengthening Devices in Previous Researches ..... **Error! Bookmark not defined.**
2.8.1 Behaviour of Patch-Repaired Concrete Structural Elements under Increasing Static Loads to Flexural Failure (Rio, et al., 2005)..... **Error! Bookmark not defined.**
2.8.2 Central peeling failure behavior of polymer cement mortar retrofitting of reinforced concrete beams (Satoh and Kodama 2005) **Error! Bookmark not defined.**
2.8.3 Strengthening and Repair of Reinforced Concrete Using External Steel Plates (Aykac, et al. 2013)..... **Error! Bookmark not defined.**
2.9 Damage Modeling in Finite Element of Composite Structure **Error! Bookmark not defined.**
2.9.1 Bond Behaviour of Composite Material.... **Error! Bookmark not defined.**
2.9.2 Concrete Column Plastic Hinge Relocation as Damage Repair Reported by Rudledge, et al. ..... **Error! Bookmark not defined.**

CHAPTER 3 CONCEPTUAL FRAMEWORK ..... Error! Bookmark not defined.
3.1 The Framework ..... **Error! Bookmark not defined.**
3.2 Expected Results ..... **Error! Bookmark not defined.**

CHAPTER 4 RESEARCH METHOD ..... Error! Bookmark not defined.
4.1 Research Place..... **Error! Bookmark not defined.**
4.2 Research Variable ..... **Error! Bookmark not defined.**
4.3 Research Equipment and Tools ..... **Error! Bookmark not defined.**
4.4 Flowchart and Procedure ..... **Error! Bookmark not defined.**
4.5 The Basic Beam Specimens..... **Error! Bookmark not defined.**
4.5.1 Beam Specimens Design ..... **Error! Bookmark not defined.**
4.5.2 Under or Over Reinforced Failure State.... **Error! Bookmark not defined.**
4.5.3 Point to Stop Preloading of Laboratory Experiment **Error! Bookmark not defined.**
4.5.4 Maximum Load Analysis ..... **Error! Bookmark not defined.**
4.6 Specimen Materials..... **Error! Bookmark not defined.**
4.6.1 Substrate Concrete..... **Error! Bookmark not defined.**
4.6.2 Steel Reinforcement Rebar..... **Error! Bookmark not defined.**
4.6.3 Patch Repair Material ..... **Error! Bookmark not defined.**
4.7 Beam Specimens Repair ..... **Error! Bookmark not defined.**
4.7.1 Staple Shape and Straight Shape of Repair Rebar **Error! Bookmark not defined.**
4.8 Repaired Beam Final Test..... **Error! Bookmark not defined.**

CHAPTER 5 RESEARCH RESULT AND ANALYSIS . Error! Bookmark not defined.

5.1 Specimens Preload ..... **Error! Bookmark not defined.**
5.1.1 Load and Beam Deflection ..... **Error! Bookmark not defined.**
5.1.2 Compression Strain and Reinforcement Strain **Error! Bookmark not defined.**
5.1.3 Crack Path of Beam ..... **Error! Bookmark not defined.**
5.1.4 Analysis of Concrete Deterioration due to Preload **Error! Bookmark not defined.**
5.2 Bonding Strength of Patch Materials ..... **Error! Bookmark not defined.**
5.2.1 Ordinary Cement Mortar ..... **Error! Bookmark not defined.**
5.2.2 Polymer Cement Mortar ..... **Error! Bookmark not defined.**
5.3 Post Repair Final Test ..... **Error! Bookmark not defined.**
5.3.1 Load and Beam Deflection ..... **Error! Bookmark not defined.**
5.3.2 Strain Observation of Concrete Compression **Error! Bookmark not defined.**
5.3.3 Strain Observation of Steel Reinforcement and Repair Rebar ..... **Error! Bookmark not defined.**
5.3.4 Crack Path of the Specimens ..... **Error! Bookmark not defined.**
5.3.5 Proposed Ultimate load Analysis Approach **Error! Bookmark not defined.**
5.3.6 Modelling of Loading Analysis using Iteration of Incremental Load **Error! Bookmark not defined.**
5.4 Analysis and Discussion ..... **Error! Bookmark not defined.**
5.4.1 The Move of Plastic Hinge ..... **Error! Bookmark not defined.**
5.4.2 Bondslip of Repair Rebar and Debonding of Patch Material ..... **Error! Bookmark not defined.**
5.4.3 Effect of Preloading Limit State to the Specimens Maximum Capacity **Error! Bookmark not defined.**

CHAPTER 6 CONCLUSION AND SUGGESTION ..... Error! Bookmark not defined.
6.1 Conclusion ..... **Error! Bookmark not defined.**
6.2 Suggestion ..... **Error! Bookmark not defined.**

BIBLIOGRAPHY ..... Error! Bookmark not defined.

APPENDIX ..... Error! Bookmark not defined.

TABLE OF FIGURES

Figure 1.1. Repeated repair on a bridge concrete pavement. (Keith K. , 2015) ..... **Error! Bookmark not defined.**
Figure 1.2 (a) Repaired reinforced concrete column using CFRP (b) Moment capacity along the column span after repaired using CFRP (Rudledge, et al., 2013) ..... **Error! Bookmark not defined.**
Figure 1.3. Repair type plot from 247 Repair Case histories of Europe Structure ..... **Error! Bookmark not defined.**
Figure 1.4. Damage mechanism on patch repair system ..... **Error! Bookmark not defined.**
Figure 1.5. Failure of patch and strengthening Repair Practice of Namira Mosque Wall ..... **Error! Bookmark not defined.**
Figure 1.6 Stitching Method for Crack Structure (ACI-Committee-224, 1998) ..... **Error! Bookmark not defined.**
Figure 2.1. General reinforced concrete restraining force composition ... **Error! Bookmark not defined.**
Figure 2.2. Reinforced Concrete Stress-strain under rectangular stirrups confinement ..... **Error! Bookmark not defined.**
Figure 2.3. Beam Stress Trajectory subjected to Uniform Load ..... **Error! Bookmark not defined.**
Figure 2.4. Key Points of Cyclic Response (Otter & Naaman, 1989) **Error! Bookmark not defined.**
Figure 2.5. Stress-Strain curve for Reloading Branch ..... **Error! Bookmark not defined.**
Figure 2.6. Comparison of experimental data reported by Aslani and Jowkarmeimandi (2012) ..... **Error! Bookmark not defined.**
Figure 2.7. Stress-strain curve of steel rebar under repeated loading **Error! Bookmark not defined.**
Figure 2.8. (a) Steel reinforcement embedded in concrete (b) Stress distribution (c) Strain distribution (d) bond stress between steel and concrete **Error! Bookmark not defined.**
Figure 2.9. (a) Hooked reinforcement in concrete (b) Stress Distribution along the length (c) Strain distribution (Alsiwat & Saatcioglu, 1992) ..... **Error! Bookmark not defined.**
Figure 2.10. Shear restraining mechanism on reinforced concrete beam. **Error! Bookmark not defined.**
Figure 2.11. Corroded Strengthening Beam Tested by Rio, et al. 2005... **Error! Bookmark not defined.**
Figure 2.12. Testing result of repaired beam specimens performed by Rio, et al. 2005 ..... **Error! Bookmark not defined.**
Figure 2.13. Strengthening Detail applied by Satoh and Kodama 2005 .. **Error! Bookmark not defined.**

Figure 2.14. (a) Several failure mode recorded (b) Central peeling failure picture (Satoh & Kodama, 2005) ..... **Error! Bookmark not defined.**
Figure 2.15. Shear Stress Distribution Scheme Proposed by Satoh and Kodama (2005) ..... **Error! Bookmark not defined.**
Figure 2.16. (a) Steel Plating Application (b) End Side Collar of the Specimens (Aykac, et al., 2013) ..... **Error! Bookmark not defined.**
Figure 2.17. Shear Peeling between the plate and concrete substrate **Error! Bookmark not defined.**
Figure 2.18. Pull out test model used (Lin & Wu, 2016) .... **Error! Bookmark not defined.**
Figure 2.19. Testing result of one of the specimens ..... **Error! Bookmark not defined.**
Figure 2.20. (a) Steel reinforcement deterioration and concrete cover spalling (b) column repair using CFRP (Rudledge, et al., 2013) ..... **Error! Bookmark not defined.**
Figure 2.21. (a) Hysteretic load-displacement curve (b) load test of repaired column **Error! Bookmark not defined.**
Figure 2.22. Scheme of nominal moment region of repaired column along its length **Error! Bookmark not defined.**
Figure 3.1. Repair concept of repair the deteriorate area by repair rebar and mortar patch ..... **Error! Bookmark not defined.**
Figure 3.2. Conceptual Framework of the research..... **Error! Bookmark not defined.**
Figure 4.1. Research Flowchart ..... **Error! Bookmark not defined.**
Figure 4.2. Beam Specimens Dimension and Cross Section **Error! Bookmark not defined.**
Figure 4.3. Moment Curvature of Analyzed Specimens with point to stop preloading ..... **Error! Bookmark not defined.**
Figure 4.4. Beam Specimen Preloading Setup ..... **Error! Bookmark not defined.**
Figure 4.5. Preload Test Setup on Laboratory Structural Testing Frame. **Error! Bookmark not defined.**
Figure 4.6. Preparation of steel reinforcement cage of strain gauge instalation ..... **Error! Bookmark not defined.**
Figure 4.7. Bond strength in flexure specimens preparation **Error! Bookmark not defined.**
Figure 4.8. Bond strength in flexure (a) specimens detail (b) testing setup ..... **Error! Bookmark not defined.**
Figure 4.9. (a) Surface preparation for direct shear specimens (b) oiured patch material to the cast ..... **Error! Bookmark not defined.**
Figure 4.10. (a) Direct Shear Test, (b) conducted direct shear on compression test apparatus ..... **Error! Bookmark not defined.**
Figure 4.11. ASTM C78 specimen specification ..... **Error! Bookmark not defined.**
Figure 4.12. General Repairing scheme ..... **Error! Bookmark not defined.**
Figure 4.13. Specimens Repaired Cross Section ..... **Error! Bookmark not defined.**
Figure 4.14. Detailed repair scheme as tabulated in Table 4.8..... **Error! Bookmark not defined.**
Figure 4.15. Preparation of substrateed concrete for patch material application ..... **Error! Bookmark not defined.**
Figure 4.16. Strain data is prior measured to make sure the strain gauge performing well before patch application..... **Error! Bookmark not defined.**

Figure 4.17. (a) Patch material pouring and casting (b) curing using plastic sheet and watering ..... **Error! Bookmark not defined.**
Figure 4.18. All beam specimens detail ..... **Error! Bookmark not defined.**
Figure 4.19. Reload (Final Test) setup ..... **Error! Bookmark not defined.**
Figure 4.20. Repaired Beam Final Loading Scheme..... **Error! Bookmark not defined.**
Figure 5.1. Load and Deflection of Control Beam..... **Error! Bookmark not defined.**
Figure 5.2. Load-Deflection graph of (a) S-4 Yield-1 (b) S-4 Yield-2 (c) S-7 Yield-1 (d) S-7 Yield-2 ..... **Error! Bookmark not defined.**
Figure 5.3. Load deflection graphs of (a) ST-4 Yield-OCM (b) ST-4 Yield-PCM (c) ST-7 Yield-OCM (d) ST-7 Yield-PCM..... **Error! Bookmark not defined.**
Figure 5.4. Load-deflection graphs of (a) S-4 Ultimate-1 (b) S-4 Ultimate-2 (c) S-7 Ultimate-1(d) S-7 Ultimate-2 ..... **Error! Bookmark not defined.**
Figure 5.5. Compression Strain of Control Beam ..... **Error! Bookmark not defined.**
Figure 5.6. Load-Compression strain graph of (a) S-4 Ultimate-1 (b) S-4 Ultimate-2 (c) S-7 Ultimate-1 (d) S-7 Ultimate-2 ..... **Error! Bookmark not defined.**
Figure 5.7. Load-compression strain graphs of (a) S-4 Yield-1 (b) S-4 Yield-2 (c) S-7 Yield-1 (d) S-7 Yield-2..... **Error! Bookmark not defined.**
Figure 5.8. Load-Tension Strain graph of (a) Control Beam (b) S-4 Ultimate-1..... **Error! Bookmark not defined.**
Figure 5.9. Crack Path of S-4 Ultimate-1 during Preload ... **Error! Bookmark not defined.**
Figure 5.10. Crack width developent during preload of S4 Ultimate-1 **Error! Bookmark not defined.**
Figure 5.11. Control Beam Preload crack path ..... **Error! Bookmark not defined.**
Figure 5.12. S7 Ultimate-1 Beam Preload Crack Path..... **Error! Bookmark not defined.**
Figure 5.13. S7 Ultimate-2 Preload Crack Path ..... **Error! Bookmark not defined.**
Figure 5.14. S7 Yield-1 Preload Crack Path ..... **Error! Bookmark not defined.**
Figure 5.15. S7 Yield -2 Preload Crack Path ..... **Error! Bookmark not defined.**
Figure 5.16. Horizontal crack propagation at the top of control beam section ..... **Error! Bookmark not defined.**
Figure 5.17. Modeled stress-strain diagram of the beam specimens.. **Error! Bookmark not defined.**
Figure 5.18. Stress-Strain Curve with plastic strain of (a) S-4 Ultimate-1 (b) S-4 Ultimate-2 (c) S-7 Ultimate-2 ..... **Error! Bookmark not defined.**
Figure 5.19. Stress-Strain curve with plastic strain of (a) S-4 Yield-1 (b) S-4 Yield-2 (c) S-7 Yield-2 ..... **Error! Bookmark not defined.**
Figure 5.20. Stress-Strain curves of concrete preloaded, unloaded and reloaded in the particular increment of strain..... **Error! Bookmark not defined.**
Figure 5.21. f_{new} line correspond to each unloading and reloading process produced using Equation 15..... **Error! Bookmark not defined.**
Figure 5.22. Scheme of development of strain and stress block during preloading, unloading, and reloading ..... **Error! Bookmark not defined.**
Figure 5.23. Concrete stress block derived from repeated loading unloading mode ... **Error! Bookmark not defined.**
Figure 5.24. Flexure tensile strength test of ASTM C-78 ... **Error! Bookmark not defined.**

Figure 5.25. Visual patch repair and substrate interfacial after given load test (a) DS-OCM 1 (b) DS-OCM 2 (c) DS OCM 3 ..... **Error! Bookmark not defined.**
Figure 5.26. Bond strength on flexure test of OCM patch material ... **Error! Bookmark not defined.**
Figure 5.27. Photo of interfacial face of OCM patch material of (a) FB-OCM 1 (b) FB-OCM 2 (c) FB-OCM ..... **Error! Bookmark not defined.**
Figure 5.28. Visual of direct shear interfacial face of (a) DS-PCM 1 (b) DS-PCM2 (c) DS-PCM 3..... **Error! Bookmark not defined.**
Figure 5.29. Visual of interfacial face of PCM bond strength in flexure of (a) FB-PCM 1 (b) FB-PCM 2 (c) FB-PCM 3..... **Error! Bookmark not defined.**
Figure 5.30. Reloading Load-Deflection curve of S-4 Ultimate-1..... **Error! Bookmark not defined.**
Figure 5.31. Reloading Load-Deflection curve of S-4 Ultimate-2..... **Error! Bookmark not defined.**
Figure 5.32. Reloading Load-Deflection curve of S-4 Yield-1..... **Error! Bookmark not defined.**
Figure 5.33. Reloading Load-Deflection curve of S-4 Yield-2..... **Error! Bookmark not defined.**
Figure 5.34. Reloading Load-Deflection curve of S7 Ultimate-1 ..... **Error! Bookmark not defined.**
Figure 5.35. Reloading Load-Deflection curve of S7 Ultimate-2 ..... **Error! Bookmark not defined.**
Figure 5.36. Reloading Load-Deflection curve of S7 Yield 1..... **Error! Bookmark not defined.**
Figure 5.37. Reloading Load-Deflection curve of S7 Yield 2..... **Error! Bookmark not defined.**
Figure 5.38. Reloading Load-Deflection curve of ST-4 Yield OCM. **Error! Bookmark not defined.**
Figure 5.39. Reloading Load-Deflection curve of ST-7 Yield OCM. **Error! Bookmark not defined.**
Figure 5.40. Reloading Load-Deflection curve of ST-4 Yield PCM . **Error! Bookmark not defined.**
Figure 5.41. Reloading Load-Deflection curve of ST-7 Yield PCM . **Error! Bookmark not defined.**
Figure 5.42. (a) Concrete concrete compression load-strain curve of S4 Ultimate-1 (b) crack propagation..... **Error! Bookmark not defined.**
Figure 5.43. Concrete concrete compression load-strain curve of S4 Ultimate-2..... **Error! Bookmark not defined.**
Figure 5.44. Concrete concrete compression load-strain curve of S7 Ultimate-2..... **Error! Bookmark not defined.**
Figure 5.45. Concrete concrete compression load-strain curve of S4 Yield -2..... **Error! Bookmark not defined.**
Figure 5.46. Concrete concrete compression load-strain curve of S7 Yield -2..... **Error! Bookmark not defined.**

Figure 5.47. Crack visual of S4-Ultimate-2, S4 Yield-1, S4 Yield-2 on their load of intersection point ..... **Error! Bookmark not defined.**
Figure 5.48. Tension reinforcement strain of S4 Ultimate-2 **Error! Bookmark not defined.**
Figure 5.49. Tension reinforcement strain of S4 Yield-1 .... **Error! Bookmark not defined.**
Figure 5.50. Tension reinforcement strain of S4 Yield-2 .... **Error! Bookmark not defined.**
Figure 5.51. Tension reinforcement strain of S7 Ultimate-1 **Error! Bookmark not defined.**
Figure 5.52. Tension reinforcement strain of S7 Yield 1 .... **Error! Bookmark not defined.**
Figure 5.53. Tension reinforcement strain of ST4-Yield OCM ..... **Error! Bookmark not defined.**
Figure 5.54. Tension reinforcement strain of ST4-Yield PCM ..... **Error! Bookmark not defined.**
Figure 5.55. Tension reinforcement strain of ST7-Yield OCM ..... **Error! Bookmark not defined.**
Figure 5.56. Tension reinforcement strain of ST7-Yield PCM ..... **Error! Bookmark not defined.**
Figure 5.57. Crack patch development during reload of specimens S4 Ultimate-1 ..... **Error! Bookmark not defined.**
Figure 5.58. Proposed force and stress scheme of beam reinforced with Staple shape rebar ..... **Error! Bookmark not defined.**
Figure 5.59. Crack width of defletion increment correspondence to Figure 5.57 ..... **Error! Bookmark not defined.**
Figure 5.60. Crack path of S4 Ultimate-1 ..... **Error! Bookmark not defined.**
Figure 5.61. Repair system failure of the S4 Ultimate-1 (a) develop plastic hinnge (b) extracted anchor legs ..... **Error! Bookmark not defined.**
Figure 5.62. Crack path of S7 Yield-1 Specimens ..... **Error! Bookmark not defined.**
Figure 5.63. Crack width with deflection increment of S7 Yield-1 ... **Error! Bookmark not defined.**
Figure 5.64. Crack path of S7 Ultimate-1 ..... **Error! Bookmark not defined.**
Figure 5.65. Crack path of S4 Yield-1 ..... **Error! Bookmark not defined.**
Figure 5.66. Crack opening width of ST4 Yield PCM ..... **Error! Bookmark not defined.**
Figure 5.67. Crack path of ST4 Yield PCM ..... **Error! Bookmark not defined.**
Figure 5.68. Crack path of ST7 Yield PCM ..... **Error! Bookmark not defined.**
Figure 5.69. ST7 Yield OCM crack path ..... **Error! Bookmark not defined.**
Figure 5.70. Crack path of ST4 Yield OCM ..... **Error! Bookmark not defined.**
Figure 5.71. Stress Block on Reloading curve on increment of ε_{un} ... **Error! Bookmark not defined.**
Figure 5.72. Plot of for the constant maximum ε_c and f'c 34Mpa .... **Error! Bookmark not defined.**
Figure 5.73. Stress Block on reloading curve on increment of ε_c with ε_{un} 0.004 ..... **Error! Bookmark not defined.**
Figure 5.74. Plot of for the increment of ε_c with particular values of ε_{un} and f'c 34Mpa ..... **Error! Bookmark not defined.**
Figure 5.75. Plot of γ_{re} for every increments of reload ε_c, for 0.004 and 0.0038 ε_{un} .. **Error! Bookmark not defined.**

Figure 5.76. Scheme of Section Force for increment load analysis ...**Error! Bookmark not defined.**
Figure 5.77. Iteration table to finde balance C-T by changing kd (larger view in appendix) .....**Error! Bookmark not defined.**
Figure 5.78.Plotted resulted empirical load on load-deflection curve of 700mm staple shape repaired specimens .....**Error! Bookmark not defined.**
Figure 5.79. Plotted resulted empirical load on load-deflection curve of straight shape repaired specimens.....**Error! Bookmark not defined.**
Figure 5.80. Plastic hinge movement in preload to postrepaired load test of S4 Ultimate-1 .....**Error! Bookmark not defined.**
Figure 5.81. required ld to the specimens load.....**Error! Bookmark not defined.**
Figure 5.82. Horizontal crack development of ST4 Yield OCM occurs at 2200Kgs...**Error! Bookmark not defined.**
Figure 5.83. Possible shear failure mechanism which induced the plastic hinge development.....**Error! Bookmark not defined.**
Figure 5.84 Section moment capacity versus given moment by given load .....**Error! Bookmark not defined.**
Figure 5.85. Diagonal shear crack development of S7 Yield-2 specimens.....**Error! Bookmark not defined.**
Figure 5.86. Diagonal shear crack development of S7 Ultimate-2 specimens (no horizontal crack occurs).....**Error! Bookmark not defined.**
Figure 5.87. Diagonal shear crack development of ST7 Yield PCM.**Error! Bookmark not defined.**
Figure 5.88. Crack path of ST4 Yield PCM.....**Error! Bookmark not defined.**
Figure 5.89. Load deflection of ST4 Yield PCM with crack point ...**Error! Bookmark not defined.**
Figure 5.90. Load-tensile strain behavior correspond to crack point of ST4 Yield PCM .....**Error! Bookmark not defined.**
Figure 5.91. Inflection point of ST4 Yield OCM repair rebar strain before reach maximum load. .....**Error! Bookmark not defined.**
Figure 5.92. Horizontal crack development of ST4 Yield OCM .....**Error! Bookmark not defined.**
Figure 5.93. Repeated stress-strain behavior of steel reinforcement rebar**Error! Bookmark not defined.**
Figure 5.94. Falling point of load of S7 Yield-2 .....**Error! Bookmark not defined.**

TABLE OF TABLES

No. Table Titles Pages

Table 1.1. Comparison table of cement based mortars and polymer modified mortars (Lukovic, et al., 2012)..... **Error! Bookmark not defined.**

Table 4.1 Testing and Recording Equiments, and Tools..... **Error! Bookmark not defined.**

Table 4.2. Required Data of Control Beam Loading Test... **Error! Bookmark not defined.**

Table 4.3.Strain gauge uses for Preload and Reload Session..... **Error! Bookmark not defined.**

Table 4.4. Strain gauge uses (a) PFL-20 (b) FLA-6 (c) YFLA-5..... **Error! Bookmark not defined.**

Table 4.5. Used polymer cement mortar (a) Sikatop 122 (b) Mixing procedure ..... **Error! Bookmark not defined.**

Table 4.6. Material Testing Specification ..... **Error! Bookmark not defined.**

Table 4.7. Technical Datasheet of the PCM..... **Error! Bookmark not defined.**

Table 4.8. Beam Specimens Specification ..... **Error! Bookmark not defined.**

Table 5.1. Unloading strain, plastic strain, compression force and Elasticity of Post-Preload ..... **Error! Bookmark not defined.**

Table 5.2. Tensile strength of OCM patch material using ASTM C78 procedure..... **Error! Bookmark not defined.**

Table 5.3. Bond strength on shear frs of OCM interfaced with substrate concrete..... **Error! Bookmark not defined.**

Table 5.4. Flexural bond strength of OCM patch material.. **Error! Bookmark not defined.**

Table 5.5. Bond strength in shear of PCM patch material .. **Error! Bookmark not defined.**

Table 5.6. Bonding strength of PCM patch material..... **Error! Bookmark not defined.**

Table 5.7. Load and Deflection Summary of 400mm staple repaired specimens..... **Error! Bookmark not defined.**

Table 5.8. Load and Deflection Summary of 700mm staple repaired specimens..... **Error! Bookmark not defined.**

Table 5.9. Load and Deflection Summary of all staple repaired specimens ..... **Error! Bookmark not defined.**

Table 5.10. Iteration formula applied in excel according to Figure 5.74 . **Error! Bookmark not defined.**

Table 5.11. Results of Iteration parameters value which process stopped to particular stop value of f_{sr}..... **Error! Bookmark not defined.**

Table 5.12. Δd before falling point of maximum load..... **Error! Bookmark not defined.**

APPENDIX LIST

Appendix 1. Preliminary analysis of beam yield and ultimate strength...**Error! Bookmark not defined.**

Appendix 2. (a) Coarse aggregat mud washing (b) Fine aggregate mud wash (c) mold preparation for Direct shear and Flexural bond test.... **Error! Bookmark not defined.**

Appendix 3. (a) Table of FLA-6 series (b) Table of PFL-20 (TML Pam E-1007A Strain Gauge Catalogue)..... **Error! Bookmark not defined.**

Appendix 4. (a) Table of YFLA-5 strain gauge (b) influence of adhesive type on strain limit of YFLA-5..... **Error! Bookmark not defined.**

Appendix 5. Stress Block of Repeated loading with constant 0.004εc and increments of εun..... **Error! Bookmark not defined.**

Appendix 6. Stress block plot area and center of grafity of ε_c increments of 0.0038 ε_{un} **Error! Bookmark not defined.**

Appendix 7. Iteration table for Control empirical analysis **Error! Bookmark not defined.**

Appendix 8. Iteration table for Repaired Empirical Analysis..... **Error! Bookmark not defined.**

SYMBOL AND NOTATION

α	=	Concrete stress block area parameter
γ	=	Concrete stress block centroid parameter
α_{re}	=	Preloaded stress block area parameter
γ_{re}	=	Preloaded stress block centroid parameter
ε_a	=	Strain value of tangential intersection line with initial curve slope
ε_c	=	Concrete strain
ε_{cm}	=	Maximum concrete strain
ε_{cc}	=	Concrete strain at peak stress of confined concrete
ε_0	=	Concrete strain at peak stress (0.002)
ε_{pl}	=	Concrete plastic strain
ε_{ro}	=	Concrete residual strain when receiving partial unloading
ε_s	=	Steel reinforcement strain, usually used for bottom reinforcement
ε_{un}	=	Unloading strain
$\varepsilon_{s'}$	=	Top reinforcement strain of reinforced concrete beam
ε_{sr}	=	Repair rebar strain
λ	=	Modification factor of lightweight concrete
φ	=	Beam curvature
A_b	=	Area of rebar for length development calculation
A_s	=	Cross section area or rebar for bottom reinforcement
A_s'	=	Cross section area of rebar for top reinforcement
A_{sr}	=	Cross section area of repair rebar
b''	=	Width of confined concrete core measured to outside of stirrups
C_c	=	Resultant of compression force by concrete stress block
C_s	=	Resultant of compression force by top steel reinforcement
C	=	Total compression force of beam cross section
e	=	Exponential number
d	=	Distance from top fiber of beam to center of bottom steel reinforcement
d_b	=	Diameter of rebar for length development
d_r	=	Distance from top fiber of beam to center of repair rebar
d'	=	Distance from top fiber of beam to center of top steel reinforcement
E	=	Material elasticity
E_S	=	Elasticity value of steel reinforcement
E_r	=	Elasticity of concrete during reloading
E_c	=	Elasticity value of concrete
f_c	=	Concrete stress
f'_c'	=	28days concrete strength tested on cylindrical specimens
f'_{cc}'	=	Maximum concrete stress of confined concrete
f_s	=	Steel reinforcement stress, usually used for bottom rebar reinforcement
$f_{s'}$	=	Top steel reinforcement stress
f_{sr}	=	Repair rebar steel reinforcement stress
f_{new}	=	Concrete stress of reloaded concrete with the same strain of its unloading strain
f_{ro}	=	Concrete stress of partially unloaded concrete
f_r	=	Tensile strength of concrete (rupture modulus)
l_d	=	Required length development of steel reinforcement

Δl	=	Length of calculated steel reinforcement
K_u	=	Unloading constant
kd	=	Distance from top fiber of beam section to beam neutral axis
S_L	=	Clear distance between ribs of deformed rebar
H_L	=	Depth of ribs of deformed rebar
u	=	Bond strength between concrete and rebar in elastic region
u_f	=	Bond strength between concrete and rebar in yield and strain hardening region
T	=	Total tension force of beam cross section
T_s	=	tension force created by bottom reinforcement
T_{sr}	=	Tension force create by repair rebar
Z	=	Confinement parameters of concrete confined by stirrups or hoops

APPENDIX

Appendix 1. Preliminary analysis of beam yield and ultimate strength

Check of Beam Failure State

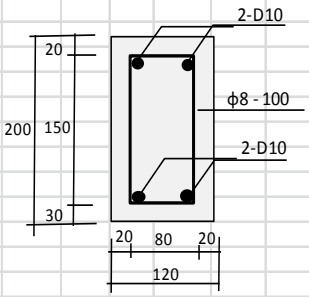

Base Specimens Data								
Top Reinf.Dia	=	10	mm	As	=	157	mm^2	
Top Reinf.Dia.	=	10	mm	As'	=	157	mm^2	
Stirrup Dia.	=	8	mm	ρ_s	=	0.019258667		
Stirrup Space	=	100	mm					
Conc.Cover Top	=	20	mm	fy	=	381	Mpa	
Conc.Cover Bot	=	30	mm	fc'	=	34	Mpa	
Conc.Cover Side	=	20	mm	Es	=	200000	Mpa	
Breadth (b)	=	120	mm	Ec	=	27405.47391	Mpa	
Heigth (h)	=	200	mm	ε_{cm}	=	0.004		
Depth (d)	=	170	mm	fr	=	3.499	Mpa	
Beam Span	=	1.8	m					

finding wheather the beam will fail in overreinforced or underreinforced

Schematic Diagram of Strain and Stress

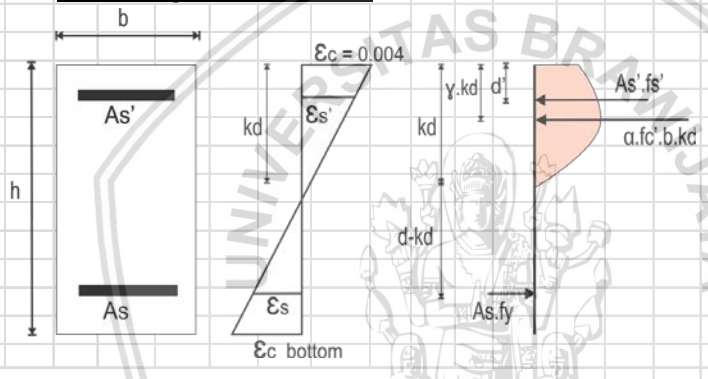

finding Z to determine the α and γ of stress function proposed by Kent and Park (1975).

from table Z of Park and Pauley (1975), we have α and γ as,

$$Z = \frac{0.5}{\frac{3+0{,}29\,fc'}{145fc'-1000} + \frac{3}{4}\rho_s\left(\frac{b''}{Sh}\right)^{1/2} - 0.002} = 35.2326777$$

ε_{cm} = 0.004
α = 0.8255
γ = 0.42775

$C = T$ with

$As'fs' + \alpha\, fc'\, b\, kd = As\, fy$ $\quad fs' = \frac{E.\varepsilon_{cm}.(kd-d')}{kd}$

$$kd = \frac{As.fy - As'.fs'}{\alpha\, fc'\, b}$$

$$kd = \frac{As.fy - \frac{As'.E.\varepsilon cm.(kd-d')}{kd}}{\alpha\, fc'\, b}$$

3368.04 kd^2 = -65783 kd + 2512000

0 = -3368.04 kd^2 -65783 kd + 2512000

kd_1 = -38.769296 mm
kd_2 = 19.2377588 mm
real kd = 19.2377588 mm

then,

$fs' = \frac{E.\varepsilon_{cm}.(kd-d')}{kd}$ $\quad f_S = \frac{E.\varepsilon_{cm}.(d-kd)}{kd}$

fs' = -31.697714 Mpa << fy = 381 Mpa = 6269.4306 Mpa > fy = 381 Mpa

underreinforced Ok!

Calculate Curvature and Ultimate moment of specimens

Mult = As'fs'(d-d')+ α f'c.b.kd (d-γkd)
= 9735237.926 Nmm
= 9.735237926 kNm

$\varphi = \frac{\varepsilon_{cm}}{kd}$
φ= 0.000208 rad/mm
φ= 0.20792 rad/m

Load Needed at Mid.Span
Mx = 9.735237926 kNm
9.735237926 = P/2 * 0.5 L (span)
P = 21.63386206 KN
P = 2.205286652 Ton

Calculate Curvature and Moment at first yield

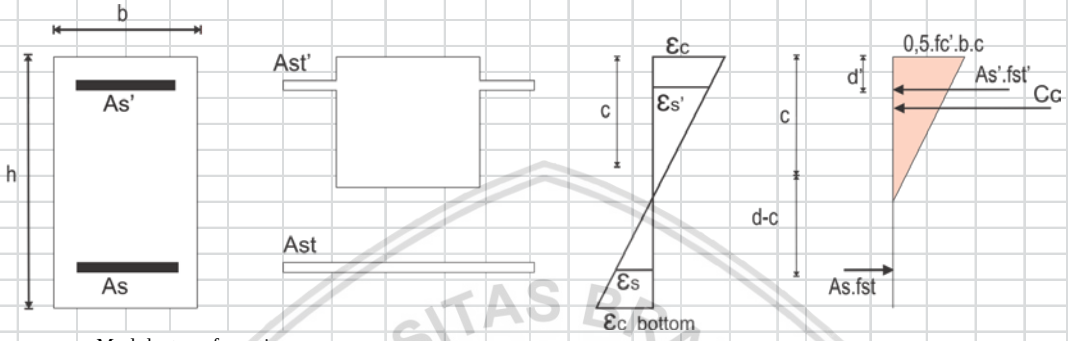

n Modular transformation

$n = \frac{E_{concrete}}{E_{steel}}$
n= 7.29781213

$k = \left((\rho + \rho')^2 n^2 + 2\rho + \left(\frac{\rho' d'}{d} \right) n \right)^{1/2} - (\rho + \rho') n$ with $p = \frac{As}{b.h}$
p= 0.0065417
p'= 0.0065417

k= 0.2448569
kd= 41.625669 mm

ε_s= 0.001905

$\varphi = \frac{\varepsilon_{cm}}{kd}$
$\varphi = \frac{fy/E}{(d-kd)}$
φ= 1.484E-05 rad/mm
φ= 0.0148394 rad/m

M= 0.5.f'c.kd.b.(d'-1/3kd)+As.fy.(d-d')
M= 8895652.034 Nmm
M= 8.895652 kNm

Calculate Curvature and Moment at first Crack (W/O Notch)

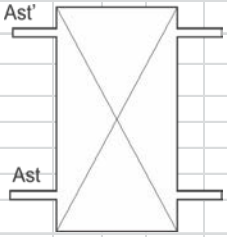

A Concrete = 24000 mm^2
As Steel Transf. = (n-1) As = 988.7565 mm^2
As' Steel Transf. = (n-1) As' = 988.7565 mm^2

$\bar{y} = \frac{\Sigma \bar{y}.A}{A}$ = 100.3806202 mm2

I_{total}= 91177874.84 mm^4

Moment at first Crack
$M = \frac{f.I}{y}$ = 3177827.361 Nmm
= 3.177827 kNm

$\varphi = \frac{\varepsilon_c}{kd}$
= 1.27176E-06 rad/mm
= 0.001271755 rad/m

Calculate Curvature and Moment at first Crack (With Notch)

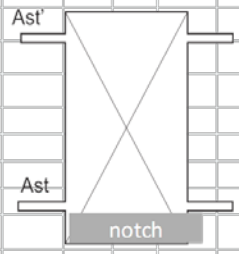

A Concrete = 20400 mm^2

As Steel Transf. = (n-1) As = 988.7565 mm^2

As' Steel Transf. = (n-1) As' = 988.7565 mm^2

$\bar{y} = \frac{\Sigma \bar{y}.A}{A}$ = 84.33722092 mm2

I_{total} = 60434878.8 mm^4

$\varphi = \frac{\varepsilon_c}{kd}$ = 1.51368E-06 rad/mm = 0.00151368 rad/m

Moment at first Crack

$M = \frac{f.I}{y}$ = 2507027.388 Nmm = 2.507027 kNm

Moment (kNm)	Curvature (rad/m)	Load Kg	
0	0	0	
2.507	0.002	0.567907439	first Crack
8.896	0.015	2.015098433	First Yield
9.735	0.208	2.205286652	Ultimate

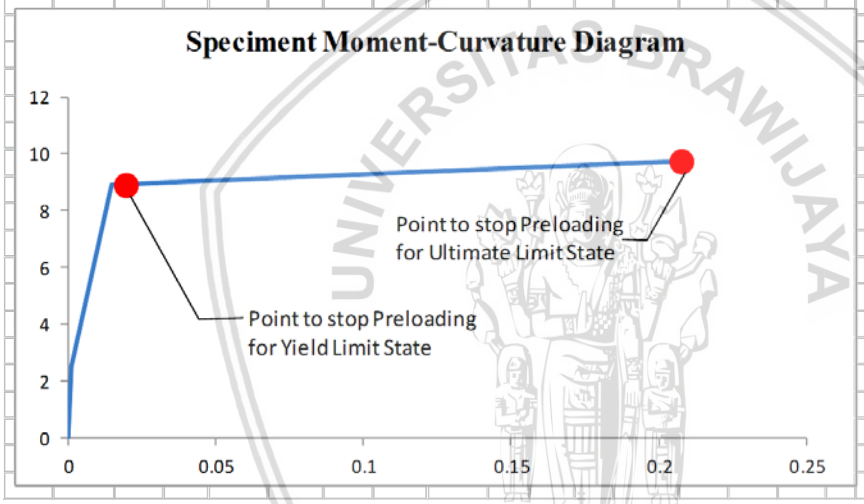

Appendix 2. (a) Coarse aggregat mud washing (b) Fine aggregate mud wash (c) mold preparation for Direct shear and Flexural bond test

(a)

(b)

(c)

Appendix 3. (a) Table of FLA-6 series (b) Table of PFL-20 (TML Pam E-1007A Strain Gauge Catalogue)

FOIL STRAIN GAUGES series F

Operating temperature range –20°C ~ +80°C

Temperature compensation range +10°C ~ +80°C

Suffix code for temperature compensation materials
-11: Mild steel (ferritic) -17: Stainless steel -23: Aluminium

For ordering, the above suffix code should be specified after basic gauge type.

Applicable adhesives

CN	–20 ~ +80°C
P-2	–20 ~ +80°C
EB-2	–20 ~ +80°C

GENERAL USE

These gauges employ Cu-Ni alloy foils for the grid and epoxy resin for the backing. The epoxy resin backing exhibits excellent electrical insulation performance, and is color-coded to identify the objective material for self-temperature-compensation. Various types of strain gauges such as for residual stress measuremenent and are available in addition to general use gauges.

Single element : FLG/FLA/FLK

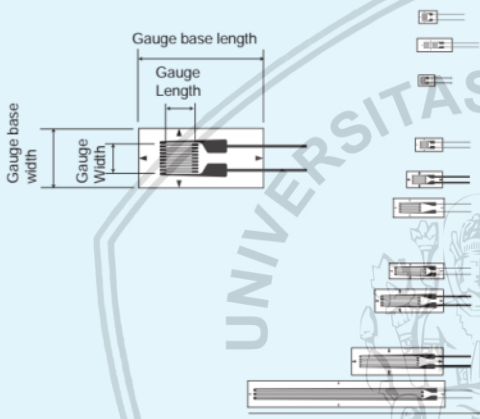

M metal G general

L : length W : width (Unit:mm)

Each package contains 10 gauges.

Basic type	Gauge size L	Gauge size W	Backing L	Backing W	Resistance Ω
FLG-02	0.2	1.4	3.5	2.5	120
FLG-1	1	1.1	6.5	2.5	120
FLA-03	0.3	1.4	3.0	2.0	120
FLA-05	0.5	1.2	5.0	2.2	120
FLA-1	1	1.3	5.0	2.5	120
FLA-2	2	1.5	6.5	3.0	120
FLA-3	3	1.7	8.8	3.5	120
FLA-3-60	3	1.2	8.0	3.0	60
FLA-5	5	1.5	10.0	3.0	120
FLA-6	6	2.2	12.5	4.3	120
FLA-6-1000	6	4.6	13.5	7.0	1000
FLA-10	10	2.5	16.7	5.0	120
FLA-30	30	2.0	36.1	5.1	120

(a)

POLYESTER STRAIN GAUGES series P/PF

Operating temperature range –20°C ~ +80°C

Temperature compensation range +10°C ~ +80°C

C concrete M mortar R rock

Applicable adhesives

CN-E	–20 ~ +80°C
RP-2	–20 ~ +80°C
PS	–20 ~ +80°C

STEEL, CONCRETE, MORTAR MATERIAL USE

series P

These are wire strain gauges utilizing a transparent plastic backing impregnated with polyester resin. The gauge length is available in 3 ranges of 60, 90 and 120mm, so it is suited to the measurement of concrete strain. Since the backing is transparent, the bonding position can easily be checked in the installation works.

Single element

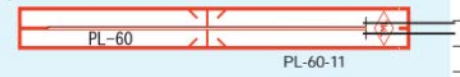

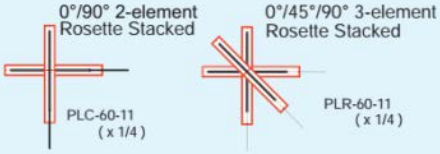

L : length W : width (Unit:mm)

Single-element Each package contains 10 gauges.

Basic type	Gauge size L	Gauge size W	Backing L	Backing W	Resistance Ω
PL-60-11	60	1	74	8	120
PL-90-11	90	1	104	8	120
PL-120-11	120	1	134	8	120

Each package contains 10 gauges.

0°/90° 2-element Rosette Stacked

PLC-60-11	60	1	74	74	120

0°/45°/90° 3-element Rosette Stacked

PLR-60-11	60	1	74	74	120

(b)

Appendix 4. (a) Table of YFLA-5 strain gauge (b) influence of adhesive type on strain limit of YFLA-5

series **YF**

These gauges are applicable to the measurement of large strain up to 15 to 20%. These are not applicable to the measurement of repeated strain in elastic range as well as in large range.

Single element

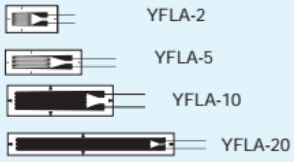

Operating temperature range

–20°C +80°C

Applicable adhesives	CN: –20 ~ +80°C; CN-Y: –20 ~ +80°C
Strain limit in room-temperature	15 ~ 20%

Each package contains 10 gauges.

YFLA-2	2	1.8	7.5	4.0	120
YFLA-5	5	1.9	12.0	4.0	120
YFLA-10	10	2.6	16.6	4.9	120
YFLA-20	20	1.8	26.0	3.7	120

(a)

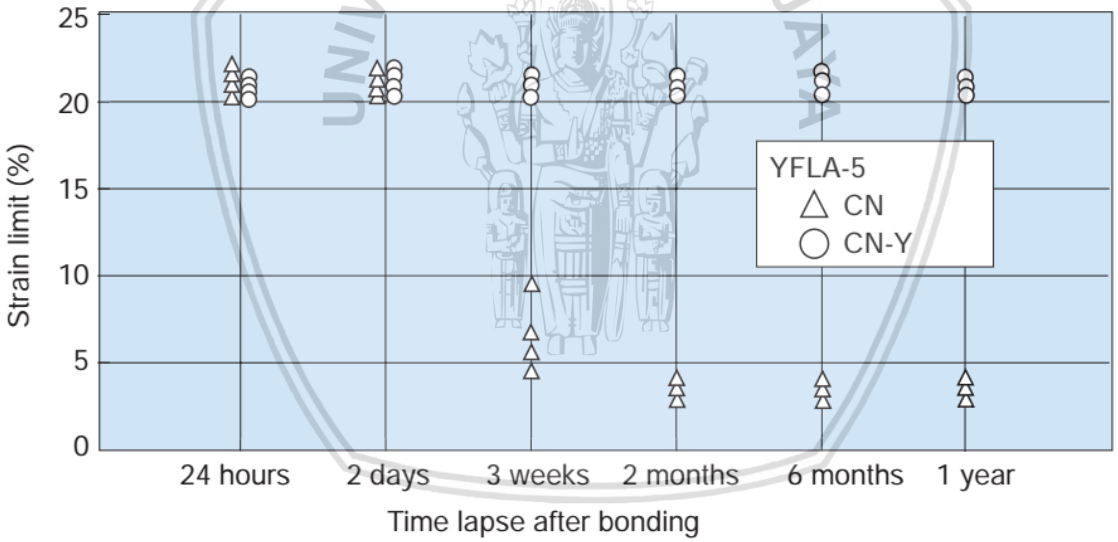

(b)

Appendix 5. Stress Block of Repeated loading with constant 0.004εc and increments of εun

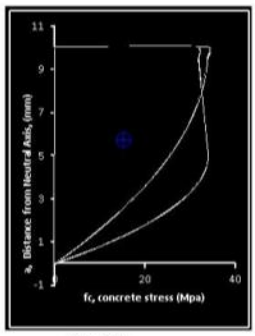

εun = 0.002
Preload Area = 1989.18
Reload Area = 2403.08
Reload CoG
CoG Y = 27.55

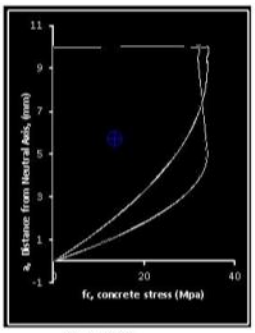

εun = 0.0022
Preload Area = 2045.12
Reload Area = 2393.06
Reload CoG
CoG Y = 27.43

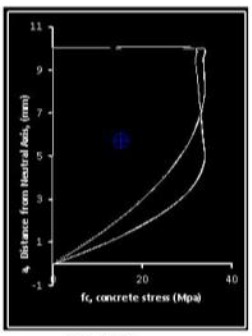

εun = 0.0024
Preload Area = 2095.30
Reload Area = 2396.68
Reload CoG
CoG Y = 27.56

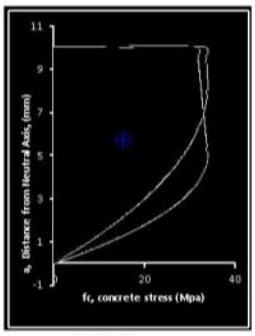

εun = 0.0026
Preload Area = 2128.11
Reload Area = 2406.87
Reload CoG
CoG Y = 27.63

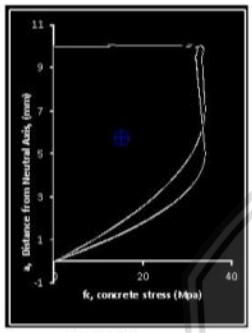

εun = 0.0028
Preload Area = 2187.53
Reload Area = 2382.39
Reload CoG
CoG Y = 27.43

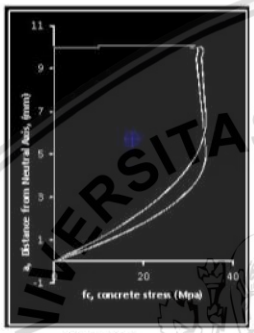

εun = 0.0030
Preload Area = 2231.43
Reload Area = 2385.94
Reload CoG
CoG Y = 27.35

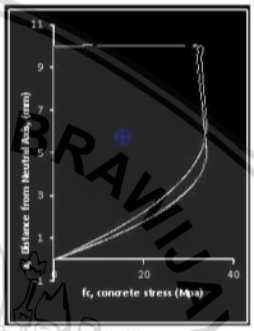

εun = 0.0032
Preload Area = 2268.9
Reload Area = 2391.85
Reload CoG
CoG Y = 27.28

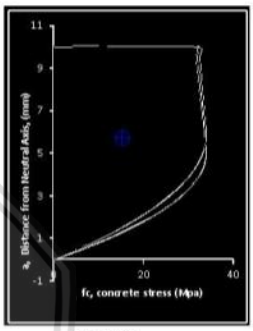

εun = 0.0034
Preload Area = 2294.17
Reload Area = 2396.66
Reload CoG
CoG Y = 27.23

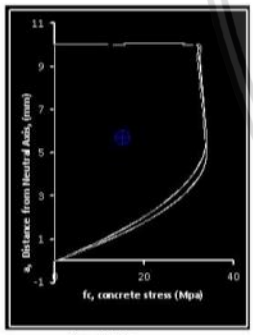

εun = 0.0035
Preload Area = 2332.4
Reload Area = 2382.95
Reload CoG
CoG Y = 27.61

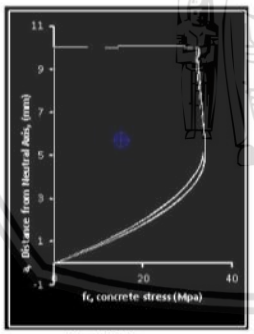

εun = 0.0036
Preload Area = 2320.67
Reload Area = 2390
Reload CoG
CoG Y = 27.51

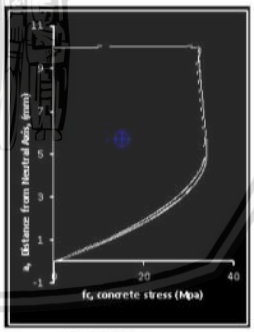

εun = 0.0037
Preload Area = 2339.91
Reload Area = 2397.55
Reload CoG
CoG Y = 27.40

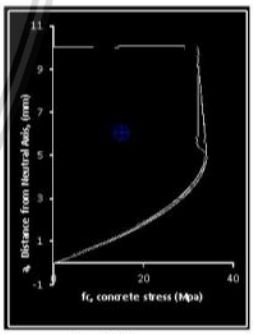

εun = 0.0038
Preload Area = 2359.26
Reload Area = 2351.51
Reload CoG
CoG Y = 27.56

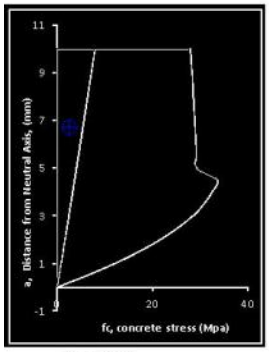

εun = 0.00025
Increment Stress Block Area = 354.53
Block CoG Y = 22.31

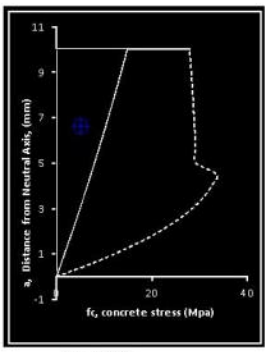

εun = 0.0005
Increment Stress Block Area = 659.4
Block CoG Y = 21.67

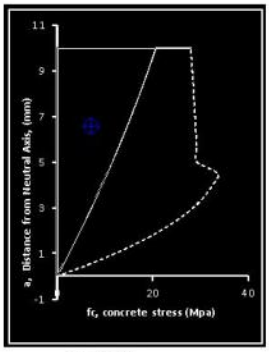

εun = 0.00075
Increment Stress Block Area = 954.8
Block CoG Y = 22.08

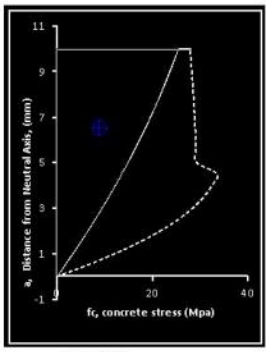

εun = 0.001
Increment Stress Block Area = 1203.94
Block CoG Y = 22.39

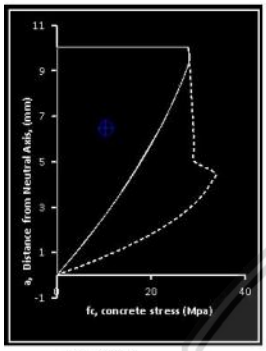

εun = 0.00125
Increment Stress Block Area = 1409.98
Block CoG Y = 22.67

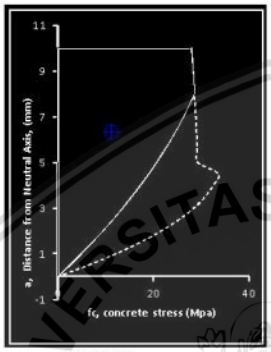

εun = 0.0015
Increment Stress Block Area = 1606.02
Block CoG Y = 23.53

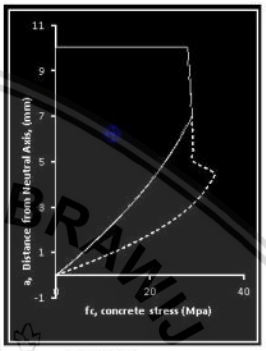

εun = 0.00175
Increment Stress Block Area = 1686.57
Block CoG Y = 24.15

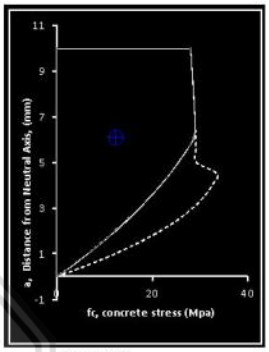

εun = 0.002
Increment Stress Block Area = 1801.47
Block CoG Y = 25.05

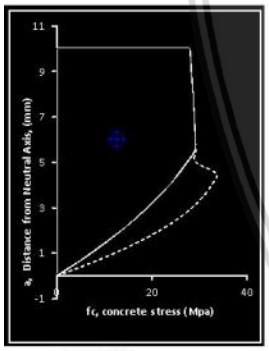

εun = 0.00225
Increment Stress Block Area = 1868.56
Block CoG Y = 25.49

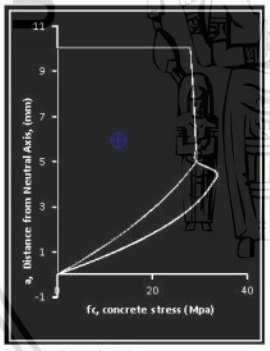

εun = 0.0025
Increment Stress Block Area = 1923.74
Block CoG Y = 25.95

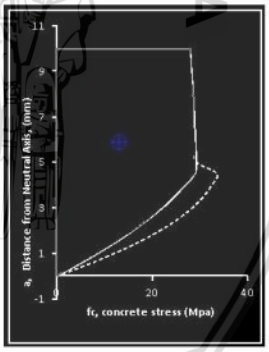

εun = 0.00275
Increment Stress Block Area = 1984.95
Block CoG Y = 26.6

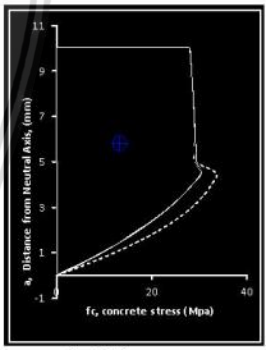

εun = 0.003
Increment Stress Block Area = 2021.98
Block CoG Y = 26.92

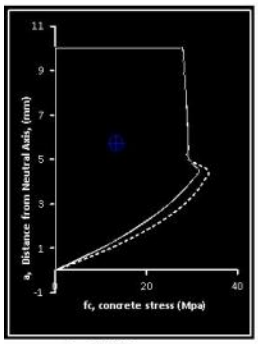

εun = 0.00325
Increment Stress Block Area = 2039.48
Block CoG Y = 27.38

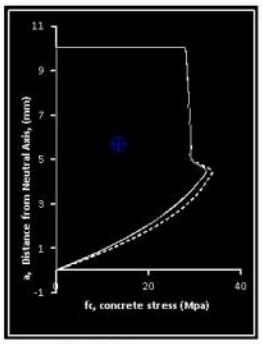

εun = 0.0035
Increment Stress Block Area = 2098.95
Block CoG Y = 27.71

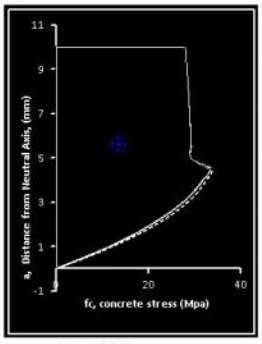

εun = 0.00375
Increment Stress Block Area = 2127.2
Block CoG Y = 27.95

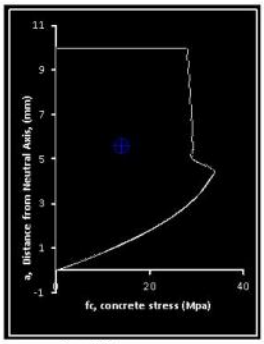

εun = 0.004
Increment Stress Block Area = 2195.43
Block CoG Y = 28.41

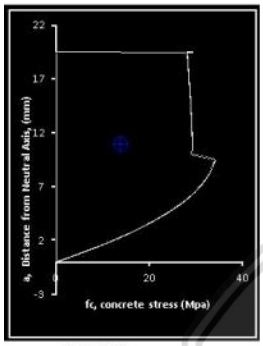

εun = 0.0041
Increment Stress Block Area = 2061.48
Block CoG Y = 26.53

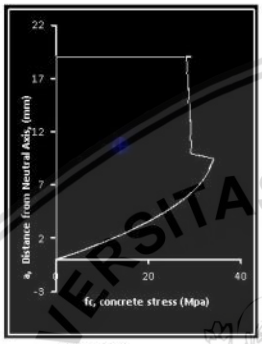

εun = 0.0042
Increment Stress Block Area = 1998.20
Block CoG Y = 25.58

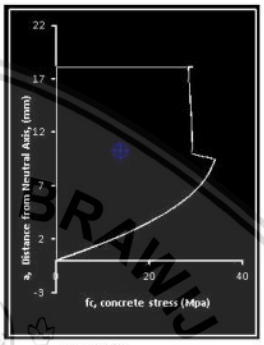

εun = 0.0044
Increment Stress Block Area = 1882
Block CoG Y = 24.25

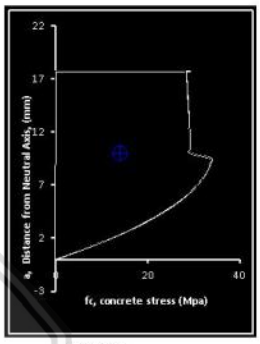

εun = 0.0045
Increment Stress Block Area = 1795
Block CoG Y = 23.47

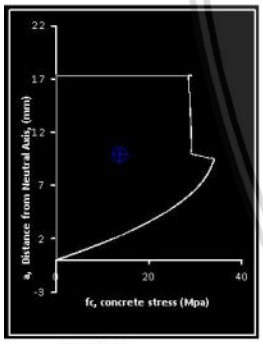

εun = 0.0046
Increment Stress Block Area = 1760
Block CoG Y = 22.92

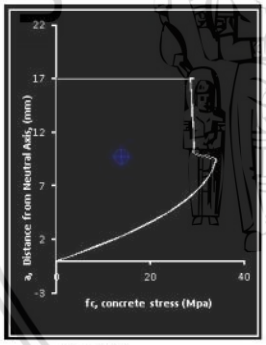

εun = 0.0047
Increment Stress Block Area = 1765
Block CoG Y = 22.54

Appendix 6.Stress block plot area and center of grafity of ε_c increments of 0.0038 ε_{un}

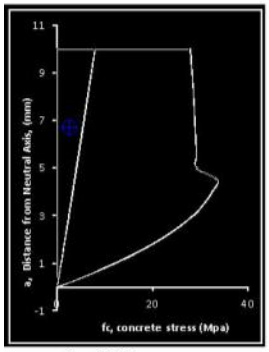

εun = 0.00025
Increment Stress Block Area = 354.53
Block CoG Y = 22.31

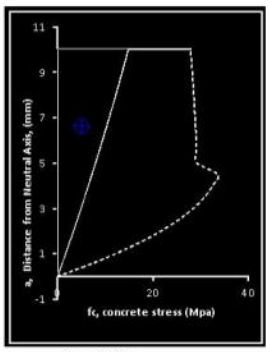

εun = 0.0005
Increment Stress Block Area = 689.4
Block CoG Y = 21.67

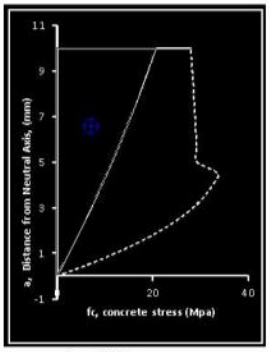

εun = 0.00075
Increment Stress Block Area = 954.8
Block CoG Y = 22.08

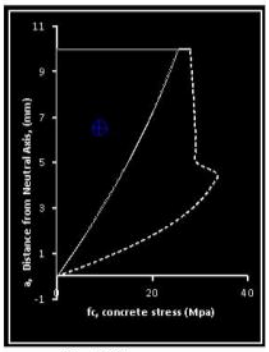

εun = 0.001
Increment Stress Block Area = 1203.94
Block CoG Y = 22.39

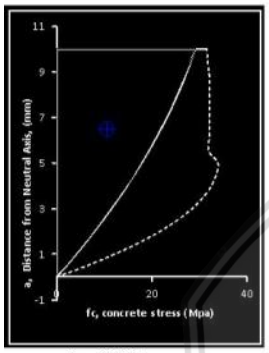

εun = 0.000125
Increment Stress Block Area = 1430
Block CoG Y = 22.73

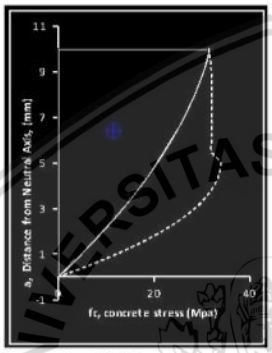

εun = 0.00015
Increment Stress Block Area = 1640
Block CoG Y = 23.14

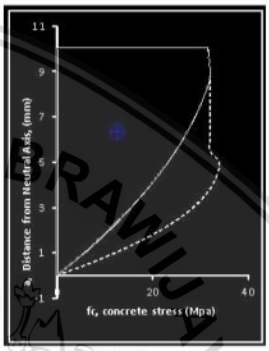

εun = 0.000175
Increment Stress Block Area = 1786
Block CoG Y = 23.55

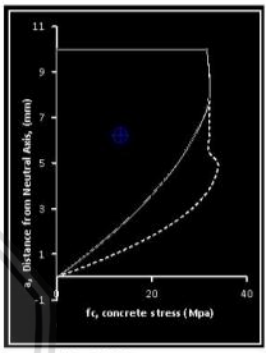

εun = 0.0002
Increment Stress Block Area = 1901.7
Block CoG Y = 24.31

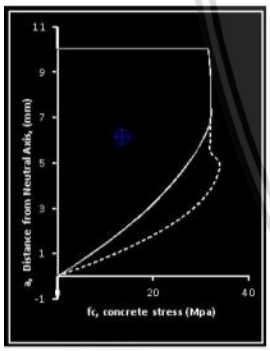

εun = 0.000225
Increment Stress Block Area = 1997.36
Block CoG Y = 24.74

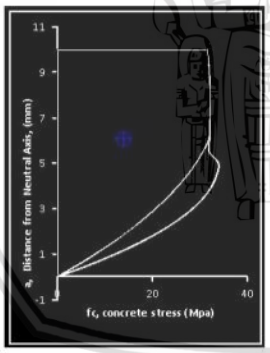

εun = 0.00025
Increment Stress Block Area = 2063
Block CoG Y = 25.34

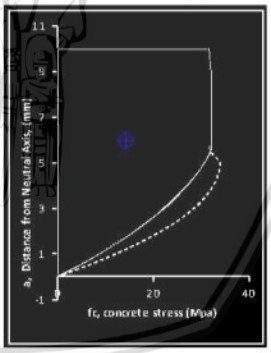

εun = 0.000275
Increment Stress Block Area = 2146.98
Block CoG Y = 25.88

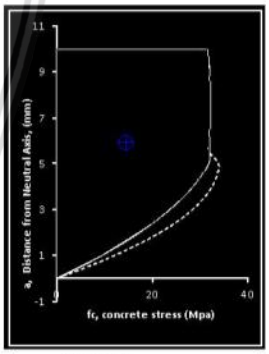

εun = 0.0003
Increment Stress Block Area = 2192.67
Block CoG Y = 26.41

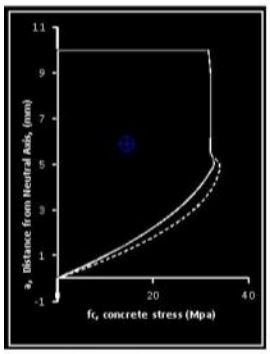

εun = 0.00325
Increment Stress Block Area = 2239
Block CoG Y = 26.70

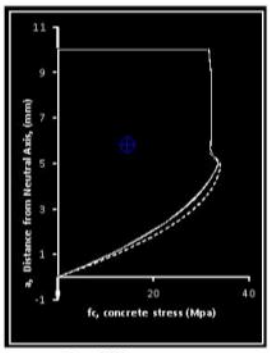

εun = 0.0035
Increment Stress Block Area = 2271.43
Block CoG Y = 26.95

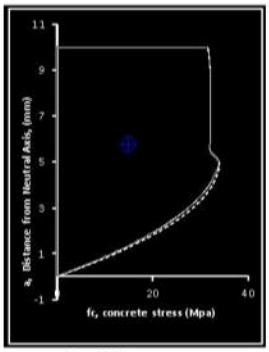

εun = 0.00375
Increment Stress Block Area = 2318.81
Block CoG Y = 27.41

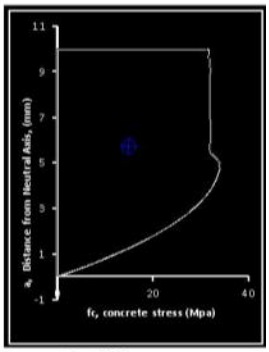

εun = 0.004
Increment Stress Block Area = 2346.98
Block CoG Y = 27.59

Appendix 7. Iteration table for Control empirical analysis

kd	$\varepsilon_{c\ Increment}$	εs	fs	εsr	fsr	Ld	εs'	fs'	α_{re}	γ_{re}	C	T	C-T	M (KNm)	Load (KN	ϕ
-1.8E-15	0	0	0			0	0	0	-0.01	0.34	7.97229E-14	0	7.97E-14	-9.3E-35	-2.1E-34	0
47.85568	0.00004	0.000102	20.41877685			0	2.328E-05	4.656614488	0.01	0.34	2233.38022	2233.38	2.93E-05	0.441942	0.982094	8.36E-07
43.09149	0.000065	0.000191	38.28622904			0	3.483E-05	6.966325995	0.03	0.34	4437.795361	4437.795	-2.3E-06	0.836879	1.859732	1.51E-06
41.48509	0.00009	0.000279	55.76144595			0	4.661E-05	9.32218283	0.04	0.34	6580.095283	6580.095	-5.9E-06	1.223177	2.718172	2.17E-06
40.70682	0.000115	0.000365	73.05269466			0	5.85E-05	11.69968298	0.05	0.34	8693.261608	8693.262	-2.7E-07	1.60531	3.567356	2.83E-06
40.26828	0.00014	0.000451	90.20718114			0	7.047E-05	14.09327281	0.07	0.34	10784.77091	10784.77	0.000955	1.9843	4.409556	3.48E-06
40.00235	0.000165	0.000536	107.2417682			0	8.25E-05	16.50096845	0.08	0.34	12857.29103	12857.29	0.00027	2.360511	5.24558	4.12E-06
39.8362	0.00019	0.000621	124.1640723			0	9.461E-05	18.92187384	0.09	0.34	14912.0303	14912.03	8.66E-05	2.734105	6.075788	4.77E-06
39.73298	0.000215	0.000705	140.9781246			0	0.0001068	21.35551475	0.10	0.34	16949.62668	16949.63	3E-05	3.105163	6.900363	5.41E-06
39.67206	0.00024	0.000788	157.6863146			0	0.000119	23.80161005	0.12	0.34	18970.45851	18970.46	1.09E-05	3.473734	7.71941	6.05E-06
39.64095	0.000265	0.000871	174.2901961			0	0.0001313	26.25997692	0.13	0.34	20974.77184	20974.77	4.08E-06	3.839846	8.532991	6.69E-06
39.63168	0.00029	0.000954	190.7908618			0	0.0001437	28.73048685	0.14	0.34	22962.73968	22962.74	1.53E-06	4.203517	9.341149	7.32E-06
39.6389	0.000315	0.001036	207.1891328			0	0.0001561	31.21304321	0.15	0.34	24934.49207	24934.49	5.68E-07	4.56476	10.14391	7.95E-06
39.6589	0.00034	0.001117	223.4856627			0	0.0001685	33.70756909	0.17	0.34	26890.13253	26890.13	2.02E-07	4.923585	10.9413	8.57E-06
39.68901	0.000365	0.001198	239.6809979			0	0.0001811	36.21400024	0.18	0.34	28829.74757	28829.75	6.63E-08	5.279998	11.73333	9.2E-06
39.72729	0.00039	0.001279	255.7756135			0	0.0001937	38.73228076	0.19	0.34	30753.41242	30753.41	1.9E-08	5.634005	12.52001	9.82E-06
39.77225	0.000415	0.001359	271.7699335			0	0.0002063	41.26236076	0.20	0.34	32661.19495	32661.19	0.0007	5.98561	13.30136	1.04E-05
39.82278	0.00044	0.001438	287.6643593			0	0.000219	43.80419303	0.21	0.34	34553.15679	34553.16	0.00018	6.334819	14.07738	1.1E-05
39.87799	0.000465	0.001517	303.4592548			0	0.0002318	46.35773473	0.22	0.34	36429.35715	36429.36	9.09E-06	6.681634	14.84808	1.17E-05
39.9372	0.00049	0.001596	319.1549749			0	0.0002446	48.92294413	0.23	0.34	38289.85204	38289.85	2.72E-05	7.026059	15.61346	1.23E-05
39.99983	0.000515	0.001674	334.7518624			0	0.0002575	51.4997809	0.25	0.34	40134.69569	40134.7	0.000136	7.368098	16.37355	1.29E-05
40.06544	0.00054	0.001751	350.2502522			0	0.0002704	54.08820563	0.26	0.34	41963.94106	41963.94	0.000276	7.707754	17.12834	1.35E-05
40.13367	0.000565	0.001828	365.6504737			0	0.0002834	56.68817957	0.27	0.34	43777.64027	43777.64	0.000412	8.04503	17.87784	1.41E-05
40.2042	0.00059	0.001905	380.9528527			0	0.0002965	59.29966438	0.28	0.34	45575.84491	45575.84	0.000524	8.379931	18.62207	1.47E-05
40.27678	0.000615	0.001981	396.1577132			0	0.0003096	61.92262198	0.29	0.34	47358.60626	47358.61	0.000598	8.71246	19.36102	1.53E-05
38.49377	0.00064	0.002186	392.2446685			0	0.0003075	61.49573678	0.30	0.34	46864.643	46864.64	2.49E-08	8.654371	19.23194	1.66E-05
37.27937	0.000665	0.002368	392.7608086			0	0.0003082	61.64685707	0.31	0.34	46916.36358	46916.36	2.95E-08	8.684692	19.29932	1.78E-05
36.17037	0.00069	0.002553	393.288617			0	0.0003085	61.69444849	0.32	0.34	46984.40673	46984.41	3.55E-08	8.713722	19.36383	1.91E-05
35.15482	0.000715	0.002743	393.8271784			0	0.0003082	61.64557697	0.33	0.34	47067.64156	47067.64	4.34E-08	8.741635	19.42586	2.03E-05
34.22243	0.00074	0.002936	394.3756168			0	0.0003075	61.50701771	0.34	0.34	47164.98398	47164.98	5.37E-08	8.768578	19.48573	2.16E-05
33.36431	0.000765	0.003133	394.9330975			0	0.0003064	61.2852438	0.35	0.35	47275.39851	47275.4	6.71E-08	8.794672	19.54372	2.29E-05
31.16326	0.00084	0.003742	396.6520668			0	0.0003009	60.18073556	0.37	0.35	47675.46409	47675.46	1.36E-07	8.868811	19.70847	2.7E-05
27.17212	0.00104	0.005467	401.4640131			0	0.0002745	54.90187504	0.44	0.35	49105.25574	49105.26	8.87E-07	9.0462	20.10267	3.83E-05
24.769	0.00124	0.007271	406.4163651			0	0.0002387	47.7497074	0.50	0.36	50820.3754	50820.38	4.48E-06	9.205291	20.4562	5.01E-05
23.22331	0.00144	0.009101	411.3560784			0	0.0001999	39.97333736	0.56	0.36	52622.14906	52622.15	1.68E-05	9.35155	20.78122	6.2E-05
22.18462	0.00164	0.010927	416.1982362			0	0.0001615	32.29961581	0.60	0.37	54395.55532	54395.56	4.9E-05	9.48691	21.08202	7.39E-05
21.46681	0.00184	0.012731	420.8977425			0	0.0001257	25.14516472	0.64	0.38	56075.17224	56075.17	0.000117	9.612341	21.36076	8.57E-05
20.96284	0.00204	0.014504	425.4328965			0	9.37E-05	18.73978897	0.67	0.39	57625.36338	57625.36	0.000236	9.728598	21.61911	9.73E-05
20.607	0.00224	0.016239	429.796093			0	6.598E-05	13.19637774	0.70	0.39	59029.05557	59029.06	0.000414	9.836438	21.85875	0.000109
20.3567	0.00244	0.017937	433.9884938			0	4.275E-05	8.550868189	0.73	0.40	60281.32141	60281.32	0.00064	9.936682	22.08152	0.00012
20.18293	0.00264	0.019597	438.0168961			0	2.393E-05	4.78561025	0.75	0.41	61385.62485	61385.62	0.000876	10.03023	22.28939	0.000131
20.06512	0.00284	0.021222	441.8918337			0	9.217E-06	1.843396066	0.76	0.42	62351.56325	62351.56	-9.4E-09	10.11803	22.48452	0.000142
19.98804	0.00304	0.022815	445.6263811			0	1.819E-06	0.363837707	0.77	0.42	63193.46908	63193.47	-1E-08	10.20112	22.66915	0.000152
19.94001	0.00324	0.024383	449.2353727			0	9.747E-06	1.949453318	0.79	0.43	63929.50596	63929.51	-9E-09	10.28052	22.84559	0.000162
19.91178	0.00344	0.02593	452.7348557			0	1.524E-05	3.048323398	0.79	0.43	64581.05893	64581.06	0.000832	10.35734	23.01632	0.000173
19.89576	0.00364	0.027462	456.1416849			0	1.907E-05	3.814099719	0.80	0.44	65172.28554	65172.29	0.000528	10.43274	23.18387	0.000183
19.88563	0.00384	0.028988	459.4731863			0	2.208E-05	4.416970881	0.81	0.44	65729.75634	65729.76	0.000249	10.50785	23.35077	0.000193
19.87598	0.00404	0.030514	462.7468578			0	2.521E-05	5.041672544	0.82	0.44	66282.12636	66282.13	3E-05	10.5838	23.51956	0.000203
19.86215	0.00424	0.03205	465.9800756			0	2.943E-05	5.885479785	0.83	0.44	66859.81021	66859.81	-1.4E-07	10.66175	23.69278	0.000213
19.84012	0.00444	0.033604	469.1897933			0	3.578E-05	7.156078159	0.83	0.43	67494.63738	67494.64	-6.4E-06	10.74284	23.87299	0.000224
19.80643	0.00464	0.035185	472.3922237			0	4.535E-05	9.069231611	0.84	0.43	68219.47719	68219.48	-6.8E-05	10.82821	24.06268	0.000234
19.7582	0.00484	0.036803	475.6025038			0	5.923E-05	11.8462296	0.86	0.42	69067.82965	69067.83	1.56E-07	10.91896	24.26436	0.000245
19.69306	0.00504	0.038468	478.8343449			0	7.856E-05	15.71113975	0.87	0.41	70073.38608	70073.39	-4.4E-08	11.01619	24.48043	0.000256
19.60917	0.00524	0.040188	482.0996764			0	0.0001044	20.88791919	0.89	0.39	71269.56989	71269.57	-1.2E-06	11.12096	24.71324	0.000267
19.50524	0.00544	0.041973	485.4082942			0	0.000138	27.59748949	0.91	0.38	72689.07199	72689.07	-7.9E-06	11.23426	24.96501	0.000279
														11.23426	24.96501	

Appendix 8. Iteration table for Repaired Empirical Analysis

kd (mm)	$\varepsilon_{c\ Increment}$	ε_s	fs (Mpa)	ε_{sr}	fsr (Mpa)	l_d	ε_s'	fs' (Mpa)	α_{re}	γ_{re}	C (kN)	T (kN)	C-T	M (KNm)	Load (KN)	ϕ
1E-07	0	0	0	0	0	0	0	0	0.00	0.34	0	0	0	0	0	0
117.7902	0.00004	1.77E-05	3.545955	2.11E-05	4.225129	11.6815	3.3E-05	6.641652	0	0.34	0	-2.5E-05	2.54E-05	0.1455472	0.3234383	3.4E-07
65.66463	0.000065	0.000103	20.65587	0.000113	22.63562	19.1364	4.5E-05	9.040486	0.01	0.34	3995.75747	3995.758	-0.00054	0.8049066	1.7886813	9.9E-07
58.82222	0.00009	0.00017	34.02115	0.000185	37.08122	26.3107	5.9E-05	11.87986	0.03	0.34	6986.88825	6986.888	3.65E-05	1.3378824	2.973072	1.53E-06
55.95873	0.000115	0.000234	46.87292	0.000255	50.98309	33.3503	7.4E-05	14.77966	0.04	0.34	9840.24787	9840.248	-2.1E-05	1.8512899	4.1139775	2.06E-06
54.41366	0.00014	0.000297	59.47804	0.000323	64.6238	40.298	8.9E-05	17.70847	0.06	0.34	12627.4357	12627.44	-0.00049	2.3549442	5.2332093	2.57E-06
53.47177	0.000165	0.00036	71.91517	0.00039	78.08665	47.1714	0.0001	20.65704	0.07	0.34	15369.5548	15369.55	7.92E-08	2.8518011	6.3373357	3.09E-06
52.8571	0.00019	0.000421	84.21631	0.000457	91.4055	53.9791	0.00012	23.62161	0.08	0.34	18075.1907	18075.19	5.39E-07	3.3430718	7.4290485	3.59E-06
52.44011	0.000215	0.000482	96.3971	0.000523	104.5969	60.7258	0.00013	26.60034	0.10	0.34	20748.5394	20748.54	2.33E-06	3.829348	8.5096622	4.1E-06
52.15184	0.00024	0.000542	108.4662	0.000588	117.6701	67.4142	0.00015	29.59221	0.11	0.34	23391.9209	23391.92	2.92E-06	4.3109544	9.5798987	4.6E-06
51.95214	0.000265	0.000602	120.4288	0.000653	130.6305	74.0464	0.00016	32.59661	0.12	0.34	26006.7413	26006.74	2.19E-07	4.7880855	10.64019	5.1E-06
51.81607	0.00029	0.000661	132.2884	0.000717	143.4819	80.6235	0.00018	35.61312	0.14	0.34	28593.918	28593.92	-0.00017	5.2608656	11.690813	5.6E-06
51.72729	0.000315	0.00072	144.0474	0.000781	156.2266	87.1466	0.00019	38.64149	0.15	0.34	31154.0879	31154.09	0.000864	5.7293791	12.731954	6.09E-06
51.67465	0.00034	0.000779	155.7074	0.000844	168.8666	93.6164	0.00021	41.68148	0.16	0.34	33687.7159	33687.72	-7E-07	6.193686	13.763747	6.58E-06
51.65027	0.000365	0.000836	167.2698	0.000907	181.4033	100.033	0.00022	44.73297	0.17	0.34	36195.1606	36195.16	-8.5E-06	6.6538306	14.78629	7.07E-06
51.64845	0.00039	0.000894	178.7357	0.000969	193.8378	106.398	0.00024	47.7958	0.18	0.34	38676.7079	38676.71	-4.7E-05	7.1098477	15.799662	7.55E-06
51.66494	0.000415	0.000951	190.1059	0.001031	206.171	112.711	0.00025	50.86989	0.20	0.34	41132.5959	41132.6	-0.00017	7.561765	16.803922	8.03E-06
51.6965	0.00044	0.001007	201.3813	0.001092	218.4037	118.973	0.00027	53.95514	0.21	0.34	43563.029	43563.03	-0.00049	8.0096059	17.799124	8.51E-06
51.74066	0.000465	0.001063	212.5624	0.001153	230.5367	125.183	0.00029	57.05148	0.22	0.34	45968.1883	45968.19	1.04E-08	8.4533902	18.785311	8.99E-06
51.79543	0.00049	0.001118	223.65	0.001213	242.5706	131.342	0.0003	60.15883	0.23	0.34	48348.2369	48348.24	3.49E-08	8.893136	19.762524	9.46E-06
51.85928	0.000515	0.001173	234.6445	0.001273	254.5059	137.451	0.00032	63.27712	0.24	0.34	50703.3263	50703.33	1.01E-07	9.3288596	20.730799	9.93E-06
51.93093	0.00054	0.001228	245.5465	0.001332	266.3434	143.51	0.00033	66.40629	0.25	0.34	53033.5985	53033.6	6.19E-09	9.7605765	21.69017	1.04E-05
52.00937	0.000565	0.001282	256.3565	0.00139	278.0834	149.519	0.00035	69.54629	0.26	0.34	55339.1889	55339.19	-6.3E-06	10.188301	22.640669	1.09E-05
52.09374	0.00059	0.001335	267.0751	0.001449	289.7265	155.477	0.00036	72.69705	0.27	0.34	57620.2281	57620.23	-0.00013	10.612048	23.582329	1.13E-05
52.18335	0.000615	0.001389	277.7025	0.001506	301.2733	161.387	0.00038	75.85853	0.28	0.34	59876.8429	59876.84	-0.00073	11.031831	24.51518	1.18E-05
52.2776	0.00064	0.001441	288.2394	0.001564	312.7241	167.247	0.0004	79.03066	0.29	0.34	62109.1585	62109.16	-1.7E-07	11.447664	25.439253	1.22E-05
52.37601	0.000665	0.001493	298.6862	0.00162	324.0795	173.058	0.00041	82.21339	0.30	0.34	64317.2967	64317.3	8.66E-05	11.859561	26.35458	1.27E-05
52.47813	0.00069	0.001545	309.0433	0.001677	335.34	178.821	0.00043	85.40667	0.31	0.34	66501.3795	66501.38	4.94E-05	12.267536	27.261191	1.31E-05
52.58362	0.000715	0.001597	319.3112	0.001733	346.506	184.535	0.00044	88.61044	0.32	0.34	68661.5278	68661.53	0.000333	12.671603	28.159118	1.36E-05
52.69216	0.00074	0.001647	329.4904	0.001788	357.5781	188.881	0.00046	91.82466	0.33	0.34	70797.8621	70797.86	-0.00028	13.071777	29.048394	1.4E-05
53.06358	0.000765	0.001686	337.1667	0.00183	366	202.93	0.00048	95.33333	0.34	0.35	73269.6582	72262.72	1006.941	13.401634	29.78141	1.44E-05
53.34035	0.00079	0.001728	345.5587	0.001876	391.3576	203.045	0.00049	98.7578	0.35	0.35	75599.1184	75599.12	-2.5E-08	13.962837	31.028527	1.48E-05
53.07939	0.000815	0.001795	359.0482	0.001949	391.566	203.16	0.00051	101.5826	0.36	0.35	77131.8564	77131.86	-3.6E-08	14.260486	31.689968	1.54E-05
52.84486	0.00084	0.001862	372.4499	0.002021	391.773	203.234	0.00052	104.4177	0.36	0.35	78650.5663	78650.57	-3.5E-08	14.555641	32.345869	1.59E-05
53.08664	0.000865	0.001905	381	0.002068	391.9065	203.441	0.00054	107.8235	0.37	0.35	80844.0149	79393.32	1450.698	14.782362	32.849693	1.63E-05
51.86583	0.00089	0.002027	391.7899	0.002199	392.2798	203.653	0.00055	109.3614	0.38	0.35	80743.0254	80743.03	1.97E-07	15.001803	33.337341	1.72E-05
50.70761	0.000915	0.002153	392.1481	0.002333	392.6626	203.869	0.00055	110.8215	0.39	0.35	80626.632	80626.63	2.07E-05	15.045836	33.435191	1.8E-05
49.62178	0.00094	0.00228	392.5125	0.00247	393.052	204.088	0.00056	112.2268	0.40	0.35	80519.5633	80519.56	2.43E-05	15.08804	33.528977	1.89E-05
48.60235	0.000965	0.00241	392.8828	0.002609	393.4476	204.31	0.00057	113.58	0.41	0.35	80421.3676	80421.37	2.81E-05	15.128583	33.619073	1.99E-05
47.64395	0.00099	0.002542	393.2587	0.00275	393.849	204.536	0.00057	114.8835	0.41	0.35	80331.6037	80331.6	3.24E-05	15.167614	33.70581	2.08E-05
46.74175	0.001015	0.002677	393.6398	0.002894	394.2559	204.764	0.00058	116.1398	0.42	0.35	80249.8411	80249.84	-2.3E-05	15.205266	33.789481	2.17E-05
45.89144	0.00104	0.002813	394.0258	0.003039	394.668	204.995	0.00059	117.3513	0.43	0.35	80175.6607	80175.66	-2.5E-05	15.241656	33.870347	2.27E-05
45.08908	0.001065	0.00295	394.4165	0.003187	395.085	205.228	0.00059	118.5204	0.44	0.35	80108.6547	80108.65	-2.8E-05	15.276887	33.948638	2.36E-05
44.33114	0.00109	0.00309	394.8115	0.003336	395.5065	205.464	0.0006	119.6493	0.44	0.35	80048.4273	80048.43	-3E-05	15.311053	34.024562	2.46E-05
43.61441	0.001115	0.003231	395.2106	0.003487	395.9322	205.702	0.0006	120.7402	0.45	0.35	79994.5946	79994.59	-3.3E-05	15.344236	34.098302	2.56E-05
42.93597	0.00114	0.003374	395.6135	0.003639	396.3619	205.942	0.00061	121.7953	0.46	0.35	79946.7852	79946.79	-3.5E-05	15.37651	34.170023	2.66E-05
42.29316	0.001165	0.003518	396.0199	0.003793	396.7953	206.184	0.00061	122.8167	0.46	0.35	79904.6397	79904.64	-3.7E-05	15.407943	34.239873	2.75E-05
41.68356	0.00119	0.003663	396.4295	0.003949	397.2321	206.428	0.00062	123.8063	0.47	0.36	79867.8111	79867.81	-3.9E-05	15.438592	34.307983	2.85E-05
41.10495	0.001215	0.00381	396.8422	0.004106	397.672	206.673	0.00062	124.7661	0.48	0.36	79835.9647	79835.96	-4.1E-05	15.468513	34.374474	2.96E-05
40.55529	0.00124	0.003958	397.2577	0.004264	398.1148	206.92	0.00063	125.6978	0.48	0.36	79808.778	79808.78	-4.2E-05	15.497754	34.439453	3.06E-05
40.03273	0.001265	0.004107	397.6757	0.004423	398.5603	207.168	0.00063	126.6034	0.49	0.36	79785.9407	79785.94	-4.3E-05	15.526357	34.503017	3.16E-05
39.53554	0.00129	0.004257	398.0961	0.004583	399.0081	207.418	0.00064	127.4845	0.49	0.36	79767.1544	79767.15	-4.4E-05	15.554364	34.565253	3.26E-05
39.06216	0.001315	0.004408	398.5186	0.004745	399.4582	207.668	0.00064	128.3428	0.50	0.36	79752.1327	79752.13	-4.5E-05	15.581808	34.626241	3.37E-05
38.61112	0.00134	0.00456	398.943	0.004907	399.9103	207.92	0.00065	129.1799	0.51	0.36	79740.6007	79740.6	-4.6E-05	15.608724	34.686053	3.47E-05
38.18107	0.001365	0.004713	399.3692	0.00507	400.3642	208.172	0.00065	129.9972	0.51	0.36	79732.2951	79732.3	-4.6E-05	15.63514	34.744755	3.58E-05
37.77078	0.00139	0.004866	399.7969	0.005234	400.8197	208.425	0.00065	130.7963	0.52	0.36	79726.9638	79726.96	-4.7E-05	15.661083	34.802406	3.68E-05
37.3791	0.001415	0.00502	400.226	0.005399	401.2765	208.679	0.00066	131.5785	0.52	0.36	79724.3658	79724.37	-4.6E-05	15.686578	34.859061	3.79E-05
37.00495	0.00144	0.005175	400.6564	0.005564	401.7346	208.933	0.00066	132.3452	0.53	0.36	79724.2706	79724.27	-4.6E-05	15.711647	34.91477	3.89E-05
36.64734	0.001465	0.005331	401.0878	0.005731	402.1938	209.188	0.00067	133.0976	0.53	0.36	79726.4586	79726.46	-4.6E-05	15.73631	34.969579	4E-05
36.30536	0.00149	0.005487	401.5201	0.005897	402.6539	209.444	0.00067	133.8369	0.54	0.36	79730.7201	79730.72	-4.5E-05	15.760588	35.023529	4.1E-05
35.97813	0.001515	0.005644	401.9532	0.006065	403.1148	209.699	0.00067	134.5644	0.54	0.37	79736.8556	79736.86	-4.4E-05	15.784496	35.076658	4.21E-05
35.66487	0.00154	0.005801	402.3869	0.006232	403.5762	209.955	0.00068	135.281	0.55	0.37	79744.6752	79744.68	-4.4E-05	15.808052	35.129004	4.32E-05
35.36482	0.001565	0.005958	402.8212	0.006401	404.0382	210.211	0.00068	135.9879	0.55	0.37	79753.9986	79754	-4.3E-05	15.831269	35.180597	4.43E-05
35.07728	0.00159	0.006116	403.2558	0.006569	404.5005	210.468	0.00068	136.6861	0.56	0.37	79764.6546	79764.65	-4.1E-05	15.854162	35.23147	4.53E-05
34.80161	0.001615	0.006274	403.6907	0.006738	404.963	210.724	0.00069	137.3764	0.56	0.37	79776.4808	79776.48	-4E-05	15.876743	35.28165	4.64E-05
34.53718	0.00164	0.006432	404.1258	0.006907	405.4257	210.98	0.00069	138.0598	0.57	0.37	79789.3235	79789.32	-3.9E-05	15.899024	35.331164	4.75E-05
34.28344	0.001665	0.006591	404.5609	0.007077	405.8883	211.237	0.00069	138.7371	0.57	0.37	79803.0377	79803.04	-3.8E-05	15.921016	35.380035	4.86E-05
34.03984	0.00169	0.00675	404.996	0.007247	406.3509	211.493	0.0007	139.4092	0.57	0.37	79817.486	79817.49	-3.6E-05	15.94273	35.428288	4.96E-05
33.80587	0.001715	0.006909	405.4309	0.007417	406.8133	211.749	0.0007	140.0767	0.58	0.37	79832.5392	79832.54	-3.5E-05	15.964175	35.475944	5.07E-05
33.58107	0.00174	0.007069	405.8657	0.007587	407.2754	212.005	0.0007	140.7404	0.58	0.37	79848.0758	79848.08	-3.3E-05	15.98536	35.523023	5.18E-05
33.36498	0.001765	0.007228	406.3002	0.007757	407.7371	212.26	0.00071	141.4009	0.59	0.37	79863.9814	79863.98	-3.2E-05	16.006295	35.569544	5.29E-05
33.15719	0.00179	0.007387	406.7343	0.007927	408.1984	212.515	0.00071	142.0589	0.59	0.38	79880.1491	79880.15	-3E-05	16.026987	35.615527	5.4E-05
32.9573	0.001815	0.007547	407.168	0.008098	408.6593	212.77	0.00071	142.715	0.59	0.38	79896.4785	79896.48	-2.9E-05	16.047444	35.660987	5.51E-05
32.76494	0.00184	0.007707	407.6012	0.008268	409.1195	213.025	0.00072	143.3696	0.60	0.38	79912.8763	79912.88	-2.7E-05	16.067673	35.705941	5.62E-05
32.57975	0.001865	0.007867	408.0338	0.008439	409.5791	213.279	0.00072	144.0234	0.60	0.38	79929.2556	79929.26	-2.6E-05	16.087682	35.750405	5.72E-05
32.4014	0.00189	0.008026	408.4658	0.00861	410.038	213.533	0.00072	144.6768	0.60	0.38	79945.5354	79945.54	-2.4E-05	16.107478	35.794395	5.83E-05
32.22958	0.001915	0.008186	408.8972	0.00878	410.4961	213.786	0.00073	145.3301	0.61	0.38	79961.6414	79961.64	-2.3E-05	16.127066	35.837924	5.94E-05
32.06399	0.00194	0.008346	409.3279	0.008951	410.9534	214.039	0.00073	145.9839	0.61	0.38	79977.5047	79977.5	-2.2E-05	16.146453	35.881006	6.05E-05
31.90434	0.001965	0.008505	409.7578	0.009121	411.4099	214.342	0.00073	146.6385	0.61	0.38	79993.0622	79993.06	-2E-05	16.165645	35.923655	6.16E-05
31.72024	0.001995	0.008697	410.2727	0.009326	411.9566	214.644	0.00074	147.4256	0.62	0.38	80011.247	80011.25	-1.9E-05	16.188426	35.974281	6.29E-05
31.54387	0.002025	0.008888	410.7864	0.00953	412.5018	214.946	0.00074	148.2148	0.62	0.39	80028.8197	80028.82	-1.7E-05	16.210945	36.024323	6.42E-05
31.37483	0.002055	0.00908	411.2988	0.009735	413.0458	215.246	0.00075	149.0066	0.63	0.39	80045.7014	80045.7	-1.6E-05	16.233211	36.073802	6.55E-05

31.90434	0.001965	0.008505	409.7578	0.009121	411.4099	214.342	0.00073	146.6385	0.61	0.38	79993.0622	79993.06	-2E-05	16.165645	35.923655	6.16E-05
31.72024	0.001995	0.008697	410.2727	0.009326	411.9566	214.644	0.00074	147.4256	0.62	0.38	80011.247	80011.25	-1.9E-05	16.188426	35.974281	6.29E-05
31.54387	0.002025	0.008888	410.7864	0.00953	412.5018	214.946	0.00074	148.2148	0.62	0.39	80028.8197	80028.82	-1.7E-05	16.210945	36.024323	6.42E-05
31.37483	0.002055	0.00908	411.2988	0.009735	413.0458	215.246	0.00075	149.0066	0.63	0.39	80045.7014	80045.7	-1.6E-05	16.233211	36.073802	6.55E-05
31.21274	0.002085	0.009271	411.8099	0.009939	413.5882	215.546	0.00075	149.8014	0.63	0.39	80061.8238	80061.82	-1.5E-05	16.255233	36.12274	6.68E-05
31.05723	0.002115	0.009462	412.3198	0.010143	414.1292	215.845	0.00075	150.5996	0.63	0.39	80077.1282	80077.13	-1.3E-05	16.27702	36.171156	6.81E-05
30.90795	0.002145	0.009653	412.8283	0.010347	414.6687	216.143	0.00076	151.4015	0.64	0.39	80091.5655	80091.57	-1.2E-05	16.298581	36.219069	6.94E-05
30.76458	0.002175	0.009844	413.3354	0.010551	415.2067	216.44	0.00076	152.2073	0.64	0.39	80105.0958	80105.1	-1.1E-05	16.319924	36.266498	7.07E-05
30.62682	0.002205	0.010034	413.8411	0.010754	415.7431	216.736	0.00077	153.0171	0.64	0.39	80117.6879	80117.69	-1E-05	16.341058	36.313463	7.2E-05
30.49438	0.002235	0.010225	414.3454	0.010958	416.2779	217.032	0.00077	153.8312	0.64	0.39	80129.3191	80129.32	-9.2E-06	16.361991	36.359981	7.33E-05
30.36698	0.002265	0.010415	414.8483	0.011161	416.8112	217.326	0.00077	154.6496	0.65	0.39	80139.975	80139.98	-8.3E-06	16.382732	36.406071	7.46E-05
30.24436	0.002295	0.010605	415.3497	0.011364	417.3429	217.62	0.00078	155.4724	0.65	0.40	80149.6491	80149.65	-7.5E-06	16.403288	36.451751	7.59E-05
30.12629	0.002325	0.010795	415.8498	0.011567	417.873	217.913	0.00078	156.2995	0.65	0.40	80158.3423	80158.34	-6.7E-06	16.423667	36.497038	7.72E-05
30.01251	0.002355	0.010984	416.3484	0.011769	418.4016	218.205	0.00079	157.1309	0.65	0.40	80166.0631	80166.06	-6E-06	16.443878	36.541951	7.85E-05
29.90282	0.002385	0.011174	416.8457	0.011972	418.9286	218.496	0.00079	157.9666	0.66	0.40	80172.8271	80172.83	-5.4E-06	16.463928	36.586507	7.98E-05
29.797	0.002415	0.011363	417.3416	0.012174	419.4541	218.786	0.00079	158.8063	0.66	0.40	80178.6567	80178.66	-4.8E-06	16.483825	36.630723	8.1E-05
29.69485	0.002445	0.011552	417.8361	0.012376	419.9781	219.076	0.0008	159.65	0.66	0.40	80183.5811	80183.58	-4.3E-06	16.503577	36.674616	8.23E-05
29.59618	0.002475	0.011741	418.3293	0.012578	420.5006	219.365	0.0008	160.4974	0.66	0.40	80187.6358	80187.64	-3.8E-06	16.523192	36.718205	8.36E-05
29.50081	0.002505	0.01193	418.8212	0.012779	421.0216	219.652	0.00081	161.3483	0.67	0.40	80190.8626	80190.86	-3.4E-06	16.542678	36.761506	8.49E-05
29.40855	0.002535	0.012119	419.3118	0.012981	421.5413	219.94	0.00081	162.2023	0.67	0.41	80193.3092	80193.31	-3E-06	16.562042	36.804537	8.62E-05
29.31925	0.002565	0.012307	419.8011	0.013182	422.0595	220.226	0.00082	163.0593	0.67	0.41	80195.0295	80195.03	-2.6E-06	16.581292	36.847315	8.75E-05
29.23275	0.002595	0.012496	420.2893	0.013384	422.5764	220.512	0.00082	163.9188	0.67	0.41	80196.0826	80196.08	-2.3E-06	16.600436	36.889857	8.88E-05
29.14889	0.002625	0.012684	420.7764	0.013585	423.0921	220.797	0.00082	164.7804	0.67	0.41	80196.5333	80196.53	-2E-06	16.619481	36.93218	9.01E-05
29.06753	0.002655	0.012873	421.2623	0.013786	423.6064	221.081	0.00083	165.6438	0.68	0.41	80196.4519	80196.45	-1.7E-06	16.638436	36.974303	9.13E-05
28.98852	0.002685	0.013061	421.7472	0.013987	424.1196	221.365	0.00083	166.5085	0.68	0.41	80195.9136	80195.91	-1.5E-06	16.657309	37.016241	9.26E-05
28.91174	0.002715	0.013249	422.2311	0.014188	424.6317	221.648	0.00084	167.3741	0.68	0.41	80194.9987	80195	-1.3E-06	16.676106	37.058013	9.39E-05
28.83706	0.002745	0.013437	422.714	0.014389	425.1427	221.93	0.00084	168.2399	0.68	0.41	80193.7924	80193.79	-1.1E-06	16.694836	37.099636	9.52E-05
28.76434	0.002775	0.013626	423.1961	0.01459	425.6527	222.212	0.00085	169.1055	0.68	0.41	80192.3843	80192.38	-9.6E-07	16.713507	37.141127	9.65E-05
28.69348	0.002805	0.013814	423.6773	0.014791	426.1617	222.494	0.00085	169.9704	0.68	0.42	80190.8691	80190.87	-8.2E-07	16.732126	37.182503	9.78E-05
28.62436	0.002835	0.014002	424.1577	0.014992	426.6698	222.775	0.00085	170.8339	0.69	0.42	80189.3454	80189.35	-6.9E-07	16.750702	37.223783	9.9E-05
28.55687	0.002865	0.01419	424.6375	0.015194	427.1772	223.056	0.00086	171.6955	0.69	0.42	80187.9164	80187.92	-5.8E-07	16.769242	37.264983	0.0001
28.4909	0.002895	0.014379	425.1166	0.015395	427.6837	223.336	0.00086	172.5544	0.69	0.42	80186.6894	80186.69	-4.9E-07	16.787754	37.306121	0.000102
28.42635	0.002925	0.014568	425.5952	0.015597	428.1896	223.616	0.00087	173.4101	0.69	0.42	80185.7756	80185.78	-4.1E-07	16.806246	37.347214	0.000103
28.36313	0.002955	0.014756	426.0733	0.015798	428.6949	223.896	0.00087	174.2618	0.69	0.42	80185.2903	80185.29	-3.4E-07	16.824726	37.388281	0.000104
28.30114	0.002985	0.014945	426.5509	0.016	429.1997	224.175	0.00088	175.1089	0.69	0.42	80185.3524	80185.35	-2.8E-07	16.843202	37.429338	0.000105
28.24029	0.003015	0.015135	427.0283	0.016202	429.7041	224.454	0.00088	175.9506	0.70	0.42	80186.0847	80186.08	-2.3E-07	16.861682	37.470404	0.000107
28.18049	0.003045	0.015324	427.5053	0.016405	430.208	224.733	0.00088	176.7861	0.70	0.42	80187.6132	80187.61	-1.8E-07	16.880173	37.511496	0.000108
28.12166	0.003075	0.015514	427.9822	0.016607	430.7117	225.012	0.00089	177.6147	0.70	0.42	80190.0676	80190.07	-1.5E-07	16.898684	37.552631	0.000109
28.06371	0.003105	0.015704	428.459	0.01681	431.2152	225.291	0.00089	178.4356	0.70	0.42	80193.5808	80193.58	-1.2E-07	16.917222	37.593828	0.000111
28.00657	0.003135	0.015894	428.9357	0.017014	431.7186	225.57	0.0009	179.248	0.70	0.43	80198.2889	80198.29	-9.1E-08	16.935796	37.635103	0.000112
27.95016	0.003165	0.016085	429.4125	0.017218	432.222	225.849	0.0009	180.051	0.70	0.43	80204.3312	80204.33	-7.5E-08	16.954414	37.676475	0.000113
27.89441	0.003195	0.016277	429.8895	0.017422	432.7254	226.128	0.0009	180.8437	0.70	0.43	80211.8498	80211.85	-7.3E-08	16.973083	37.717962	0.000115
27.83925	0.003225	0.016468	430.3667	0.017627	433.229	226.407	0.00091	181.6254	0.71	0.43	80220.9896	80220.99	-7.2E-08	16.991811	37.759581	0.000116
27.7846	0.003255	0.016661	430.8442	0.017832	433.7329	226.686	0.00091	182.395	0.71	0.43	80231.8986	80231.9	-7E-08	17.010607	37.801349	0.000117
27.7304	0.003285	0.016854	431.3221	0.018038	434.237	226.966	0.00092	183.1518	0.71	0.43	80244.727	80244.73	-6.8E-08	17.029478	37.843285	0.000118
27.67659	0.003315	0.017047	431.8005	0.018245	434.7416	227.246	0.00092	183.8948	0.71	0.43	80259.6277	80259.63	-6.7E-08	17.048433	37.885406	0.00012
27.62311	0.003345	0.017241	432.2795	0.018452	435.2467	227.526	0.00092	184.623	0.71	0.43	80276.756	80276.76	-6.5E-08	17.067479	37.92773	0.000121
27.5699	0.003375	0.017436	432.7592	0.01866	435.7525	227.807	0.00093	185.3355	0.71	0.43	80296.2695	80296.27	-6.3E-08	17.086624	37.970275	0.000122
27.51689	0.003405	0.017631	433.2396	0.018869	436.2589	228.088	0.00093	186.0313	0.72	0.43	80318.328	80318.33	-6.1E-08	17.105876	38.013057	0.000124
27.46404	0.003435	0.017827	433.7209	0.019078	436.7662	228.369	0.00093	186.7095	0.72	0.43	80343.0933	80343.09	-6E-08	17.125243	38.056095	0.000125
27.41129	0.003465	0.018024	434.2032	0.019288	437.2743	228.651	0.00094	187.369	0.72	0.43	80370.7291	80370.73	-0.00015	17.144733	38.099407	0.000126
27.35859	0.003495	0.018222	434.6865	0.0195	437.7834	228.934	0.00094	188.0088	0.72	0.43	80401.4012	80401.4	-5.6E-08	17.164354	38.143009	0.000128
27.3059	0.003525	0.018421	435.1709	0.019712	438.2937	229.217	0.00094	188.628	0.72	0.43	80435.2766	80435.28	-5.5E-08	17.184114	38.18692	0.000129
27.25315	0.003555	0.01862	435.6565	0.019925	438.8051	229.501	0.00095	189.2255	0.72	0.43	80472.5245	80472.52	-5.3E-08	17.20402	38.231156	0.00013
27.20032	0.003585	0.018821	436.1435	0.020139	439.3177	229.786	0.00095	189.8002	0.73	0.44	80513.3151	80513.32	-5.1E-08	17.224081	38.275736	0.000132
27.14734	0.003615	0.019023	436.6319	0.020354	439.8318	230.072	0.00095	190.3512	0.73	0.44	80557.8202	80557.82	-4.9E-08	17.244304	38.320676	0.000133
27.09419	0.003645	0.019225	437.1218	0.020571	440.3473	230.358	0.00095	190.8772	0.73	0.44	80606.2129	80606.21	-4.8E-08	17.264697	38.365993	0.000135
27.04082	0.003675	0.019429	437.6133	0.020788	440.8645	230.646	0.00096	191.3774	0.73	0.44	80658.6673	80658.67	-4.6E-08	17.285267	38.411705	0.000136
26.98719	0.003705	0.019634	438.1065	0.021007	441.3832	230.934	0.00096	191.8506	0.73	0.44	80715.3586	80715.36	-4.4E-08	17.306023	38.457829	0.000137
26.93327	0.003735	0.01984	438.6014	0.021227	441.9037	231.223	0.00096	192.2957	0.74	0.44	80776.4628	80776.46	-4.3E-08	17.326972	38.504383	0.000139
26.87902	0.003765	0.020047	439.0983	0.021448	442.4261	231.514	0.00096	192.7116	0.74	0.44	80842.1567	80842.16	-4.1E-08	17.348122	38.551382	0.00014
26.8244	0.003795	0.020256	439.5971	0.021671	442.9504	231.805	0.00097	193.0973	0.74	0.44	80912.6179	80912.62	-4E-08	17.36948	38.598844	0.000141

26.8244	0.003795	0.020256	439.5971	0.021671	442.9504	231.805	0.00097	193.0973	0.74	0.44	80912.6179	80912.62	-4E-08	17.36948	38.598844	0.000141
26.76939	0.003825	0.020466	440.0979	0.021895	443.4768	232.098	0.00097	193.4517	0.74	0.44	80988.0243	80988.02	-3.8E-08	17.391053	38.646785	0.000143
26.71395	0.003855	0.020677	440.601	0.02212	444.0053	232.392	0.00097	193.7735	0.74	0.44	81068.5545	81068.55	-3.6E-08	17.41285	38.695223	0.000144
26.65806	0.003885	0.02089	441.1062	0.022347	444.536	232.688	0.00097	194.0619	0.75	0.44	81154.3871	81154.39	-3.5E-08	17.434878	38.744173	0.000146
26.60169	0.003915	0.021104	441.6138	0.022576	445.069	232.984	0.00097	194.3155	0.75	0.44	81245.701	81245.7	-3.3E-08	17.457144	38.793653	0.000147
26.5448	0.003945	0.02132	442.1238	0.022806	445.6044	233.282	0.00097	194.5334	0.75	0.44	81342.6752	81342.68	-3.2E-08	17.479655	38.843678	0.000149
26.48739	0.003975	0.021537	442.6362	0.023038	446.1423	234.001	0.00097	194.7144	0.75	0.44	81445.4886	81445.49	-3E-08	17.502419	38.894266	0.00015
26.11511	0.004005	0.022066	443.8787	0.0236	447.44	234.057	0.00094	187.5621	0.78	0.44	82769.6826	82769.68	-2.4E-08	17.575115	39.055811	0.000153
26.24082	0.004035	0.022106	443.9711	0.023643	447.5403	234.113	0.00096	191.9277	0.77	0.44	82174.6056	82174.61	-2.5E-08	17.569328	39.04295	0.000154
26.36506	0.004065	0.022146	444.0653	0.023688	447.6424	234.171	0.00098	196.2747	0.76	0.44	81582.6263	81582.63	-2.7E-08	17.563843	39.030762	0.000154
26.48778	0.004095	0.022187	444.1614	0.023733	447.7466	234.23	0.001	200.6016	0.75	0.44	80993.9726	80993.97	-2.9E-08	17.558669	39.019264	0.000155
26.60892	0.004125	0.022229	444.2597	0.023779	447.8529	234.29	0.00102	204.9071	0.74	0.44	80408.8733	80408.87	-3.1E-08	17.553813	39.008474	0.000155
26.72841	0.004155	0.022272	444.3601	0.023826	447.9615	234.352	0.00105	209.1898	0.73	0.44	79827.5585	79827.56	-3.4E-08	17.549284	38.99841	0.000155
26.84621	0.004185	0.022316	444.463	0.023875	448.0725	234.415	0.00107	213.4483	0.72	0.44	79250.259	79250.26	-3.6E-08	17.54509	38.989088	0.000156
26.96225	0.004215	0.022361	444.5683	0.023924	448.1862	234.479	0.00109	217.6812	0.72	0.44	78677.2069	78677.21	-3.9E-08	17.541237	38.980527	0.000156
27.07646	0.004245	0.022407	444.6762	0.023975	448.3025	234.545	0.00111	221.8871	0.71	0.44	78108.6348	78108.63	-4.1E-08	17.537734	38.972743	0.000157
27.1888	0.004275	0.022455	444.7869	0.024027	448.4218	234.613	0.00113	226.0646	0.70	0.44	77544.7761	77544.78	-4.4E-08	17.534589	38.965752	0.000157
27.2992	0.004305	0.022503	444.9005	0.02408	448.544	234.682	0.00115	230.2123	0.69	0.44	76985.865	76985.86	-4.7E-08	17.531807	38.959571	0.000158
27.4076	0.004335	0.022554	445.0171	0.024135	448.6694	234.754	0.00117	234.3287	0.68	0.43	76432.1358	76432.14	-5E-08	17.529397	38.954217	0.000158
27.51394	0.004365	0.022605	445.1369	0.024191	448.798	234.827	0.00119	238.4125	0.68	0.43	75883.8235	75883.82	-5.3E-08	17.527366	38.949703	0.000159
27.61816	0.004395	0.022658	445.26	0.024249	448.9301	234.902	0.00121	242.4622	0.67	0.43	75341.163	75341.16	-5.7E-08	17.525721	38.946047	0.000159
27.7202	0.004425	0.022712	445.3865	0.024309	449.0657	234.979	0.00123	246.4764	0.66	0.43	74804.3895	74804.39	-6E-08	17.524468	38.943263	0.00016
27.82	0.004455	0.022768	445.5166	0.02437	449.2051	235.058	0.00125	250.4537	0.65	0.43	74273.738	74273.74	-6.4E-08	17.523615	38.941366	0.00016
27.91751	0.004485	0.022826	445.6504	0.024432	449.3483	235.14	0.00127	254.3927	0.65	0.43	73749.4433	73749.44	-6.8E-08	17.523167	38.94037	0.000161
28.01267	0.004515	0.022885	445.7881	0.024497	449.4954	235.224	0.00129	258.2918	0.64	0.43	73231.7397	73231.74	-7.1E-08	17.523131	38.94029	0.000161
28.10543	0.004545	0.022946	445.9297	0.024563	449.6467	235.31	0.00131	262.1498	0.63	0.43	72720.8611	72720.86	-7.5E-08	17.523513	38.94114	0.000162
28.19572	0.004575	0.023009	446.0754	0.024632	449.8022	235.399	0.00133	265.9652	0.63	0.43	72217.0405	72217.04	-8E-08	17.52432	38.942933	0.000162
28.28349	0.004605	0.023074	446.2253	0.024702	449.9622	235.49	0.00135	269.7366	0.62	0.43	71720.51	71720.51	-8.4E-08	17.525557	38.945683	0.000163
28.36869	0.004635	0.02314	446.3796	0.024774	450.1266	0	0.00137	273.4626	0.62	0.43	71231.5005	71231.5	-8.8E-08	17.527231	38.949403	0.000163

CHAPTER 2
LITERATURE REVIEW

2.1 Concrete Beam Stress-Strain Behavior

During loading, a reinforced concrete beam will experience stress thorough the section. Composite action of the beam composer is provided by the structure composer such as concrete and steel reinforcement. In regular beam, concrete is designed to restrain the compression stress while steel restrain the tension stress. The stress-strain diagram showed in Figure *2.1* is widely understood as derivation of flexural theory with several basic behavior assumptions (Park & Paulay, 1974). The non-linear form of the stress diagram of compression area is caused by the eccentricity of the force created by moment action due to beam geometry correspond to basic concrete behavior which contains stress hardening branch and falling branch. Meanwhile, the stress of steel reinforcement is assumed as uniform along the section..

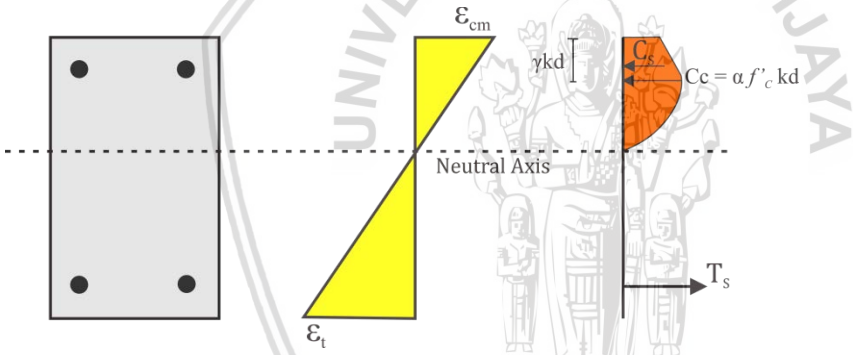

Figure 2.1. General reinforced concrete restraining force composition

The stress block assumed on the Figure *2.1* were already confirmed by C-Shape test or also known as PCA test. The PCA test will resulting on several parameters such as k_1,k_2, and k_3 that will confirm the stress block to be converted as rectangular stress block diagram for ultimate strength of concrete beam (Mattock, et al., 1961) or already wide known as whitney's stress block diagram. However, this study more focusing on the basic stress block diagram which derived from the stress-strain diagram of cylindrical compression specimens, especially to calculate the α and γ that much more convenient for non-ultimate state.

α is average stress factor that formed by integration of average stress multiplied by area above neutral axis then divided by maximum concrete stress multiplied the strain at maximum. While γ is centroid of stress block factor in perpendicular axis to the neutral axis. In Kent and Park (1971), α has been proposed as expressed in Equation 1, while γ is expressed on Equation 2.

$$\alpha = \frac{\int_0^{\epsilon_{cm}} f_c \, d\epsilon_c}{f'_c \, \epsilon_{cm}}$$ Equation 1

$$\gamma = 1 - \frac{\int_0^{\epsilon_{cm}} \epsilon_c f_c d\epsilon_c}{\epsilon_{cm} \int_0^{\epsilon_{cm}} f_c d\epsilon_c}$$ Equation 2

Several stress-strain diagram models for confined concrete have been proposed by many researchers (Park & Paulay, 1974). One proposed models is considered close to real stress-strain behaviour happen at the beam section and used as concrete stress model in this research is the model proposed by Kent and Park (1971). The function of proposed model for confined concrete is expressed in Equation 3. The function of fc is only valid for parabolic function, and limited to ε_0 equals to 0.002. The assumed value of 0.002 is still accepted for confined as the rectangular stirrups may have small influence than radial stirrups. For falling branch, another function is proposed in Equation 4 and, with linear result of graph.

$$f_c = f'_c \left[\frac{2 \in_c}{\epsilon_0} - \left(\frac{\in_c}{\epsilon_0} \right)^2 \right]$$ Equation 3

2.1.1 Confinement Effect of Rectangular Stirrups

Stirrups or spiral hoops can be considered as passive confinement in reinforced concrete beam. However, they have very much different effect than triaxial confinement subjected by liquid pressure. According to previous study of concrete under confinement, stirrups or hoops affect and work as confining device to concrete only if they stressed enough to bear the lateral strain of inner concrete. When the stirrups or hoop is started to stressed, microcracks and strain of the concrete will be restrained by the stirrups or hoops and make the concrete having higher strain before failure. Although significant and effective passive confinement is only achieved by circular hoops, the study also shown that rectangular stirrups still giving better behavior in extending the beam ductility (Park & Paulay, 1974).

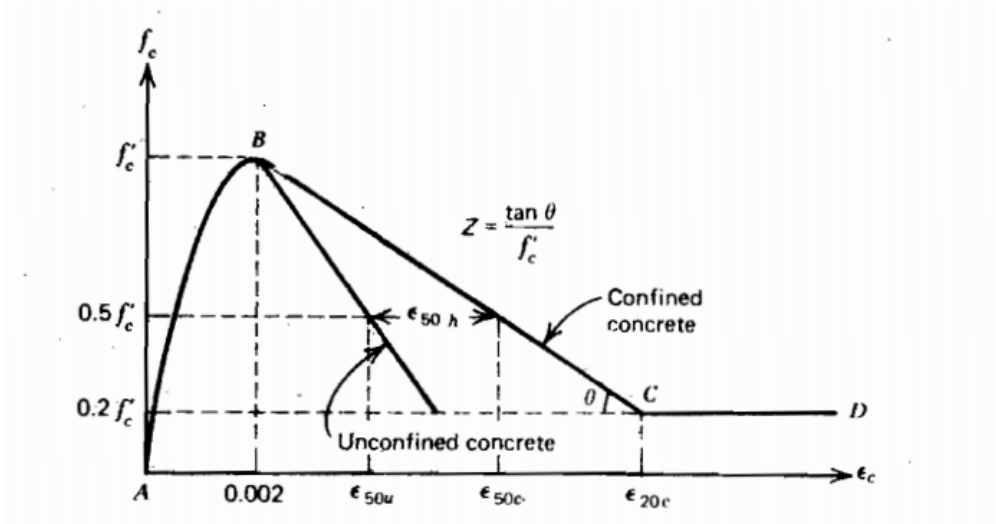

Figure 2.2. Reinforced Concrete Stress-strain under rectangular stirrups confinement (Park & Paulay, 1974)

However, previous study (Kent & Park, 1971) has prove that there is no or very small increasing of concrete stress with given passive confinement. Kent and Park (1971) proposed the effect of stirrups confinement by introducing parameter of Z which govern the falling branch of the conrete stress-strain curve as shown in Figure 2.2 which is also derive flexure member stress-block. The falling branch of concrete confined by stirrups is expressed in Equation 4 while the Z parameters is expressed in Equation 5.

$$fc = f'_c[1 - Z(\epsilon_c - \epsilon_0)] \qquad \text{Equation 4}$$

$$Z = \frac{0.5}{\frac{3 + 0.29f'c}{145f'c - 1000} + \frac{3}{4}\rho_s\left(\sqrt{\frac{b''}{S_h}}\right) - \epsilon_0} \qquad \text{Equation 5}$$

ε_0 is the strain when concrete reach f'c, ε_c is the concrete strain during loading, ρ_s is the stirrups area ratio to the concrete section, b" is the confined area by the stirrup, and S_h is stirrups spacing. The Equation 5 is already set to SI units, with the literature may be showed in British unit.

2.2 Limit State of a Structure

Generally, a structure is considered failure if the structure has collapse and cannot carry the designated load. However, the term “failure” may covering a wide range of type of failure to a structure and very much depend on the purpose of the structure. With different purpose of structure, comes different terms which we called it a limit state.

A limit state of a structure may be defined as the boundary between the desired condition and undesired condition that may happen to it (Nowak & Collins, 2000). For example, limit state for a bridge span may defined by particular deflection value. The bridge considered as fail when the displacement exceed the limit that have been specified. The bridge may also another limit state such as crack width and fatigue limit at the same

time. Then, the failure of the bridge determined by the first limit state exceeded. With this concept of failure by limit state, a failure of a structure may be defined by several limit state, included first crack, yield of reinforcement, and other limit state that may be added by designer considering function of the structure.

2.3 Deterioration of Reinforced Concrete Structure

2.3.1 Cracks on Concrete Beam

Crack on reinforced concrete (RC) beam may be induced by several causes, such as overloading, shrinkage during concrete hardening, or delamination over different material or time-gap in its casting (Leonhardt, 1988). However, the principal causes of a concrete to crack is the tensile stress of the concrete that exceeding the designation tensile strength. Code provision (BSNI, 2013) has been define the stress of the concrete that will induce cracks as expressed in Equation 6.

$$f_r = 0{,}62\ \lambda\sqrt{f'_c} \qquad \text{Equation 6}$$

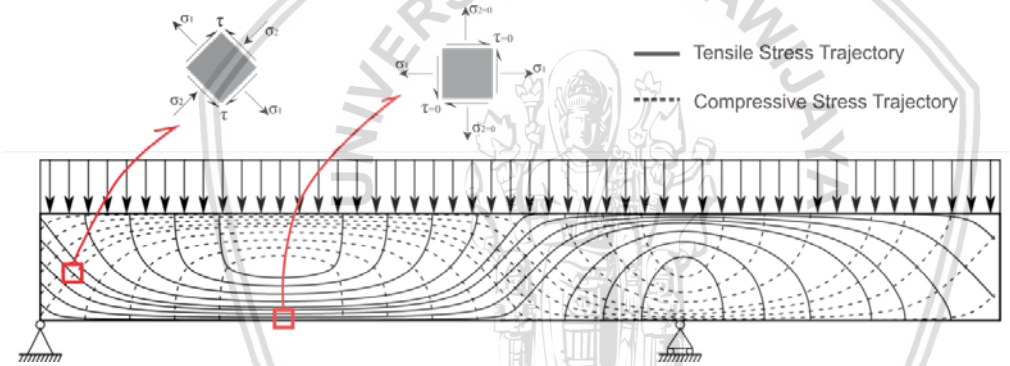

Figure 2.3. Beam Stress Trajectory subjected to Uniform Load

The tensile strength of concrete is well known to significantly small compare to the compressive strength. Tensile strength is also usually assumed be neglected on regular reinforced concrete beam design (Park & Paulay, 1974). However, the properties still very important that a small crack happen on a structure will induce deterioration to the structure such as corrosion attack by sulphate and salt ion.

2.4 Concrete Deterioration

Structural failure is commonly induced by insufficient strength of a part of the structure, which in reinforced concrete it may be started by either failure of the steel reinforcement or the concrete. In several case, the failure were simply failed by insufficient available strength compared to the given load or stress, while other were caused by deterioration of one of its structural composer, or all together at the same time.

2.4.1 Composer Deteroriation

Deterioration of concrete structure may happen to a part or all structure depending on the situation given. An aggressive environment such as high concentration of sulfate or chloride may deteriorate both the concrete and its reinforcement rebar, while exposed normal environment will majoring in attacking the rebar. Several laboratory experiments attempting to simulate the aggressive environment in accelerated way were conducted by many researchers (Badawi & Soudki, 2010) (Rio, et al., 2005). The result of their experiment show that aggression attacks the reinforcement rebar makes the specimens loss the area of steel reinforcement by corrosion and also causing concrete cover to peel, which in real environment., the corrosion may be progress even faster. The loss steel reinforcement area also makes the specimens to fail suddenly without any sign, which is strictly avoided in most designed structure.

As a solution to the deteriorate problem, in the study several repair procedure have been proposed to make sure the deteriorated structure may service for expected age. Repair procedure such as patch repair is conducted to replace the spalling and cracked concrete cover using repair mortar, while the other procedure are using strengthening rebar addition to regain the flexural strength of the structure. Both of the repairing procedure will be applied to this current research. However, deterioration will be carried by mechanical action of preloading session. Brief discussion for both literature and repairing detail method will be discussed on other point of CHAPTER 2 and CHAPTER 4 respectively.

2.4.2 Microscopic Deterioration during Loading

Concrete is a material with widely well-known has non elastic properties with non-linearity of stress-strain behaviour, and often called brittle material. The non-elastic behaviour is caused by forming micro cracks of concrete in every given stress. Therefore, a reinforced concrete beam will have tendency to deteriorate after receiving a certain degree of load. Therefore, the regular stress block of concrete derived from stress-strain calculation is no longer précised for strength calculation. Hence, a new approach for reinforced concrete beam after given preload is needed.

Early studies of concrete have considered that stress strain behaviour of concrete is consists of two linear, elastic and brittle (ACI-Committee-224, 1998). The idea considers the concrete will perform in elastic manner until a certain degree of stress than start to form microcracks then failed in brittle manner. However, the development of concrete studies of around 1970s found that cement paste is non-linear softening materials and the non-linearity is much depends on the constitutive of both cement paste and aggregate. Thus may explain that the concrete does not have elasticity like the steel does. The behaviour make concrete having a permanent plastic deformation after given load.

Extensive observations have been conducted to establish the relationship of concrete after given load and the stress-strain behaviour after receiving load (Aslani & Jowkarmeimandi, 2012) (Barros, et al., 2000) (Mander, et al., 1988) (Otter & Naaman, 1989). On the references, the term ε_{pl} of plastic strain is used to describe the permanent

deformation in the term of length or size extension of concrete after given pre-load. The studies have also shown that the curve of repeated loading will always form the envelope curve of stress-strain curve of concrete under monotonic loading (Barros, et al., 2000) (Mander, et al., 1988). Many study of this plastic strain behavior were performed to establish the behavior of concrete under cyclic load such as in seismic activity or under earthquake load.

Several researcher has found that in short-time loading duration, with the stress of loading is not exceeding than 30% of its compressive strength, the concrete will not form an additional crack than earlier cracks induced by shrinkage (Hsu, et al., 1963). After exceeding 30% stress, microcracks are occur on cement paste and combined to form a parallel cracks and propagate thorough matrix with larger cracks form.

2.5 Concrete Behavior during Repeated Loading

Vast experiment and report of concrete behavior during cyclic loading has been done by many researchers. Some of the reports has been discussing on high rate cyclic loading behavior (Otter & Naaman, 1989) while other developing repeated loading behavior of concrete in quassi-static loading (Mander, et al., 1988) (Aslani & Jowkarmeimandi, 2012). The reports with also supported by extensive laboratory experiments show that concrete stress during repeated loading is always forming the envelope curve of normally quassi-static loading stress-strain behavior. The term of plastic strain of ε_{pl}, ε_{un}, f_{un}, f_{new} are used by the previous researcher.

2.5.1 Repeated loading by Otter and Naaman

After concrete experienced a certain magnitude of load there will be a plastic strain result on the concrete. And that point of plastic strain will be a starting point of strain for next given load. The model of plastic strain due to repeated or cyclic loading has been proposed by previous researcher (Otter & Naaman, 1989) by count the key points of cyclic response as shown in Figure *2.4*.

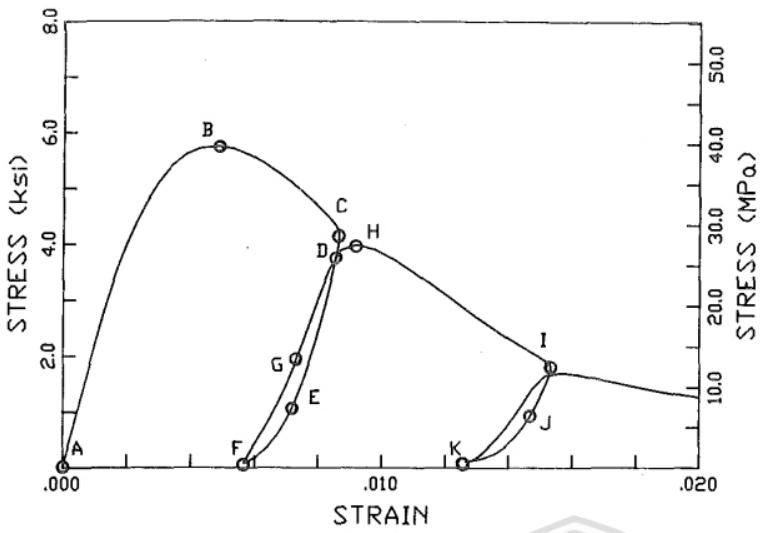

Figure 2.4. Key Points of Cyclic Response (Otter & Naaman, 1989)

Point C and I of Figure *2.4* are the unloading point, where the load is started to be released. Point F and K is considered as plastic strain. Point D is the intersection point of the reloading strain and the unloading strain path. Point H is reloading point as it will create a continue envelope curves. Point B is the inflection point that marks the maximum stress and ε_0 of the concrete.

Analytic model for plastic strain point of the concrete has also been proposed by the researcher (Otter & Naaman, 1989) as shown in Equation 7. Where ε_p = plastic strain, ε_0 = Strain at inflection point of maximum stress, ε_u = unloading strain, and k_U = unloading constant. Based on their observation, 0.8 is proposed as unloading constant that will fit the expression formula. For the stress of re-loaded condition, a single continuous function was proposed by early researcher as expressed in Equation 8.

$$\frac{\epsilon_p}{\epsilon_0} = \frac{\epsilon_u}{\epsilon_0} - k_u\left(1 - e^{-\epsilon_u/(k_u\epsilon_0)}\right) \qquad \text{Equation 7}$$

$$\frac{f}{f_{un}} = (1-p)\left(\frac{\epsilon - \epsilon_p}{\epsilon_u - \epsilon_p}\right) + p\left(\frac{\epsilon - \epsilon_p}{\epsilon_u - \epsilon_p}\right)^{n_{uc}} \qquad \text{Equation 8}$$

2.5.2 Unloading and Reloading Branches by Mander, Priestley and Park

Study on the reports by Mander, et al., (1988) devide the cycling process into two parts of unloading process and reloading process. The unloading process will determine the plastic strain produced after given loading which is stop to unloading strain ε_{un}. ε_a is needed to determined first. ε_a is taken as the tangential intersection line with first loading slope of Ec from f_{un} as explained in their report.

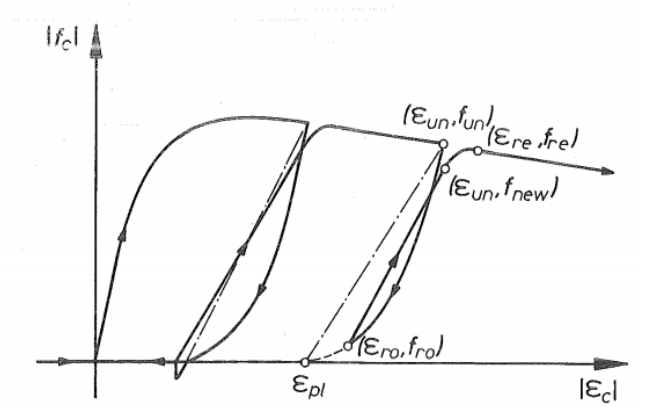

Figure 2.5. Stress-Strain curve for Reloading Branch

ε_{pl} may stay in stressed or unstressed, depending on given unloading, whether fully unloaded or partially unloaded. If concrete is given partial unloading, means that there present f_{ro} stress remains in the structure, and leave ε_{ro} as starting point for next reloading process.

Reloading process will again stressing the unloaded concrete. However, if the unloading process is given after concrete passing its ε_0, the concrete will not reach the same stress with the same given strain. Introducing f_{new} as new stress point at the same strain was unloading ε_{un} of is performed. 0.92 is proposed by the researcher as coefficient of the f_{new} as the function of f_{un} and f_{ro}.

$$\varepsilon_a = a\sqrt{\varepsilon_{un}\varepsilon_{cc}} \qquad \text{Equation 9}$$

$$a = \frac{\varepsilon_{cc}}{\varepsilon_{cc} + \varepsilon_{un}} \qquad \text{Equation 10}$$

$$f_{new} = 0.92 f_{un} + 0.08 f_{ro} \qquad \text{Equation 11}$$

$$E_r = \frac{f_{ro} - f_{new}}{\varepsilon_{ro} - \varepsilon_{un}} \qquad \text{Equation 12}$$

$$\varepsilon_{re} = \varepsilon_{un} + \frac{f_{un} - f_{new}}{E_r\left(2 + \frac{f'_{cc}}{f'_{co}}\right)} \qquad \text{Equation 13}$$

2.5.3 Mathmatical Model of Stress-Strain for Concrete Under Cyclic Loading by Ashlani and Jowkarmeimandi.

Similar model to earlier researcher (Mander, et al., 1988) (Otter & Naaman, 1989), Aslani and Jowkarmeimandi (2012) propose further development for practical significance of the mathmatical model of the problem. The envelope curve, unloading curve, partial unloading and reloading curve has been developed and described in summary on their

report. The empirical model is also confirm other experiment result for comparation for the model accuration.

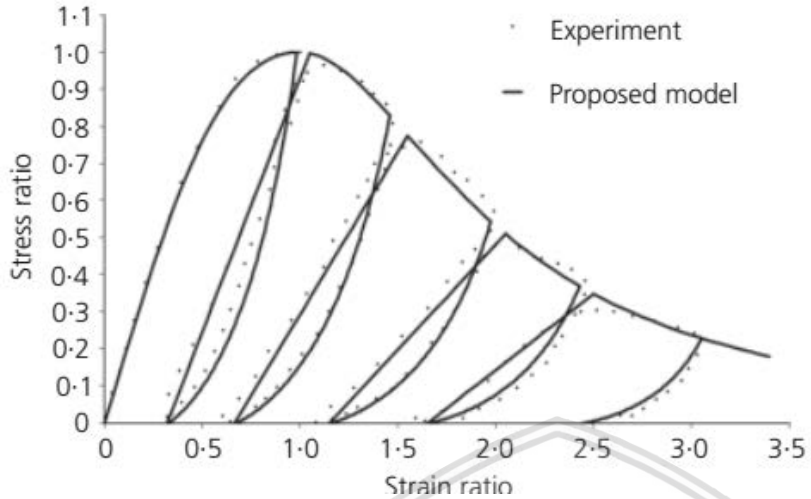

Figure 2.6. Comparison of experimental data reported by Aslani and Jowkarmeimandi (2012)

$$f_c = f_{ro} + E_r(\varepsilon_c - \varepsilon_{pl}) \qquad \text{Equation 14}$$

Different than proposed by Mander, Priestley and Park (1988), f_{new} of the concrete stress loaded at same strain to unloading strain is exspressed by Equation 15. In the analysis, this expression showing much realistic and non linear solution for concrete deterioration during repeated loading than model proposed by earlier study. For total unloading, ε_{ro} may substitute by $\varepsilon_{pl.}$ Reloading curve is expressed by Equation 15.

$$f_{new} = f_{un}\left[1 - 0.09\left(\frac{\epsilon_{un}}{\varepsilon_{ro}}\right)^{0.5}\right] \qquad \text{Equation 15}$$

$$f_c = f_{un}\left(\frac{1 - [(\varepsilon_c - \varepsilon_{un})/(\varepsilon_{pl} - \varepsilon_{un})]}{1 + 1.2[(\varepsilon_{un} - \varepsilon_{un})(\varepsilon_{pl} - \varepsilon_{un})]}\right)^{1.2} \qquad \text{Equation 16}$$

2.5.4 Repeated Loading of Steel Reinforcement

Steel bar usually used as concrete reinforcement has known have three distinct state during given stress. There were elastic, yield plateau and strain hardening despite each state is different for every steel grade. If creep is not under consideration, steel rebar has known to behave as always back to original position of unloading strain and stress when receiving repeated loading (Park & Paulay, 1974). Then, when the stressing is released at the strain hardening state, re-stressing will make the steel reaching its original un-stressing position with gradient of E_S before continue to form its original monotonic stress-strain curve. The behavior may be explained on Figure *2.7.*

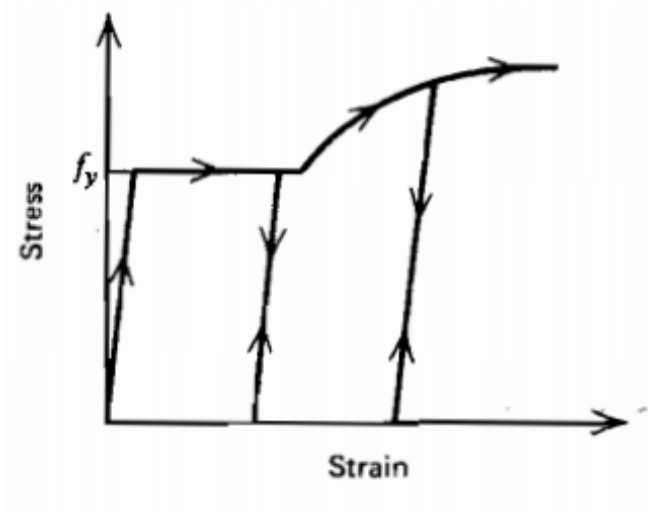

Figure 2.7. Stress-strain curve of steel rebar under repeated loading

2.6 Bond Strength and Anchorage Development of Steel Reinforcement

The bond between concrete and reinforcement steel has been acknowledge as the key to performance of reinforced concrete structure since early study of concrete (Committee-408, 2003). This is obvious since reinforced concrete is a one type of composite structures that combine the benefit of compression strength of concrete and high tensile strength of steel. Then a bond strength to make those two materials work together is a necessity. The interaction and force restrain mechanism has been explained and imaged in Figure *2.1*. To define the repaired this current experiment beam behaviour, which repaired using additional rebar, the mechanism of this bond strength model has to be well understand.

2.6.1 Yield Penetration Mechanism

Three rebar reinforcement stress regions have been discussed on the previous research (Alsiwat & Saatcioglu, 1992). The sub region of steel reinforcement is distinct by the steel stress state whether its elastic, yield or in strain hardening state. However, these distinctions are not necessarily always happen, rather depend on the length of the reinforcement development length. Short length development may result on the steel slip with it only experience yield state or even still in elastic state. With sufficient length it is possibly to apply those three regions in the stress analysis. The scheme is explained in Figure *2.8*.

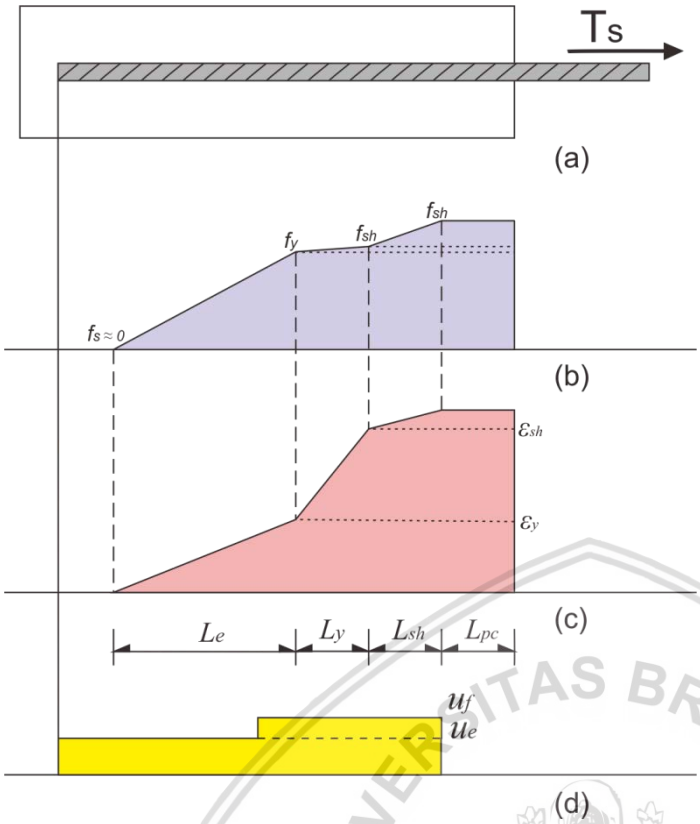

Figure 2.8. (a) Steel reinforcement embedded in concrete (b) Stress distribution (c) Strain distribution (d) bond stress between steel and concrete (Alsiwat & Saatcioglu, 1992)

When steel reinforcement passed its yield state, strain hardening is taking over and create more displacement. Large displacement creates slip to concrete which considered that no more bonding strength available in the concrete pullout area of Lpc. The stress released by Lpc then bear by adjacent steel area of Lsh which considered as steel area experiencing strain hardening, followed by area experiencing yield state and elastic state, as explained by Figure *2.8* (b).

Alsiwat & Saatcioglu, (1992) has summerized the stress formula created by a force acting on the certain length of rebar as expressed in Equation 17 with fs is steel stress, d_b is bar diameter and l is the length of rebar. While the length of l_d required for the steel could reach yield state is provised by Equation 18 in inch and psi. l_d expressed by Equation 18 may apply as elastic length of Le of Figure *2.8* (c).

$$u = \frac{U}{\Sigma_o} = \frac{\Delta T}{\Delta l \Sigma_o} = \frac{\Delta f_s A_b}{\Delta l \Sigma_o} = \frac{\Delta f_s d_b}{4 \Delta l} \qquad \text{Equation 17}$$

$$l_d = \frac{440 A_b}{K\sqrt{f'_c}} \frac{f_y}{400} \qquad \text{Equation 18}$$

To calculate the embedded nominal stress of the concrete, Alsiwat and Saatcioglu (1992) has summarize the nominal bond stress as a function of rib dimension and space, and square root of f'c. Equation 19 expreses the stress rest on the steel bond strength, with

S_L as the space between ribs and H_L is the high of rib measured from the round surface of the steel. This formula may apply for both yield region and strain hardening region. Then, the yield penetration is may cosidered be limited to Lpc + Lsh + Ly using Equation 20, while Le has been considered to remain elastic.

$$u_f = \left(5.5 - 0.07\frac{S_L}{H_L}\right)\sqrt{\frac{f'_c}{27.6}}\ \text{MPa} \qquad \text{Equation 19}$$

$$L_y = \frac{\Delta f_s d_b}{4u_f} \qquad \text{Equation 20}$$

2.6.2 Analysis of Hook Development

If straight development of steel reinforcement does not has enough length to restrain tension force, hook development is needed to applied. Code provision (BSNI, 2013) has regulate that hook length of reinforcement rebar is $12d_b$, which ACI code provision limit the length development is also around that value with no strength formula to calculate the force strength the hook could carried. Previous researcher (Alsiwat & Saatcioglu, 1992) has also been summarizing the hook role on the stress and strain development of anchoring steel reinforcement. Figure *2.9* explain that the elastic length development can considered continuing to the hook branch as continuing stress-and strain. Then, Equation 18 may apply to the hook length development as well.

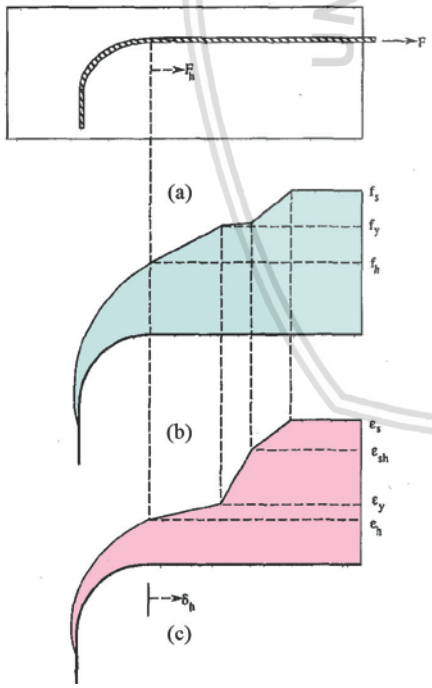

Figure 2.9. (a) Hooked reinforcement in concrete (b) Stress Distribution along the length (c) Strain distribution (Alsiwat & Saatcioglu, 1992)

2.7 Reinforced Concrete Failure Mechanism on Shear

Shear in reinforced concrete structure has complex mechanism. many published paper shows the problem with complexity of how the shear failure occur in a such structure

(Park & Paulay, 1974). However, there evidence that shear resistance is combination for several restraining action such as,

1. Shear force of compressed concrete acting along compression section Vc,
2. Dowel mechanism transmitted by flexural reinforcement in (usually) a cracked section V_T,
3. Shearing mechanism by interlocking of aggregate particles v_a,
4. Vertical reinforcement force created by stirrups or hoops Vs.

which may be explained by Figure *2.10*.

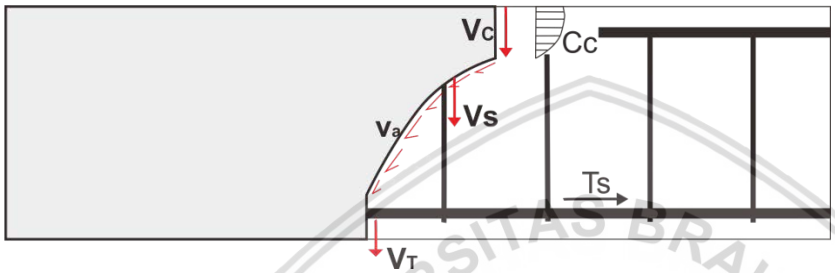

Figure 2.10. Shear restraining mechanism on reinforced concrete beam

2.8 Repair Method using Strengthening Devices in Previous Researches

2.8.1 Behaviour of Patch-Repaired Concrete Structural Elements under Increasing Static Loads to Flexural Failure (Rio, et al., 2005)

A research observing patch repair performance on prior reduced strength by accelerated corrosion process has been reported by Rio, et al. (2005). In addition, repair rebars were also added in several of their specimens to replace the loss steel area due to corrosion process. However, the result of the final test does not showing a satisfactory strength for the repaired beam. The outcome of adding strengthening rebar yield the same value of ultimate load with other specimens which only repaired by patch repair.

The specimens are repaired by three different patch materials, and strengthening rebars are added for particular specimens. The loss of reinforcement section area is varying from 8-24% of its area due to corrosion process. Its reported that the specimens, which strengthened by a ϕ8mm rebar, as shown in Figure *2.11*, failed suddenly in brittle manner, show that the strengthening rebar did not perform well. The author of the report mentioned that an adequate anchorage length is needed especially exceeding to the outside of maximum moment area, which will be applied on this current research as specimens repair variable.

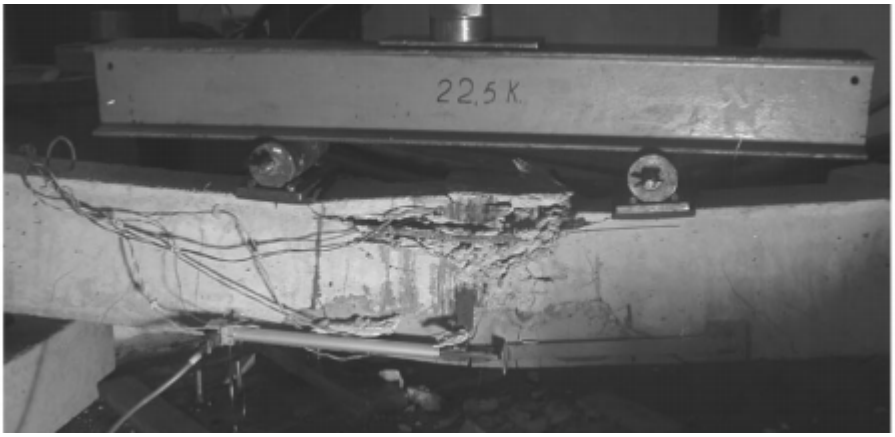

Figure 2.11. Corroded Strengthening Beam Tested by Rio, et al. 2005

The absence of the stirrups at the mid span of the beam was also pointed as one of the cause of brittle failure. With large loss area, the specimens did not have sufficient tensile restraining part and the compression area of the specimens was not confined which will limit the concrete compression strain. Instead, the stirrups on this current research will be made narrower in spacing which aimed to confine compression concrete and limiting the crack occurring as will be briefly discussed on chapter 4. Such precaution is necessary as decreasing strength treatment of this current research is performed by preloading, that may break the specimens that could make the repair much more difficult to perform, yet having unreliable result.

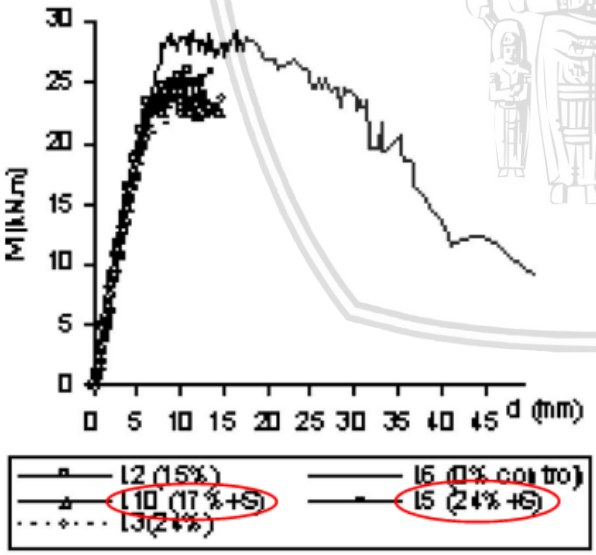

Figure 2.12. Testing result of repaired beam specimens performed by Rio, et al. 2005 (the S suffix, mark the specimens with strengthening rebar)

2.8.2 Central peeling failure behavior of polymer cement mortar retrofitting of reinforced concrete beams (Satoh and Kodama 2005)

Reinforced Concrete beam which retrofitted by anchored strengthening rebar were reported by Satoh and Kodama (2005). The result of some of tested specimens showing an

expected behavior that the anchored strengthening rebar, together with overlayed PCM mortars, forming composites action with substrate structure. The report show that the bond behavior at PCM-Substrate Concrete interface influence the structural behavior of the tested beams and slabs. Debonding failure behavior was studied by the author and has objectives to derive a relationship between debonding failure mechanism and strengthening procedure.

The beam specimens were made with length variation from 1000mm to 2700mm, which affecting the shear span and its fail behavior. The strengthening rebars were anchored using dynabolt look achors which tied to the rebar using steel plate. The strengthening rebar anchoring were placed at almost the end of the length, then all the bottom of the specimens were shot (sprayed) by PCM (Polymer Composite Mortar). The result shows that specimens with 8.0 shear span ratio, failed by flexure manner with no overlay peeling. Other retrofitted specimens with less shear span ratio failure with either peeling in central zone or at anchorage zone which shown on Figure *2.14*. central peeling were occurred when the strain of the strengthening bar exceeding the yielded strain, which show a optimum strengthening rebar work but failed on shear bond strength.

The report show that anchoring the strengthening rebar could solve the rebar-substrate bonding problem. The comparison with normal tested beam also show significant incrasing flexural strength. But the way of anchoring detail and PCM shotcrete method may considered as quite difficult method for other practician. This current research will take similar repairing approach but tend to be a simple and traditionaly look method that may be done by any practician as long the engineering adjustment is applied.

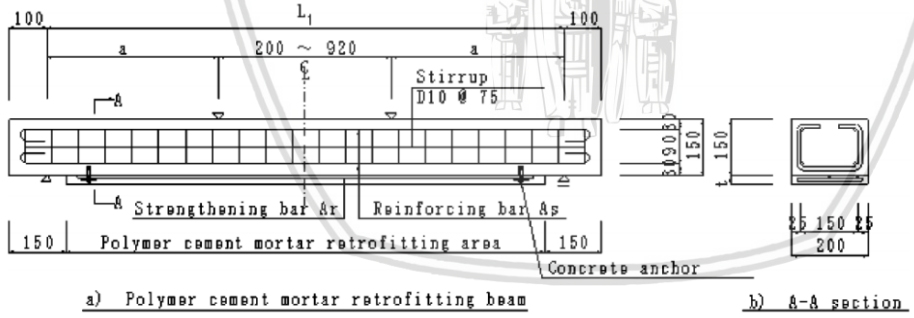

Figure 2.13. Strengthening Detail applied by Satoh and Kodama 2005

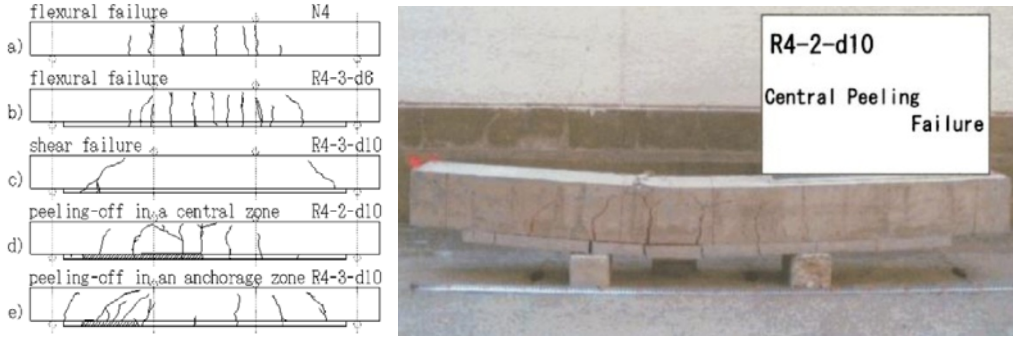

(a) (b)

Figure 2.14. (a) Several failure mode recorded (b) Central peeling failure picture (Satoh & Kodama, 2005)

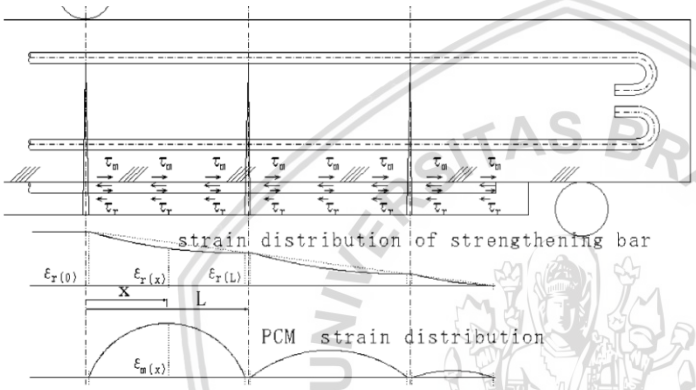

Figure 2.15. Shear Stress Distribution Scheme Proposed by Satoh and Kodama (2005)

2.8.3 Strengthening and Repair of Reinforced Concrete Using External Steel Plates (Aykac, et al. 2013)

Externally platted strengthening is a well-known method for strengthening a concrete structure with a simple technique. Another RC beam strengthening method which has been reported by Aykac, et al. (2013) is using external steel plate anchored to the bottom side of repaired beam specimens. Various 1.5mm to 6mm thick plate were installed as tensile reinforcement for both pretested and un-pretested beam. The plates were extended from one support to another, so that the bottom of the beams were covered by steel plate. The plates were anchored using M12 high strength bolt, with 200mm anchoring space for some specimens.

The result of the final test showing a significant increasing strength compared to the control (basic) beam for all non-pretested specimens. The increasing strength was the outcome steel plate tensile strength contribution which 1.5mm thick plate is may equal to adding more than 1xϕ19mm reinforcement rebar to the cross section, but in more lever arm length to the Neutral Axis. However, for the heavily strengthened beam, which using 6mm thick plates, the deflection before failure show significantly lower than control beam, which show the beam was over reinforced that the compression concrete crushed before further displacement, despite its significantly larger restrained load.

The externally strengthening plate seems showing a promising result. However the effort to install and plating cost is quite high, despite its simplicity and low technology procedure. Other problem was also the plate anchor may installed prior to concrete cover, which may not transfering the given stress properly to the inner beam core. Anchoring system to un-confined concrete, which not restrained by stirrups, will also a major problem of failed by plate peeling followed by its anchored concrete cover. As mentioned by the report, that, side collars and more deeper anchor is needed to significantly reduce the premature peeling of the beam specimens.

(a) (b)

Figure 2.16. (a) Steel Plating Application (b) End Side Collar of the Specimens (Aykac, et al., 2013)

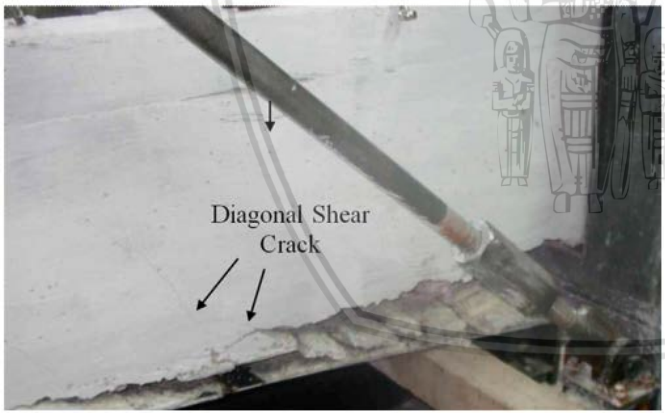

Figure 2.17. Shear Peeling between the plate and concrete substrate

2.9 Damage Modeling in Finite Element of Composite Structure

2.9.1 Bond Behaviour of Composite Material

Several modelling of concrete composites system involving damage plasticity model have been done by many researcher. With damage plasticity model, a failure of structure, which always ignited by crack can be simulated, together with its propagation behaviour. In general, damage model works on measuring the mesh stress, which the limit stress has been defined, and then “delete” the mesh if its stress exceeding the limit. The model is mimic how the crack happening in real practice.

An interfacial bond behaviour of eternally bonded FRP to a RC beams which has been reported by Lin and Wu 2016 shown a well modelled composites structure. The concrete is modeled by damage plasticity available in finite element software ABAQUS. The finite model is using a constitutive model of concrete materials as shown in Equation 2. In which σ_e and ε_e are compressive stress and strain respectively, σ_p and ε_p are experimentally determined maximum stress and its coressponding strain, which are in the research set to f'_c and 0.002 respectively. However, because this current research ispossible to find out the maximum tensile strain of the concrete, the maximum strain will be taken from the loading test of the control beam, which will be discussed on Chapter 4.

$$\sigma_c = \frac{E_0 \varepsilon_c}{1 + (E_0 \varepsilon_P / \sigma_p - 2)(\varepsilon_c / \varepsilon_p) + (\varepsilon_c / \varepsilon_p)^2}$$ Equation 21

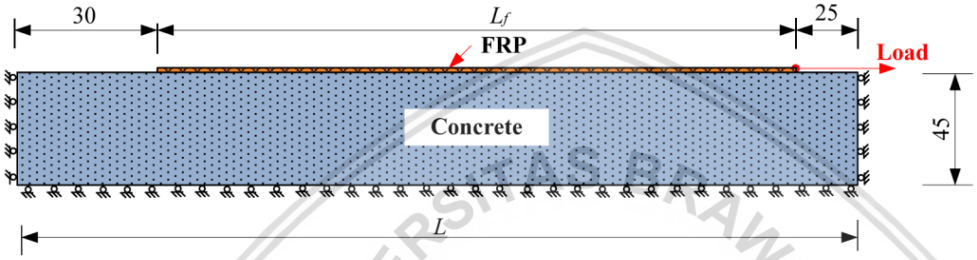

Figure 2.18. Pull out test model used (Lin & Wu, 2016)

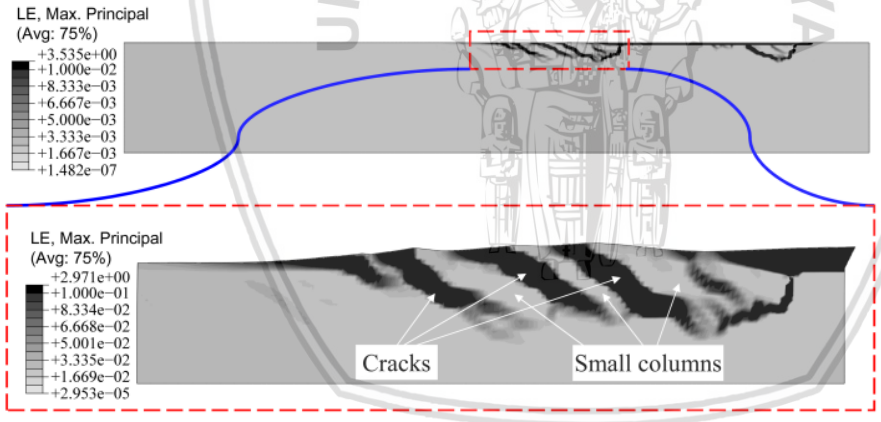

Figure 2.19. Testing result of one of the specimens

In their study, only the desirable and adequate failure mode is considered. Therefore, undesirable failure modes, such as interfacial debonding between FRP layer and concrete substrate which "glued" by epoxy layer are ignored. It is clear that the failure are modelled only by bond failure between substrate particles –concrete particles, where the constitutive properties of tensile strength were defined to the model. However, although several peeling fail of FRP Layered specimens on the other research observation were occur between concrete substrate itself, other peeling behaviour were occur at the interfacial bond between FRP sheet and substrate concrete –fail in epoxy layer- as reported by Li and Kai (2011). Hence, in this current research, the interfacial bond strength between

patch material and conctrete substrate will be briefly examined and modelled to gain more realistic behavior of the patch repair treatment.

2.9.2 Concrete Column Plastic Hinge Relocation as Damage Repair Reported by Rudledge, et al.

A Comprehensive study of plastic hinge relocation as a column repair has been reported by Rudledge, et al., (2013). There are three full scale bridge column specimens used in the research. All column lower level reinforcements has been deteriorated by corrosion with concrete covers have been spalling. One of them has been reported rupture almost completely as seen in Figure *2.20* (a). according to the report, the columns has been subjected by modelled earthquake load and has pass their ultimate load. The tensile strength of the reinforcement has been passed and experience rupture for some specimens.

(a) (b)

Figure 2.20. (a) Steel reinforcement deterioration and concrete cover spalling (b) column repair using CFRP (Rudledge, et al., 2013)

Repair using CFRP and pacth materials filling the spalled concrete cavity was performed to restore column strength. The results of reloading test shows that strength restoration can be achieved by repairing with confining the deteriorated area of prior plastic hinge which the structure will create new plastic hinge adjacent to the repaired area.

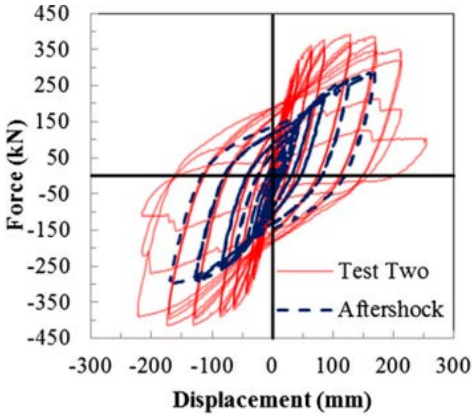

(a) (b)

Figure 2.21. (a) Hysteretic load-displacement curve (b) load test of repaired column

The result of conducted reload test as shown in Figure *2.21* (a) and (b) has shown that the repaired columns strength have been restored and reach even higher restraining load. The higher load may be achieved by stiffening column base by given CFRP lamination and CFRP anchoring device as detailed in the report. Therefore, with stiffer base, required load to create ultimate moment is need to be increased as the low stiffness of column length is decreased. According to the Figure *2.22*, the moment capacity of the concrete column has been partially increased by the applied repair. Thus makes the plastic region of column moves to higher level where the demand moment meets the moment capacity of the column.

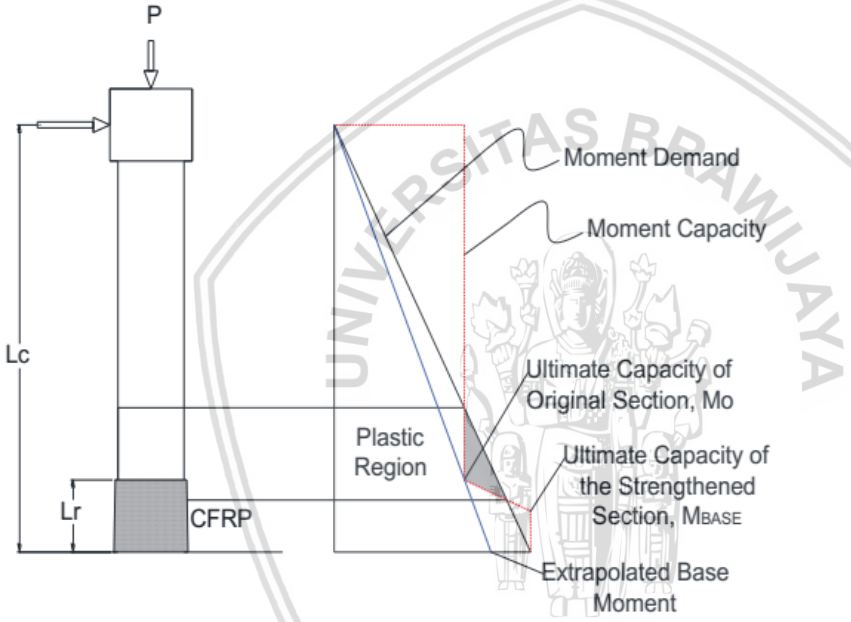

Figure 2.22. Scheme of nominal moment region of repaired column along its length

CHAPTER 3
CONCEPTUAL FRAMEWORK

3.1 The Framework

A reinforced concrete beam which has reached ultimate bearing capacity will deteriorate and leaving a plastic deformation after the load has been released. A large number of repair methods has been practiced and reported by many practician with many kind of behavior. Especially for beam structure, high bond strength is not the only requisite for applied repair material. The compatibility, deflection behavior and post fail behavior are other things that engineer have to be confirmed to make sure the repair works is considered safe. This study will experiment the beam behavior which has been deteriorated by mechanical means, and apply some repair procedure of patch repair with addition of repair rebar.

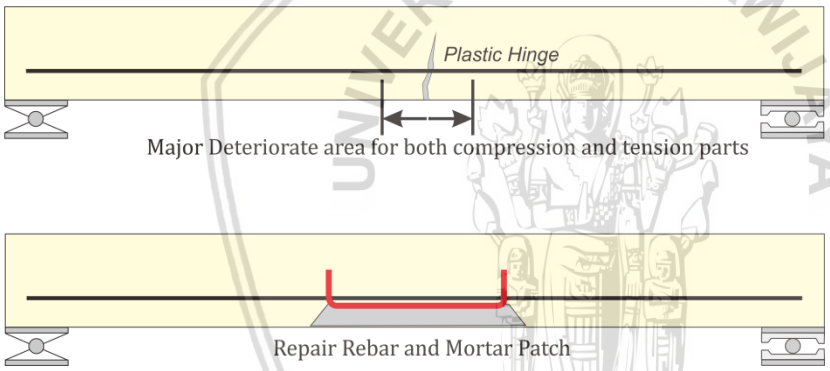

Figure 3.1. Repair concept of repair the deteriorate area by repair rebar and mortar patch

Similar with previous studies of reinforced concrete repair (Rio, et al., 2005) (Rudledge, et al., 2013), the concept of repair procedure conducted in this study is to repair the deteriorated area which contains deteriorated compression concrete and tension steel reinforcement as the concept may be enhanced by Figure *3.1*. According to the theory of plastic hinge development discussed on CHAPTER 2, reinforcement next to yield penetration area may remain in elastic state. According to the study of concrete under repeated loading, compression concrete may still has available strength to carry the load despite prior developed plastic strain.

As for discussion convenience, introducing two systems that will distinct the post repaired beam structure entities. The substrate system and repair system. Substrate system is the original body beam specimens being repaired by repair system. The repair system is the unity of repair component of patch material and repair reinforcement rebar. Reason for distinct the two is that each of them has tendency to acting separately in particular condition, or being debonded. The base concept of the experiment is to observe the overall

repaired specimens which contain those two entities and also the detail interaction between them.

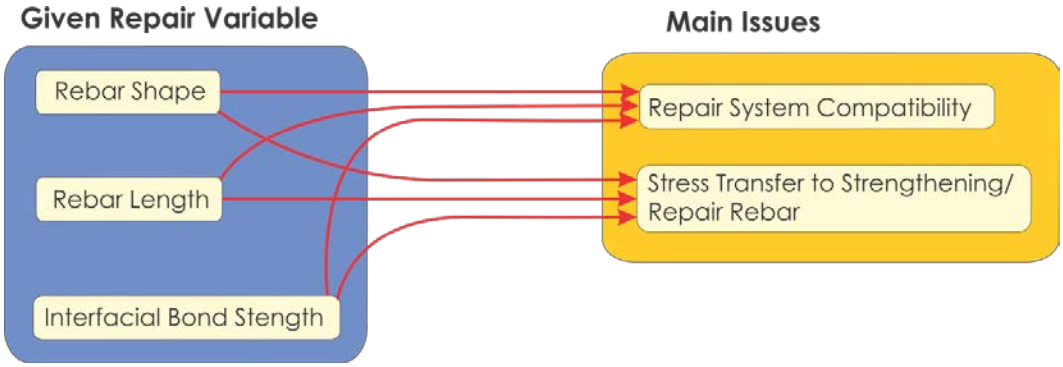

Figure 3.2. Conceptual Framework of the research

As mentioned on research problem, the main issues that will be studied on this research are the repair system compatibility and the stress transfer of strengthening or repair rebar. To understand the compatibility and stress-transfer on strengthening rebar added on patch repair, several variables will be given to the experiment object/specimens such as repair/strengthening rebar shape, rebar length and patch material properties correspondent to its interfacial bond-strength to substrate material. Figure *3.2* show the relationship between the given variable and the main issues to be studied.

To accommodate the research purposes, three type of repair system are employed to the specimens,

1. Repair system with staple shape reinforcement rebar, short as staple rebar,
2. repair system with straight shape reinforcement rebar patched with Ordinary Cement Mortar (OCM),
3. Repair System with straight shape reinforcement rebar patched with Polymer Cement Mortar (PCM).

As for comparison with different type of deterioration, two limit states are also given to beam specimens,

1. Beam specimens preloaded until reach yield state,
2. Beam specimens preloaded until reach ultimate state.

Good repair practice is achieved by adequate bonding strength of repair system to the substrate system. Repair system with staple rebar is used to give better stress transfer from substrate system to the repair system the anchor legs of staple shape is planted to the substrate system to receive stress from substrate concrete then transferred to its own body. Bond strength of the patch material is also expected to give more compatibility effect during loading process.

From the research reported by Satoh and Kodama (2005), it is conclusion that an anchoring to the substrate material will give a better stress-transfer from the substrate structure to the added strengthening rebar. However, they applied the anchor on the concrete cover surface which may break the concrete due to unconfined and un-restrained concrete by any stirrups. Anchoring method will be adopted to this research by using staple shape rebar. For better achoring system, the repair/strengthening rebar will be direcly anchored to concrete confined by stirrups by prior concrete cover removal.

Differently, repair system with straight shape has known to depend completely to the interfacial bonding strength of patch material. Interfacial bond strength is also has a significant relationship to the compatibility as well as stress transfer to the repair system (Satoh & Kodama, 2005) (Lukovic, et al., 2012) (Minoru, et al., 2001). Hence, two patch materials are employed to this shape of rebar. The ordinary cement mortar (OCM) is expected to give lower bond strength than polymer cement mortar (PCM). With higher bond strength of patch repair, beam specimens with PCM patch material is expected to perform better than OCM. This higher strength of one type to another may be quite clearly imagined. However, how exactly the interaction of the repair system to the substrate system in every increment of load is the point of interest of this research as the previous researches only discuss the maximum load capacity at the end of the loading session (Rio, et al., 2005), and the results of this study do showing quite interesting behavior which will be briefly discussed in CHAPTER 5.

Other factor that will highly affecting the strength of post repaired beam is the length of the repair system. The length variation for each repair/strengthening rebar will also given to study whether the length will affect the compatibility, stress-transfer as well as the flexural strength improvement. Hence, two lengths of 400mm and 700mm of both staple shape and straight shape repair rebar are provided to this experiment.

3.2 Expected Results

With brief and comprehensive observation in every step of the experiment, sufficient data of materials, loads, strain, crack path, and visual detail is expected to be obtained. Start from preload session, all loading data, strain, crack path and post preload data such as plastic strain and plastic deformation are recorded. Then the data is used to calculate the deterioration of the concrete strength by preloaded session, and predict several specimens constituent stress during given final load as well as their ultimate strength. Both of experiment and calculation results will be analyzed and discussed to yield overall specimens behavior during loading and their failure mechanism.

CHAPTER 4
RESEARCH METHOD

4.1 Research Place

This research is consists of laboratory experiment and empirical analysis which is the laboratory experiment were conducted at "Laboratorium Struktur dan Teknologi Beton" of Civil Engineering Department of Universitas Brawijaua. All concrete mixing activity, rebar arrangement, casting and concrete material testing are conducted at the same area to minimize any changing on transporting and handling the specimens.

4.2 Research Variable

Independent variables which needed to yield the objectives are,

a. Repair rebar shape
b. Rebar and Patch length
c. Patch Material Properties
d. Preloading state of the beam specimens

4.3 Research Equipment and Tools

Testing Apparatus, recording equipments and tools are tabulated in Table 4.1.

Table 4.1 Testing and Recording Equiments, and Tools

	Testing Apparatus and Recording Equipments		Tools
1	Compression Test Machine	1	Power Tools (Grinder, Cutting Wheel, Drill, etc)
2	UTM (Universal Testing Machine)	2	Air Compressor 1PK
3	Frame Structure	3	Concrete Mixer 300Lt
4	Hidraulic Pump and 5 Ton Load Cell	4	Concrete Mixer 100Lt
5	Load Monitor	5	Handtools
6	LVDT	6	Rebar Bender
7	Strain Meter	7	Laboratory Forklift
8	Camera and Handycam		
9	Crack MicroScope 500X Magnification		

4.4 Flowchart and Procedure

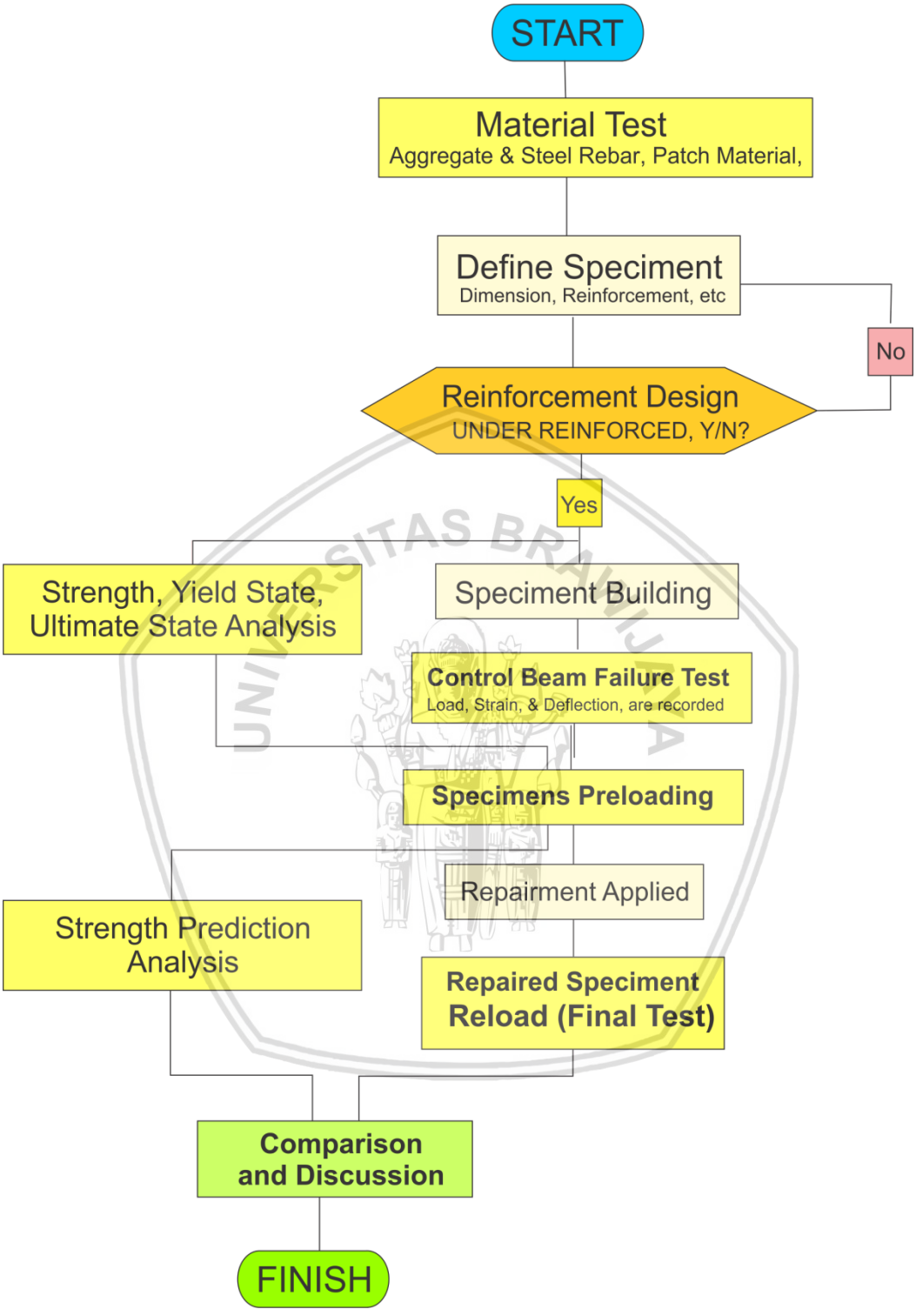

Figure 4.1. Research Flowchart

4.5 The Basic Beam Specimens

Thirteen beam specimens were made for laboratory experiments. All of the specimens ware built identical specimens at the first place, then variations were given to ten specimens according to the experiment objectives, leaving one remaining specimens as control beam or benchmark specimen. The control beam was tested as a plain specimen without any preload or repairing procedures.

The variations which are given to four specimens are derived from the setting of research specimens which were conducted by previous researcher (Rio, et al., 2005). In the research report, several patch repaired beams, which added by a straight strengthening rod/rebar to restore tension steel section, did not giving any strength improvement or even any difference with similar specimens but without a strengthening rebar. The report said that, anchoring length of the strengthening rod govern the interaction between beam and strengthening rod. Hence, the specimens will be given length variation of the rebar length, that the result may validates the researcher statement and compare the other present research specimens result at the same time.

Meanwhile, eight other specimens were given repair variation originally designed for the main purpose of this research. The repairing procedure however, is using the same repair procedure with the other fives, but with different rebar shape. The rebar shape given has anchoring legs that forming a “staple” shape, regarding to the proportion of its main length and legs length. The legs of the rebar were anchored to substrate concrete using an anchor chemical adhesive.

Most of previous researches are using a repair device placed on surface of specimen body (Aykac, et al., 2013) (Satoh & Kodama, 2005), while this research will place the repair device inside the specimens geometry by concrete cover peeling and re-cover it the repair with patching technique. Such effort may be need in actual application to maintain the original dimension of the specimens. However, the main purpose is to confine the anchoring legs with the stirrups cage as close as possible, which will be explained in the next discussion in this paper. Two different patch materials, Polymer Cement Mortar (PCM) and Ordinary Cement Mortar (OCM) are employed at this research to observe the repair device behavior correspondence to each patch materials.

4.5.1 Beam Specimens Design

The specimens built in this experiment are designed by considering the size for material constitutive, readability of failure and crack propagation, the size of frame test, testing equipment capacity, lifting equipment capacity, and other workability factors. Hence, the specimens are designed has 120mm breadth, 200mm in height, with 2000mm span. The specimens length and cross section dimension has the same value with previous patch repair researcher (Rio, et al., 2005), so that may deliver a better benchmarking to confirm the research result.

As the purposes of the research is to repair a particular deteriorate area of reinforced beam, 30mm depth of cross notch with 5mm wide is given at mid bottom face of the beam to make sure the plastic hinge are built around the area. As the notch is built near to the reinforcement position, yield penetration is expected to reach notched cross section.

The reinforcement rebar designed as 2x10 mm deformed steel rebar for both compression and tension reinforcement. While repair rebar has 13mm in diameters. As shown Figure *4.2*, the stirrups have 100mm space in between along the beam length, which considered being quite dense and very conservative to restrain shear force considering specimen's dimensions. However, the purpose of closer stirrups is that they will hold the concrete and make a better confinement so that the concrete will not crushed too much and make less repair procedure of compression zone, since the repair of compression zone is not part of the research objectives. According to the material test result, the concrete has average value of 34Mpa of compression strength. From the material test, it is found that steel has 384 Mpa, 381 Mpa, and 366 Mpa for 8, 10 and 13 diameters respectively.

However, steel material measurement results that there are deviation on the reinforcement diameter than its designation diameters. The 8mm plain bar has shown 8mm in measurement, while 10 and 13mm deformed rebar have 9.2mm and11.5 mm of diameter respectively. The diameters of deformed bar are measured on clear diameter without rebar ribs.

4.5.2 Under or Over Reinforced Failure State

As a base of testing procedure, the specimen should be analyzed to acquire several testing parameters. From the analysis, with several pre-adjustment and assumption of specimen's properties, some parameters and behavior may be predicted by the result. Hence, the first analysis was the failure state of the specimens, whether the beam will fail on underreinforced state or overreinforced state. Previous research reports that there were difficulties on specimen behaviour observation, as their resulted in over-reinforced state (Rio, et al., 2005). Underreinforced state of failure is expected to take place so that the failure process could be observed well. To achieve the desired state, the tension reinforcement designed as two 10mm diameter of rebars with confirmed stress and strain analysis on Appendix 1**.** More closer stirrups than the necessity to carry shear stress was also designed to make more confinement to its compression concrete, so that the concrete has more strain but delayed in crushing (Park & Paulay, 1974). From the result of analysis the beam specimens should be failed on under reinforced state, so that the fail process along with change of strain and displacement could be observed well.

4.5.3 Point to Stop Preloading of Laboratory Experiment

The moment-curvature graph also yielded from the analysis, which is useful for determining the point to stop preloading. Point to stop preloading has to be determined before the preloading of specimens is conducted. From Figure *4.3*, the preloading is expected to stop right after first yield state. after the first yield of tension reinforcement,

the beam seems may not has much further strength yet the compression concrete area may not crushed nor cracks too much to be repaired by mortar injection. With less cracks on compression area and less strength that the beam could be carried, the point to stop preloading right after first yield may give convenience condition for further treatment.

The point to stop loading may be limited by a given number of loading magnitude which converted from the first yield moment, or may be limited by a calculated yield strain, which can be observed by putting a strain gauge at designated point. However, exact limited number of magnitude will also be observed by several observations during control beam loading which will be loaded until reach ultimate state. Several behavior of beam, including yield strain and first yield load and deformation, was also take as consideration of determining the point to stop loading.

4.5.4 Maximum Load Analysis

By several pre-adjustment and assumptions of beam specimens properties, the maximum load that needed to make the beam reach the ultimate state is about 2.2 tons. Which means that a 5-tons of hydraulic jack is sufficient to be used as the loading gear. The load is performed using three point bonding (single point load) to make sure the crack and yield state of the steel is occurred at mid span of the beam specimens.

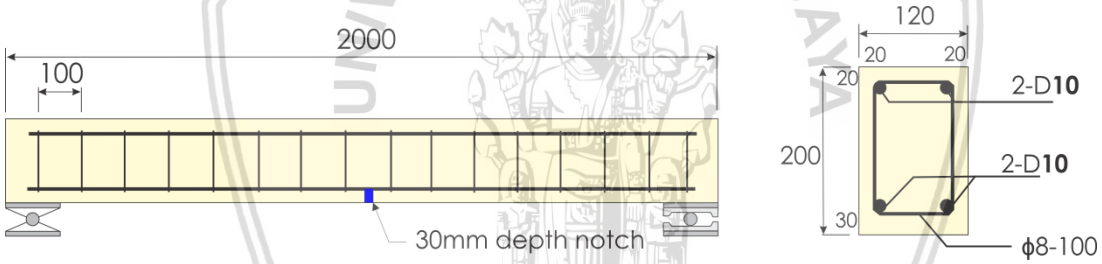

Figure 4.2. Beam Specimens Dimension and Cross Section

Table 4.2. Required Data of Control Beam Loading Test

No.	Data Type	Measured Object	Unit	Measuring Tools	Placement
1	Load	Entire Beam	KN	Load Cell + Monitor	Top of Beam surface (mid-span)
2	Displacement	Entire Beam	mm	LVDT + Monitor	Bottom Side-Mid Span
3	Compression Strain	Concrete	mm/mm	Strain Gauge + Strain Meter	Top Fiber-Mid Span
4	Tensile Strain	Reinforce.Rebar	mm/mm	Strain Gauge + Strain Meter	Tensile Rebar Surface-Mid Span
5	Crack Propagation	Entire Beam	-	Camera	-
6	Crack Width	Entire Beam	mm	Microscope + Milimeter Gauge	-

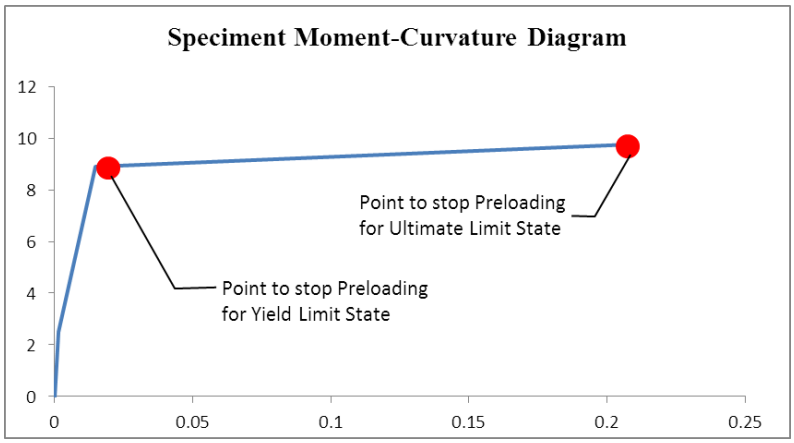

Figure 4.3. Moment Curvature of Analyzed Specimens with point to stop preloading

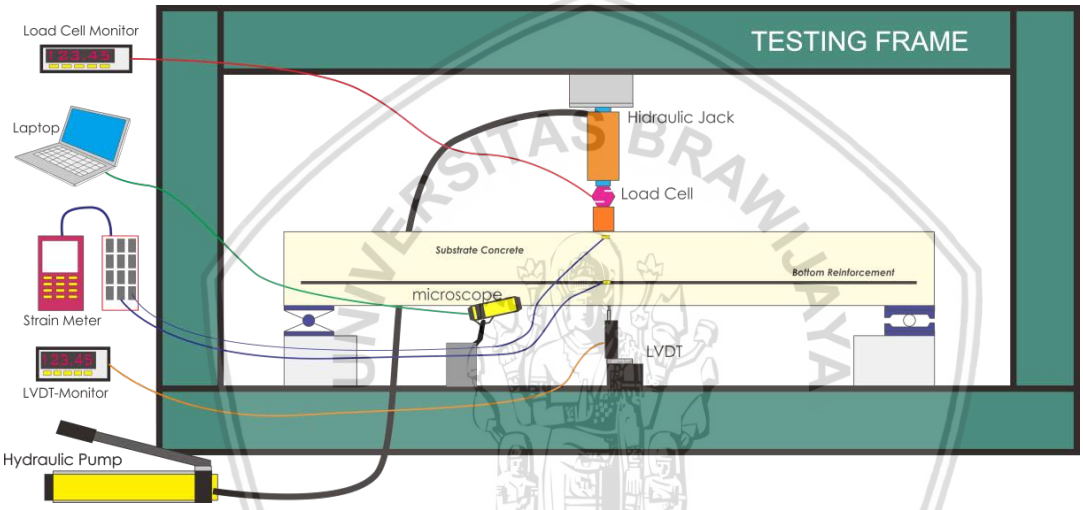

Figure 4.4. Beam Specimen Preloading Setup

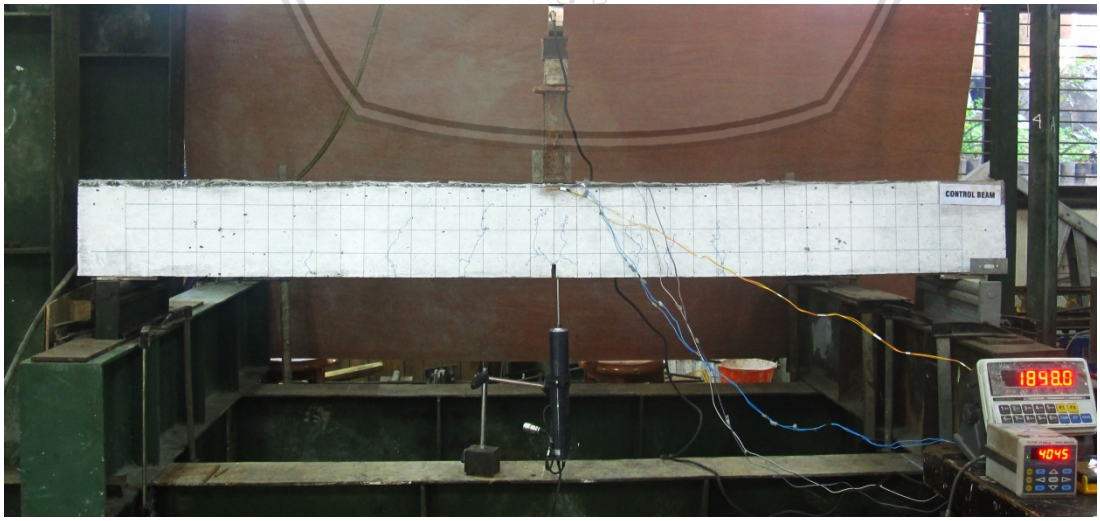

Figure 4.5. Preload Test Setup on Laboratory Structural Testing Frame

4.6 Specimen Materials

4.6.1 Substrate Concrete

As mentioned on 4.5.1, the concrete which considered as substrate concrete, regarded to its interfacial with patch material, is designed to achieve compression strength 34Mpa of 28days age. The concrete is normal concrete without any additive addition, significantly high or low water cement ratio, or any special aggregate. For uniformity of concrete strength, aggregate used, for both coarse and fine aggregate were washed to clean them from any mud and silty materials, then the quality of mix is may considered as well controlled.

Concrete samples use 150Dia. x 300 mm^3 cylindrical molds and were tested by compression testing equipment with 5 concrete samples to achieve the minimum statistic number. Concrete elasticity was not tested, but was acquired using actual concrete weight and actual compression strength. Similarly, concrete rupture value was only calculated using compression strength parameters. As that concrete rupture among concrete substrate particles is not necessarily needed to be observed.

4.6.2 Steel Reinforcement Rebar

The yield stress and rupture stress was be acquired by universal testing machine (UTM), as well as its elasticity. From the test, it is found that steel has 384 Mpa, 381 Mpa, and 366 Mpa for 8, 10 and 13 diameters respectively. However, steel material measurement results that there are deviation on the reinforcement diameter than its designation diameters. The 8mm plain bar has shown 8mm in measurement, while 10 and 13mm deformed rebar have 9.2mm and11.5 mm of diameter respectively. The diameters of deformed bar are measured on clear diameter without rebar ribs.

Rebar cage arrangement was carefully built. The stirrups distance is distributed evenly and the reinforcement was firmly tied to prevent change of shape during concrete pouring.

Figure 4.6. Preparation of steel reinforcement cage of strain gauge instalation

4.6.2.1 Strain gauge Installation

Three types of strain gauge are employed on this experiment. The types of strain gauges are used according to the placement and the strain target of the measured material. All of the strain gauges brand Tokyo Sokki which matched with existing laboratory strain meter.

For measurement of concrete strain, PFL-20 is used. It has 20mm gauge length with is suitable for concrete and mortar strain measurement. Maximum strain capacity is 2%, or 0.02 of original gauge length. The strain gauge was applied to control beam and all specimens repaired using staple rebar before preload session is started. For measurement of steel reinforcement strain, FLA-6 and YFLA-5 are used.

FLA-6 has 6mm gauge length. The strain capacity is about 5%. This strain gauge is used on the predicted lower strain of staple rebar. The detail strain gauge uses is tabulated on Table *4.4*.

To accommodate longer yield strain which predicted to occur on original rebar, YFLA-5 is employed. This strain gauge only has 5mm gauge length, but has high advantage for recording very long elongation as could records until 20% capacity. However, strain gauge manual book (TML Pam E-1007A Strain Gauge Catalogue, p. 70) shows that the strain capacity will be dropped by longer waiting time with uses of generic cyanoacrilic, which may also be found in Appendix 4. According to the manual, capacity of YFLA may drop to 10% or 0.1 of strain by using the adhesive. However, regarding to the steel maximum possible recorded strain, this limit value may not be a problem as the strain reached by the steel only reach 0.018 of tensile strain.

*Table 4.3.*Strain gauge uses for Preload and Reload Session

Specimen Code	Concrete in Compression		Steel in Tension			
	Concrete Strain Gauge	Max strain (mm/mm)	Original Reinforcement	Max strain (mm/mm)	Repair Rebar	Max strain (mm/mm)
Control Beam	PFL-20	0.02	FLA-6	0.02	-	-
S4 Ultimate-1	PFL-20	0.02	FLA-6	0.02	FLA-6	0.02
S4 Ultimate-2	PFL-20	0.02	FLA-6	0.02	FLA-6	0.02
S7 Ultimate-1	PFL-20	0.02	FLA-6	0.02	FLA-6	0.02
S7 Ultimate-2	PFL-20	0.02	FLA-6	0.02	FLA-6	0.02
S4 Yield-1	PFL-20	0.02	YFLA-5	0.15	YFLA-5	0.15
S4 Yield-2	PFL-20	0.02	FLA-6	0.02	FLA-6	0.02
S7 Yield-1	PFL-20	0.02	YFLA-5	0.15	YFLA-5	0.15
S7 Yield-2	PFL-20	0.02	FLA-6	0.02	FLA-6	0.02
ST4 Yield OCM	-	-	YFLA-5	0.15	FLA-6	0.02
ST7 Yield OCM	-	-	YFLA-5	0.15	FLA-6	0.02
ST4 Yield PCM	-	-	YFLA-5	0.15	FLA-6	0.02
ST7 Yield PCM	-	-	YFLA-5	0.15	FLA-6	0.02

(a) (b) (c)

Table 4.4. Strain gauge uses (a) PFL-20 (b) FLA-6 (c) YFLA-5

4.6.3 Patch Repair Material

Ordinary Cement Mortar (OCM) and Polymer Cement Mortar (PCM) will be used as one of research variable that expected to have many differences in its properties but has similarity of the number of uses on many repair practices.

4.6.3.1 Ordinary Cement Mortar (OCM)

Ordinary cement mortar is the most used patch material regarding to its benefits of availability, easy of mix and application, and relatively cheap price. The uses are not only limited in regular home repair, but also in high rise building repair despite its unreliable properties as patch repair material. The reason for taking OCM as one of patch material is according its benefits and its extensive uses in repair practices.

Component ratio of mortar is 1:3 of Portland composite cement (PCC), and fine sand respectively. To gain low shrinkage patch mortar, low water content of 0.45 is applied to the mortar mix. The mix ratio may be resulted on poor workability so super-plasticizer is added to the mix with ratio of 0.85% to the cement weight. The result of the mix was

relatively good in workability with little sign of bleeding. The ratio of 0.85% of super-plasticizer and 0.45 water cement ratio was the result of several workability trial and error.

The compression test of 50mm cube mortars will be conducted. The mould used is 50x50x50mm cube, with 5 samples of mortar will be tested. The Mortar was tested after 28days curing age by compression testing equipment. The shrinkage is also observed but not discussed as major study of the research as OCM is well-known has a great possibility to process more shrinkage than polymer cement mortars.

4.6.3.2 Polymer Cement Mortar

Polymer cement mortar (PCM) used is Sikatop 122, which has specialization uses on concrete patch repair application. The PCM consist of two separate components that have to be mixed before patching application, which are the cement-aggregate components and polymer liquid component. No water needed for the mix. The properties of PCM are provided by product datasheet as shown in Table *4.7*. However several material parameters, especially Tensile Adhesion Strength, or referred as Interfacial Strength Properties will be retested with current substrate concrete to get more accurate data for analysis and Finite Element Analysis.

(a) (b)

Table 4.5. Used polymer cement mortar (a) Sikatop 122 (b) Mixing process

4.6.3.3 Interfacial Test of Patching Mortars

Interfacial test will be conducted to acquire real interfacial strength between substrate concrete and patch material. With the possibilities of several bond failures which may occur on the repaired structure between substrate and patch material, patch material interfacial bond will be tested by several testing procedures. For tensile bond strength, the procedure used is flexure bond test which may result tensile bond strength which may be compared to concrete rupture value. On the other hand, shear bond strength will also be tested by direct shear test.

a. Flexural Bond Test

The flexural bond test setup as shown on Figure *4.8* is derived from the research report of evaluation of bond properties (Minoru, et al., 2001). The specimens have 350x100x150 mm in length, width and height respectively. The specimens were also having a 25mm depth notch at the bottom of interfacial face to ensure debonding propagate from the notch point. With the setup, several behaviour, and parameter such as interfacial tensile strength may be acquired. However, other properties which found on the reference such as such as tension softening behaviour, crack mouth will not be briefly discussed.

Figure 4.7. Bond strength in flexure specimens preparation

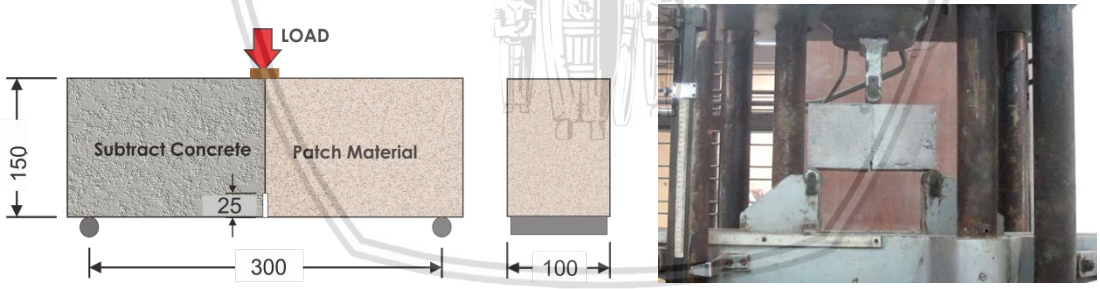

(a) (b)

Figure 4.8. Bond strength in flexure (a) specimens detail (b) testing setup

b. Direct Shear Test

Direct Shear test setup was also adopted from research reference of interfacial bond strength that has been proposed and reported by Momayed, et al., (2005). This method may result closer real interfacial shear than the interfacial bond test provided by ASTM C882 of slant shear test, as found that it has there is compression strength effect of the specimen to the shear strength result, according to Pattnaik (2015). The specimens will have 150x150x150 mm^3 dimensions, with 2/3 and 1/3 part of the section will be the concrete substrate and patch material

respectively. Shear bond strength will be calculated by fail load given divided by the area restraining shear stress. With modified specimens base, made from 2mm steel, the direct shear test may performed using regular compression test equipment.

(a) (b)

Figure 4.9. (a) Surface preparation for direct shear specimens (b) oiured patch material to the cast

(a) (b)

Figure 4.10. (a) Direct Shear Test, (b) conducted direct shear on compression test apparatus

c. Flexural tensile strength of ASTM C78

Flexural tensile strength for ordinary cement mortar is tested according ASTM C78. This test using four point bending creating moment to the tested specimens. The result of given moment is the crack propagate from the bottom fiber of the specimens as a function of tensile strength of the concrete. This tensile procedure is conducted for OCM patch material to provide the tensile strength data as PCM material has been provided by its datasheet.

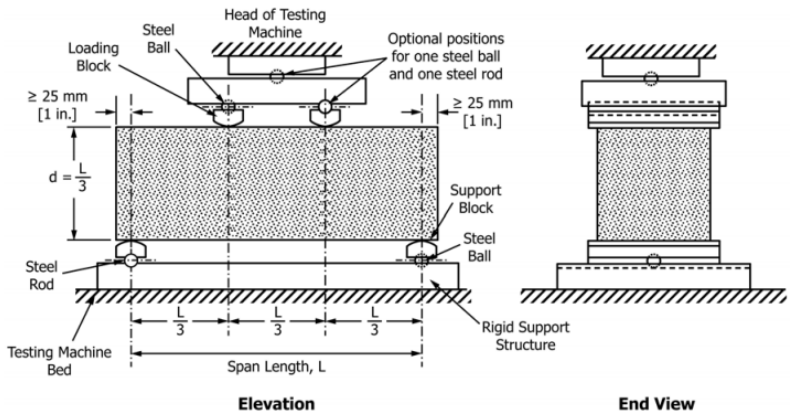

Figure 4.11. ASTM C78 specimen specification

Table 4.6. Material Testing Specification

No.	Specimen Code Name	Speciment Content	Dimension			Quantity (Ea)	Testing Procedure
			Length (mm)	Width / Diametre (mm)	Height (mm)		
1	C34	Concrete 34Mpa	-	150	300	5	Compression Test
2	ST13	Carbon Steel	20	19	-	3	Tensile Test
3	ST10	Carbon Steel	20	13	-	3	Tensile Test
4	ST8	Carbon Steel	20	8	-	3	Tensile Test
5	OCM	Portland Cement Mortar	50	50	50	3	Compression Test
6	FB-OCM	Concrete-OCM	300	100	150	3	Flexural Bond Test
7	FB-PCM	Concrete-PCM	300	100	150	3	Flexural Bond Test
8	DS-OCM	Concrete-OCM	150	150	150	3	Direct Shear Test
9	DS-PCM	Concrete-PCM	150	150	150	3	Direct Shear Test
10	FT-OCM	Portland Cement Mortar	340	80	100	3	Flexure Tensile Test

Table 4.7. Technical Datasheet of the PCM

Flexural Strength (ASTM C-348)	**28 days**	50 – 70 kg/ cm^2
Bond Strength to concrete	**28 days**	≥15 kg/ cm^2 (concrete failure)
Compressive Strength (ASTM C-109)	**3 days**	350 kg/ cm^2
	7 days	400 kg/ cm^2
	28 days	520 kg/ cm^2

4.7 Beam Specimens Repair

Repair treatments are given after preloading session of twelve beam specimens. The repair procedures given to the specimens are the point of interest of this research. As discussed on CHAPTER 3, the repaired structure will be consist of two system of substrate system and repaired system. The result of final loading of post-repair beam specimens will show whether given repair system will working effectively with the subtract system.

Repair treatment of the beam specimens is divided by two major groups, the specimens repaired using staple shape rebar and other with straight shape rebar. The beam specimens which have been pass designated limit state (yield and ultimate) after given preloading will be installed a staple shape rebar which aimed to replace the yielded As of bottom tensile reinforcement. The concrete cover will prior peeled to 30cm depth and the legs of the staple rebar will be anchored to the concrete substrate using chemical anchor to restore the original reinforcement-rebar. In the other hand, straight shape rebar will be applied with the same manner to the staple shape rebar but without anchoring procedure. Patch repair will be applied to the beam to cover the added repair rebar.

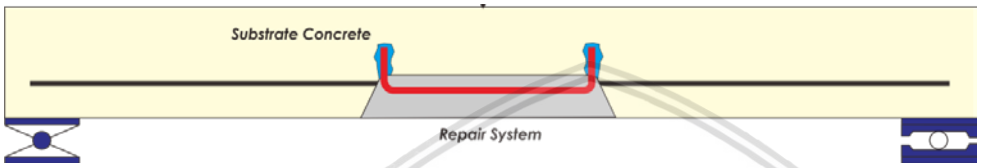

Figure 4.12. General Repairing scheme

4.7.1 Staple Shape and Straight Shape of Repair Rebar

The previous research of strengthening repaired beam using straight rebar (Rio, et al., 2005) yield a result that the strengthening procedure was not effective where there was bond slip occur between rebar and concrete interfacial face. The straight repair-rebar is then carried out on this research to see whether more rebar length will give the repaired beam a better reinforcement, and may compares to the result of previous research. On the other hand, repair method using the staple form rebar is aiming to eliminate the bond slip behavior between rebar and the concrete, which expected to establish full reinforcement action as replacement of prior yielded reinforcement.

The repair-rebar is only provided by a single rod rebar which has a purpose to make the strain measurement is more accurate to observe, and strain gauge may applied only to one repair rebar, rather than two gauges for two double repair rebar. Hence, the single rod rebar designed to have 13mm in diameter which only has small different of section area than original embedded rebar which has 2x10mm in diameter. The specimens repair treatments are tabulated in Table *4.8*.

All specimens has the same mid-span cross section as shown in Figure *4.13*. as detailed in Table *4.8*, both two groups of specimens with staple shape and straight shape rebar has two variation of rebar length, 400mm and 700mm. this variation is expected to show the influence of the rebar length correspond to repaired substrate system and the repair system itself. The different patch material is only applied on straight repair rebar groups as this effectively of this group repair system will be much depends on the interfacial bond strength.

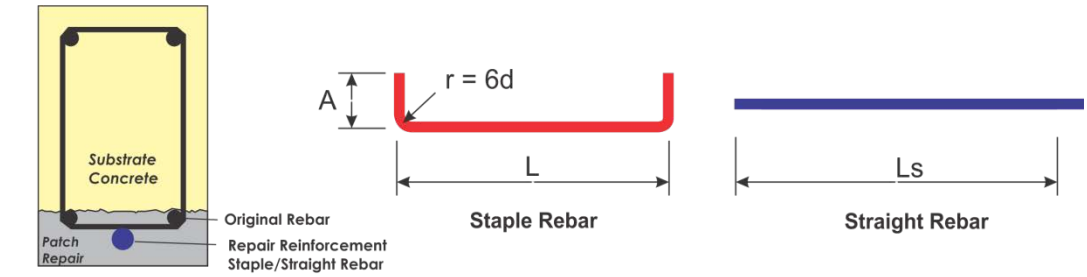

Figure 4.13. Specimens Repaired Cross Section

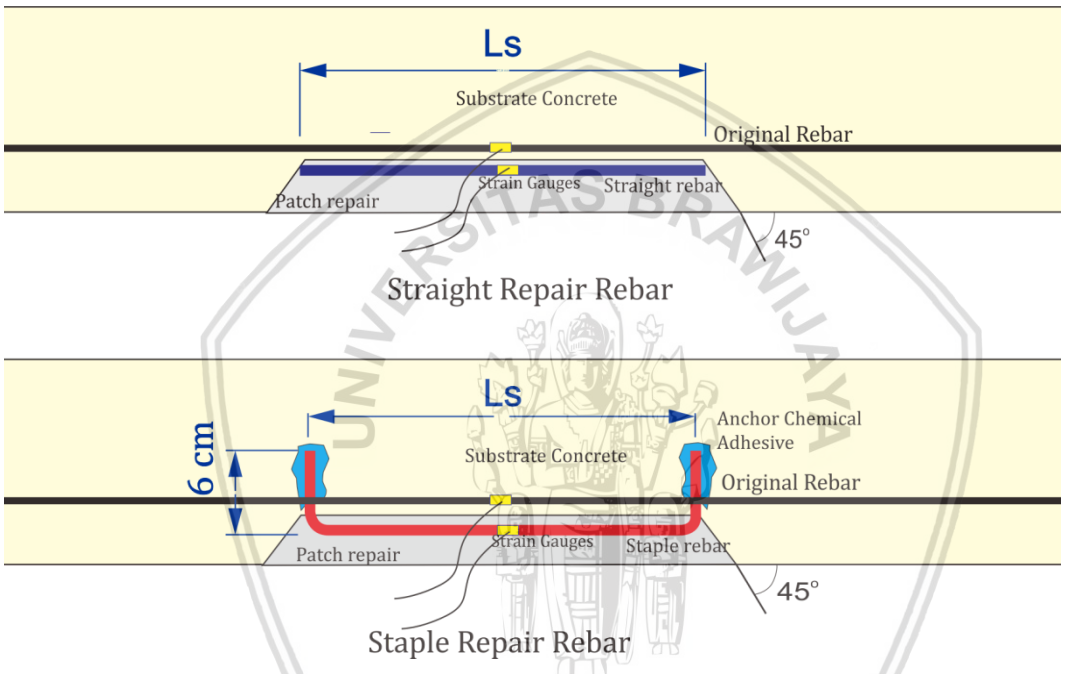

Figure 4.14. Detailed repair scheme as tabulated in Table *4.8*

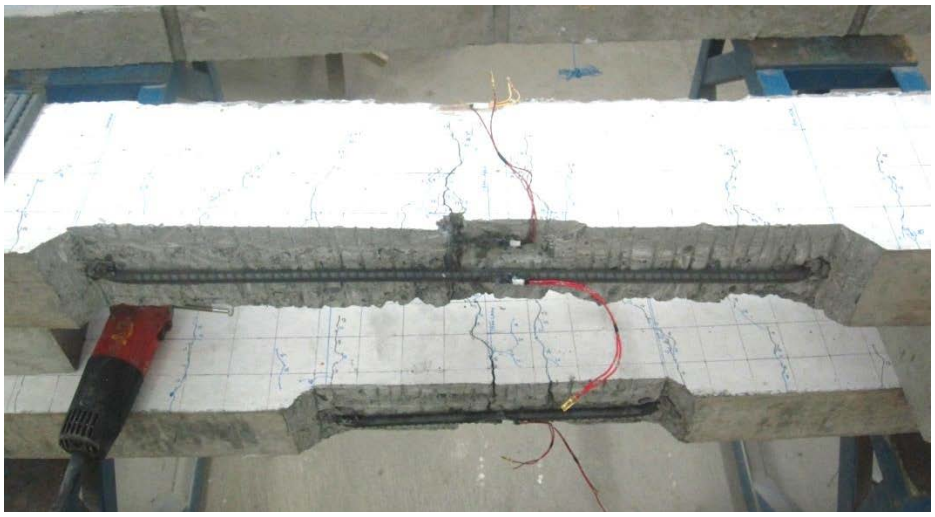

Figure 4.15. Preparation of substrateed concrete for patch material application

Staple form rebar will be installed by create two anchoring holes. Anchoring strength will be provided by chemical anchoring adhesive of Sikafix-2, which is a heavy duty chemical anchor adhesive of SIKA**.** On the other hand, straight repair-rebar is tied to the stirrup without any anchoring or special tie treatment. Strain gauge will be installed for both original rebar and straight/staple rebar as detailed in 4.6.2.1. Compression strain gauge of PFL-20 will use prior installed gauges which have been used on preload session.

The strain measurement of both original and repair-rebar is aiming to observe the repair-rebar behaviour and the interaction with the substrate concrete. Whether the repair-rebar will work effectively may be showed by incrementally increased strain between the two during final loading. Before pouring of patch material, all installed strain gauge were measured to ensure they will be works and may record the strain well. The measurement of repair-rebar are shown in Figure *4.16*.

Figure 4.16. Strain data is prior measured to make sure the strain gauge performing well before patch application

(a) (b)

Figure 4.17. (a) Patch material pouring and casting (b) curing using plastic sheet and watering

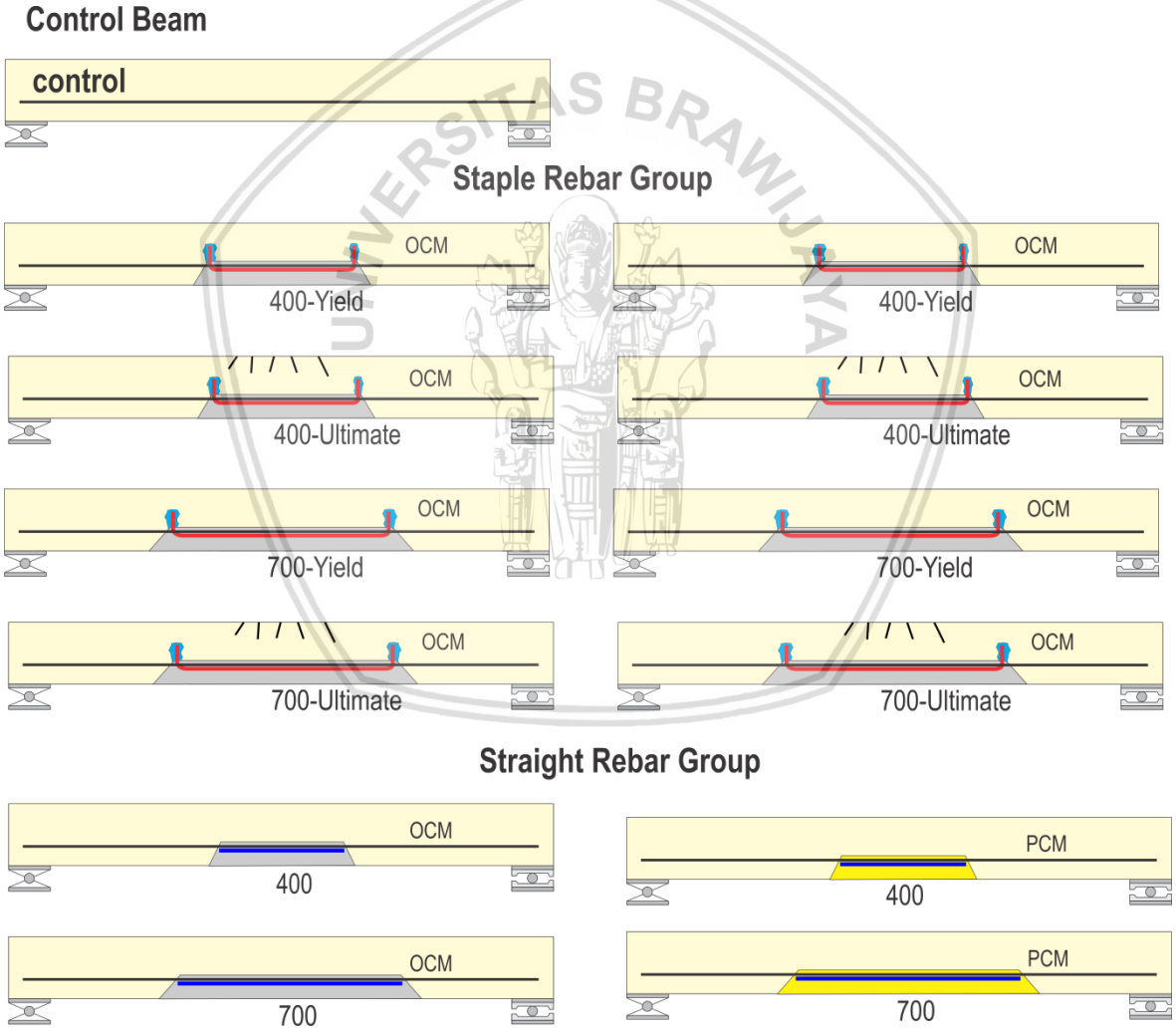

Figure 4.18. All beam specimens detail

After patch material pouring, curing of poured material is provided by moisturising. To prevent frequent moisturising during curing time, a layer of plastic sheet is employed to covering the patch material. However, this method was not fully effective to prevent the

loss of moisture as subtract concrete absorb the moisture and distribute to the concrete substrate body. The distributed moisture may evaporated through the subtract concrete surface. Hence, the moisturising by water may still applied about every 2-3 days.

The prior developed cracks during preloading session were not injected by any form of polymer injection material. For final load crack path observation convenience, exposed cracks are covered with regular wall paint putty.

4.8 Repaired Beam Final Test

After all given repair treatments of preloaded beam specimens, the next step is final load test. The loading test of repaired beam specimens was conducted after applied repair pass 28 days of curing age. In this loading session, the specimens will be given a load and displacement until reaching their collapse state. Such treatment is needed to gain all possibly recorded data and visual behavior of the loaded specimens. The strain of original rebar, repair-rebar, interfacial shear line, together with crack propagation, load given and displacement will be real time recorded. Detailed testing setup and measurement are shown in Figure *4.20*.

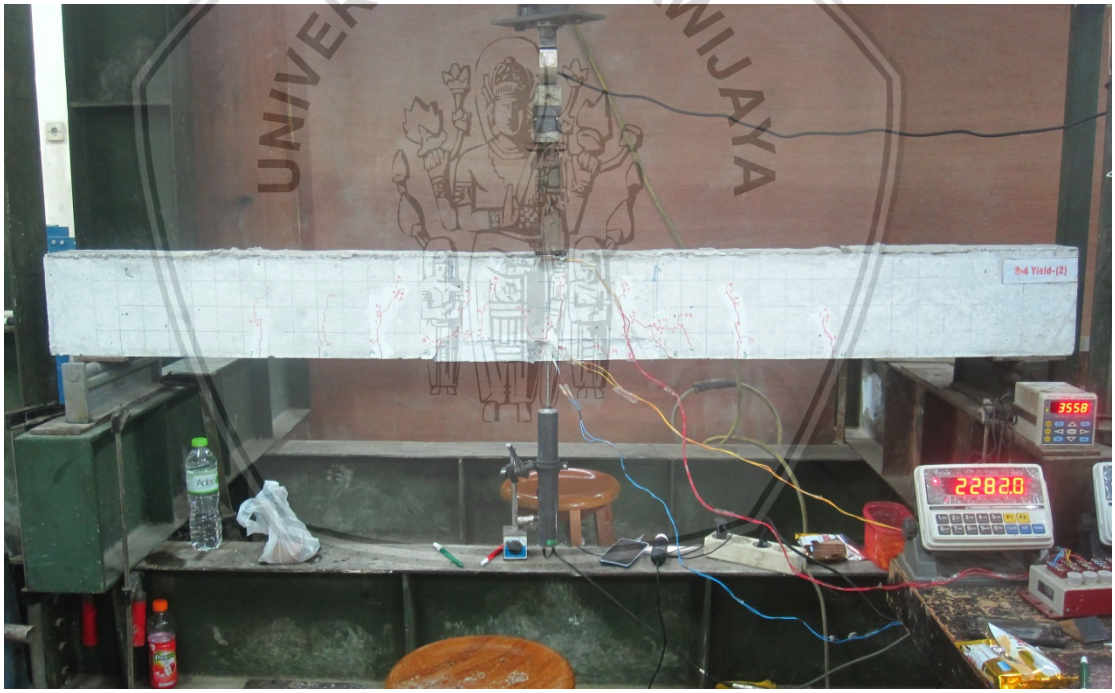

Figure 4.19. Reload (Final Test) setup

Table 4.8. Beam Specimens Specification

Speciment Code Name	Repair Rebar Type	L or Ls (mm)	State Given	Patch Material
Control	-	-	Maximum	-
S-4 Yield (1)	Staple	400	Yield	OCM
S-4 Yield (2)	Staple	400	Yield	OCM
S-7 Yield (1)	Staple	700	Yield	OCM
S-7 Yield (2)	Staple	700	Yield	OCM
S-4 Ultimate (1)	Staple	400	Ultimate	OCM
S-4 Ultimate (2)	Staple	400	Ultimate	OCM
S-7 Ultimate (1)	Staple	700	Ultimate	OCM
S-7 Ultimate (2)	Staple	700	Ultimate	OCM
S-4 Yield OCM	Straight	400	Yield	OCM
S-7 Yield OCM	Straight	700	Yield	OCM
S-4 Yield PCM	Straight	400	Yield	Polymer Cement
S-7 Yield PCM	Straight	700	Yield	Polymer Cement

* OCM = Ordinary Cement Mortar

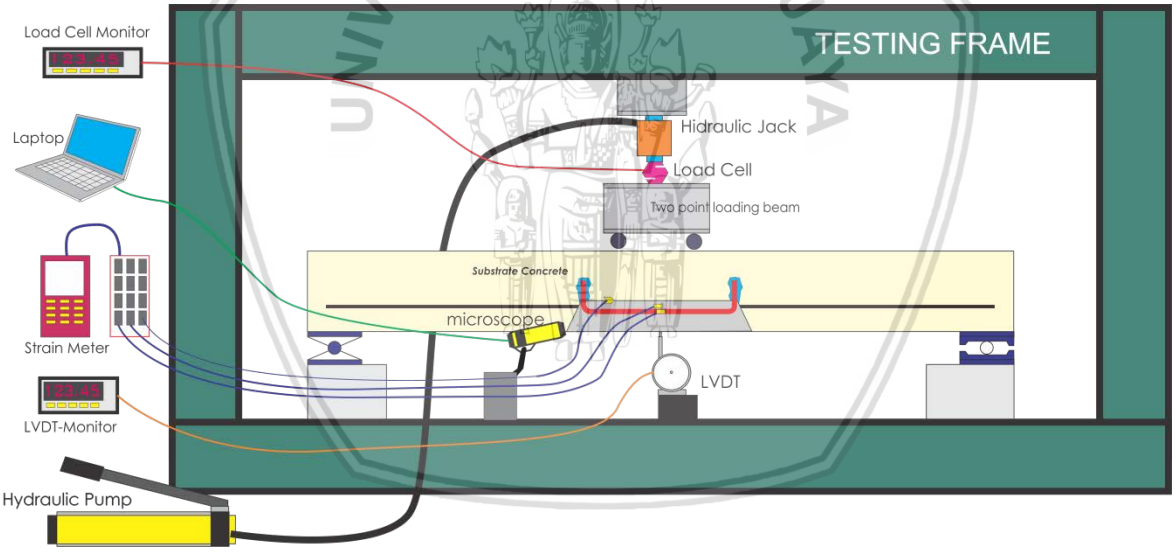

Figure 4.20. Repaired Beam Final Loading Scheme

CHAPTER 1
RESEARCH RESULT AND ANALYSIS

1.1 Specimens Preload

Thirteen specimens were built with the same detail specification and treatment procedures were given a preload session at the first place. One specimen was designated as control beam as a benchmark specimens, while twelve other specimens were given several variations for the specific research purposes. The specimens detail has been discussed in 4.5.1. As one of the objectives of the research is to observe the variations of repair procedure correspondence to each deterioration state, deterioration is needed to be given to the specimens. Rather to create a deterioration of specimens using chemical process as other previous research (Rio, et al., 2005) (Mangat & O'Flaherty, 2000), a preload is given to the twelve specimens to create a deterioration which may categorized as deterioration induced by mechanical force.

Three limit state of preload were given to the specimens. One of the specimens is control beams that used as a benchmark. Limit state of the control beam is total collapse with maximum load and deflection. It was loaded until reach the maximum load and deflection and shows the built-up a plastic hinge to make sure it reached ultimate load and pass its reinforcement hardening. Four of the remaining twelve specimens were loaded until reach its ultimate state but stop not far from falling branch inflection point. While other eight specimens were loaded until reach its yielded state of its reinforcement. All of preload limit states were confirmed by the pre-analysis of the specimens as well as all specimen strain and load measurements.

1.1.1 Load and Beam Deflection

Single point load or three point bending were applied to the specimens, as shown in Figure *4.4*. The load is given as static deflection created by hydraulic jack forced to the beam. The correspondence reaction is read by the load cell and transmitted to the monitor. The load is given incrementally to observe the deflection, strain and crack path of the specimens. All the specimens are given the same load and deflection measurement, as well as compression strain measurement except the tension strain measurements which will be discussed on 5.1.2.

1.1.1.1 Maximum Load and Deflection of Control Beam Specimen

The load-deflection chart of control beam is shown on Figure *5.1*. The control beam was reached maximum load of 2690 Kgs. This is 24% larger than calculated in pre-analysis of the specimens. However, the value has been confirmed by other specimens preloaded to ultimate limit state which are reach close value. There is no sign of falling branch of the load until it reached the maximum load. Yield inflection point was occurring on 2150 Kgs due to yield of tension reinforcement then goes flat until increasing again to

maximum load. From Figure *5.5*, it shows that the concrete is not reach its designated maximum strain of 0.004, but still at 0.0019, then the load reach up until 0.00408. After reach the maximum load, falling branch occurs and the loading was stopped to 2300Kgs due to maximum capacity of LVDT.

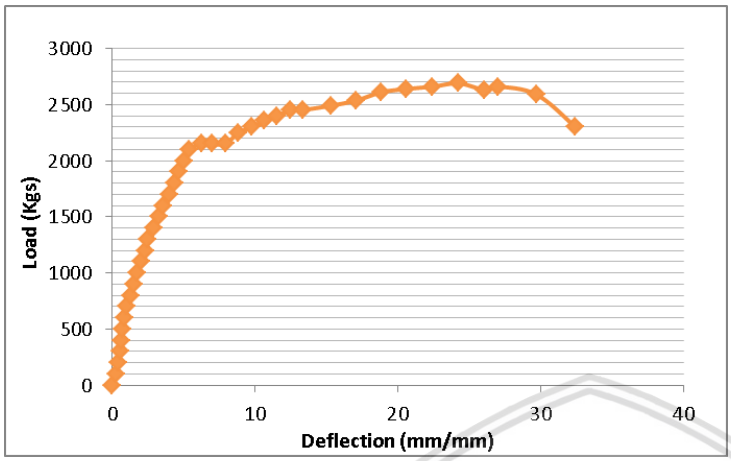

Figure 5.1. Load and Deflection of Control Beam

1.1.1.2 Yield State of the Yield Type Specimens

There are eight designated yielded specimens which are detailed on Figure *5.2* and Figure *5.3*. The behaviour of eight specimens are supposed to have same deflection manner as there is no different of treatment and specification of all the specimens. The average values of yield state load of the eight specimens are 2125Kgs, which ranging from 1900Kgs to 2300 Kgs. Those load values are confirmed by the pre-analysis that yielded values of 1940 Kgs. also, the yield state is confirmed by the strain measurement of the ultimate specimens of S-4 Ultimate-1 as shown in Figure *5.8*. The figure showed that the second inflection point of the graph is the yield state of the bottom reinforcement, seen by the strain with almost plateau manner. Thus was also confirmed with the load-deflection of the Figure *5.4*(a) which the inflection point with load of 2000 Kgs are match with the load-strain graph inflection point.

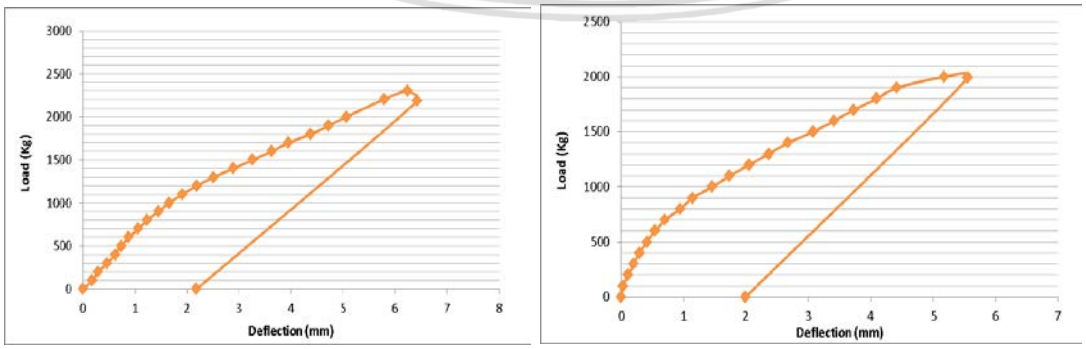

(a) (b)

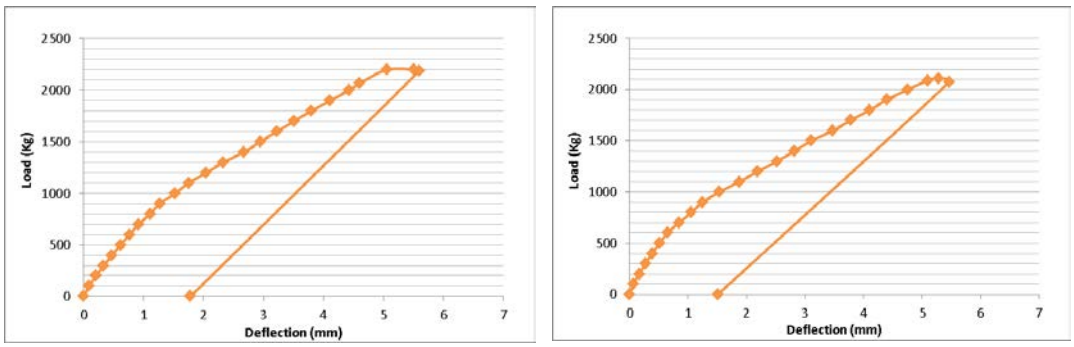

(c) (d)

Figure 5.2. Load-Deflection graph of (a) S-4 Yield-1 (b) S-4 Yield-2 (c) S-7 Yield-1 (d) S-7 Yield-2

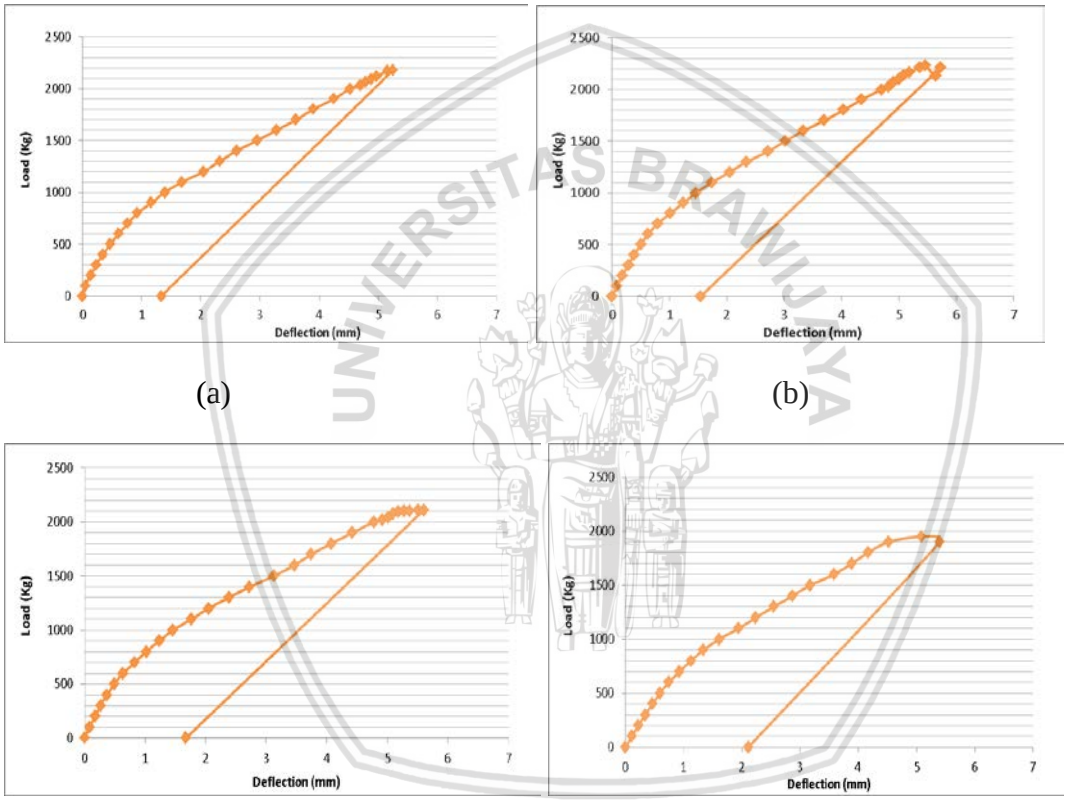

(a) (b)

(c) (d)

Figure 5.3. Load deflection graphs of (a) ST-4 Yield-OCM (b) ST-4 Yield-PCM (c) ST-7 Yield-OCM (d) ST-7 Yield-PCM

1.1.1.3 Ultimate State of the Ultimate Type Specimens

Four ultimate specimens were loaded until pass the ultimate state. As shown on Figure *5.4*, the deflection when stop the loading are ranging 13mm to 15.2mm, far beyond deflection of yield state. The ultimate state of the specimens were confirmed by the inflection point of the graph which are start to showing a falling branch, or the carriage load is decrease. The ultimate state was also confirmed by the strain of the beam which reach 0.004 which has stated as ultimate strain from the pre-analysis calculation on 4.5.4.

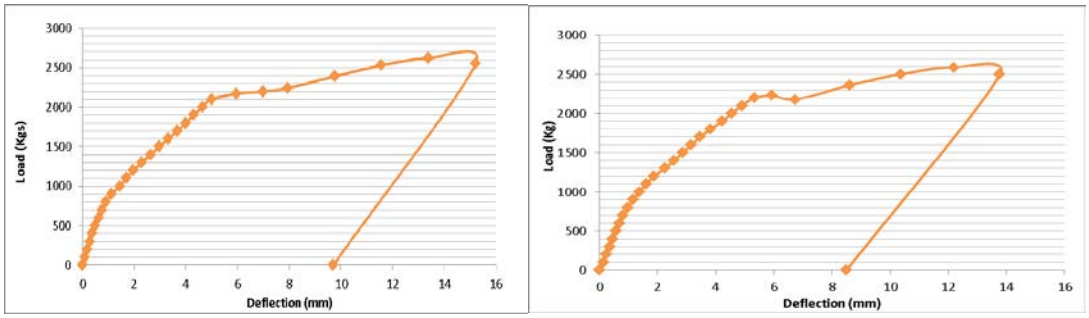

(a) (b)

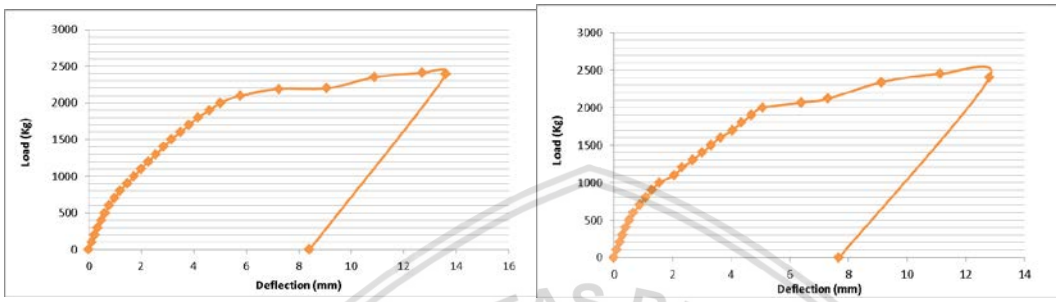

(c) (d)

Figure 5.4. Load-deflection graphs of (a) S-4 Ultimate-1 (b) S-4 Ultimate-2 (c) S-7 Ultimate-1(d) S-7 Ultimate-2

Point to stop loading of ultimate specimens is controlled by real-time observation to the load monitor and the graph path. The loading process is immediately stopped when the specimens reach suspected ultimate state, which is showing a third inflection point after suspected yield state, and the carried load is starting to decrease. There is a possibility of the ultimate specimen reach higher of load, however to create the same deterioration for all specimens, the loading of ultimate specimens are stopped at the same behaviour. It is necessary to control propagation of cracks and also to maintain the same deteriorate condition to all of the ultimate type specimens.

1.1.2 Compression Strain and Reinforcement Strain

Nine specimens were equipped by PFL-20 type of strain gauge with gauge length of 20mm. There are control beam, and eight other specimens designated to be repaired using staple rebar. Compression strain gauges were placed to them to observe the change and development of strain before and post-repair condition. however, only Control beam and S-4 Ultimate-1 were give tension strain gauge for economical reason, as the needed of tension strain at pre-loading were only for confirming the yield state and ultimate state for the specimens and not used to control “point to stop loading”.

From Figure *5.6*, compression strain for ultimate type specimens is ranging from 0.0037 to 0.0042. This is close to designated compression strain of 0.004. The specimens with recorded strain below 0.004 value, such as at S-4 Ultimate-1 and S-4 Ultimate-2 may be caused by the compression strain gauges were not positioned right to the top edge of the

beam because of irregularities of top edge due casting process. However, from the compression strain data, it may be considered that the ultimate type specimens have reached their ultimate state, with similarity of deterioration condition.

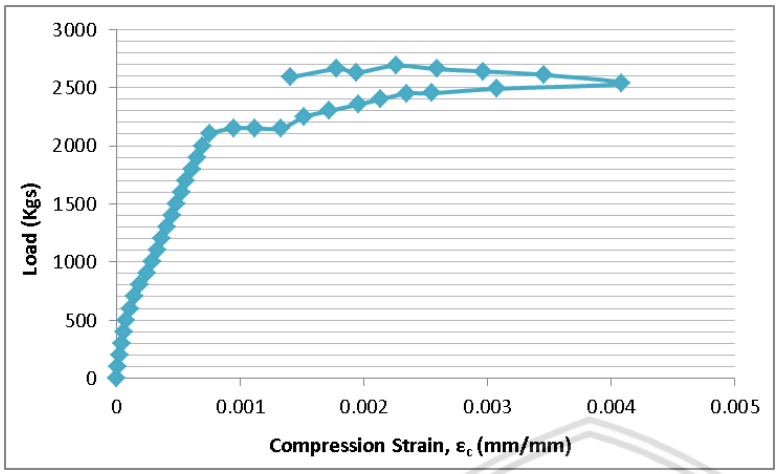

Figure 5.5. Compression Strain of Control Beam

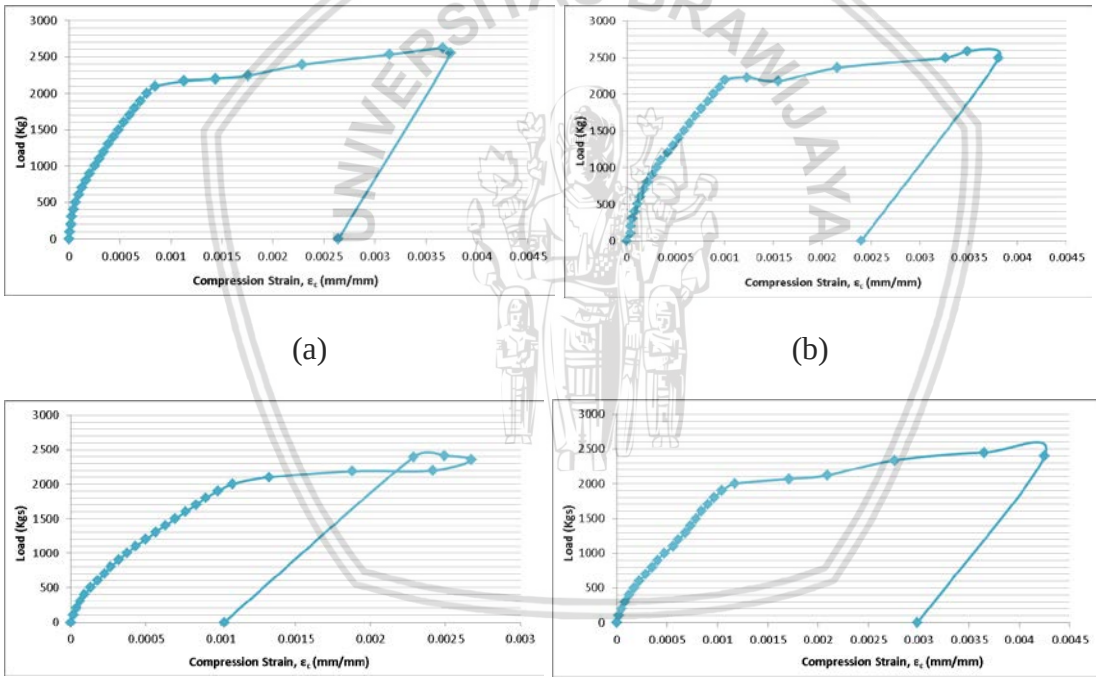

Figure 5.6. Load-Compression strain graph of (a) S-4 Ultimate-1 (b) S-4 Ultimate-2 (c) S-7 Ultimate-1 (d) S-7 Ultimate-2

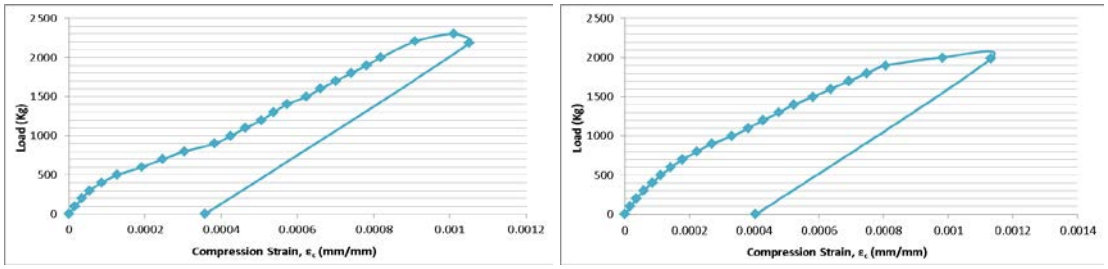

(a) (b)

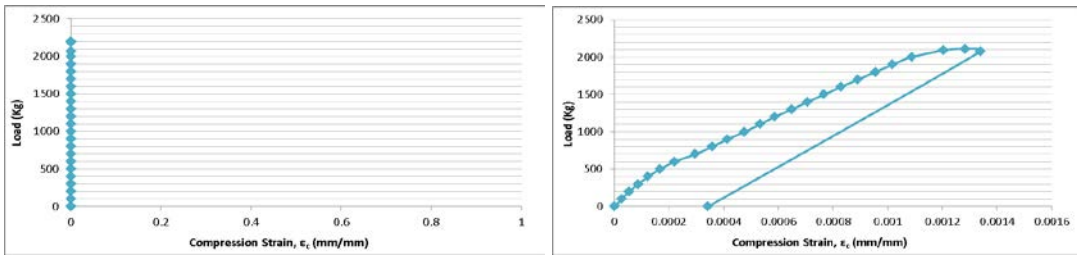

(c) (d)

Figure 5.7. Load-compression strain graphs of (a) S-4 Yield-1 (b) S-4 Yield-2 (c) S-7 Yield-1 (d) S-7 Yield-2

Compression strain for yielded specimen show that strains at stopping point of the load were ranging from 0.0010 to 0.0013. However, the strain gauge of S-7 Yield-1 was failed to show any strain data, which may induced by defect strain gauge due to patch material pouring process. The load-compression strain gauge graphs were also showing the same pattern for three specimens as the first inflection point is the first crack occurrence, and the second inflection point is the yield state of the specimens.

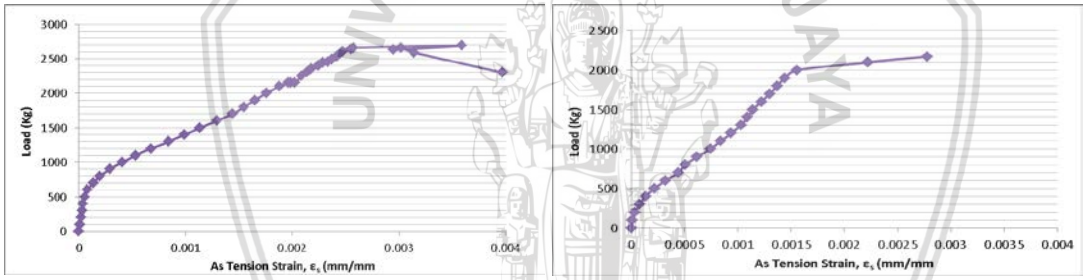

(a) (b)

Figure 5.8. Load-Tension Strain graph of (a) Control Beam (b) S-4 Ultimate-1

Figure *5.8* shows strain development of bottom reinforcement of control beam and S-4 Ultimate-1 specimens. From the figure, the yield state of bottom shows that the reinforcement yield after reach 0.0025 of tension strain. That is also confirmed with the strain measurement of post-repaired specimens which will be briefly discussed on 5.3.3. The graphs are also showing that the first inflection point is the value of the first crack was firstly occurred. The inflection point tells that after the role of concrete tension adjacent to the reinforcement area is disappeared, the stress then fully transferred to the tension rebar. It showed by the tension strain is abruptly increased after the cracks were observed.

1.1.3 Crack Path of Beam

The specimens were applied preload step with given notch at the bottom of the mid span. The result of deterioration was going as expectation that the major crack was propagating right after the notch as well as the plastic hinge. Figure *5.9* show the crack

path of several increments of given loads of S4 Ultimate-1 specimen with its crack development showed on Figure *5.10*.

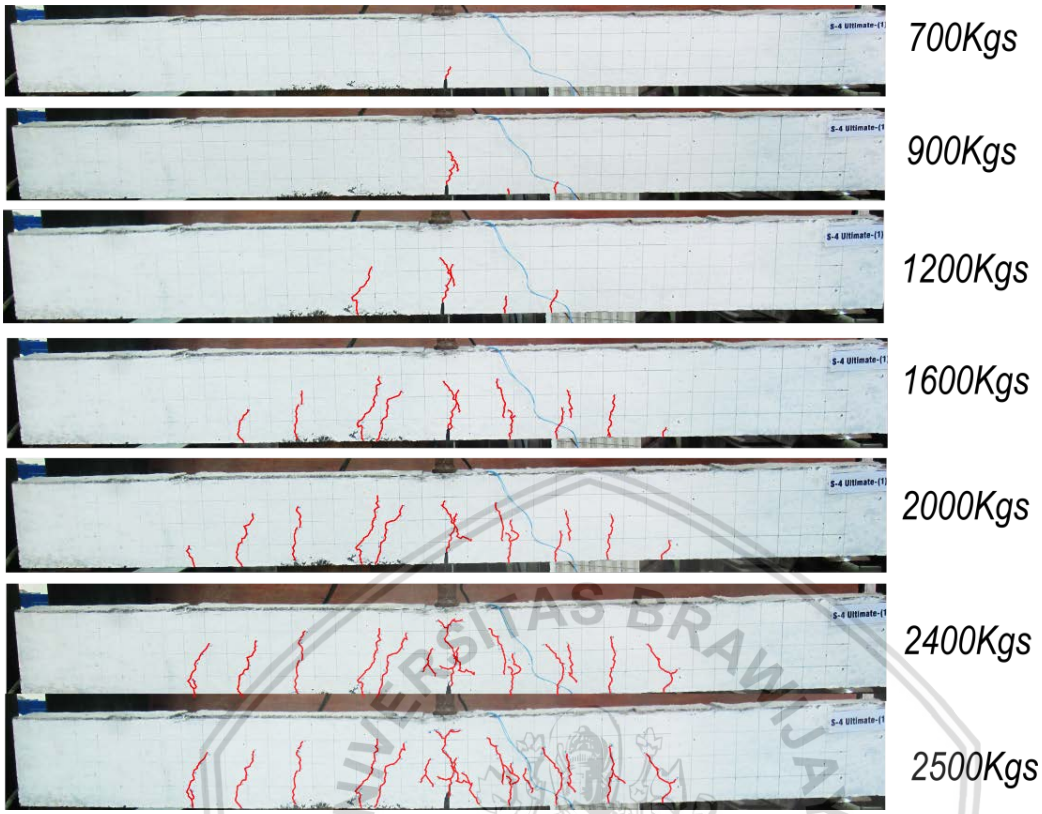

Figure 5.9. Crack Path of S-4 Ultimate-1 during Preload

The cracks pattern shows that the specimens were deteriorate by flexural mechanism. The cracks propagate from the bottom to upper level in vertical manner. As all preloaded specimens have the same base design, other preloaded specimens were also resulting similar crack propagation behavior.

uring preload, the all specimens are successfully deteriorated at the same area by the given notch. Thus will ensure calculation and analysis could be simplified. If the deterioration and yielded area of steel cannot be determined, the analysis of pre-repair to post-repair may be difficult to be established.

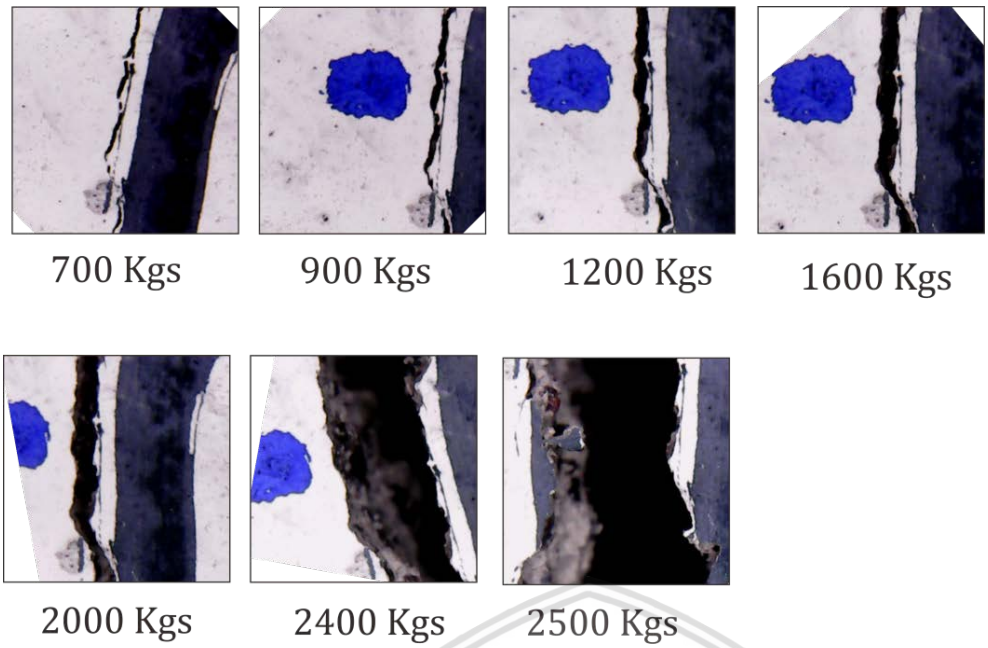

Figure 5.10. Crack width develompent during preload of S4 Ultimate-1

Figure 5.11. Control Beam Preload crack path

Figure 5.12. S7 Ultimate-1 Beam Preload Crack Path

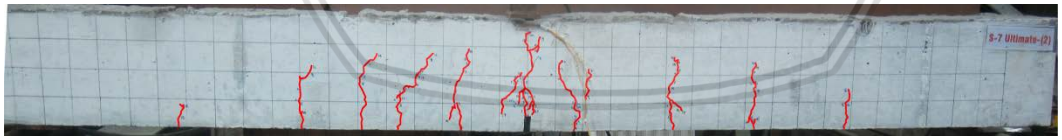

Figure 5.13. S7 Ultimate-2 Preload Crack Path

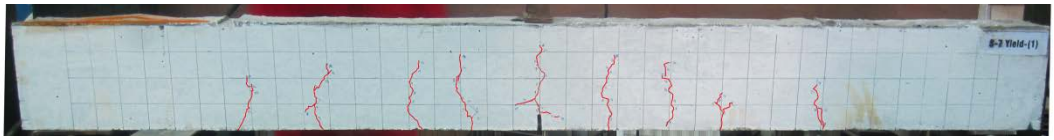

Figure 5.14. S7 Yield-1 Preload Crack Path

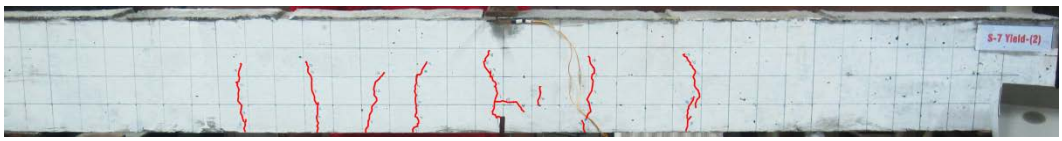

Figure 5.15. S7 Yield -2 Preload Crack Path

Figure *5.11* shows that plastic hinge is formed by several cracks are jointed together after several path propagations. Crack paths of Figure *5.12* to Figure *5.15* may show the prospective pattern of the plastic hinge later showed on fully loaded of Control Beam. It could be seen that if other specimens are fully loaded to maximum deflection, it will have similar pattern of crack propagation and plastic hinge with control beam. The plastic hinge crack pattern may also be confirmed by the crack propagation pattern showed by Figure *5.10*.

The control beam was also experienced a crack with horizontal propagation at the top of concrete section showed on Figure *5.11* and Figure *5.16*. It may be caused by excessive compression strain that the poisson ratio makes top of concrete experienced a tension stress which is confirmed the Figure *2.3* of stress trajectory of beam. Excessive compression of concrete makes the compression strain gauge bend and debonded at their mid, which are may create inaccurate of strain reading. Thus confirmed the Figure *5.5* that compression strain is abruptly decreased at the certain point of loading.

Figure 5.16. Horizontal crack propagation at the top of control beam section

1.1.4 Analysis of Concrete Deterioration due to Preload

After given preload, all of the specimens show deterioration of both concrete and steel reinforcement. Early investigator has observed the plastic strain behavior in both concrete and steel reinforcement with several mathematical model for it (Mander, et al., 1988) (Otter & Naaman, 1989) (Aslani & Jowkarmeimandi, 2012). With installed measurement in this current laboratory experiment, the plastic strain may clearly showed by strain monitoring at the specimens. From the strain measurement showed in Figure *5.6* and Figure *5.7*, average plastic strain of 0.00263 and 0.000385 for ultimate specimens and yielded specimens respectively. From the model proposed by early researcher, the deterioration factor of the concrete could be derived from the modeled stress-strain curve after unloading and re-loaded for final test.

1.1.4.1 Model of Stress-Strain Curve

According to 2.1, the stress-strain of beam specimens could be modeled using approaching formula of Equation 3 and Equation 4. The equation is consists of function of ε_c with f'c and ε_0 as a constant. ε_0 is assumed as 0.002 which is commonly used as the strain in which the concrete reach maximum stress f'c equals 34Mpa, To Calculate Z, Equation 5 is used and resulting on Z equals to 34.98. A modeled stress-strain diagram is shown in Figure *5.17*.

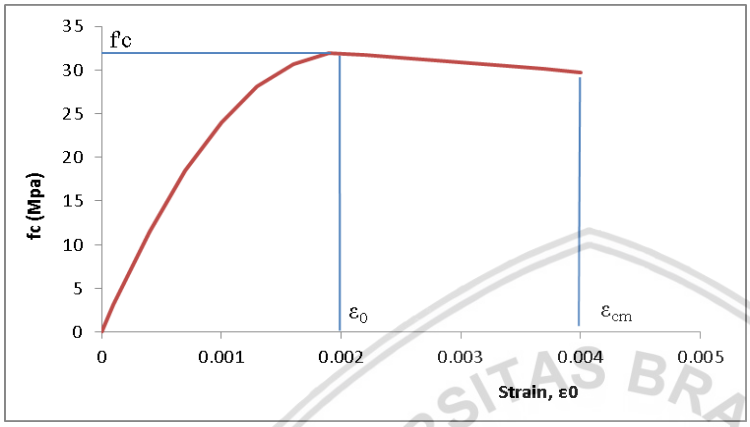

Figure 5.17. Modeled stress-strain diagram of the beam specimens

1.1.4.2 Plastic Strain of Preloaded Specimens

Load and strain data have been recorded from the preload step. After receiving a particular preload, all specimens show deterioration sign as the deflection was not back to zero, which indicate that there was a plastic strain lies in the specimen body. Plastic strain was well noticed from load-strain curves showed in Figure *5.6* and Figure *5.7*, although some of them are showing an error gauge behavior such as S-7 Ultimate-1 and S-7 Yield-1. Although load-strain curves could show a certain deterioration value of the specimens, the analysis of the reduction of the specimens load capacity cannot be delivered from the data.

Hence, stress-strain curve derived from curve shown in Figure *5.17* is employed. The curve was modeled using proposed model of Kent and Park (1971) which showing more realistic curve than other proposed models, especially for confined concrete (Park & Paulay, 1974). Although deviations are present in concrete compression test result, average stress of 34Mpa is set as the value of f'c of compression stress of cylindical specimens for analysis convinience. Table *5.1* show the calculated concrete stress and strain during unloading and reloading. ε_{un} is the unloading strain where the load is started to be released, which can also be confirmed on Figure *5.6* and Figure *5.7*. f_{un} is the compression stress right at the released load derived from Kent and Park model.

f_{new} is the calculated compression stress of when reload is given with the same strain development as the ε_{un}. The plastic strain and unloading stress is showed on Figure *5.18* and Figure *5.19*. ε_{re} is calculated from Equation 13, which the projected strain after reload is given in final loading.

Table 5.1. Unloading strain, plastic strain, compression force and Elasticity of Post-Preload

Specimens	ε_{un}	ε_{pl}	f_{un} (Mpa)	f_{ro} (Mpa)	f_{new} (Mpa)
S-4 Ultimate-1	0.00374	0.00264	30.052	0	27.64784
S-4 Ultimate-2	0.003807	0.0024	29.977	0	27.57884
S-7 Ultimate-1					
S-7 Ultimate-2	0.00424	0.00299	29.492	0	27.13264
S-4 Yield-1	0.00105	0.000357	24.78	0	22.7976
S-4 Yield-2	0.00113	0.000405	25.944	0	23.86848
S-7 Yield-1					
S-7 Yield-2	0.00133	0.000343	28.408	0	26.13536

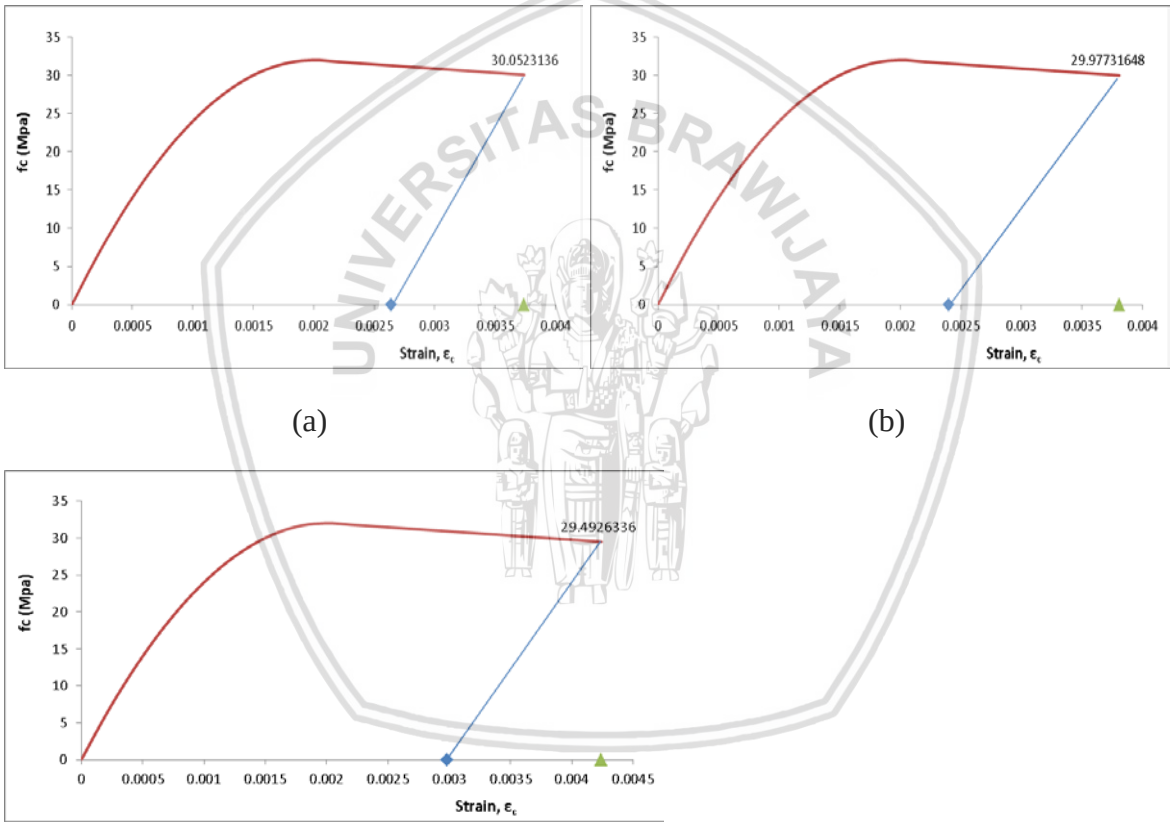

(a) (b)

(c)

Figure 5.18. Stress-Strain Curve with plastic strain of (a) S-4 Ultimate-1 (b) S-4 Ultimate-2 (c) S-7 Ultimate-2

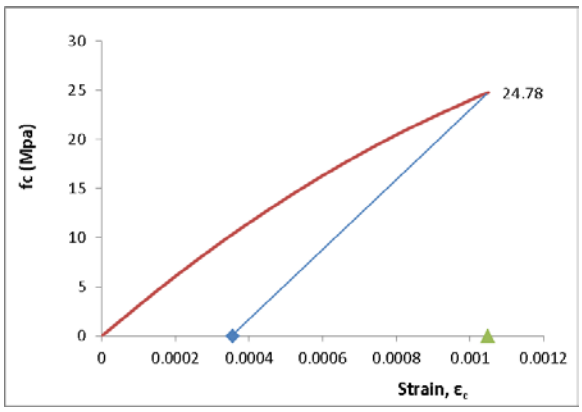

(a)

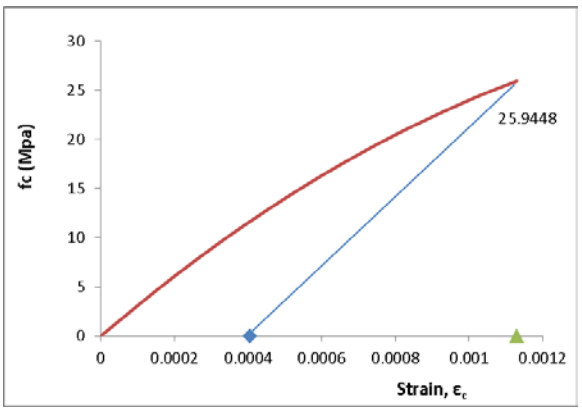

(b)

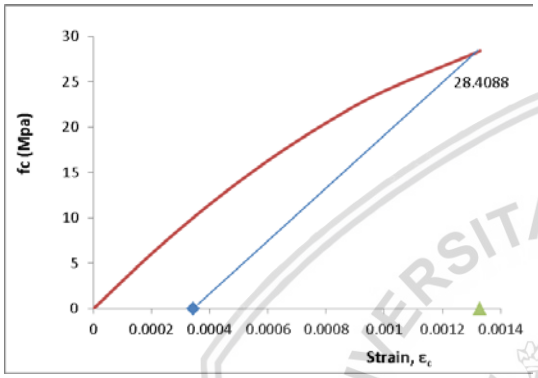

(c)

Figure 5.19. Stress-Strain curve with plastic strain of (a) S-4 Yield-1 (b) S-4 Yield-2 (c) S-7 Yield-2

After the f_{new} are defined, remaining concrete stress block could be derived from residual stress-strain curve of f_{new}. The report of concrete stress-strain behavior (Kent and Park 1971) proposed parameters α and γ which are calculated from Equation 1 and Equation 2 as discussed in CHAPTER 2. In the same way, stress block with deteriorated concrete by prior preload may be delivered from parameters α and γ derived from stress envelope curve of f_{new} on reloading process.

1.1.4.3 Preloading, Unloading, and Reloading Stress-Strain Model

Deterioration of preloaded concrete has to be determined to establish an analysis for the remaining strength of the beam, so the strength of repaired beam can be compared to the unrepaired beam after given preload, not to freshly producted beam. From the comprehensive trial of stress-and strain modelling, three reports were used to establish an apropriate model of stress and strain model (Aslani & Jowkarmeimandi, 2012) (Mander, et al., 1988) (Otter & Naaman, 1989). Figure *5.20* show the stress-strain relation of concrete being stressed by any load in close increments of strain, ε_c.

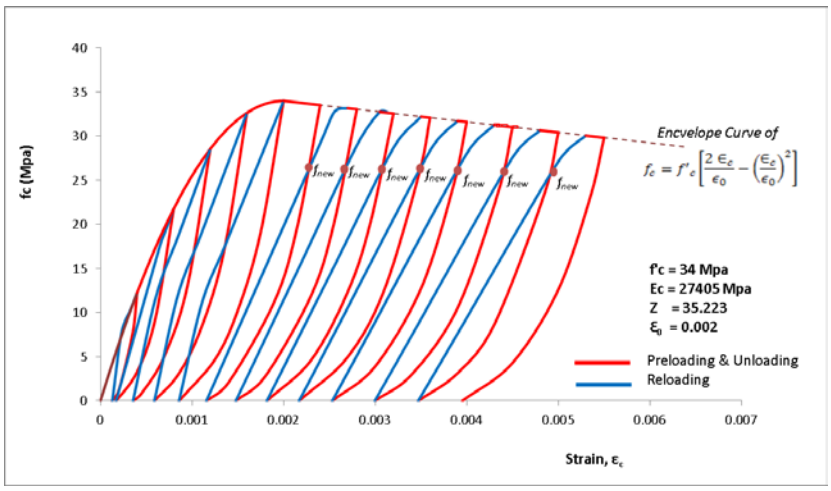

Figure 5.20. Stress-Strain curves of concrete preloaded, unloaded and reloaded in the particular increment of strain

The red line are showing the stress development during preloading and unloading, where the preloading is stopped in incremental of strain. The stress goes to zero due to full unloading and leave a plastic strain ε_{pl}. Then reloading is given to a relatively little strain pass the unloading strain to continue the preload. Then unloading and reloading process are repeated until pass 0.005 of strain. This repeated unloading and reloading processes do not including the decreasing stress due to a lot of repeated process such as reported on the reference (Otter & Naaman, 1989). However, this model is considered more convinience that the specimens of this study only finished one complete process of preloading, unloading and reloading. The modelling of repeated processes are necessary to create the beam stress block which are the stress state on stress block is depend variation range of strain from the neutral axis to the edge of compression fiber.

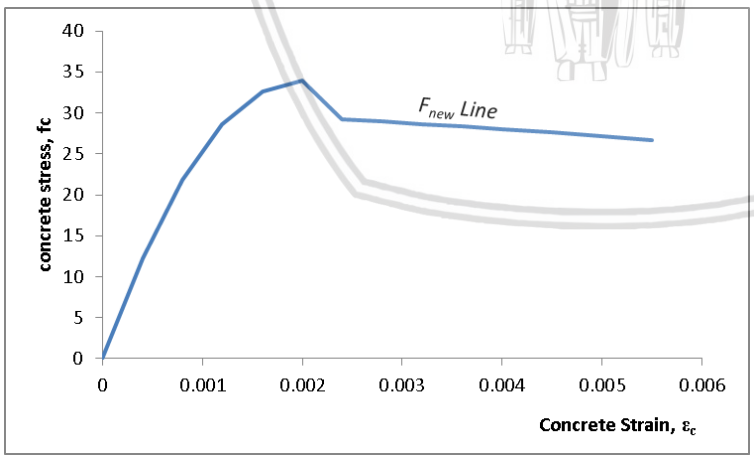

Figure 5.21. f_{new} line correspond to each unloading and reloading process produced using Equation 15

After given preload, concrete stress strain model show deteriorated curve with the stress that did not reach its original stress value on the same given strain. The new stress values are marked as f_{new} with the envelope of the stress magnitude are shown in Figure *5.21*. From the model, stress of the concrete are showing a deterioration after

reaching ε_0 of 0.002, which is confirm the models which have been established by previous researcher. The f_{new} resulted from the model is about 88% of the magnitude of unloading stress, f_{un}.

As vast observation of cyclic loading on concrete were showing that the stresses will always form the envelope curve with given cyclic load, this model is also confirm the same behavior. A certain strain of concrete is needed to result the maximum remaining stress of the concrete. Thus, conclude that deterioration of concrete are marked by the decreasing of stress capacity of the concrete and increasing of strain needed to reach such stress. The model simulates the concrete which is strain is developed until reach more than 0.005.

1.1.4.4 Concrete Compression Stress Block Modeling after Preload

Model of concrete compression during given strain of normally loaded concrete beam has been established in the early work of concrete research, and well-refined with the next researchers (Kent & Park, 1971). In the report, concrete stress block was derived from the stress-strain diagram. The stress-strain diagram model showed in Figure *2.2* is working well in quasi-static loading. However, in cyclic loading or repeated load, concrete stress-strain curve has been re-modeled as shown in Figure *2.4*, and Figure *5.20* and well proven to derive the compression stress block. However, there is a very limited report that has been reported on compression stress block due to repeated loading.

By using the established models reported on the references (Mander, et al., 1988) (Aslani & Jowkarmeimandi, 2012) (Otter & Naaman, 1989), the stress block of reloading beam may be created. The stress value at every millimeters of increment of concrete fiber from neutral axis and top compression fiber are calculated with corresponding unloading strain of ε_{un}, and plastic strain of ε_{pl} after given preload. The strain and stress block development are showed in Figure *5.22* and then plotted to the curve of stress and fiber distance from the neutral axis as shown in Figure *5.23*. With the stress block is already determined, the force distance factor of γ can be defined using common center of gravity for the stress block function.

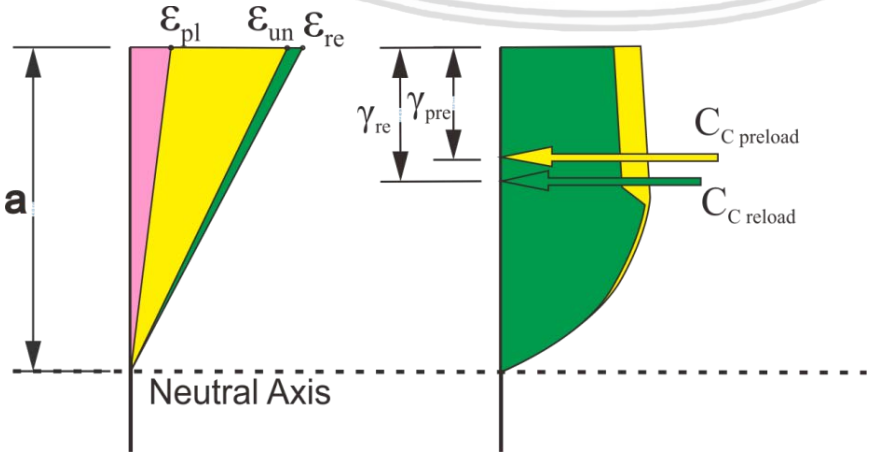

Figure 5.22. Scheme of development of strain and stress block during preloading, unloading, and reloading

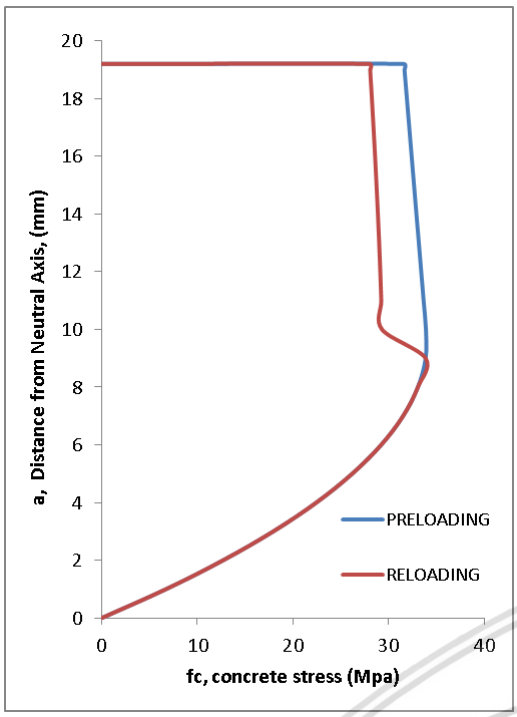

Figure 5.23. Concrete stress block derived from repeated loading unloading mode

1.2 Bonding Strength of Patch Materials

In composite structure, bonding strength between different material determine whether the composite structure will perform well or not. In this experiment, the composite action is designed to work not only between the concrete and the steel reinforcement, but also with the patch material which is covering the repair rebar. Then, to perform a well worked repair, the patch material should have adequate bonding. Thus, have to be measurable so that the limit state of the repair composite structure could be calculated.

Two patch materials are employed in this experiment, which are the Ordinary cement mortar (OCM) and polymer cement mortar (PCM). Ordinary cement mortar is employed as patch material to the staple shape repair specimens, as the stress transfer from the repair system to the substrate concrete expected to be done by the anchored legs of the staple shape rebar. In the other hand, specimens with straight shape rebar are very much depend on the interfacial bonding strength of the patch material. Hence, both OCM and PCM mortar are employed to the specimens to observe the behavior correspond to the different bonding strength

1.2.1 Ordinary Cement Mortar

Ordinary Cement Mortar (OCM) is concrete mix consist of portland composite cement and fine aggregate. Water cement ratio for this mix is set to 0.45 to prevent excessive shrinkage strain due to loss of unused water. Super-plasticizer is also added to the mix to make the mortar has adequate workability to fill the patch space. Although the bond strength is not the primary purpose for this experiment, they will support the data for concrete analysis.

During mortar patching, cube sample is taken for individual material test of the mortar as well as sample for shear strength and flexure bond strength test. Compression strength of the mortar was taken from 5x5x5 cm^3 mortar cube. Five mortar samples were taken to provide more representative data of compressive strength. The compression test resulting average 41.46Mpa of compressive strength. Using rupture modulus formula of Equation 6, the tensile strength in rupture is 4.199 Mpa. Those values are the compression and tension strength of individual mortar itself. The interaction with other material, which resulting in bonding stress are provided in bond strength on shear and bond strength on flexure test.

The tensile strength, f_r of the patch material was also confirmed by flexure tensile strength test procedure of ASTM C-78. Three molded patch mortar with dimension of 34x10x8 cm^3 is tested using UTM (universal testing machine) which has been detailed in 4.6. Because of the fracture is initiated within middle third of the span (ASTM, 2015), using tensile stress formula provided by the code, average value of tensile strength yielded value of 4.2 Mpa. Thus, confirm the value of f_r derived from the mortar compression strength.

Table 5.2. Tensile strength of OCM patch material using ASTM C78 procedure

b = 80 mm
d = 100 mm

Specimen	Load (KN)	P (N)	L (mm)	fr (Mpa)
FT-OCM 1	14.5	14500	240	4.35
FT-OCM 2	14	14000	240	4.2
FT-OCM 3	13.5	13500	240	4.05
	Average Tensile Strength, f_r			**4.2**

Figure 5.24. Flexure tensile strength test of ASTM C-78

1.2.1.1 Bond Strength on Shear

The bond strength on shear is performed by direct shear test using concrete compression test apparatus. Detailed setup of the specimens has been discussed on 4.6. The test was showing load received by the direct shear specimens. Using measured area of the interface surface, the bond strength is calculated as load divided by section srea restraining the shear stress. Bond strength on shear is resulting on 3.355Mpa of average value of three specimens. Each specimens calculation is present on Table *5.3*.

Table 5.3. Bond strength on shear frs of OCM interfaced with substrate concrete

Specimen	Load (KN)	A (mm^2)	f_{rs} (Mpa)
DS-OCM 1	83	237.15	3.500
DS-OCM 2	70	238.64	2.933
DS-OCM 3	85	234.08	**3.631**
Average of bond strength			**3.355 Mpa**

(a) (b)

(c)

Figure 5.25. Visual patch repair and substrate interfacial after given load test
(a) DS-OCM 1 (b) DS-OCM 2 (c) DS OCM 3

Observation on the surface of the interfacial face between OCM patch material and substrate concrete show less detached subtrate concrete which expected to stick to the patch material as f_r of patch repair has higher value of 4.199 Mpa than f_r of the substract concrete of 3.499 Mpa. Observation to the interfacial surface confirm the calculated f_{rs} of

the bonding strength on shear is smaller than f_r of concrete tensile strength substrate concrete, which make the splitting of two materials happening with loose of the interfacial face, not failure on the substrate concrete. However, small part of substrate concrete is observed has stick to the patch material as shown in Figure *5.25* (a) and (b).

1.2.1.2 Bond Strength on Flexure

As the beam specimens will also be loaded and create moment interaction to the section, debonding which is caused by flexure may be firstly happen than debonding caused by shear. Then bond strength on flexure is performed using specimens specification is derived from previous debonding material experiment report (Minoru, et al., 2001).

Using equation of beam stress due to moment, yielding the average bond strength has value of f_{rf} of 3.827 Mpa. This value is quite higher than the bond strength on shear. Figure *5.27* shows that there was an adequate bonding between the patch material and substrate concrete. Observation on specimens FB-OCM 1 interface shows that there is relatively wide area of tear off substrate concrete and stick to the patch materials. Similarly on FB-OCM 2 specimen, smaller area has tear off from substrate concrete. Thus tell that ordinary cement mortar may give an adequate bonding strength with the failure on the substrate concrete. However, as explained in 4.7, the substrate concrete has to be roughened and cleaned well before the application of the patch material. A bonding agent will also improve interfacial bonding strength.

Table 5.4. Flexural bond strength of OCM patch material

Specimen	Load (KN)	M (N.mm)	I (mm^4)	y	fr (Mpa)
FB-OCM 1	14	910000	24414063	125	4.6592
FB-OCM 2	11.5	747500	24414063	125	3.8272
FB-OCM 3	9	585000	24414063	125	2.9952
				Average Bond Strength f_{rf}	**3.8272**

Figure 5.26. Bond strength on flexure test of OCM patch material

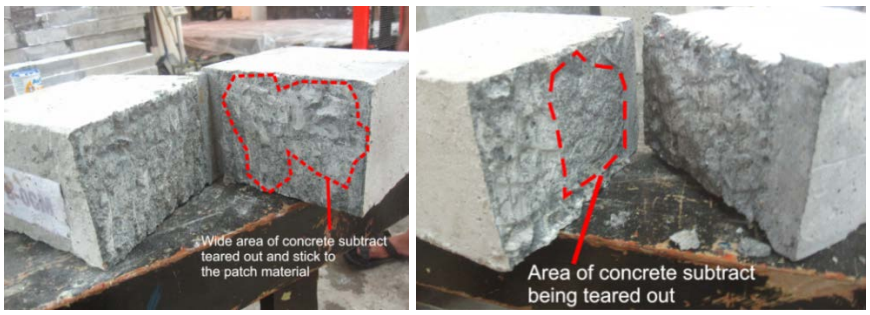

(a) (b)

(c)

Figure 5.27. Photo of interfacial face of OCM patch material of (a) FB-OCM 1 (b) FB-OCM 2 (c) FB-OCM

1.2.2 Polymer Cement Mortar

For comparison with Ordinary Cement Mortar (OCM), Polymer Cement Mortar (PCM) is also employed to observe the specimens behavior correspond to different patch material, especially for specimens repaired with straight shape rebar. PCM used in the experiment is Sikatop 122, which has 51 Mpa of compression strength in 28 days, 4.9Mpa of individual flexural tensile strength, and 1.49Mpa of flexural bond strength to concrete, based on its datasheet (SIKA, 2005).

To confirm the data gathered from technical datasheet, material testing for PCM was also performed for compression strength and bond strength on shear and flexure, as performed on OCM patch material. From the test, 28days compression strength of the PCM has result 51.2 Mpa, The value was converted from the 41 Mpa of 21 days testing age. The value confirms the compression strength provided in product datasheet.

1.2.2.1 Bond Strength in Shear

Bond strength in shear of PCM is showing higher average value of 4.441 Mpa than resulted from OCM bond shear strength. Figure *5.28* confirm the lowest value of DS-PCM 1 which has minimum of tear off of substrate concrete to the patch material or vice versa. In the other hand, DS-PCM 2 shows that there is a few of patch material stick to the substrate concrete, with increasing of load carried by the specimens. Similar with OCM patch material, both DS-PCM 2 and DS-PCM 3 showed a failure at PCM patch material instead failure at substrate concrete. Different from bonding strength on flexure test that

the substrate concrete stick to the patch material as shown in Figure *5.26*, in this failure mechanism, coarse aggregate interlocking contribute significant portion of keeping the substrate material in place. Thus confirmed by both OCM and PCM patch material has minimum interlocking that they only have fine aggregate.

Other aspect that may explain the failure on PCM patch material is deficient of tensile strength due to insufficient of PCM age. As the specimens are being tested at 21days age, bonding strength of the PCM patch material may have significant effect from its age. However, more comprehensive experiment has to be conducted to confirm this statement.

Table 5.5. Bond strength in shear of PCM patch material

Specimen	Load (KN)	A (mm^2)	f_{rs} (Mpa)
DS-PCM 1	70	237.15	2.951718
DS-PCM 2	116	238.64	4.860878
DS-PCM 3	129	234.08	5.510936
Average of bond strength			**4.441**

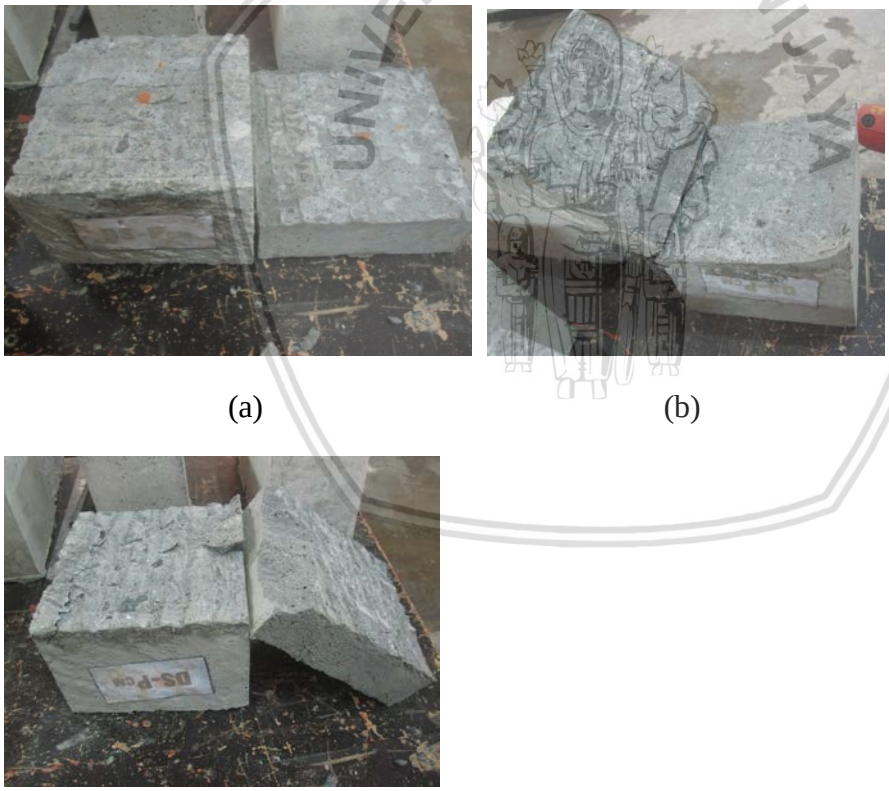

(a) (b)

(c)

Figure 5.28. Visual of direct shear interfacial face of (a) DS-PCM 1 (b) DS-PCM2 (c) DS-PCM 3

1.2.2.2 Bond Strength in Flexure

Bond strength in flexure for the PCM patch material is showing much lower despite the higher value of the bond strength in shear. Although the value is higher than stated in the product datasheet (SIKA, 2005), the average value of 2.77 Mpa is much slower than OCM's bonding strength in flexure. Figure *5.29*.(a) and Figure *5.29*.(c) show that there small area is being tear off from substrate concrete and stick to PCM patch material, which is caused by higher tensile strength of the PCM patch material than substrate concrete. However Figure *5.29*(b) shows no failure happening on both materials, and bond failure completely caused by patch material adhesive to the substrate concrete.

Table 5.6. Bonding strength of PCM patch material

Specimen	Load (KN)	M (N.mm)	I (mm^4)	y	fr (Mpa)
FB-PCM 1	8.5	552500	24414063	125	2.8288
FB-PCM 2	6	390000	24414063	125	1.9968
FB-PCM 3	10.5	682500	24414063	125	3.4944
				Average Bond Strength f_{rf} =	**2.7733**

(a)

(b)

(c)

Figure 5.29. Visual of interfacial face of PCM bond strength in flexure of (a) FB-PCM 1 (b) FB-PCM 2 (c) FB-PCM 3

Compared to the OCM patch material, PCM patch material seems showing high inconsistency result despite its careful handling and application. Bond strength in flexure

which is expected to be higher than OCM patch material has shown much lower values. Moreover, high deviation of bond strength value occurs in its group itself. Either there were many factor affecting the bond strength or the testing age is the only problem, more comprehensive experiment is needed to confirm this behaviour.

1.3 Post Repair Final Test

Final load is reloading test of the specimens which will show how the specimens will behave correspond to each given repair. Comprehensive observation is performed to gain more data so that any behavior can be explained. In line with the purpose of this study, post repair final load activity is expected to explain how the strain behavior after given repair, specimens behavior of deflection, crack path, maximum load that the specimens could carried, how the analysis could be performed, and what limit state should be put on any structure repaired with this procedure. As additional discussion, the plastic hinge behavior will also be discussed in this section.

1.3.1 Load and Beam Deflection

Deflection value for each load increment has been recorded on final load session of the laboratory experiment. Observation of deflection behaviour has been observed with increment of load is 100kgs. The increment value is considered relatively fine and specimens behaviour is captured well. However, as seen in further discussion, there is no significant behaviour in load and deflection curve between specimens loaded ultimately or only to yield state. Hence, load beam discussion will be grouped according to the given repair type.

Ductility of beam specimens could be an interesting topic in repaired beam experiment, however, that would not be an issue in this discussion. Different range of point to stop loading on reloading session is more caused by limited range of LVDT apparatus and trial and error of measurement placement setup on one after another specimens . Hence, several beam such as S-4 Ultimate-2, S-7 Ultimate-1 and S-7 Ultimate-2 have lower point to stop loading value than others specimens due to their early test of final load. Fortunately, as seen in specimens repaired by 700mm staple shape rebar, which are expected has highest performance, has back to original beam capacity before the LVDT apparatus meets its limit displacement. Thus conclude that ductility measurement of beam to total collapse is not necessary.

As conducted repair procedure has propped the beam specimens during repair process, there was a indeterminant zero deflection after released by load. However, there was a measurement of concrete strain before and after specimens movement from loading frame to repair area. The measurement shows that there is no significant change of compression strain. After given repair, initial displacement is set as zero for convenience of comparation.

1.3.1.1 Load-Deflection Behaviour of Specimens Repaired by 400mm Staple Shape Rebar

Result of reloading or final load session to the specimens has resulting load and deflection summarized in Table *5.7*. The loading test shows an increasing of load capacity for all specimens tabulated in column Load Relative to Control Beam, which is compared as increasing capacity from control beam. 2690Kgs of control beam load has been confirmed with other ultimate specimens which no one reach the value, despite its ultimate state. About 108% of load capacity could be taken with ultimate specimens and 103-104% capacity for the yield specimens. Deflection at Max load is the deflection measured from its post-repair initial position, while Relative Deflection at Max Load is deflection relative to the base initial position.

Table 5.7. Load and Deflection Summary of 400mm staple repaired specimens

Specimen	Preload (Kgs)	Final Load (Kgs)	Load Relative to Control Beam (%)	Deflection at Max Load (mm)
Control Beam	-	2690	**100.00**	24.23
S-4 Ultimate (1)	2620	2925	**108.74**	17.027
S-4 Ultimate (2)	2587	2920	**108.55**	14.7
S-4 Yield (1)	1600	2780	**103.35**	24
S-4 Yield (2)	1400	2800	**104.09**	22.15

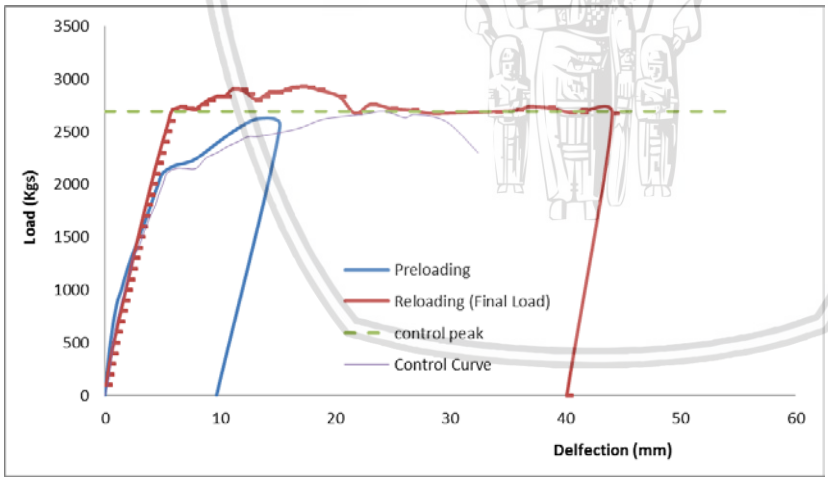

Figure 5.30. Reloading Load-Deflection curve of S-4 Ultimate-1

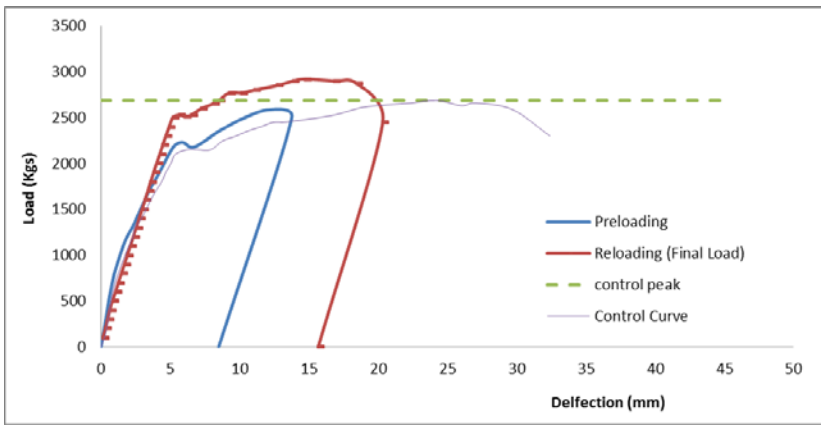

Figure 5.31. Reloading Load-Deflection curve of S-4 Ultimate-2

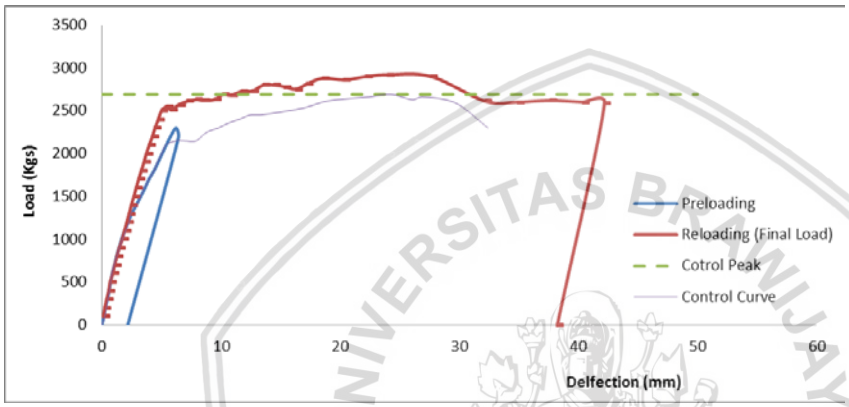

Figure 5.32. Reloading Load-Deflection curve of S-4 Yield-1

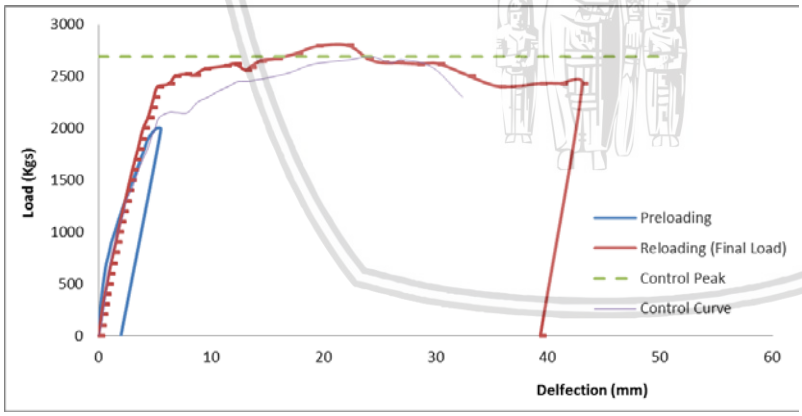

Figure 5.33. Reloading Load-Deflection curve of S-4 Yield-2

Control beam peak load of 2690Kgs is also plotted to the graph of Figure *5.30*, Figure *5.31*, Figure *5.32*, Figure *5.33* as a benchmark to the reloaded load-deflection curve. Although only 8% maximum of load increasing, which is not significant compared to the 700mm staple repaired specimens, the effect of the staple rebar seems certain. More comprehensive discussion for the effect of the staple repair rebar is need the strain data correspond to given load, which will be discussed in 5.3.2.

1.3.1.2 Load-Deflection Behaviour of Specimens Repaired by 700mm Staple Shape Rebar

Significant increasing load capacity is well observed from specimens with 700mm staple shape repair rebar. Having benchmarked with control beam, about 32.34% increasing capacity was achieved by S7 Ultimate-1 specimens. Relatively to the its preload load value, the load capacity increasing to 47%. However, it may not convenience to be taken as benchmark load as there still possibilities of increasing load after point to stop load at reloading session due to strain hardening of the steel reinforcement.

The control beam load-deflection curve is also plotted to the curves to showing significances of increasing capacity. For further study development, it also possible to analyse and compare the restrain energy for repaired beam to the base preloaded beam using two plotted load-deflection curves. As explained from earlier session, that point to stop loading which is stop at about 29-30mm for S-7 Ultimate-1 and S-7 Ultimate-2 is not the point of total collapse of the beam specimens, but because of early trial and error to find correct installation setup to gain maximum recording data. However, Figure *5.36* and Figure *5.37* show that after the specimens reaching about 25 to 28mm of deflection, the load carried started to drop and developing to follow the base or control beam curve path. Detailed information of beam behaviour has to be countered with stress and strain behaviour of the steel reinforcement, steel rebar and compression concrete.

Table 5.8. Load and Deflection Summary of 700mm staple repaired specimens

Specimen	Preload (Kgs)	Final Load (Kgs)	Load Relative to Control Beam (%)	Deflection at Max Load (mm)
Control Beam	-	2690	**100.00**	24.23
S-7 Ultimate (1)	2410	3560	**132.34**	18.63
S-7 Ultimate (2)	2450	3300	**122.68**	14.7
S-7 Yield (1)	2200	3460	**128.62**	13.02
S-7 Yield (2)	2110	3260	**121.19**	16.46

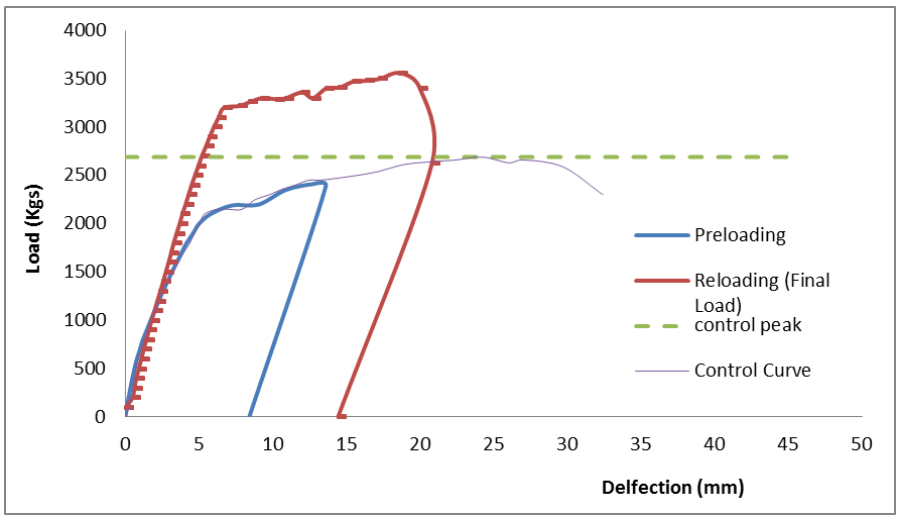

Figure 5.34. Reloading Load-Deflection curve of S7 Ultimate-1

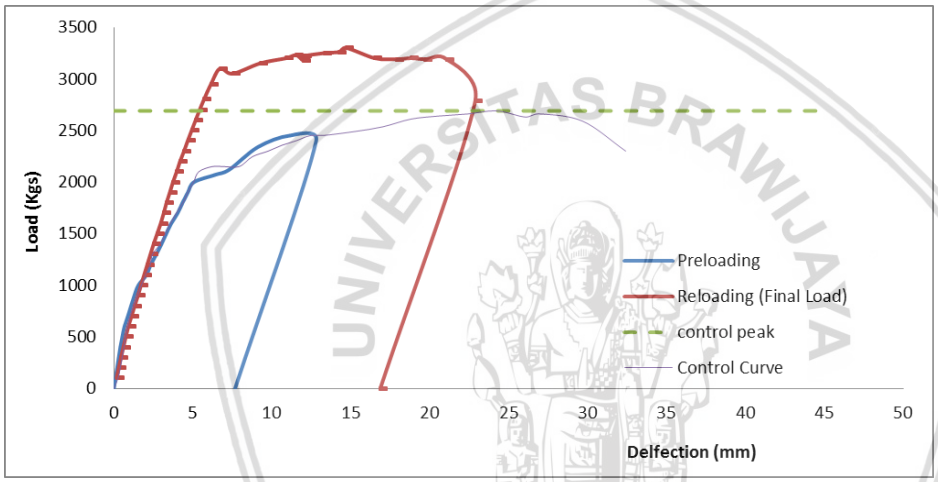

Figure 5.35. Reloading Load-Deflection curve of S7 Ultimate-2

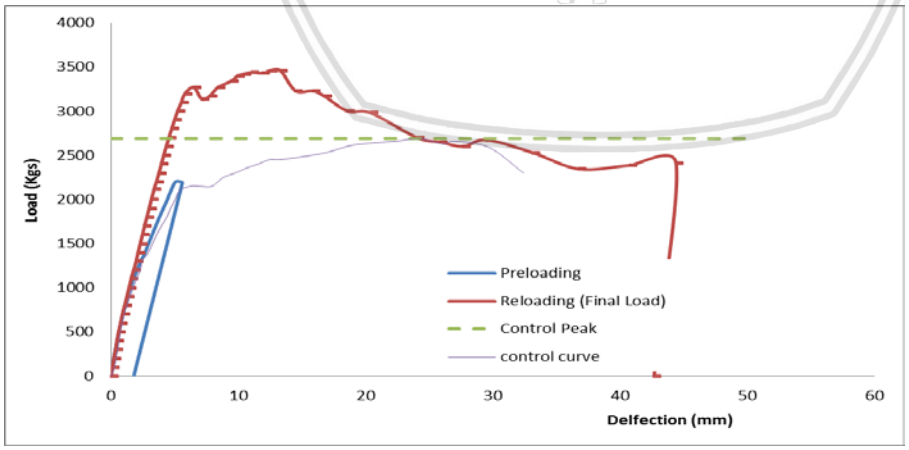

Figure 5.36. Reloading Load-Deflection curve of S7 Yield 1

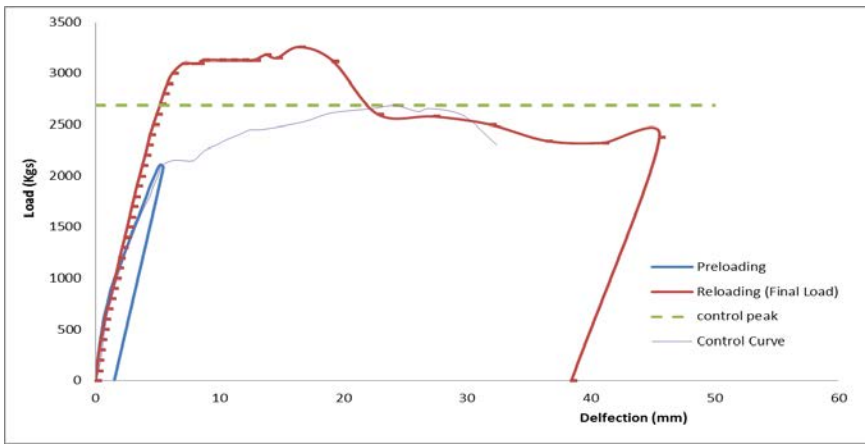

Figure 5.37. Reloading Load-Deflection curve of S7 Yield 2

1.3.1.3 Load-Deflection Behaviour of Specimens Repaired by 400mm and 700mm Straight Shape Rebar

Different behaviour is showed on specimens repaired using straight shape repair rebar, which each specimens of this group has unique pattern of load-deflection curve. Increasing of load capacity is only occur for specimens which are repaired using 700mm rebar, while the repaired specimens which are use 400mm rebar do not show higher load capacity compared to the control beam.

Although both specimens repaired using straight rebar do not show any increasing load capacity, they show slightly different deflection pattern. ST4 Yield PCM, as shown in Figure *5.40* has higher early load than ST4 Yield OCM. PCM adhesive seems do the bonding well at first, which could make the specimens increase its load capacity almost reach control beam peak load. However, it drop after some interface bond is break out. In the other hand, ST4 Yield OCM as shown in Figure *5.38* do show higher early strength compared to control beam, although not as high as with PCM patch material, then drop and following base specimens load-deflection curve.

The specimens repaired with 700mm straight repair rebar are showing about 11-13% of higher load capacity than control beam specimens. Specimens with OCM patch material, as shown in Figure *5.39* showing high early load capacity and drop abruptly after receiving more deflection, which is caused by lower bonding strength and lack of tensile strength reinforcement such as fiber. In the other hand, specimens with PCM patch material as shown in Figure *5.41*, has inflection point after reaching control beam peak load, and then develop to its maximum load capacity. Detailed discussion of the cause of its behaviour, and what bonding strength which has much affection will be discussed on strain and bonding strength session.

Table 5.9. Load and Deflection Summary of all staple repaired specimens

Specimen	Preload (Kgs)	Final Load (Kgs)	Load Relative to Control Beam (%)	Deflection at Max Load (mm)
Control Beam	-	2690	**100.00**	24.23
ST-4 Yield OCM	2172	2670	**99.26**	23.609
ST-7 Yield OCM	2110	3000	**111.52**	5.95
ST-4 Yield PCM	2210	2740	**101.86**	16.69
ST-7 Yield PCM	1900	3040	**113.01**	9.61

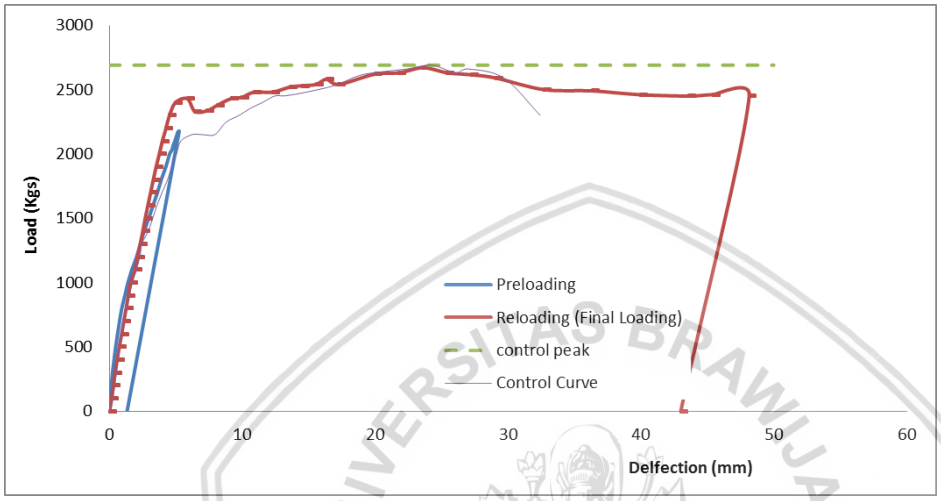

Figure 5.38. Reloading Load-Deflection curve of ST-4 Yield OCM

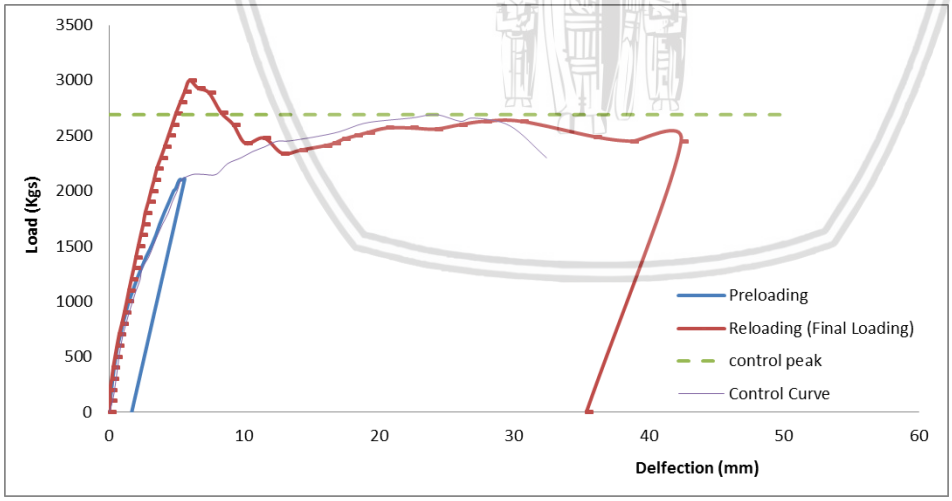

Figure 5.39. Reloading Load-Deflection curve of ST-7 Yield OCM

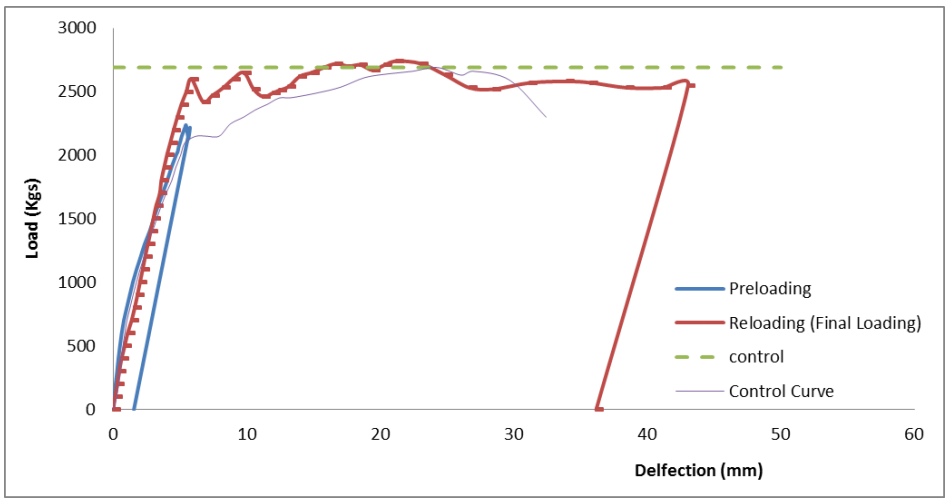

Figure 5.40. Reloading Load-Deflection curve of ST-4 Yield PCM

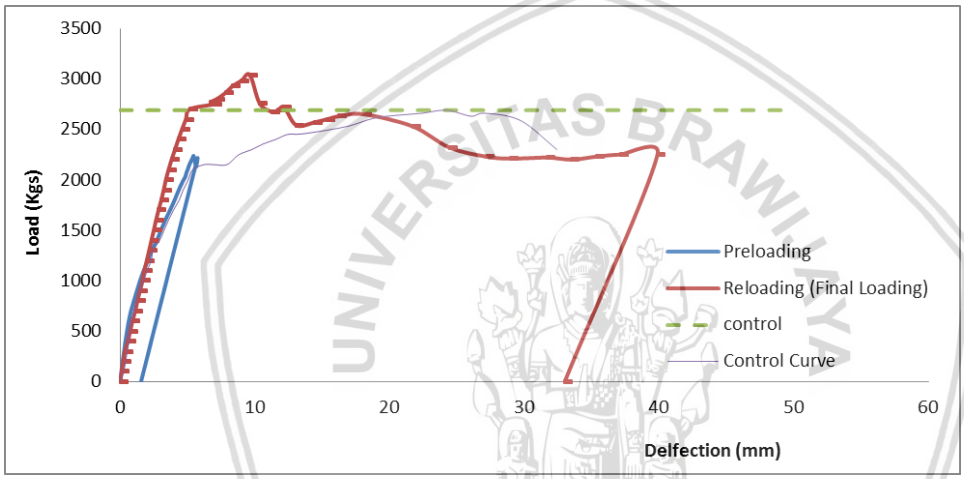

Figure 5.41. Reloading Load-Deflection curve of ST-7 Yield PCM

1.3.2 Strain Observation of Concrete Compression

All repaired specimens have been preloaded with ultimate and yield state. Therefore, plastic strain occurs after specimens are given unloading procedure. After given repair, the specimens are then reloaded until meet their maximum state and collapse. For compression strain measurement, concrete strain gauge of PFL-20 is applied to top beam surface before given preload. The strain gauges were not removed during repairing process and reused on final loading session to maintain its constant strain measurement. On the curve plot, the preload and reloading curve are plotted together with the plastic strain point as the assemble point of the two curves. Strain change during repairing procedure is considered as zero, as the handling procedure is taken carefully and controlled as detail discussed on CHAPTER 4. Only specimens repaired with staple shape rebar which provide compression strain data, as specimens with straight shape rebar is not equipped with concrete strain gauge.

1.3.2.1 Specimens with Ultimate State Preload

According to 5.1.4, concrete always shows a lower elasticity slope of reloading curve after given unloading process. However, as shown in Figure *5.42*(a), the specimens show steeper reloading curve than preloading curve. It may happen because of given addition reinforcement of repair rebar. More reasonable answer for the behaviour is that highest compression stress is moved to the next crushed concrete position, which is no longer positioned at the middle of the beam spans, where the strain gauge is placed. Additional repair rebar creates abrupt changes of beam flexure capacity along the beam length, hence there is high possibilities of the plastic hinges is moved to the where abrupt change is placed. Figure *5.42*(b) shows that the widest crack develops at the end of repair rebar and directed to the load point.

However, the crack cannot propagates to reach the centre of the beam. Plateau line strain on reloading curve, showed in Figure *5.42*(a) is not necessary mean that the concrete strains very quickly as steel does. It is caused by concrete crush which the spalling of the concrete cover reaches the strain gauge position. Figure *5.42*(b) shows that after the loading reach more than 2700kgs, the concrete near loading point is crushed and affect the strain gauge.

Another specimens, the S4 Ultimate-2, which is the crushed concrete is has a distance shows that the strain gauge could provide stable data during loading as shown in Figure *5.43*. It's load-strain graph shows that the compression concrete at the beam mid span reach its maximum strain of 0.004 with the load reaching 2920 Kgs, but then the crush is moved to about 15cm from beam mid span and makes the load carried is drop to about 2500 Kgs. It could be possible that the strain at crushed position reach far more than 0.004.

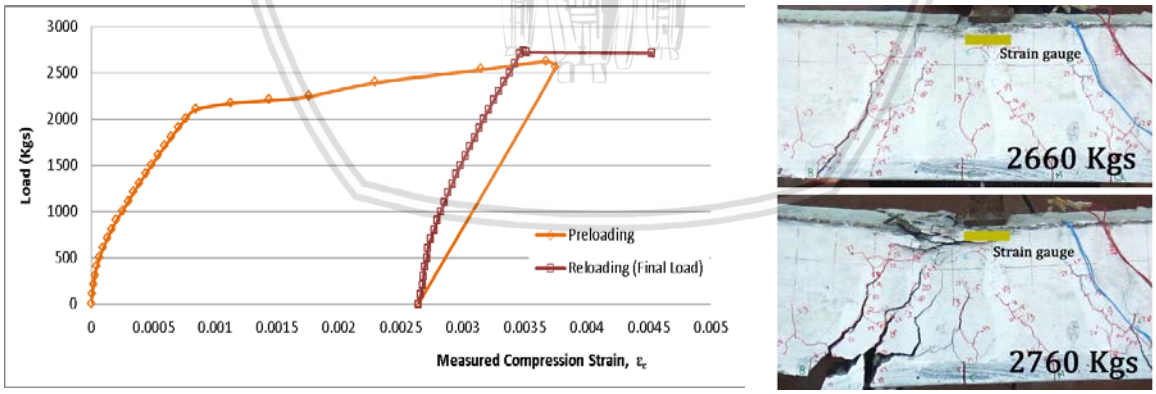

(a) (b)

Figure 5.42. (a) Concrete concrete compression load-strain curve of S4 Ultimate-1 (b) crack propagation

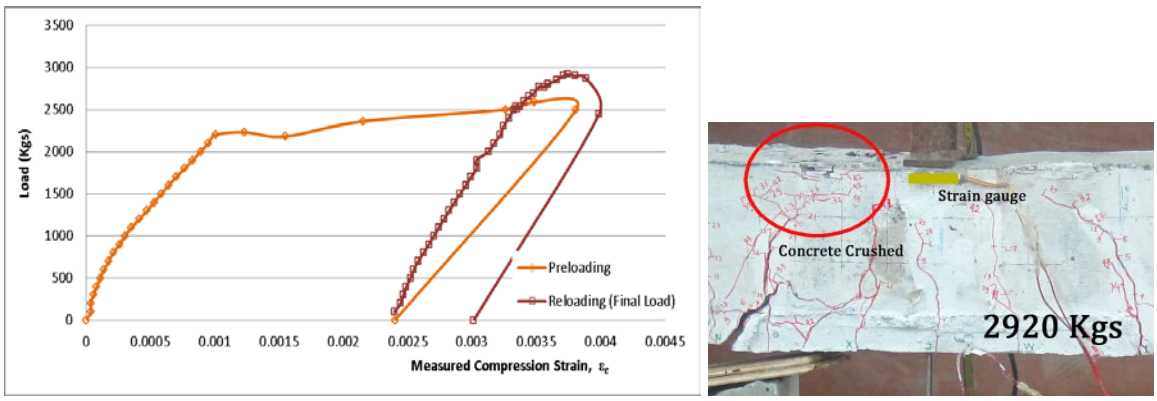

(a) (b)

Figure 5.43. Concrete concrete compression load-strain curve of S4 Ultimate-2

Different reloading curve is showed by 700mm staple repaired specimens. The compression strain curve is showing a inflection point after climbing to 600 Kgs, where first tension crack is occurred. This confirms the reloading curve behaviour discussed in 5.1.4.3 which the concrete will show lower Er of reloading, when the unloading strain ε_u is exceeding ε_0 of 0.002. The unloading strain of this specimen preload may provide big difference to the reloading curve behaviour, as S7 Ultimate-2 is unloaded on ε_u equals to 0.00424. That relatively higher than other ultimate specimens which are unloaded on ε_u equals 0.0037 to 0.0038. The much higher unloading strain of S7 Ultimate-2 may create futher deterioration to the concrete and affect the unloading behaviour. Further experiment is needed to confirm this behaviour.

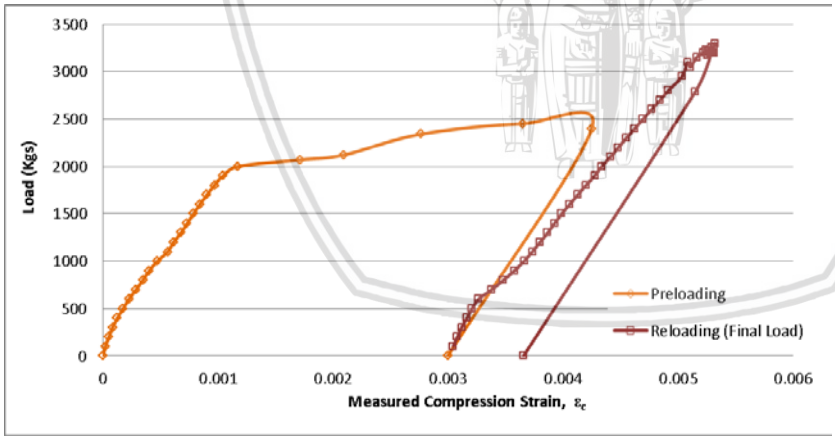

Figure 5.44. Concrete concrete compression load-strain curve of S7 Ultimate-2

1.3.2.2 Specimens with Yield State Preload

Similar with ultimate state specimens, the yield state specimens has reach 0.004 strain value then experience a strain decreasing due to crush of compression concrete. However, different than S4 Ultimate-1 which the strain gauge show error result, both S4 yield-2 and S7 Yield S-2, as shown in Figure *5.45* and Figure *5.46* show decreasing of strain due to increasing of loading. This is may be caused strain relaxation of the compressed concrete at the middle beam due to concrete crush adjacent to the strain gauge.

As seen in Figure *5.45*(a) and (b), the strain gauge showing a decreasing of concrete strain after the concrete looks crushed adjacent to the strain gauge. After the most stressed section is crushed, with about 1 centimeters from the top fiber, the higher stress is moved to the lower section which is the area strain gauge placement released from stress. Similiarly, same strain behaviour occurs on the S7 Yield-2 specimen. It strain is decreased after concrete crush adjacent to the strain gauge placement area.

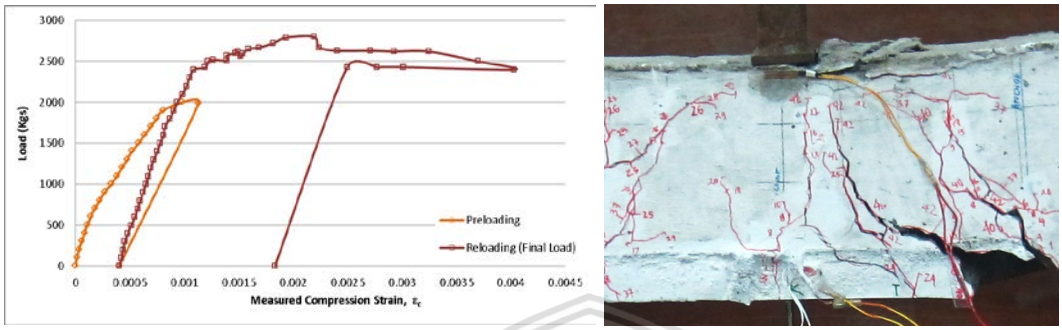

(a) (b)

Figure 5.45. Concrete concrete compression load-strain curve of S4 Yield -2

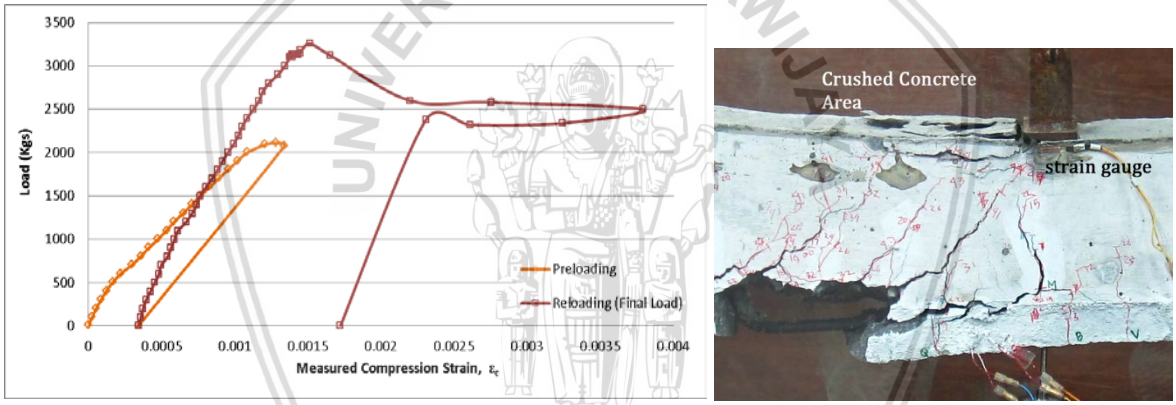

(a) (b)

Figure 5.46. Concrete concrete compression load-strain curve of S7 Yield -2

1.3.3 Strain Observation of Steel Reinforcement and Repair Rebar

Steel strain gauges were place to the both original rebar and repair rebar. Strain observation shows that there is a good compatibility for repair system consists of steel repair rebar and patch material to the substrate concrete until certain magnitude of given load. After observation to all strain curve behaviour, the split process of the repair system from the substrate system may be marked with the intersection of the two strain curves. That means the repair system, especially for repair rebar, experiences stress relaxation due to either debonding of patch material from the substrate concrete or bond slip between rebar and the surrounding concrete.

Although carefully installation was performed to the strain gauge, there are several errors occur at the strain gauge. S4 Ultimate-1 and S-7 Ultimate-1, and ST7 OCM are

showing error in original rebar strain gauges; while S7 Yield-2 is showing error in repair rebar strain gauge. However, as there only one strain gauge was failed at one specimen, the strain curve may still observable.

1.3.3.1 Strain Behaviour of Original Reinforcement and Repair Rebar Reinforcement of Specimens with 400mm Staple Shape Rebar

Observation on the strain behaviour for both original reinforcement and repair rebar reinforcement shows that average intersection point, which the repair system start to split from the substrate concrete in 2180 Kgs. The value is only 76% of average maximum load capacity of specimens repaired with 400mm staple shape rebar. Decreasing strain of means that there is stress relaxation experienced on rebar which could be caused by debonding of patch material or bond slip of the rebar. Vertical crack propagation is well noticed in crack observation shown in Figure *5.47*, however, there is no sign of horizontal crack that could be sign of debonding process of the patch material. Therefore, the stress relaxation of the repair rebar is caused by the rupture of the concrete, marked by the vertical crack on around staple legs anchoring point. The crack tends to separate the repair system to the substrate concrete.

Figure 5.47. Crack visual of S4-Ultimate-2, S4 Yield-1, S4 Yield-2 on their load of intersection point

However, after load of curve intersection is passed, there is no sign of inflection point of load and deflection curve for S4 Ultimate-2 and S4 Yield-1 as may be observed in Figure *5.31* and Figure *5.32*. Means that repair system is still giving significant contribution to load capacity of the specimens. Differently, Figure *5.33* shows that inflection point of load-deflection curve happening at the intersection curve point of the S4 Yield-2 on Figure *5.50*. It means that the repair system is starting to split from the substrate system at that point although still giving strength contribution until totally spitted.

The splitting process of S4 Yield-2 specimen is also marked by sudden decrease of repair rebar strain and sudden increase of original rebar strain. The similar behaviour is also well noticed on S4 Ultimate-2 and S4 Yield-1 specimens, but happened in higher load value than load of the intersection point. After the specimens reach their maximum load, and the repair system is completely split, load capacity is drop to load capacity of the base specimen without repair and the original rebar is starting to gain longer strain.

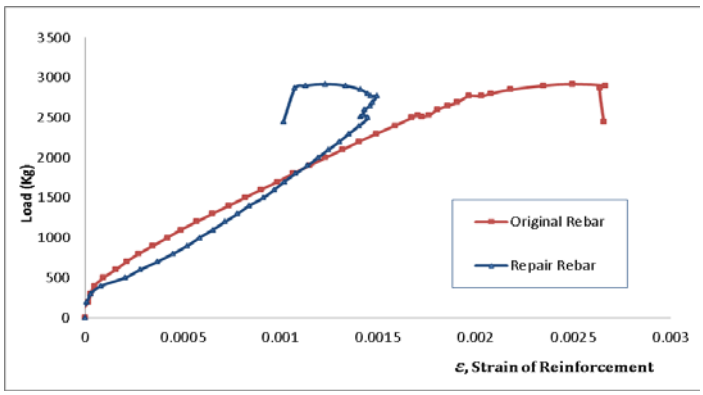

Figure 5.48. Tension reinforcement strain of S4 Ultimate-2

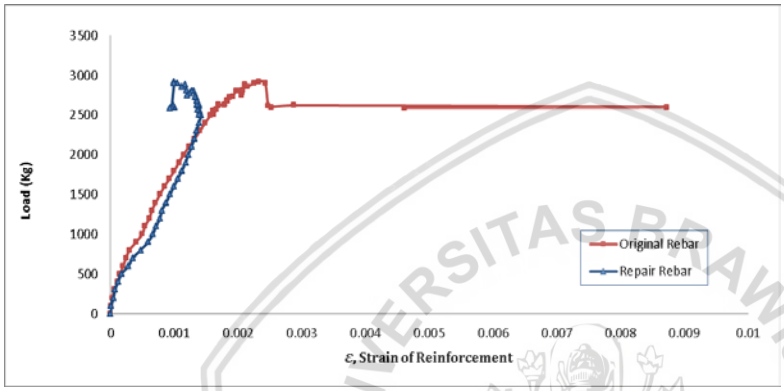

Figure 5.49. Tension reinforcement strain of S4 Yield-1

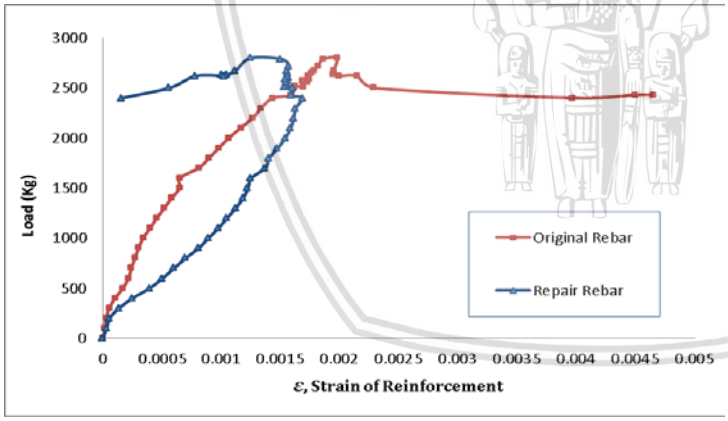

Figure 5.50. Tension reinforcement strain of S4 Yield-2

1.3.3.2 Strain Behaviour of Original Reinforcement and Repair Rebar Reinforcement of Specimens with 700mm Staple Shape Rebar

Well observable data is provided by specimens repaired with 400mm staple rebar. In the other hand, only one specimen of 700mm staple repaired beam which provide well observable data as shown in Figure *5.52*, while others show zero strain data of either original rebar or repair rebar strain. Despite lack of data, the behaviour of the specimens may still be observed well using information provided with other specimens.

Better performance of 700mm staple repaired specimens is confirmed by the load-strain curves. As shown in Figure *5.51*, S7 Ultimate-1 specimen shows that the repair rebar is experiences yielding process after reach more than 0.002 of strain while none of 400mm staple repaired specimens experience yielding process. Decreasing strain occurs after the load reach 3000 Kgs and continue to decrease to steel plastic strain of 0.002 while the load is still increase to the maximum load of 3470 Kgs.

Similarly, S7 Yield-1 repair rebar was also experiencing a yielding process. It is believed that the specimens has better compatibility than S7 Ultimate-1, which the strain of the repair rebar could reach maximum load while yielding process still continues and not to decrease. After that, the strain is starting to decrease and the strain of original rebar experience large yield strain with the load continue to drop.

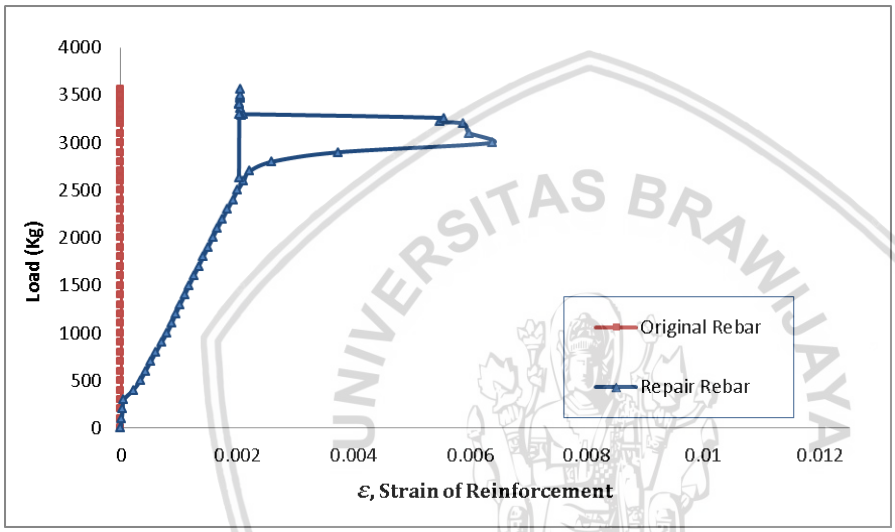

Figure 5.51. Tension reinforcement strain of S7 Ultimate-1

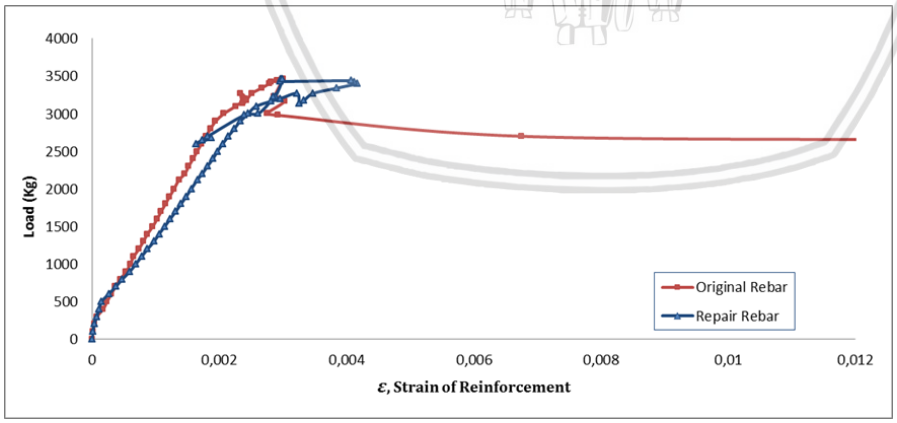

Figure 5.52. Tension reinforcement strain of S7 Yield 1

1.3.3.3 Strain Behaviour of Original Reinforcement and Repair Rebar

Reinforcement of Specimens with Straight Shape Rebar

Poor performance of repair system is confirmed by the load-strain data of the specimens repaired using straight shape rebar, especially for those repaired using 400mm

straight shape rebar. Despite their poor performance, very good compatibility is showed on the early loading, with the two strain curves are developing at the same slope, as shown in Figure *5.53*, Figure *5.55*, and Figure *5.56*. This is not happening with the staple shape rebar, as the shape of the rebar may be the causes of different slope developing between the two curves.

Poor performance is marked by the decreasing rate of strain development during loading, and the repair system is start to split from substrate system in relatively early strength, without any further contribution to flexure strength. This is showed by sudden decrease of strain of repair rebar on 2400Kgs and 2600Kgs for the S4 Yield OCM and S4 Yield PCM with no significant load increase after that while the original rebar strain start to continues to experiences large yield strain from that point. Sudden decrease of the strain, which also means sudden stress relaxation, is caused by debonding process of the patch material from substrate concrete.

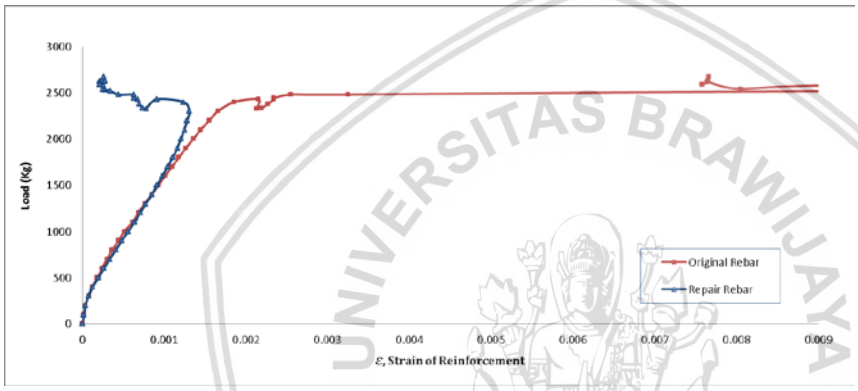

Figure 5.53. Tension reinforcement strain of ST4-Yield OCM

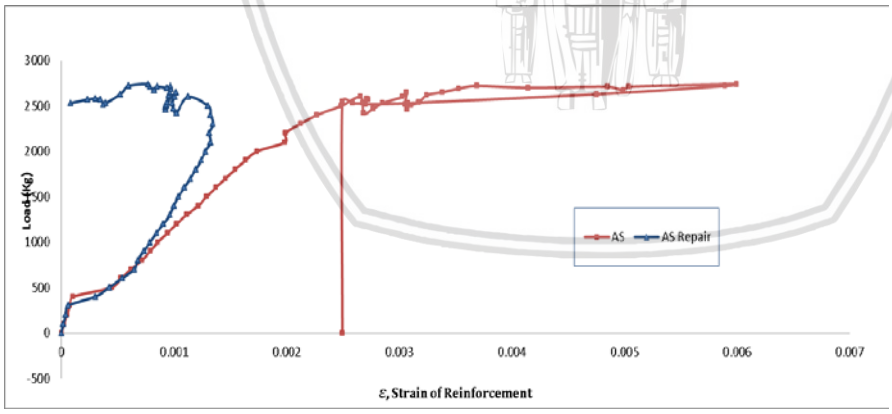

Figure 5.54. Tension reinforcement strain of ST4-Yield PCM

On the other hand, good performance is confirmed by load-strain curves for specimens repaired with 700mm straight shape repair rebar. Despite error strain reading of original rebar strain, repair rebar strain of ST7 Yield OCM showing good performance which reaching specimens maximum load before experiences sudden decrease of strain as shown in Figure *5.55*. Poor bonding strength of OCM patch material may cause the repair system having more incompatible behaviour along two developing curves.

ST7 Yield PCM also confirm good performance and good compatibility as the two strain curves are developing proportionally to each other as shown in Figure *5.56*. The repair rebar was also experiencing the yield strain and continuously to strain until reach specimens maximum load. With decrease of rebar strain, the load carried is drop and the two curves is directing to different directions.

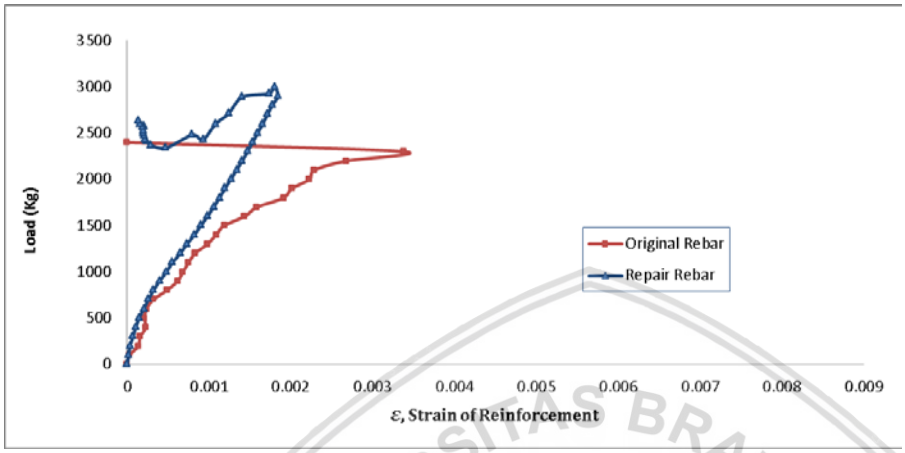

Figure 5.55. Tension reinforcement strain of ST7-Yield OCM

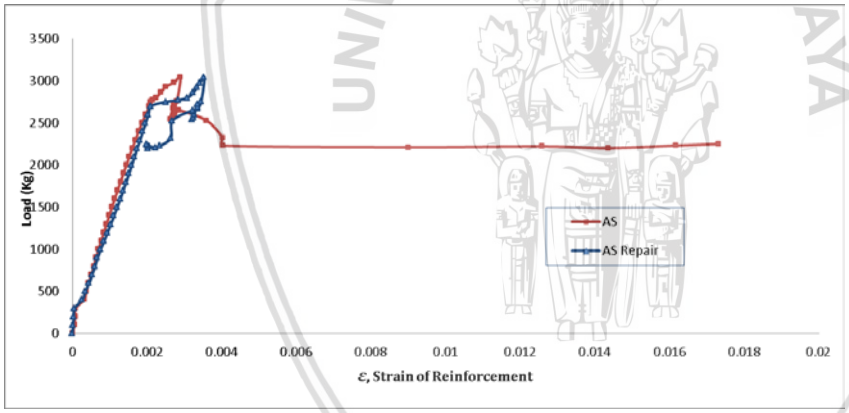

Figure 5.56. Tension reinforcement strain of ST7-Yield PCM

1.3.4 Crack Path of the Specimens

Crack path during final loading session is observed and documented. Every crack development of each load increments is recorded and marked. The main purpose of crack path observation is to understanding and confirm others data such deflection, concrete strain, and reinforcement strain to conclude the behaviour of the loaded specimens. Proposed analysis approach result may also to be confirmed using crack path behaviour of the specimens. For convenience of the discussion, all specimens will be group into three groups, the specimens repaired using staple rebar, the specimens repaired rebar with OCM patch material, and the specimens repaired rebar with PCM patch material, which three of group has distinct crack behaviour.

After given preload, all the specimen cracks are patched in the surface using wall paint putty compound to cover early developed crack. Hence, during reloading session, there are cracks path that actually present before first load is applied. However, for area which has covered by patch repair mortar, both OCM and PCM, all the crack have been covered by about 3cm depth of patch repair. So there will be no cracks acting as notch around the bottom of mid span of the specimens. Despite of the treatment, new cracks are developed at the same area of the specimens. a comprehensive discussion of crack development will explain the behaviour.

1.3.4.1 Crack Path of Specimens Repaired with Staple Shape Rebar

The crack propagation on the specimens with staple shape rebar showed with mostly following the early crack path development. Although not all early crack is reopened during reload, Figure *5.64* clearly show that new crack develop further from the crack path developed from preload session.

Figure *5.57* shown that the first crack of S-4 Ultimate-1 specimen which patched using OCM, was occur at one of two vertical interfacials between the patch material and substrate concrete, and so do the S-4 Ultimate-2, S-4 Yield-1, S-4 Yield-2. Schematic terminology of stress and force transfer from the concrete substrate to the repair rebars and patch material may be explained by Figure *5.58*. The anchor legs of repair rebar transfer the force carried by rebar body from bottom strain of the concrete. The force which is stopped to the end of anchor legs create a tension to adjacent concrete toward the support side, makes the interfacial face to debond. There is no significant difference between the yield specimens or the ultimate specimens.

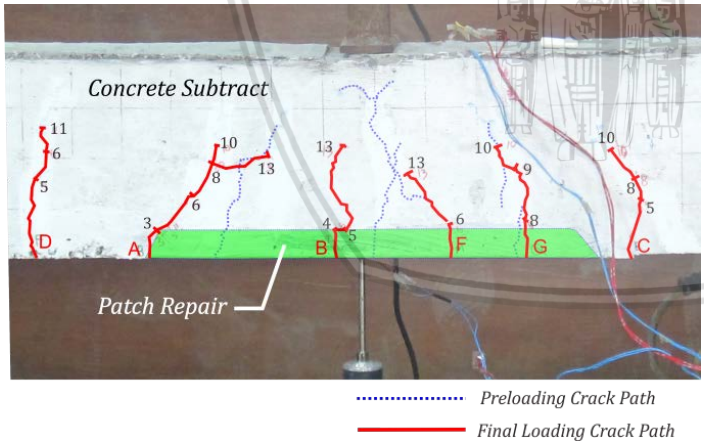

Figure 5.57. Crack patch development during reload of specimens S4 Ultimate-1

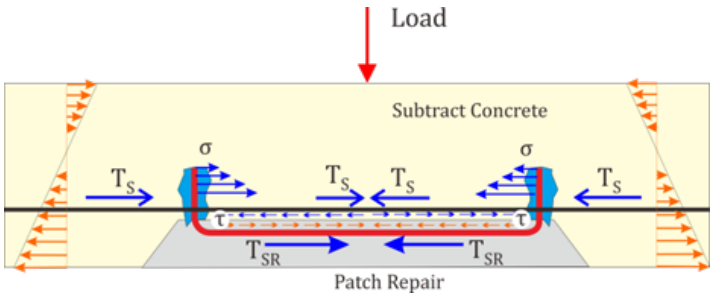

Figure 5.58. Proposed force and stress scheme of beam reinforced with Staple shape rebar

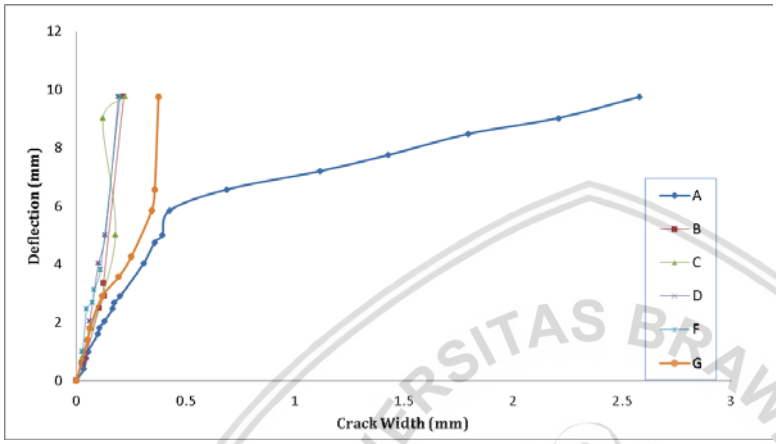

Figure 5.59. Crack width of defletion increment correspondence to Figure *5.57*

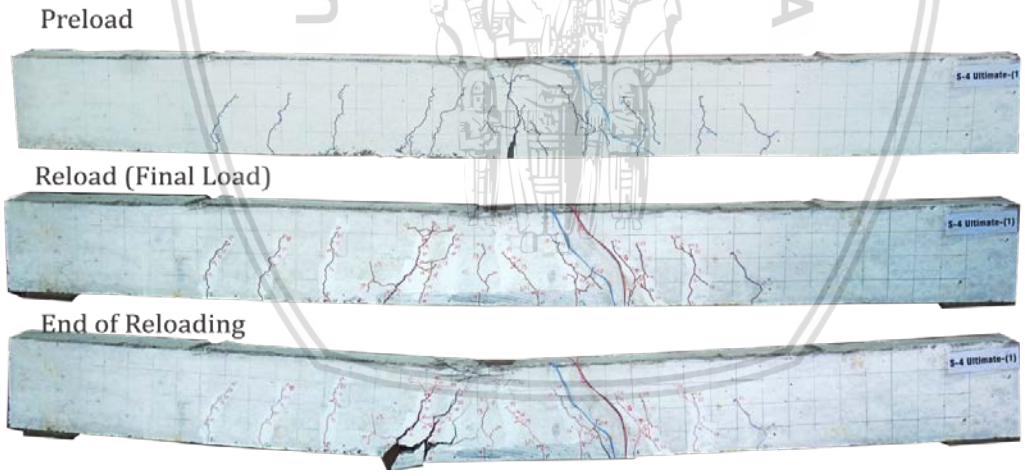

Figure 5.60. Crack path of S4 Ultimate-1

(a) (b)

Figure 5.61. Repair system failure of the S4 Ultimate-1 (a) develop plastic hinnge (b) extracted anchor legs

From the Figure *5.57* some crack paths are propagating vertically to previous developed crack path of preload session, but some of previous cracks were not followed by the new cracks. This may be happened because of changing stress trajectory of the repaired beam specimens, which create different stress state for each body particle of the structure.

Load-strain curve of Figure *5.48* may explain that the repair system remains functioned until the anchor legs are extracted from its hole as shown in Figure *5.61*. Another specimens of S4 Yield-1, failure state of the repair system happen when the load reaching 2400Kgs, with the relaxation of repair rebar stress, as shown in Figure *5.49*. It shows that after the specimen carries 2400Kgs, the strain of repair rebar is decreased and strain of original rebar suddenly increased. There is no sign of horizontal delamination of patch interfacial during failing process of repair system. The horizontal crack were mostly propagated on the concrete substrate itself.

Meanwhile, first crack of specimens with 700mm staple rebar is occurring at mid-point of the specimens. Figure *5.58* may explain that the stress transfer τ of shear stress between the patch interfacial to the repair system is capable to extend the stress from the substrate concrete to repair system. Other reason is that smaller tension stress present on the interfacial face of the patch material to the substrate concrete compared to the specimens repaired with 400mm rebar.

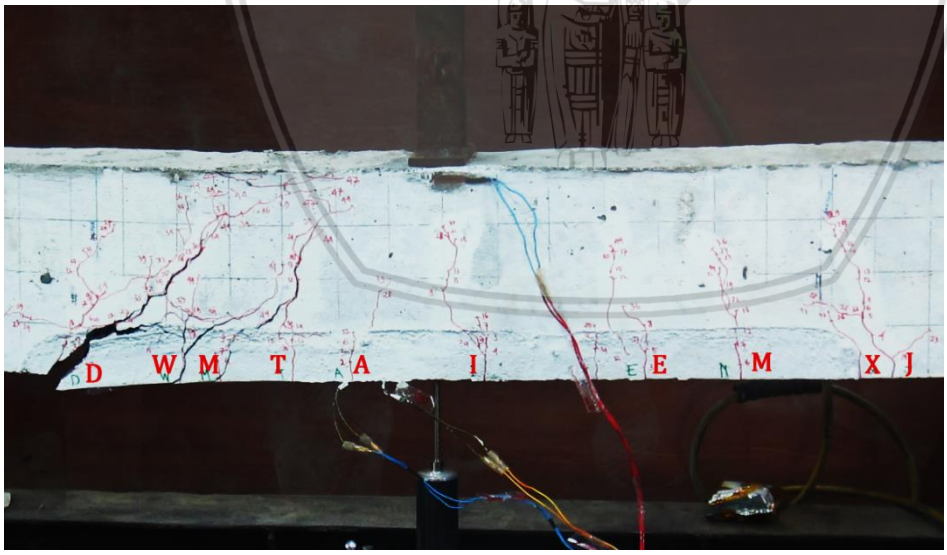

Figure 5.62. Crack path of S7 Yield-1 Specimens

Other observation result of the crack path is that all the beam specimens repaired using staple shape rebar is failed by occurring of diagonal cracks started from the anchor legs line toward load point. This developing of cracks is very different than cracks developed at preloading session, which in preloading session cracks propagate in vertical manner where built plastic hinge is relatively occur in narrow area. As shown in

Figure 5.62. Crack path of S7 Yield-1 Specimens, the cracks was started at legs anchorage cross line, and not from the interfacial face of patch material, then diagonally propagate toward center of the beam where the load point is placed. However, by the present of stirrups, the cracks cannot developed excessively then another cracks propagate adjacent to the first large crack toward the same direction.

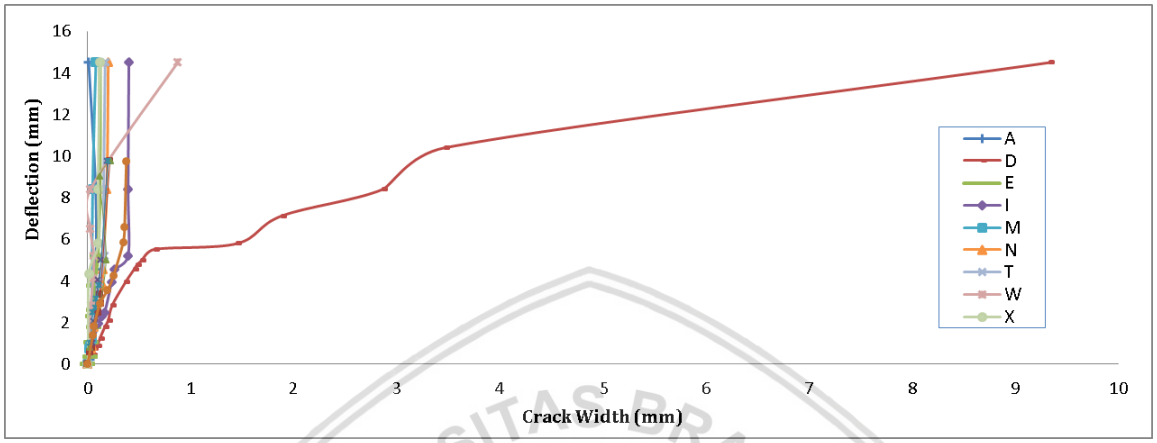

Figure 5.63. Crack width with deflection increment of S7 Yield-1

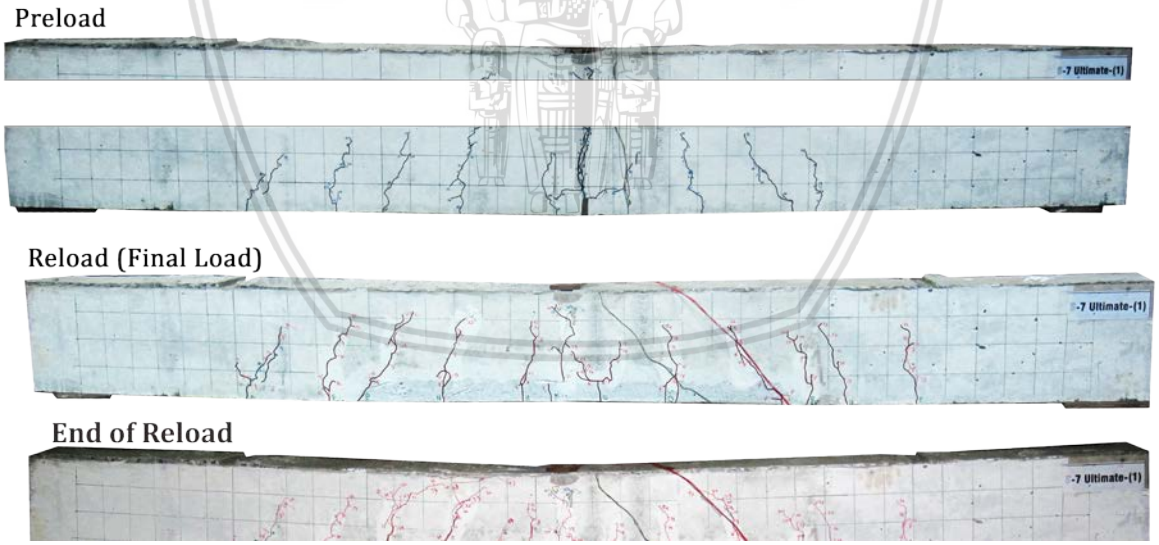

Figure 5.64. Crack path of S7 Ultimate-1

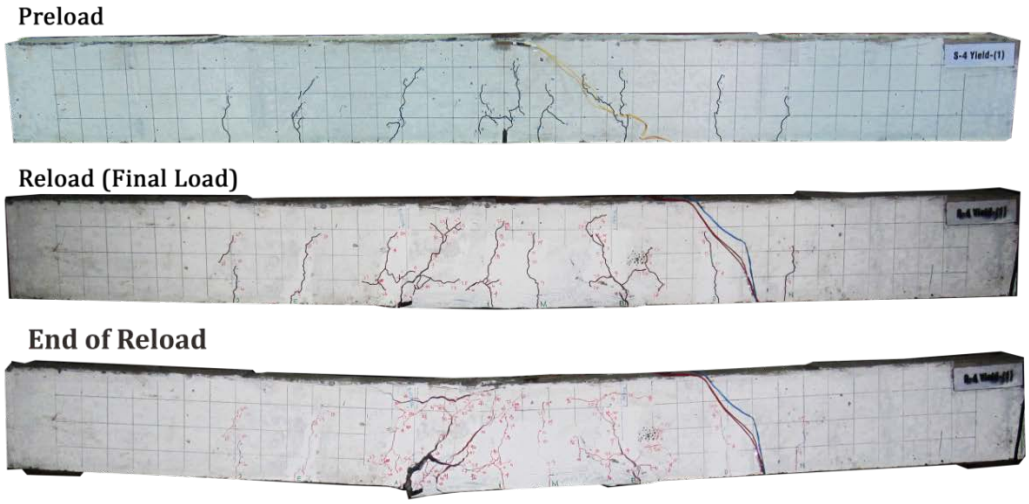

Figure 5.65. Crack path of S4 Yield-1

1.3.4.2 Crack Path of Specimens Repaired with Straight Shape Rebar

Observation of crack path on the specimens repaired using straight shape rebar with PCM mortar shows that similar crack propagation to the staple shape rebar is also achieved. After several increments of load, beam specimens of ST4 Yield PCM started to show diagonal crack started from the end of the straight rebar line toward load point as shown in Figure *5.67* and Figure *5.66* for crack opening width. This crack propagation behaviour in also shown in ST7 Yield PCM as shown in Figure *5.68*. However, different than specimens repaired using staple rebar, in these specimens, horizontal cracks is always occurs on the interfacial line of the patch material near the maximum load of the specimens.

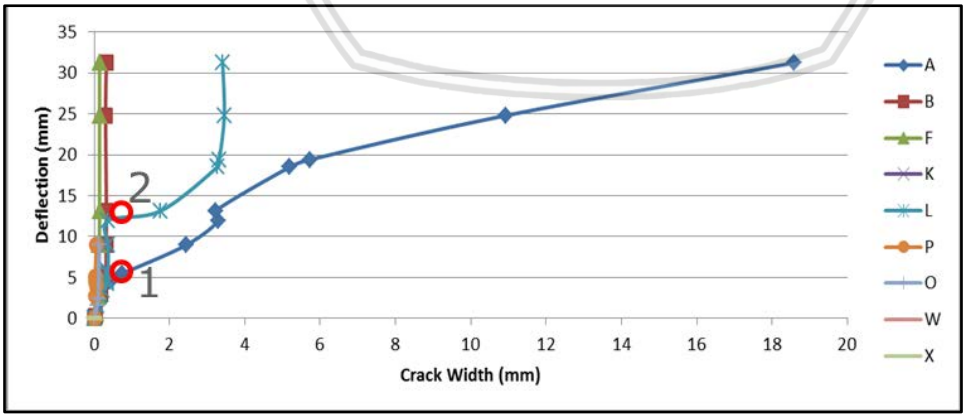

Figure 5.66. Crack opening width of ST4 Yield PCM

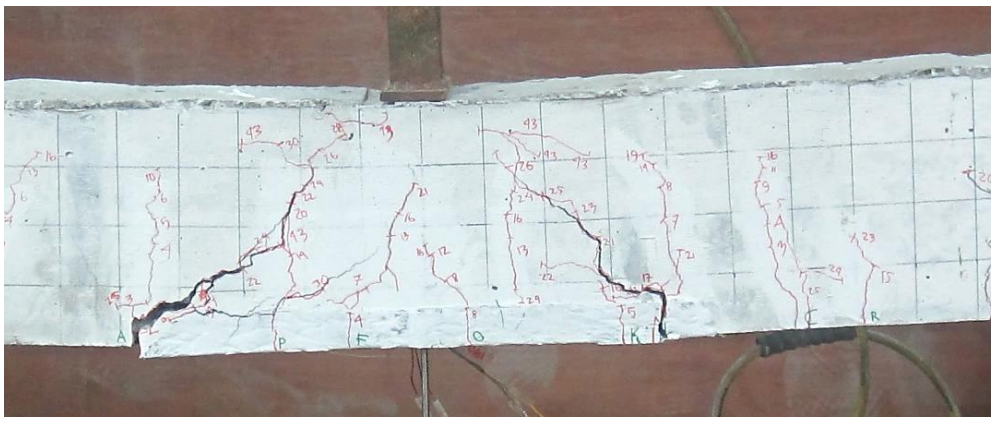

Figure 5.67. Crack path of ST4 Yield PCM

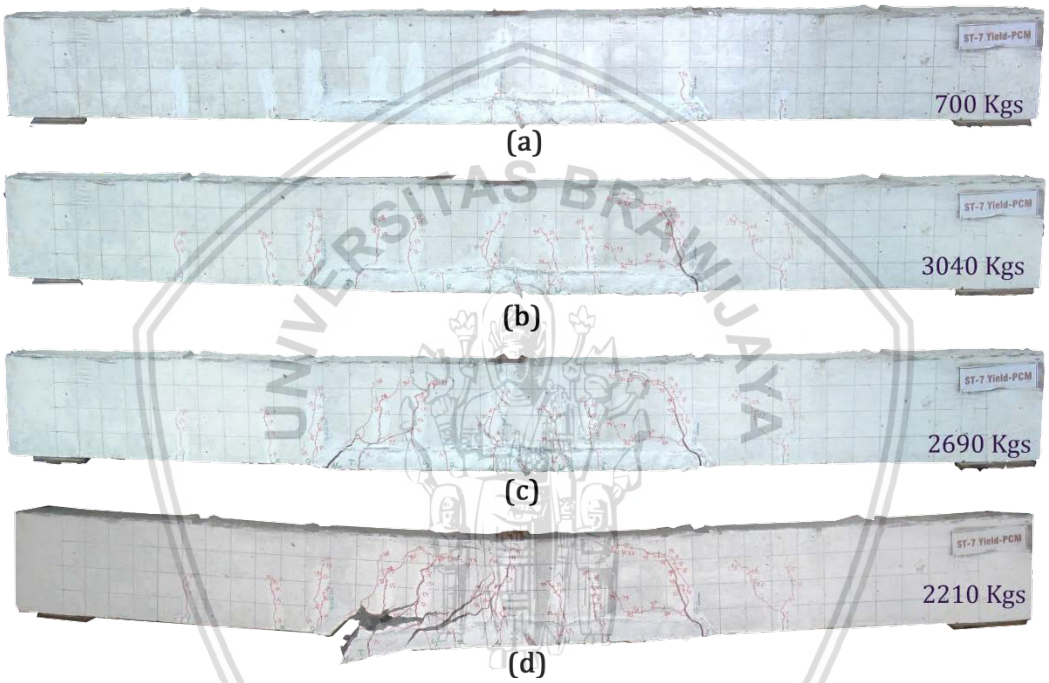

Figure 5.68. Crack path of ST7 Yield PCM

In the other hand, crack path of specimens repaired with straight shape rebar with OCM patch mortar showing different cracks development behavior. As shown in Figure *5.69*, horizontal crack of ST7 Yield OCM was occur at maximum load of 2900Kgs. However, specimens of ST4 Yield OCM shows that the horizontal cracks was occur in much lower load than its maximum load as shown in Figure *5.70*. No dominant diagonal cracks was occur in ST4 Yield OCM specimen. According to the reference (Park & Paulay, 1974) this behavior may confirm that the specimens may failed because of either bondslip of the repair rebar or the debonding of the patch material.

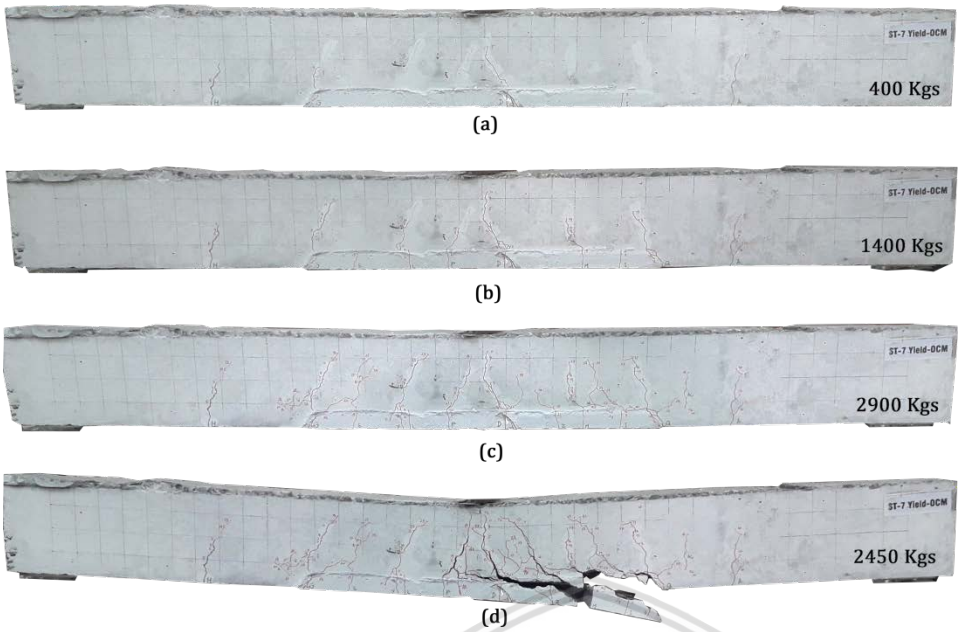

Figure 5.69. ST7 Yield OCM crack path

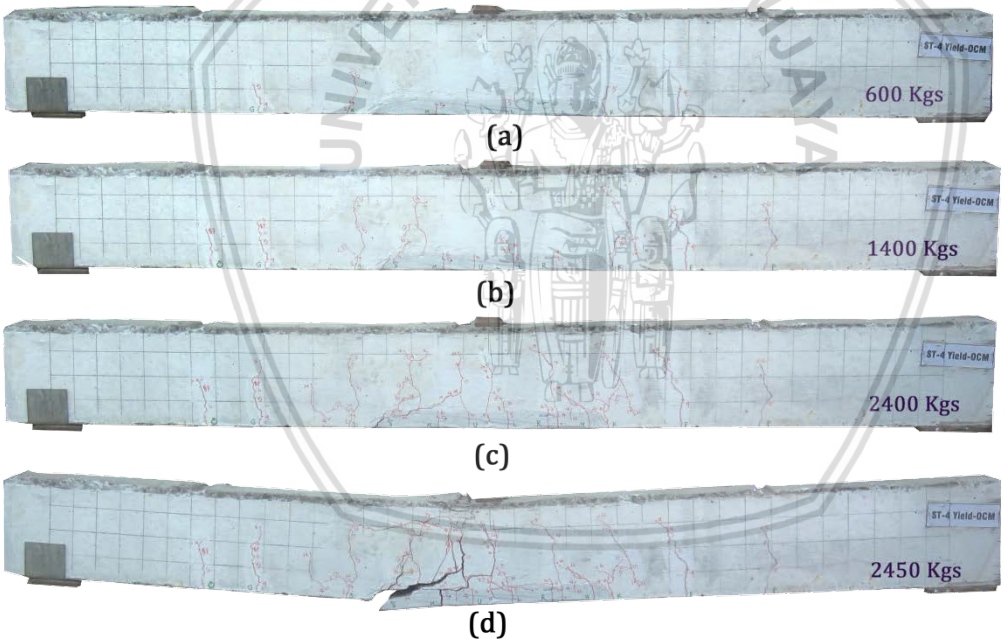

Figure 5.70. Crack path of ST4 Yield OCM

1.3.5 Proposed Ultimate load Analysis Approach

As post repair beam specimens cross section is remain the same as regular reinforced concrete beam section, with only additional strengthening rebar, the base analysis of ultimate strength and service load during loading may still the analysis for regular reinforced concrete beam. However, with deteriorated steel reinforcement, several parameters and coefficients adjustment have to be determined in the first place. In

addition, with the behaviour of the repair system that always has tendency to be separated from substrate system, additional limit state for the analysis should be added to the model.

1.3.5.1 Concrete Stress Block on Repeated Loading

According to the discussion on 5.1.4, stress-strain curve of concrete under repeated loading may be derived using mathematical model proposed by previous researcher (Otter & Naaman, 1989) (Aslani & Jowkarmeimandi, 2012) (Mander, et al., 1988). Similar with developed theory of concrete stress block which is derived from stress curve with the neutral axis to top fiber dimension, stress block of preloaded reinforced concrete beam may also derived from stress-strain curve of concrete under repeated loading.

Concrete plastic strain ε_{pl} of the concrete stress-strain behaviour which is used to yield Figure *5.20* were derived from Otter and Naaman (1989) proposed model which rewriten as Equation 22. The value of ε_{pl} itself is enough to create reloading curve and f_{new}, however, the unloading curve is also determined for continuity of the preloading, and reloading curve envelope. Then Equation 23 is used to provide well smooth unloading curve, which is derived from Aslani and Jowkarmeimandi (2012) formula.

$$\varepsilon_{pl} = \varepsilon_0 \left(\frac{\epsilon_{un}}{\epsilon_0} - k_{un}\left[1 - e^{-\epsilon_{un}/(k_{un}\varepsilon_0)}\right] \right) \quad \text{Equation 1}$$

$$f_c = f_{un} \left(\frac{1 - \left[(\varepsilon_c - \varepsilon_{un})/(\varepsilon_{pl} - \varepsilon_{un})\right]}{1 + 1.2\left[(\varepsilon_{un} - \varepsilon_{un})(\varepsilon_{pl} - \varepsilon_{un})\right]} \right)^{1.2} \quad \text{Equation 2}$$

$$f_{new} = f_{un} \left[1 - 0.09 \left(\frac{\epsilon_{un}}{\varepsilon_{ro}} \right)^{0.5} \right] \quad \text{Equation 3}$$

With determined of f_{new} and ε_{pl}, E_r of reloading Elasticity, or reloading slope gradient could be calculated using Equation 25. Then for the reloading curve line, could be yielded by simple mathematical expression as Equation 26.

$$E_r = \frac{f_{ro} - f_{new}}{\varepsilon_{pl} - \varepsilon_{un}} \quad \text{Equation 4}$$

$$f_c = f_{ro} + E_r(\varepsilon_c - \varepsilon_{pl}) \quad \text{Equation 5}$$

1.3.5.2 Stress Block of Repeated Loading Stopped in Particular Value of Unloading Strain ε_{un}

As preloaded of any beam could be stopped in any strain, than stress block with particular ε_{un} and reloading ε_c have to be determined. Using those equations, the stress

block of concrete state with constant maximum strain of ε_c 0.004, and ε_{un} from 0.002 to 0.004, the formulas yield stress block as shown on Figure *5.71*. Finer increment of this stress block complete with stress block area and centre of gravity of the stress block can be found in Appendix 5.

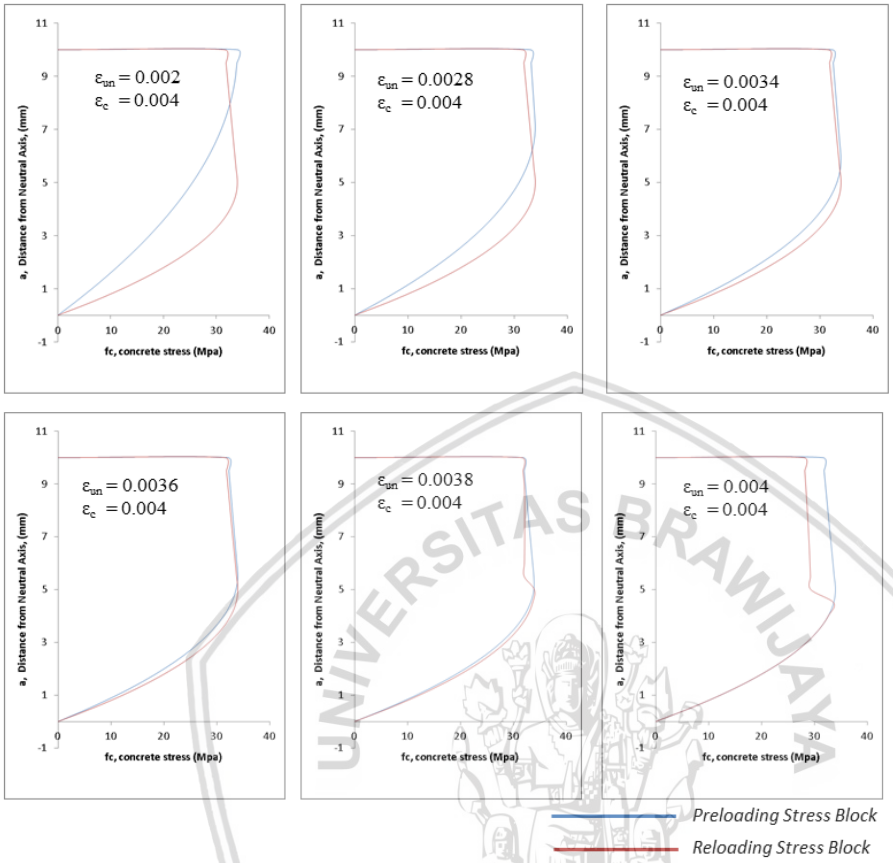

Figure 5.71. Stress Block on Reloading curve on increment of ε_{un}

As its well noticed that there is a decreasing area of reloading stress block, we need new parameters for more close approximation. Introducing α_{re} as stress block shape factor of concrete under repeated loading. the value of α_{re} may be derived using expression proposed by previous reports (Kent & Park, 1971) to be expressed as Equation 27. With finer increment of the stress block modelling, and calculation of every stress block formula, the value result the plot of α_{re} for every increment of unloading strain as shown in Figure *5.72*. Assumption is made that the concrete could reach 0.0045 of unloading strain.

$$\alpha_{re} = \frac{\int_0^{\epsilon_{cm}} f_{c\,re}\, d\epsilon_c}{f'_c\, \epsilon_{cm}} \qquad \text{Equation 6}$$

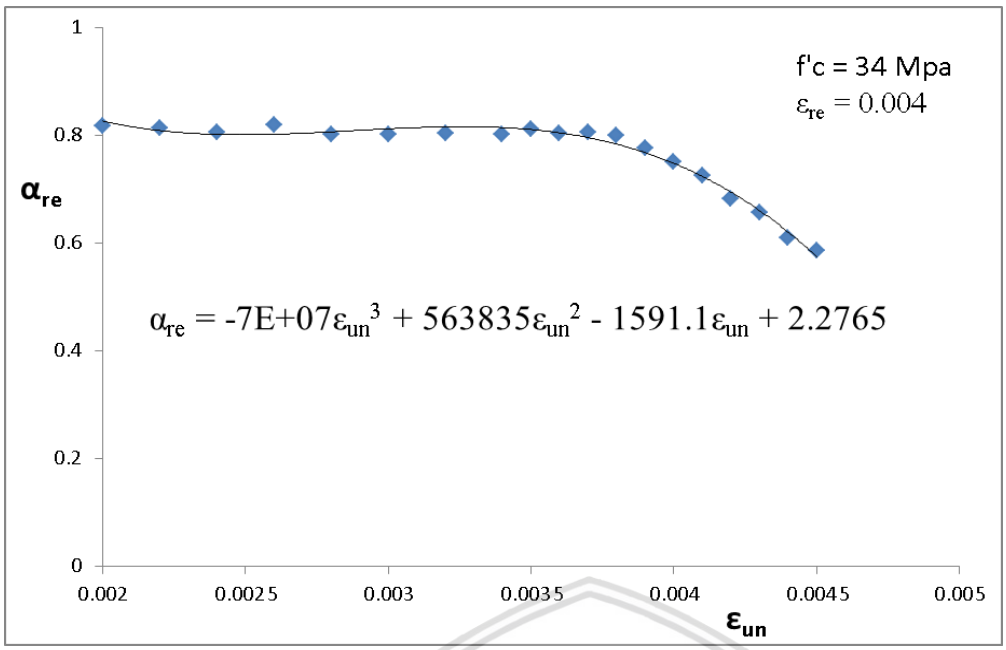

Figure 5.72. Plot of for the constant maximum ε_c and f'c 34Mpa

From the plot, the decrease of α_{re} value is well noticed. The decrease of α_{re} means the calculated stress block will also decrease with every increasing of ε_{un}. Thus may explain the deterioration result of repeated loading of the concrete beam. However, as this trend is derived from mathematical model, expense and comprehensive experiment is needed to confirm this behaviour.

1.3.5.3 Reload Stress Block Stress Shape Factor of α_{re} of each increment ε_c and constant ε_{un}

The ε_{un} effect for the α_{re} has been figured in Figure *5.72*. However, for service load behaviour analysis of the preloaded beam, stress block in each increment of ε_c has to be determined to calculate the stress force provided by compression stress block, as discussed in 2.1. By using the same method used in calculating α_{re} for increment of $\varepsilon_{un.}$, α_{re} for each increment of ε_c may also be determined. calculation to yield the stress block in every increment of ε_c performed for two unloading strain of 0.0038 and 0.004. The overview of the stress block for 0.004 ε_{un} resulted from discussed empirical model is presented on Figure *5.73*.

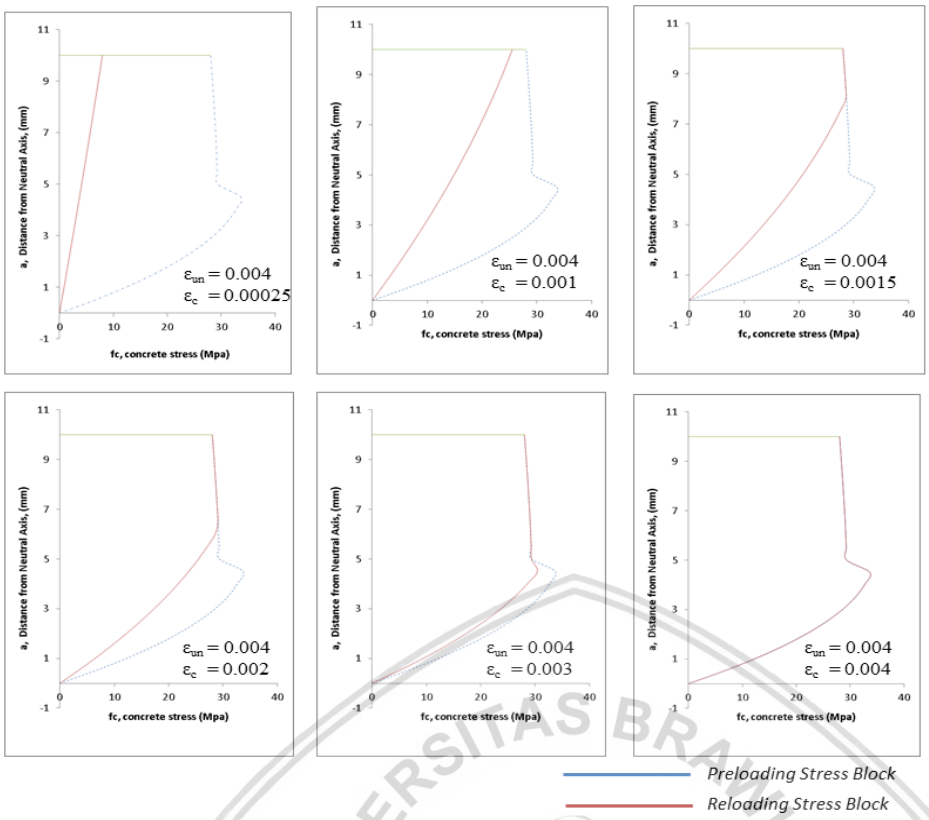

Figure 5.73. Stress Block on reloading curve on increment of ε_c with ε_{un} 0.004

Finer increment of ε_c, and calculation of all area and center of gravity for 0.0038 and 0.004 ε_{un} results the plot graph of α_{re} value for each loading step. Detailed and finer increment of stress block with area calculation and center of grafity could be found in Appendix 6.

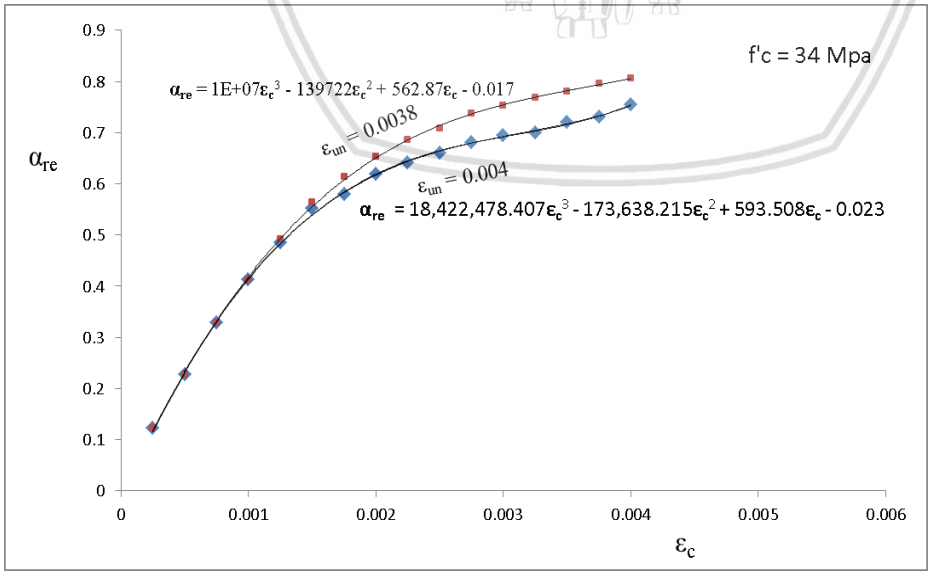

*Figure 5.74.*Plot of for the increment of ε_c with particular values of ε_{un} and f'c 34Mpa

1.3.5.4 Reload Stress Block Centroid Factor γ_{re}

Another parameter that is part of concrete strength beam calculation is γ. In the references (Park & Paulay, 1974), γ described as the distance factor of the stress block centroid. As the change of stress block shape and area due to preload, this value is has to be determined to gain accurate strength and service load behaviour analysis.

Introducing γ_{re} as the distance factor of reload stress block. Using the same way to produce plot in Figure *5.73* which has been detailed in Appendix 6, γ_{re} of each increment of reloading ε_c may be plotted as shown in Figure *5.75*.

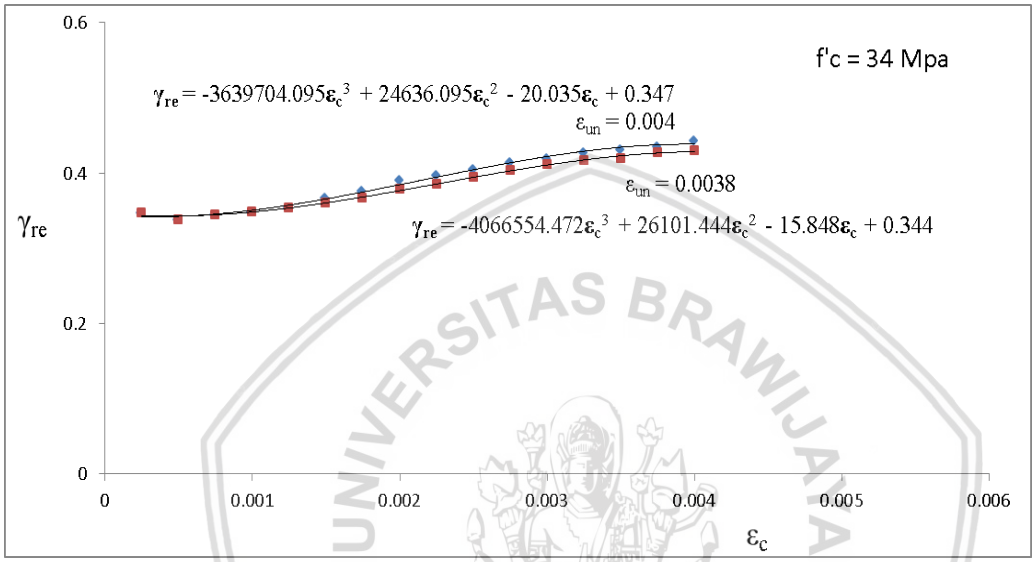

Figure 5.75. Plot of γ_{re} for every increments of reload ε_c, for 0.004 and 0.0038 ε_{un}

1.3.6 Modelling of Loading Analysis using Iteration of Incremental Load

The parameters of stress block after given preload has been defined on previous section. The α_{re} and γ_{re} obtained can be used for beam strength analysis combined with established calculation formula as described in 2.1 by early researcher. Analysis is performed using iteration process to find unknown value of changing kd to gain balance of compression force generated by stress block and compression steel, and tension force which is generated by tension reinforcement and repair rebar reinforcement. For analysis of beam preloaded until ε_{un} equals to 0.004, Equation 29 and Equation 30 is used for α_{re} and γ_{re} respectively.

C – T = 0 Equation 7

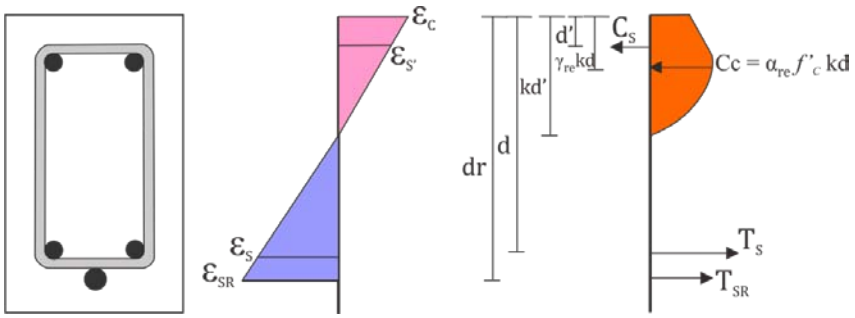

Figure 5.76. Scheme of Section Force for increment load analysis

$$\alpha_{re} = 18{,}422{,}478.407\varepsilon_c^3 - 173{,}638.215\varepsilon_c^2 + 593.508\varepsilon_c - 0.023 \quad \text{Equation 8}$$

$$\gamma_{re} = -3639704.095\varepsilon_c^3 + 24636.095\varepsilon_c^2 - 20.035\varepsilon_c + 0.347 \quad \text{Equation 9}$$

kd (mm)	$\varepsilon_{c\ Increment}$	ε_s	fs (Mpa)	ε_{sr}	fsr (Mpa)	l_d	ε_s'	fs' (Mpa)
1E-07	0	0	0	0	0	0	0	0
117,7902	0,00004	1,77E-05	3,545955	2,11E-05	4,225129	3,00903	3,3E-05	6,641652
65,66463	0,000065	0,000103	20,65587	0,000113	22,63562	16,1205	4,5E-05	9,040486
58,82222	0,00009	0,00017	34,02115	0,000185	37,08122	26,4083	5,9E-05	11,87986
55,95873	0,000115	0,000234	46,87292	0,000255	50,98309	36,3088	7,4E-05	14,77966
54,41366	0,00014	0,000297	59,47804	0,000323	64,6238	46,0234	8,9E-05	17,70847
53,47177	0,000165	0,00036	71,91517	0,00039	78,08665	55,6112	0,0001	20,65704
52,8571	0,00019	0,000421	84,21631	0,000457	91,4055	65,0966	0,00012	23,62161

Cont →

	fs' (Mpa)	α_{re}	γ_{re}	C (kN)	T (kN)	C-T	M (KNm)	Load (KN)	ϕ
0	0	0,00	0,34	0	0	0	0	0	0
5	6,641652	0	0,34	0	-2,5E-05	2,54E-05	0,1455472	0,3234383	3,4E-07
5	9,040486	0,01	0,34	3995,75747	3995,758	-0,00054	0,8049066	1,7886813	9,9E-07
5	11,87986	0,03	0,34	6986,88825	6986,888	3,65E-05	1,3378824	2,973072	1,53E-06
5	14,77966	0,04	0,34	9840,24787	9840,248	-2,1E-05	1,8512899	4,1139775	2,06E-06
5	17,70847	0,06	0,34	12627,4357	12627,44	-0,00049	2,3549442	5,2332093	2,57E-06
1	20,65704	0,07	0,34	15369,5548	15369,55	7,92E-08	2,8518011	6,3373357	3,09E-06
2	23,62161	0,08	0,34	18075,1907	18075,19	5,39E-07	3,3430718	7,4290485	3,59E-06

Cont →

Figure 5.77. Iteration table to finde balance C-T by changing kd

Part of iteration table used for determining unknown kd for balance C-T is showed on Figure *5.77* with complete table could be found in Appendix 8. Using goal seek analysis, by setting C-T value is equal to zero (0), the program seek automatically for the suitable value of kd which has been linked to all parameters data of cross section analysis. With established kd and other parameters, moment, load and curvature can be acquired.

In this study, the limitation is present on the f_{sr} analysis which there is no suitable approaching method for the repair rebar failing process. Since all the laboratory specimens has the same mid-span section, iteration only provided with single analysis of one type of specimen with no limitation of repair rebar length. Iteration result of unrepaired (control) specimens and repaired specimens could be found of unrepaired (control) specimens and repaired specimens can be found on Table *5.11*.

Table 5.10. Iteration formula applied in excel according to Figure *5.77*

Parameters	Formula in iteration table	Note

kd	-	Target value
ε_c	-	Increments of 0.000025
ε_s	$\varepsilon_s = \varepsilon_c \frac{(d-kd)}{kd}$	As reinforcement strain
f_s	**IF** ε_s < (fy/Es) ; $fs = \frac{Es.\varepsilon_c\,(d-kd)}{kd}$; fs = -12846,571 $\varepsilon_s^{\,2}$ + 2908,887 ε_s + 385,946	fs of As
ε_{sr}	$\varepsilon_s = \varepsilon_c \frac{(dr-kd)}{kd}$	As-repair rebar strain
f_{sr}	**IF** ε_{sr} < (fy/Es) ; $fsr = \frac{Es.\varepsilon_c\,(d_r-kd)}{kd}$; fsr = -12846,571 $\varepsilon_s^{\,2}$ + 2908,887 ε_s + 385,946	fsr of Asr
ld	$ld = Le + Ly + Lsh = \left(\frac{440A_b}{3d_b}\frac{f_y}{400}\right) + 0 + \frac{\Delta f_s d_b}{4\left((5.5 - 0.07\frac{S_L}{H_L})\sqrt{\frac{f'c}{27.6}}\right)}$	Repair rebar length development needed
ε_s'	**IF** kd > d' ; $\varepsilon_s = \varepsilon_c \frac{(kd-d')}{kd}$; $\varepsilon_s = \varepsilon_c \frac{(d'-kd)}{kd}$	As' reinforcement strain
f_s'	**IF** ε_s' < (fy/Es) ; $fs' = \frac{Es.\varepsilon_c\,(kd-d')}{kd}$; fsr = -12846,571 $\varepsilon_s^{\,2}$ + 2908,887 ε_s + 385,946	fs' of As'
α_{re}	γ_{re} = -3639704.095$\varepsilon_c^{\,3}$ + 24636.095$\varepsilon_c^{\,2}$ - 20.035ε_c + 0.347	Stress block area parameter
γ_{re}	α_{re} = 1E+07$\varepsilon_c^{\,3}$ - 139722$\varepsilon_c^{\,2}$ + 562.87ε_c - 0.017	Stress block centroid parameter
C-T	$(-\alpha_{re}.f'c.kd.b) + As\,.\,fs_{re} + As_r.fs_r + As'.fs'_{re} = 0$	Target balance of compression and tension = zero (0)
Moment	$M = As'.f_s'(kd-d') + \alpha_{re}.b.f_c'.kd(kd-\gamma_{re}kd) + As.f_s(d-kd) + Asr.f_{sr}(dr-kd)$	Internal Moment couple
Load	$P = \frac{2.M}{L}$	Concentrated load at mid.span
φ	$\varphi = \varepsilon_c/kd$	Beam Curvature

Table 5.11. Results of Iteration parameters value which process stopped to particular stop value of f_{sr}

Parameters	Value				
	Control (preload)	**Repaired with continous *fsr***	**Repaired with ε_{sr} stopped at Yield**	**Repaired with ε_{sr} stopped at 0.00416**	**Repaired with ε_{sr} stopped at 0.0016**
kd (mm)	19.8760	26.1151	53.0636	41.1049	52.4781
$\varepsilon_{c\ Increment}$	0.0040	0.0040	0.0008	0.0012	0.0007
ε_s	0.0305	0.0221	0.0017	0.0038	0.0015
fs (Mpa)	462.7469	443.8787	337.1667	396.8422	309.0433
ε_{sr}	-	0.0236	0.0018	0.0041	0.0017
fsr (Mpa)	-	447.4400	366.0000	397.6720	335.3400
Ld (mm)	-	234.0568	188.8808	206.4281	173.0582
ε_s'	-	46451.5461	37996.7475	41284.8139	34813.7412
fs' (Mpa)	-	4.2267	3.4574	3.7566	3.1678
α_{re}	0.8173	0.7768	0.3384	0.4760	0.3106
γ_{re}	0.4378	0.4380	0.3453	0.3560	0.3442
C (KN)	66282.13	82769.68	73269.66	79835.96	66501.38
T (KN)	66282.13	82769.68	72262.72	79835.96	66501.38
C-T	0.0000	0.0000	1006.9412	0.0000	0.0000
M (KNm)	10.5838	17.5751	13.4016	15.4685	12.2675
Load (KN)	**23.5196**	**39.0558**	**29.7814**	**34.3745**	**27.2612**
ϕ	0.0002033	0.0001534	0.0000144	0.0000296	0.0000131

Table *5.11* provide the strength value of repaired concrete with or without repair rebar strength contribution. Assuming that repair rebar will continuously contribute until total failure, the iteration are continued with no f_{sr} loss or falling value until the end of iteration. In the other hand, to accommodate the loss of repair rebar strength contribution, iteration stopped to particular ε_{sr} value according to the higher inflection point of strain falling branch value gathered from laboratory experiment. For specimens repaired by 400mm staple shape repair rebar, maximum ε_{sr} was reaching 0.0016, while specimens repaired by 700mm staple shape rebar was reaching about 0.00416.

Length development required is also calculated at each increment of iteration process. it could be noticed that needed ld, assuming that repair rebar will continuously contribute to the beam strength is about 234mm, which is much shorter than 350mm of 700mm repair rebar development length. While the column which ε_{sr} is stopped at 0.0016, which is maximum strain acquired by 400mm rebar, required ld is 173mm, which is relatively close to the available development length of 200mm.

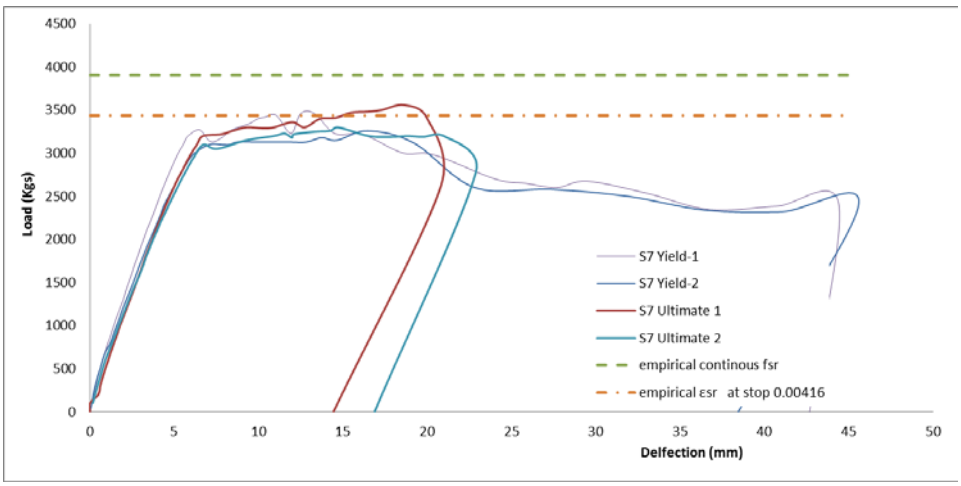

Figure 5.78. Plotted resulted empirical load on load-deflection curve of 700mm staple shape repaired specimens

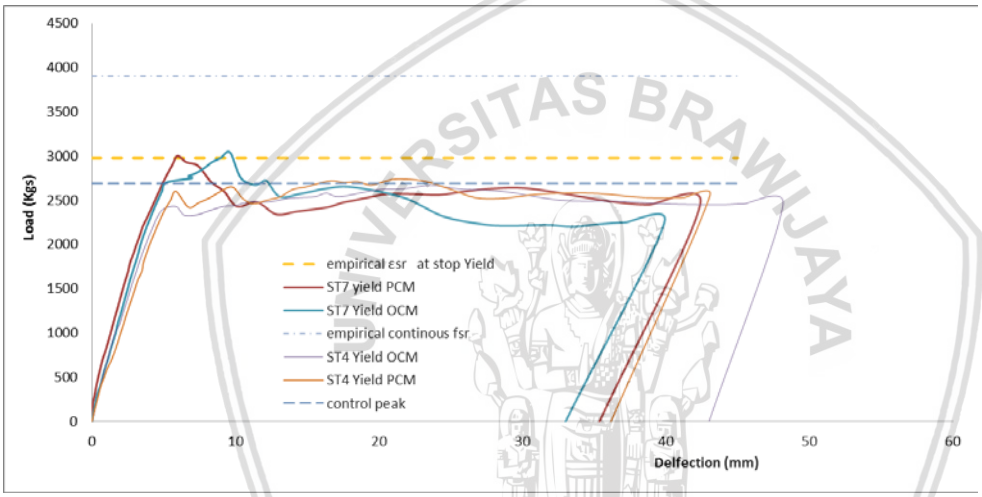

Figure 5.79. Plotted resulted empirical load on load-deflection curve of straight shape repaired specimens

1.4 Analysis and Discussion

1.4.1 The Move of Plastic Hinge

Rudledge, et al. (2013) has been reporting an extensive report of plastic hinge relocation of of failed bridge coloumn using CFRP repair. According to the report, base of the column has been failed significantly by corroded reinforcements, with some of them has been ruptured. With the repair procedure, the plastic hinge is moved to upper level of the column and resulting acceptable performance repaired columns. Similiarly, the results of this research has been showing restoration of structure strength followed by hinge movement to adjacent prior plastic hinge area.

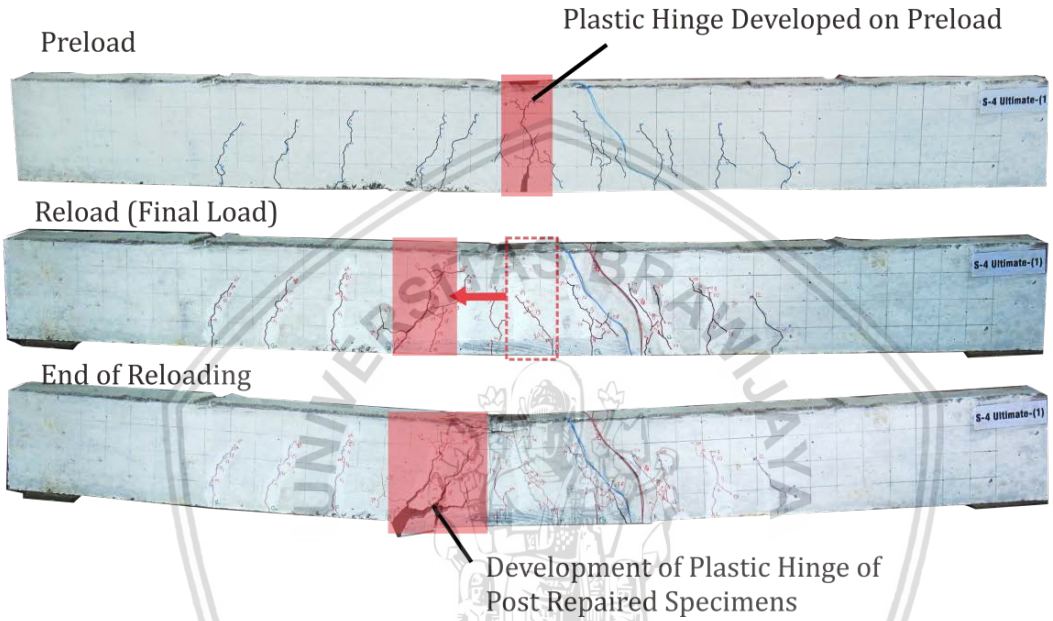

Figure 5.80. Plastic hinge movement in preload to postrepaired load test of S4 Ultimate-1

Plastic hinge usually built up on higher external force location correspond with its local strength capacity. According to previous repair observation report (Rudledge, et al., 2013) which is previous plastic hinge is built up at the bottom of the column, where largest moment is placed, the repair procedure creates significantly higher stiffeness on the area. Similiarly, with higher stiffness area on the mid-span of the beam, where repair procedure is applied, the plastic hinge tend to move to lower stiffness area, which is an abrupt change of beam cross section. As discussed on previous section, there are many factors that may be induced the development of plastic hinge. However. the detailed discussion will be performed in this section.

1.4.1.1 Required Repair Rebar Development

Many references (Alsiwat & Saatcioglu, 1992) (Committee-408, 2003) have been reporting on the behaviour and requirement of rebar development in concrete. Tension strength of the development is the main objective in rebar development design, which is the function of rib dimension and space, rebar length and concrete compression strength. For particular case, a concrete cover is also a major parameter.

In this study, the required rebar development has been calculated and summarized in Figure *5.81*. Calculation is based on the ld requirement as discussed in CHAPTER 2. From the iteration analysis, it may clearly observed that for specimens repaired using staple shape rebar of both 400mm and 700mm rebar, also for straight shape repair rebar for 700mm has available development length beyond the requirements. only specimens repaired using 400mm straight shape repair rebar which do not have sufficient available length to restrain the tensile force to supposed maximum capacity which is described on continuous f_{sr} column ofTable *5.11*. This behaviour may be confirmed by the horizontal crack of ST4 Yield OCM which already occurs at 2200Kgs, far below its maximum load.

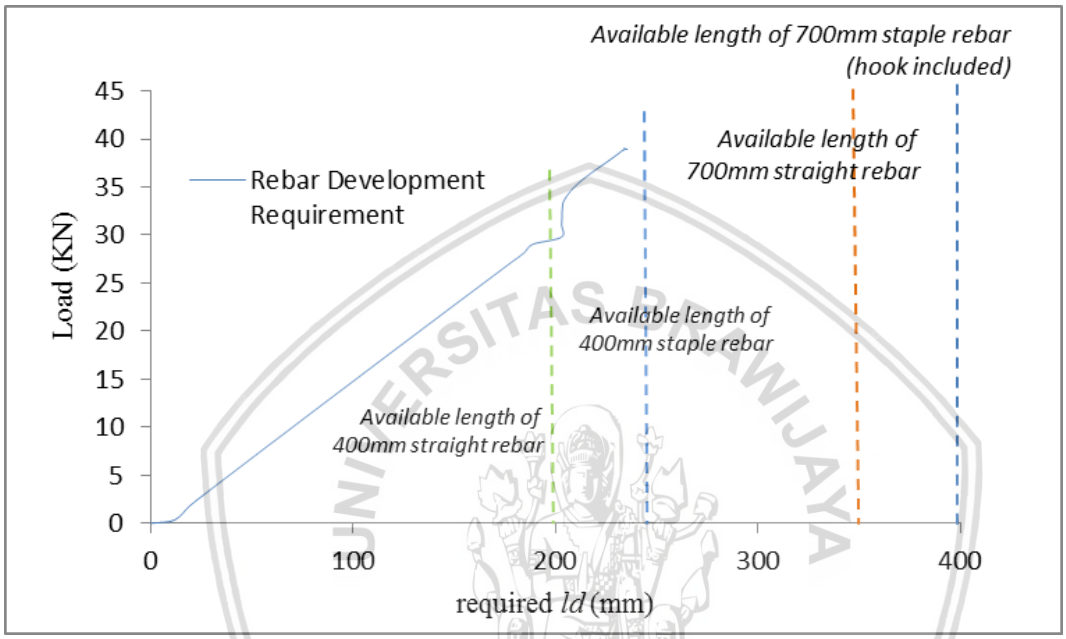

Figure 5.81. Required ld to the specimens load

Differently, no horizontal crack occur in other specimens than straight rebar with length 400mm before larger crack mouth opening is occur, which also the sign of plastic hinge development. According that those specimens has beyond available rebar development, another failure approach analysis is needed more than just rebar development requirement.

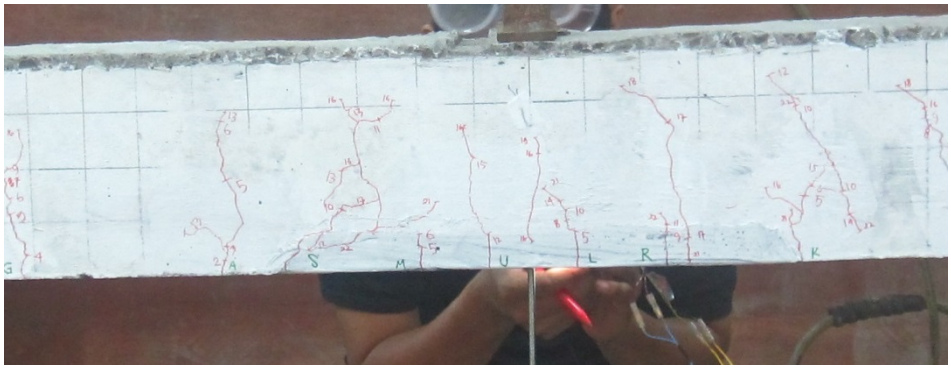

Figure 5.82. Horizontal crack development of ST4 Yield OCM occurs at 2200Kgs

1.4.1.2 Failure by Shear and Flexural Mechanism

The specimens in this study originally subjected to flexure load with less expectation of failing in shear. Hence, the specimens are designed with high span to depth ratio to 15. However as discussed in CHAPTER 2, shear mechanism is a complex event that may occur in any structure and cannot be neglected in structure fail behaviour (Committee-408, 2003). With plastic hinge development behaviour combined with rebar development requirement analysis, the specimens with sufficient anchorage length show failure in combination of shear and flexural manner.

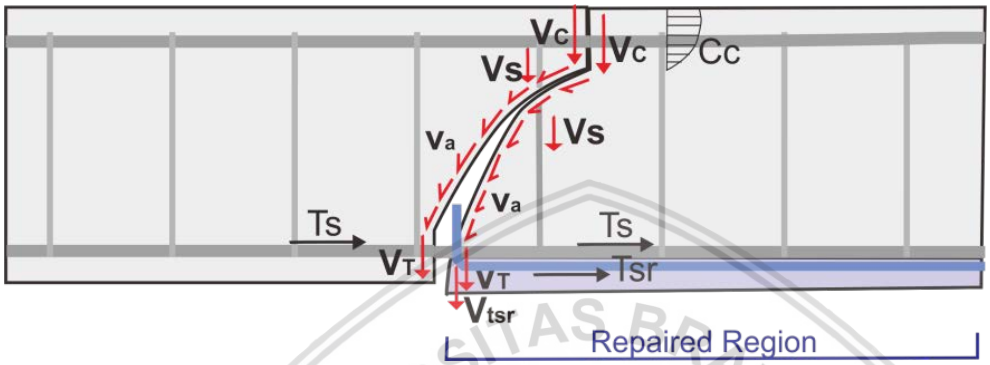

Figure 5.83. Possible shear failure mechanism which induced plastic hinge development

Observation on the crack path of specimens during final load shows evidence that shear mechanism is what inducing the hinge development on the specimens. For specimens repaired using staple repair rebar, which both of 400mm and 700mm type has sufficient length development, diagonal wide crack is always occur before horizontal crack on repair rebar line as shown in Figure *5.85* and Figure *5.86*.

According to the references (Park & Paulay, 1974) (Committee-445, 1999) , shear given by external load is restrained by three to four internal shear counteract force created by concrete compression stress of Vc, aggregate interlocking force of va, dowel action of longitudinal reinforcing rebar of Vt (and Vtsr) and lateral reinforcement of Vs. refer to the shear mechanism theory, addition of repair rebar creating stiffer region corresponding to shear stress acting on the specimens.

With the same shear flow along the length of the beam and shear crack is usually occur near one third of beam span, it is hard to conclude that plastic hinge is induced by a shear mechanism itself. Then, it is more convenience to take the flexural mechanism which also takes place to induce plastic hinge as shown in Figure *5.84*. The figure shows the plot of section moment capacity which has abrupt change of moment capacity on the repaired area. Increments of moment created by given load are also plotted. From the plot it may be seen that section moment capacity may be overpowered by moment by given load in three point. As may be seen in moment plot created by 35kN, overpowering moment happen in abrupt moment change location on two side and at the mid span of the beam.

As shear flow of the beam has the same magnitude along the beam length, which created by single concentrated load, combined by large flexural moment near mid span,

makes the shear failure occurs at abrupt section change between repaired and unrepaired region. This failure behavior was occurred on all of the specimens repaired using staple repair rebar and also specimens with 700mm straight repair rebar However, this mechanism is rather complicated to analysis by current available data. Possible mechanism may be explained by Figure *5.83*.

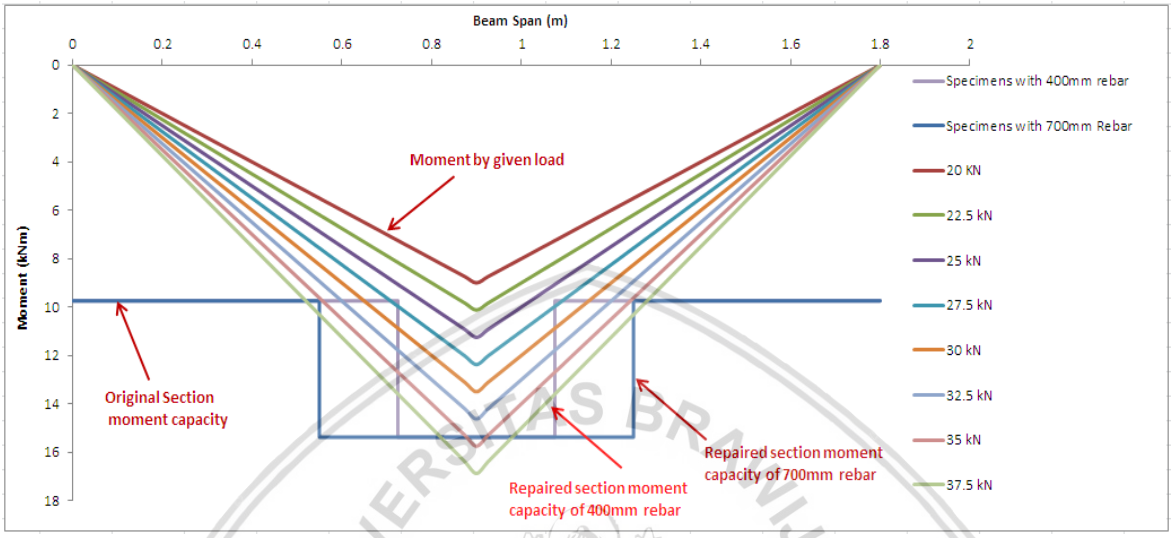

Figure 5.84 Section moment capacity versus given moment by given load

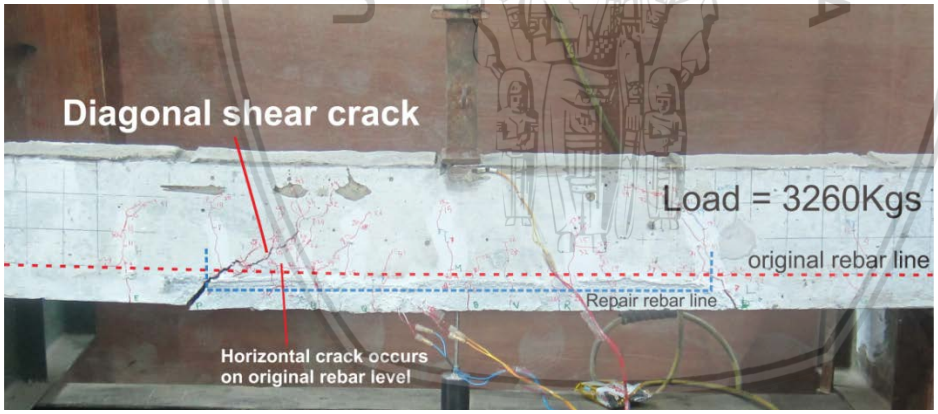

Figure 5.85. Diagonal shear crack development of S7 Yield-2 specimens

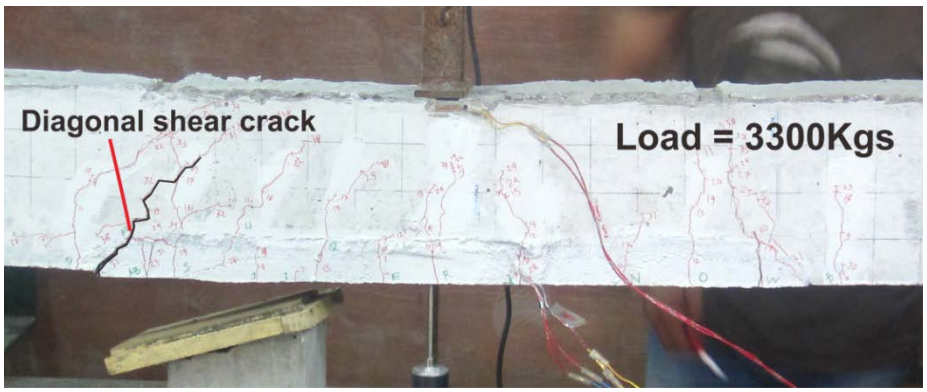

Figure 5.86. Diagonal shear crack development of S7 Ultimate-2 specimens (no horizontal crack occurs)

Figure 5.87. Diagonal shear crack development of ST7 Yield PCM

1.4.2 Bondslip of Repair Rebar and Debonding of Patch Material

As prior discussed on 5.3.4, the specimens repaired with straight shape rebar have shown horizontal cracks pattern during final load session. For specimens of ST4 Yield PCM, horizontal crack was occur after large diagonal cracks were developed. This behavior may be seen in Figure *5.88*. According to the load deflection curve shown in Figure *5.89*, the left hand side diagonal crack was suddenly larger in load point 1, while right hand side diagonal crack was suddenly larger in load point 2. The horizontal crack later occurred in load point 3.

It may be seen that after reach load point 1, the load curve suddenly drop but later increase until reach point 2. However, the collapse of the specimens was not happened after reach point 2. After several increasing of load and deflection, the load curve was suddenly drop followed by horizontal crack development in interfacial face of patch material. From Figure *5.90*, it well observed that rebar strain curve has inflected and softened after reach about 2300Kgs of load. However, no sudden drop of strain curve when the load reach load point 1 and 2. Strain curve then significantly drop after load curve reach load point 3. This behavior may explain that failure mechanism of ST4 Yield PCM was taken by combination of shear and flexural mechanism at the earlier of structure collapse. However, with excessive strain and slip happened with the repair rebar, rebar

bond slip take place and create horizontal crack pattern. With more increments of load and deflection, this horizontal crack continue to debond the patch material.

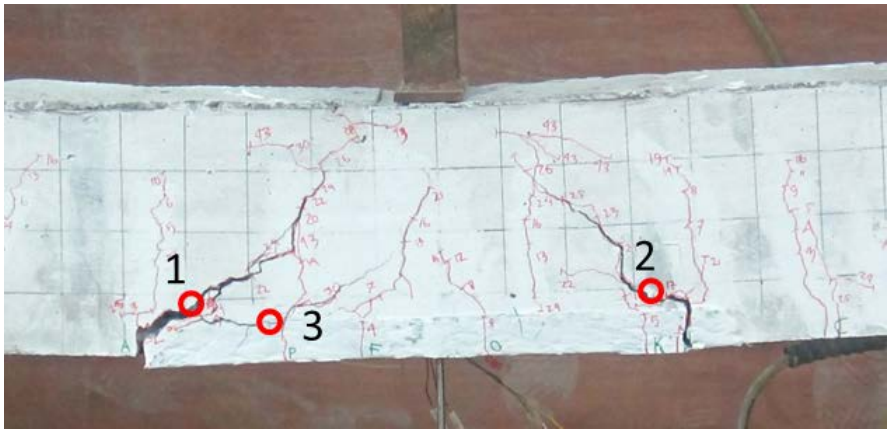

Figure 5.88. Crack path of ST4 Yield PCM

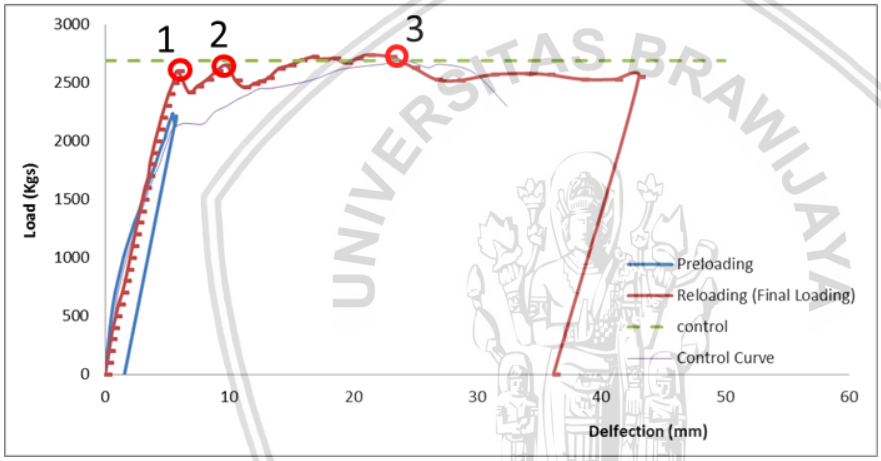

Figure 5.89. Load deflection of ST4 Yield PCM with crack point

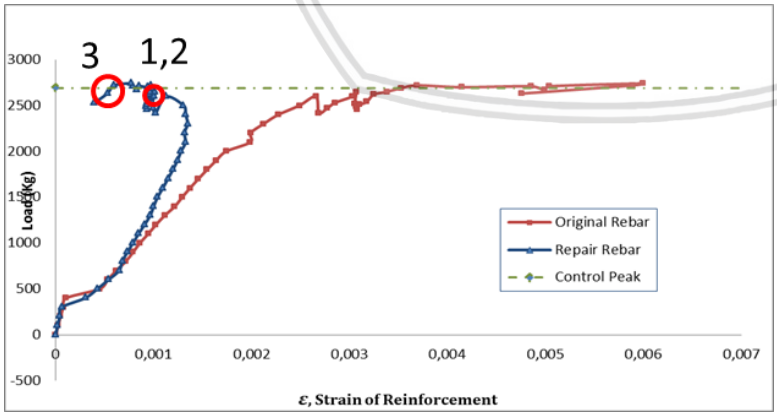

Figure 5.90. Load-tensile strain behavior correspond to crack point of ST4 Yield PCM

In contrast, specimen of ST4 Yield OCM was not show any sign of combination of shear-flexural mechanism. The failure mechanism was started by bondslip of the repair rebar and continue to debond the patch material. After the repair system was no longer

functioned, the specimens continue to fail with flexural mechanism similar with base specimens or control beam with dominantly vertical crack development. This behavior may be shown by Figure *5.91* which the repair rebar strain was inflecting and release it strain before the specimens reach its maximum load. Horizontal cracks was first occur on 2400Kgs as shown in Figure *5.92* which is relatively far below specimens maximum load.

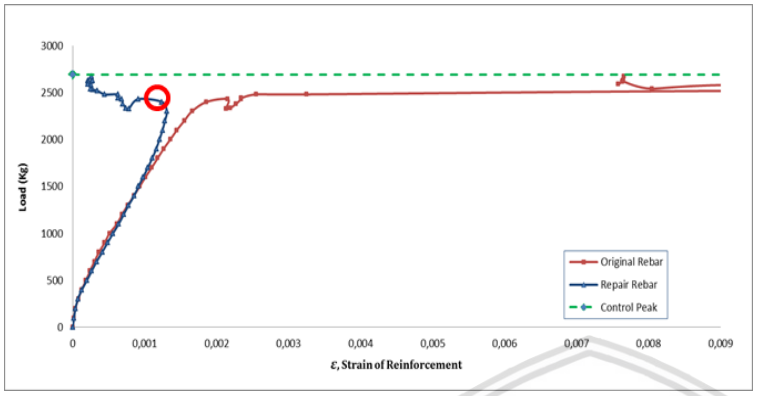

Figure 5.91. Inflection point of ST4 Yield OCM repair rebar strain before reach maximum load.

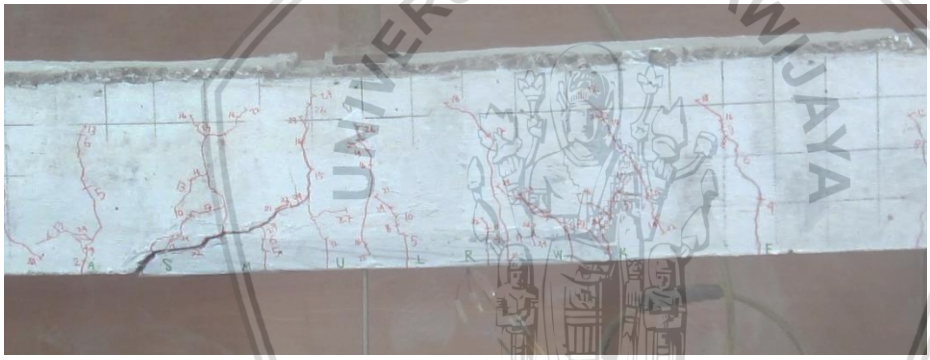

Figure 5.92. Horizontal crack development of ST4 Yield OCM

1.4.3 Effect of Preloading Limit State to the Specimens Maximum Capacity

Ultimate limit state and yield limit state have been applied to the beam specimens before the repair system was applied. Load record on final load session has shown that there are slight differences of maximum load between ultimate specimens and yield specimens. Rather than showing higher maximum load due to its low prior deteriorated material, the yield specimens were showing lower maximum load than ultimate specimens. This behaviour can be found in Table *5.7* and Table *5.8*, where maximum load of yield specimens with 400mm staple rebar is about 4% lower than maximum load of ultimate specimens. However, this behaviour cannot be clearly concluded for the specimens with 700mm staple rebar, as the maximum load of S7 Ultimate-2 was found lower than S7 Yield-1.

If maximum load of S7 Ultimate-2 is considered as deviated sample, the behaviour may be explained by the steel unloading state. Despite error of further recording of original

rebar as seen from Figure *5.8*, it may be clearly seen that the strain of original rebar has been reach more than 0.0028 of strain as seen in the curve plot. Considering the plot and ultimate analysis provided in Appendix 1, it is convenience to assume that repair rebar has reach strain hardening state. In the other hand, original rebar on yield state was expected and maintained to reach first inflection point of yield state then stopped.

According to the theory of repeated loading of steel reinforcement rebar as explained on the reference (Park & Paulay, 1974), steel rebar will always forming the envelope curve with the same curve gradient in elastic region. This behavior may be explained on Figure *5.93*.

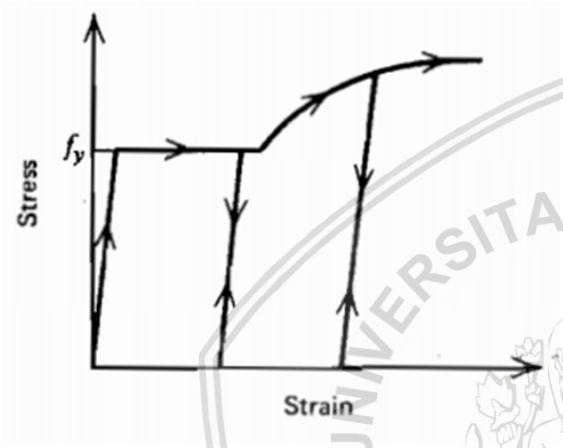

Figure 5.93. Repeated stress-strain behavior of steel reinforcement rebar

Assumed that the repair system contribution to substrate system is limited to the falling point of load as shown in Figure *5.94*, the summary of Δd from zero to deflection before the load is drop may is tabulated on Table *5.12*. As beam deflection is a function of concrete and steel reinforcement strain, it can be concluded that the repaired beam has limited value for the developing strain of repair system. From the table, it may be concluded that there is no significant different in maximum deflection between ultimate specimens and yield specimens.

According to the Figure *5.93* and the reinforcement condition post preloading session for each ultimate and yield specimen, the original rebar of ultimate specimens may has been reach the strain hardening region while original rebar of the yield specimens still in the plateau region with the same strain or the same given deflection. The earlier increasing stress of original rebar of ultimate specimens results the specimens reaching higher load before the repair system start to fail. However, this behaviour has to be confirmed by further comprehensive experiment.

Table 5.12. Δd before falling point of maximum load

Specimens	Deflection		Δd (mm)
	First inflection point (mm)	falling point (mm)	
S7 Ultimate-1	6.69	20	13.31
S7 Ultimate-2	6.718	21	14.352
S7 Yield-1	5.8	20.4	14.6
S7 Yield-2	7.06	19.19	12.13

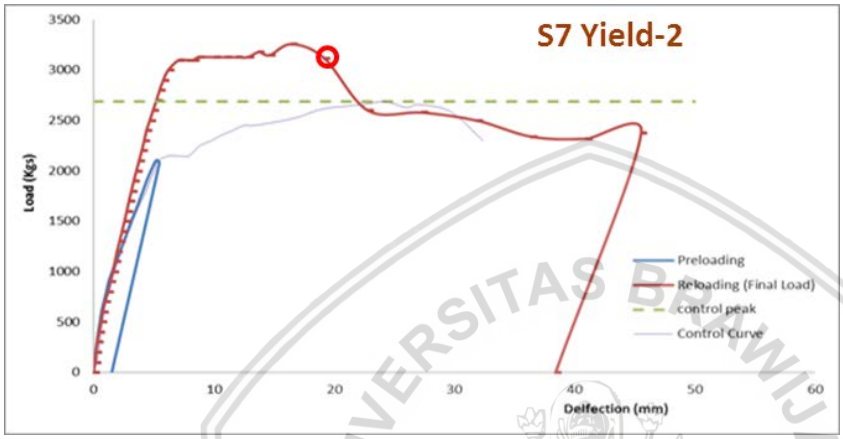

Figure 5.94. Falling point of load of S7 Yield-2

CHAPTER 6
CONCLUSION AND SUGGESTION

6.1 Conclusion

Comprehensive experiment and analysis has been performed to obtain well observed behavior of the preloaded reinforced concrete beam repaired using three type of repair system. From the experimental observation, the specimens repaired using staple shape rebar has showing a significant improvement especially for specimens with 700mm staple shape rebar with 22 to 32% higher than control load. The specimens with 400mm staple shape rebar are also showing an increasing in load capacity with around 4 to 8% higher than control load. The specimens repaired with 700mm straight rebar also showing increasing strength of 11 to 13% higher than control load. However, no significant increasing load is showed by specimens with 400mm straight shape rebar.

The length of the repair system is the most affecting factors of the compatibility of the repair system which longer length of repair rebar as well as patch material will create longer composite action than shorter repair rebar and patch material. This behavior may fill the gap of reported repair experiment by Rio, et al., (2005). However, there still indeterminate failure mechanism which causing the total collapse of the specimens. For specimens repaired with staple rebar, all failure mechanism was shown by diagonal cracks which usually caused by shear mechanism. However, flexural mechanism seems showing significant portion to induce the total collapse mechanism. This indeterminate of combination of failure mechanism may be answered by eccentric load with the same repair position or vice versa.

In the other hand, combination of shear-flexural mechanism with bondslip and debonding mechanism was also shown by ST4 Yield PCM specimens. Despite its short repair rebar, the specimens experience shear-flexural fail mechanism as the large diagonal cracks was also occur during final load. This is may be caused by high strength bond between patch material to the rebar and between patch material to the substrate concrete. However, debonding failure has taken over the failure process as the horizontal crack was developing followed by drop of load curve. In contrast, ST4 Yield OCM was failed by bondslip and debonding of repair system due to lower bond strength to the substrate system.

The effect of different prior limit state of preloaded beam has shown different maximum load of the repaired beam. From preliminary analysis it may be concluded that the earlier increasing stress of original rebar of ultimate specimens results the specimens reaching higher load before the repair system start to fail. This makes the ultimate specimens may reach higher maximum load than yield state.

As conclusion, the experiment and analysis of preloaded beam repaired using several repair system has been conducted. The result shows significant improvement especially for preloaded beam repaired using staple shape rebar. However, there are still indeterminate mechanism and behaviours of the specimen failure process. Therefore, more experiment and analysis have to be conducted to gain more understanding in the behaviour of the repair system correspond to the subtract system.

6.2 Suggestion

1. More comprehensive experiment need to be performed with eccentric position of loading point and repair system to gain more understanding in specimens failure mechanism.
2. Finite element model in detailed manner is needed to observe the stress and force trajectory of repaired specimens.
3. More comprehensive experiment is needed to confirm the proposed analysis, especially for the proposed value of γ_{re} and α_{re}.
4. There is a well noticed difference between the PCM bond strength in flexure and bond strength in shear, where bond in flexure is far below bond in shear. A comprehensive experiment is needed to confirm this experiment result.

BIBLIOGRAPHY

ACI-Committee-224. (1998). ACI 224R-01 Control of Cracking of Concrete Structures. Farmington Hills: American Concrete Institute.

Alsiwat, M., & Saatcioglu, M. (1992, September). Reinforcement Anchorage Slip under Monotonic Loading. Journal of Structural Engineering, 118(9), 2421-2438.

Aslani, F., & Jowkarmeimandi, R. (2012). Stress-strain model for concrete under cyclic loading. Magazine of Concrete Research, 64(8), 673-685.

ASTM. (2015). C78 - Standard Test Method for Flexural Strength of Concrete (Using Simple Beam with Third-Point Loading). ASTM.

Aykac, S., Ilker Kalkan, S., Aykac, B., Karahan, S., & Kayar, a. S. (2013). Strengthening and Repair of Reinforced Concrete Using External Steel Plates. JOURNAL OF STRUCTURAL ENGINEERING - ASCE.

Badawi, M., & Soudki, K. (2010). CFRP Repair of RC Beams with Shear-Span and Full-Span Corrosion. JOURNAL OF COMPOSITES FOR CONSTRUCTION - ASCE, 323-334.

Baluch, M. H., Rahman, M. K., & Al-Ghadib, A. H. (2002). Risk of Cracking and Delamination in Patch Repair. Journal Material of Civil Engineering - ASCE, 294-302.

Barros, J. A., Cruz, J. M., Delgado, R. M., & Costa, A. G. (2000). REINFORCED CONCRETE UNDER CYCLIC LOADING. 12Th World Conference on Earthquake Engineering. Auckland.

BSNI. (2013). SNI 2847:2013 - Persyaratan Beton Struktural Untuk Bangunan Gedung. Jakarta: BSNI.

Coakley, E. (2009). Behaviour of Continous Reinforced Concrete Beams During the Patch Repair Process. Heriot Watt University. Edinburgh: Heriot Watt University.

Committee-408. (2003). Bond and Development of Straight Reinforcing Bars in Tension. American Concrete Institute - ACI.

Committee-445, J. A.-A. (1999). Recent Approaches to Shear Design of Structural Concrete. American Concrete Institute - ACI.

Committee-562, A. (2013). Code Requirements for Evaluation, Repair, and Rehabilitation Concrete Buildings (ACI-562-13) and Commentary. Farmington Hills: American Concrete Institute.

Hsu, T. T., Slate, F. O., Sturman, G. M., & Winter, G. (1963). Microcracking of Plain Concrete and the Shape of the Stress-Strain Curve. ACI Journal, Proceedings, 209-224.

Keith, K. (2015). ACI 562 - The Concrete Repair Code. Forensic Engineering.

Keith, K., & Kevin, C. (2014). ACI 562 - Development of a building code for existing Concrete Structure. NCSEA Annual Conference. New Orleans: NCSEA.

Kenkyujo, T. S. (n.d.). TML Pam E-1007A Strain Gauge Catalogue. Product Catalogue. Tokyo, Japan: Tokyo Sokki Kenkyujo.Ltd.

Kent, D. C., & Park, R. (1971). Flexural Members with Confined Concrete. Journal of Structural Division, 1969-1990.

Leonhardt, F. (1988). Cracks and Crack Control in Concrete Structures. PCI Journal.

Lin, J. P., & Wu, Y.-F. (2016). Numerical Analysis of Interfacial Bond Behaviour of Externally Bonded FRP-to-Concrete Joints. Journal of Composites Construction.

Lukovic, M., Ye, G., & Breugel, K. v. (2012). Reliable concrete repair - a critical view. 14th International Conference Structural Faults and Repair. Edinburgh: TU Delft.

Mander, J., Priestley, M., & Park, R. (1988, August). Theoretical Stress-Strain Model for Confined Concrete. Journal of Structural Engineering, 114, 1804-1826.

Mangat, P., & O'Flaherty. (2000). Factors Affecting the Efficiency of Repair to Propped and Unpropped Bridge Beams. Magazine of Concrete Research, 4(52), 303-319.

Mattock, A. H., Kriz, L. B., & Hognestad, E. (1961). Rectangular Concrete Stress Distribution in Ultimate Strength Design. Journal of The American Concrete Institute, 875-928.

Minoru, K., Toshiro, K., Yuichi, U., & Keitetsu, R. (2001). Evaluation of Bond Properties in Concrete Repair Materials. JOURNAL OF MATERIALS IN CIVIL ENGINEERING - ASCE, 98-105.

Momayed, A., Ehsani, M., Rajaie, R., & Ramenzanianpour. (2005). Cylindrical specimen for measuring shinkage in repairing concrete members. Construction Building Material, 107-116.

Nowak, A. S., & Collins, K. R. (2000). Reliability of Structures. Boston: McGraw.Hill.

Otter, D. E., & Naaman, A. E. (1989). Model for Response of Concrete to Random Compressive Loads. Journal of Structural Engineering, 115, 2794-2809.

Park, R., & Paulay, T. (1974). Reinforced Concrete Structures. New York: John Wiley & Sons.

Pattnaik, R. R. (2015, April). Investigation on ASTM C882 Test Procedure of Slant Shear Bond Strength of Concrete Repair Material. International Journal of Civil, Structural,

Enviromental and Infrastructure Engineering Research and Development (IJCSEIERD), 5(2).

REMR-CS-2. (1985). The Condition of Corps of Engineers Civil Works - Concrete Structures.

Rio, O., Andrade, C., Izquierdo, D., & Alonso, C. (2005). Behaviour of Patch-Repaired Concrete Structural Elements under Increasing Static Loads to Flexural Failure. JOURNAL OF MATERIALS IN CIVIL ENGINEERING - ASCE, 168-177.

Rudledge, S. T., Kowalsky, M. J., Seracino, R., & Nau, J. M. (2013). Repair of Reinforced Concrete Bridge Columns Containing Buckled and Fractured Reinforcement by Plastic Hinge Relocation. Journal of Bridge Engineering - ASCE.

Salathiel, M., Leopold, M., & Moyo, P. (2016). Finite Element Modeling of Reinforced Concrete Beam Patch Repaired and Strengthened With Fiber-Reinforced Polymers. International Journal of Engineering and Technical Research (IJETR), 47-54.

Satoh, K., & Kodama, K. (2005). Centra peeling faulire behavior of polymer cement mortar retrofitting of reinforced concrete beams. Journal Material Civil Engineering, 126-136.

SIKA. (2005). Sikatop 122 - Fiber Reinforce, Polymer Modified Repair Mortar. Technical Data Sheet. SIKA.

Tao, Y., & Chen, J. (2014). Concrete Damage Plasticity Model for Modelling FRP-to-Concrete Bond Behavior. Journal of Composite Structure - ASCE.

Tilly, G., & Jacobs, J. (2007). Concrete Repairs: Performance in Practice and Current Service. Garston: CONREPNET.